

Investigations into the surface antigens of Hepatitis B Virus

By

Reginald Francis Clayton

A thesis presented for the degree of
Doctor of Philosophy

In

The Faculty of Science
At the University of Glasgow

Institute of Virology
Church Street
Glasgow G11 5JR

July 2000

ProQuest Number: 13818552

All rights reserved

INFORMATION TO ALL USERS

The quality of this reproduction is dependent upon the quality of the copy submitted.

In the unlikely event that the author did not send a complete manuscript and there are missing pages, these will be noted. Also, if material had to be removed, a note will indicate the deletion.



ProQuest 13818552

Published by ProQuest LLC (2018). Copyright of the Dissertation is held by the Author.

All rights reserved.

This work is protected against unauthorized copying under Title 17, United States Code
Microform Edition © ProQuest LLC.

ProQuest LLC.
789 East Eisenhower Parkway
P.O. Box 1346
Ann Arbor, MI 48106 – 1346



12038 - Copy 1

Acknowledgements

I thank Professor Duncan McGeoch for granting me the opportunity to study at the MRC Division of virology.

I also thank Dr Arvind Patel for direction and supervision throughout the course of my training.

Many people deserve acknowledgement and thanks for academic-related matters, and this serves to satisfy some of the relevant people:

Susan Graham for generation of monoclonal antibodies: Adrian Abbots for assistance in purifying those antibodies: Dr. Roger Everett for training concerning confocal microscopy: Mr. Jim Aiken for splendid assistance with electron microscopy: Mr. Connal McCaughey for some rather useful antisera: Dr Ania Owsianka for numerous things: Prof. R. Elliott for encouragement, Dr N. Stow for encouragement, Dr. H. Marsden for advice.

Furthermore, some people who deserve thanks for non-academic related matters: Ms I Konig for support: Mr C. F. Clayton (RIP), and Mrs C. F. Clayton: Prof. C. R. Clayton: Mrs P. J. M. Clayton for encouragement: Dr R. A. Bulman for encouragement (Nil carborundum, etc.). Mrs W. Harris B.Sc. for encouragement and a great deal more: Mr A. J. Duncan B.Sc. for still hanging on: Mr P. Rycraft B.Sc. for encouragement: Dr. C. Moncreiff, for many things: Mr M. Gooch, and Mr. S. Gooch for infallible southern wit (Mornin' Judge): Mr S. Chivers and Ms P. Bisley for motivation: Drs Bhella, Goodfellow, Pollit, and Ms. Y. Chaudhury, for being top people: Ms. P. Murad B.Sc., M.Sc., for making Glaswegian life more tolerable: Ms J. Kean B.Sc. for also making Glaswegian life more tolerable: Ms. K Foster B.Sc. for making Glaswegian life even more tolerable. Also, acknowledgements are due to Mr P. Anselmo *et al* for inspiration: Mr R. Flynn *et al* for inspiration: Mr J. Hetfield *et al*: Mr P. Hamilton for passing on the knowledge from the Joe Pass School: Mr. P Keenan *et al*. Acknowledgements are due to the late Mr. E. Stuart B.Sc.

Lastly, acknowledgements to my late father, Mr. A. F. Clayton.

The author was in receipt of a Medical Research Council studentship throughout the course of this work. Except where stated, the work presented in this thesis was carried out by the author.

Reginald Francis Clayton.

August 2000.

Summary

The small (S), medium (M), and large (L) surface antigens of Hepatitis B virus (HBV) are found in the virion envelope. They are initially synthesised in infected cells as multispinning transmembrane proteins of the endoplasmic reticulum (ER). These proteins perform many roles in the life cycle of the virus. Specifically, they play a crucial role in initiating the infection through virus attachment and entry into the target cells, and subsequently in the assembly and morphogenesis of the HBV virion. The surface antigens mediate these processes through interaction with each other, with HBV core and viral nucleic acid, and with host cell proteins. The major aim of this study was to investigate the protein-protein interactions of the HBV structural proteins in order to enhance our understanding of the mechanisms involved in these processes. To carry out this work, an extensive array of specific reagents was initially generated in house and characterised. These include monoclonal and polyclonal antibodies (MAbs and PABs, respectively) to the preS1 domain of the HBV L protein, and novel cell lines derived from primary human hepatocytes. Additional reagents were obtained from elsewhere. Furthermore, the genes encoding the HBV surface antigens and core were cloned and expressed using a recombinant vaccinia virus and bacterial systems. Using specific antibodies, the heterologous expression of the HBV proteins was confirmed in several assays.

HBV displays a strong tropism for human hepatocytes and cannot be propagated efficiently in cell culture. However, under certain conditions, the virus can replicate in cell lines of hepatic origin. Most hepatocyte cell lines in existence are derived from tumours, thus are likely to display aberrant gene expression in comparison with healthy hepatocytes. The failure of the virus to replicate efficiently in cell culture may be due to the lack of certain hepatocyte-specific functions in the cells. In this study, two hepatocyte cell lines, H5 and H16 were generated in house from healthy liver tissue and were examined for expression of certain proteins known to be associated with hepatocyte phenotype. The results suggested that cell lines H5 and H16 are likely to have retained at least some of the hepatocyte gene expression, and have not reverted to a fibroblast phenotype. Both cell lines H5 and H16, as well as established cell lines (such as HepG2) were used for the study of the protein-protein interactions of the HBV structural antigens.

A detailed antigenic characterisation of the anti-L MAbs showed that all recognised a linear epitope on the preS1 domain of the L protein. Interestingly, a previously uncharacterised anti-S MAb, 6B1, specific for a conformation-sensitive epitope in S, recognised S and M proteins, but not L in immunoprecipitation and immunofluorescence assays. These results provide the first biochemical evidence for the existence of important structural differences in the S moiety of L from that in M and S. Such differences have not been predicted in existing models of HBV surface antigen topology. The significance of a difference in the topology or conformation of the S domain of L in comparison with that of HBsAg is discussed.

The intracellular distribution of the HBV proteins expressed in this study was in keeping with previously published data. Recent studies show that amino acid peptides corresponding to regions within L and S bind HBV core in *in vitro* assays. However, to-date these interactions have not been demonstrated in cell culture. In this study, the interaction of the surface antigens with the core protein was investigated. Confocal microscopy analysis showed that the core protein when expressed singly localised throughout the cytoplasm and the nucleus. However, in the presence of the L protein the intracellular distribution of core changed to a tightly defined perinuclear region where L is normally localised, indicating co-localisation of core with the L protein. Furthermore, the core protein also co-localised with a secreted form of L (L_x) protein. In confocal microscopy assays, the L (or L_x) protein co-localised with core was readily detected by three out of four of our anti-L MAbs. However, one MAb, RC28, failed to recognise L co-localised with core. This indicated that the amino acid residues in the epitope of preS1 recognised by MAb RC28 may play a critical role in L-core interaction. Alternatively, the failure of MAb RC28 to recognise L bound to core may be due to conformational changes in the preS1 domain of L induced by the interaction. In contrast with L (and L_x), the M and S proteins failed to affect the cellular distribution of core. The failure of core to co-localise with M or S in the confocal microscopy assay is not consistent with the published *in vitro* binding data. It is likely that L is fulfilling a scaffolding role in the virion morphogenesis process, where there is a small contribution to the L-core binding from the S domain of L. It is furthermore likely that S is unable to bind sufficiently strongly to the core to

facilitate an intracellular redistribution, pointing to a minor role, if any, of S in the morphogenesis process. Taken together, this data adds considerably to the existing body of literature, and enhances our understanding of the virion morphogenesis process.

The HBV L protein has been implicated in binding via its preS1 domain to a cell surface receptor. To further understand the mechanism of the attachment of the L protein to cells, the preS1 domain was expressed in bacteria and purified. This protein was investigated for its ability to bind hepatocytes by flow cytometry. A specific and inhibitable binding of the preS1 domain of HBV L protein to HepG2 and H5 cell lines, but not other non-human or non-hepatocyte cell lines, was demonstrated. This indicated that the preS1 domain recognised a human hepatocyte-specific receptor(s). Interestingly, the preS1 domain bound to H5 cells much more efficiently than to HepG2 and the binding was subject to inhibition by the peptide corresponding to amino acid 21-27 of the preS1 domain, which has been implicated in receptor recognition. Thus, the flow cytometry assay developed in this study and the availability of cell lines such as H5 should aid in future studies to identify and clone the receptor(s) for preS1.

Table of contents

	<u>Page</u>
ACKNOWLEDGEMENTS	i
SUMMARY	ii
TABLE OF CONTENTS	v
LIST OF FIGURES AND TABLES	viii
ABBREVIATIONS	x
<u>Chapter 1 Introduction.</u>	1
1.1 Genome organisation.	2
1.2 Polypeptides encoded by HBV.	3
1.2.1 The core and pre-core proteins.	3
1.2.3 The X Protein.	5
1.2.3 The surface antigens.	6
1.2.4 The polymerase.	10
1.3 Virion Morphogenesis.	11
1.4 Existing <i>in vitro</i> systems for the propagation of HBV.	13
1.5 Putative receptors for HBV and mechanisms of uptake.	15
1.5.1 Receptors for L protein.	15
1.5.2 Receptors for the M protein.	18
1.5.3 Receptors for S protein.	18
1.5.4. Receptors for Duck Hepatitis B Virus.	20
1.6 Project aims.	23
<u>Chapter 2 Materials and Methods.</u>	24
Radiochemicals.	24
Solutions.	24
Chemicals and reagents.	24
2.1 Bacterial strains.	25
2.2 Expression and purification of the preS1 domain.	26
2.3 Nucleic acid manipulations.	26
2.4 Electrophoresis of nucleic acids.	27
2.5 Sodium-dodecyl sulphate polyacrylamide gel electrophoresis.	27
2.6 Western blotting.	28
2.7 Immunoprecipitations.	29
2.8 Preparation of samples for Cryo-Electron Microscopy.	30
2.9 Scanning electron microscopy.	31
2.10 Generation of Polyclonal antibodies.	31
2.11 Generation of monoclonal antibodies.	32
2.12 Purification of MAb RC28.	33
2.13 Production of peptides representing the preS1 domain.	34
2.14 Epitope mapping of monoclonal antibodies.	34
2.15 Cell culture.	35
2.16 Purification of vLx.	35
2.17 Generation of the hepatocyte-derived cell lines.	36
2.18 Cloning of HBV structural genes.	36
2.19 Generation of the recombinant vaccinia viruses.	38
2.20 Confocal microscopy.	39
2.21 Fluorescence-Activated Cell Sorting.	40

<u>Chapter 3 Generation and Characterisation of reagents.</u>	42
3.1 Expression and purification of the preS1 domain.	42
3.2 Generation and characterisation of recombinant vaccinia viruses expressing HBV structural proteins.	44
3.2.1 Expression of L, Lx, M, S and core in cells.	44
3.3 Generation and Characterisation of Antisera.	46
3.3.1 Polyclonal Antisera 142 and 143.	46
3.3.2. Monoclonal antibodies.	47
3.3.3. Monoclonal Antibody 6B1.	49
3.3.4. Isotype determination.	50
3.4 Peptide characterisation.	50
3.5. Epitope Mapping of MAbs.	51
3.6 Purification of MAb RC28.	52
3.7 Preparation and Characterisation of Proteins for Ligand-Binding Assays.	53
3.8 Discussion.	54
<u>Chapter 4 Generation and partial characterisation of novel hepatocyte-derived cell lines.</u>	56
4.1 Analysis of novel and established cell lines for expression of hepatocyte-specific proteins.	58
4.1.1. Cytokeratins 8 and 18.	58
4.1.2 Albumin.	58
4.1.3. Alpha-fetoprotein.	59
4.1.4. Alpha (1)-antitrypsin.	59
4.1.5. Apolipoprotein-1a.	60
4.1.2. Annexin V.	61
4.2 Discussion.	62
<u>Chapter 5 Investigations into the structure of the surface antigens of HBV.</u>	65
5.1 Intracellular localisation of HBV surface antigens.	66
5.2 Evaluation of anti-S MAbs for antigen recognition.	67
5.3 Co-expression of L and S.	68
5.4 Analysis of the interactions between L, Lx, M and S by immunoprecipitation.	70
5.5 Discussion.	71
<u>Chapter 6 Investigation of the interaction between HBV core and L proteins.</u>	75
6.1 Intracellular localisation of HBV core protein.	76
6.2 Co-expression of L and core.	76
6.3 Co-expression of Lx and core.	78
6.4 Co-expression of Core with M and S.	79
6.5 Discussion.	79

<u>Chapter 7 Ligand binding assays.</u>	84
7.1. Binding of preS1 domain to hepatocytes.	84
7.2. Binding of HepB3 and Lx protein to hepatocytes.	87
7.3 Discussion.	89
<u>Chapter 8 Conclusions.</u>	91
<u>Appendix 1</u> Antisera	95
<u>Appendix 2</u> Sequence information	96
Bibliography.	98

<u>List of Figures.</u>	<u>Follows page</u>
Figure 1.1. Organisation of the HBV genome.	2
Figure 1.2. Morphology of the virion and sub-viral particles.	3
Figure 1.3. Putative model of spatial arrangement of HBsAg envelope proteins.	3
Figure 2.1. Plasmid constructs used in this study.	38
Figure 3.1. Expression and purification of HBV preS1 domain from <i>E. Coli</i> .	43
Figure 3.2. Verification of the identity of the purified protein as the preS1 domain fusion protein.	43
Figure 3.3. Characterisation of HBV structural antigens.	45
Figure 3.4. Characterisation of HBV structural antigens.	45
Figure 3.5. Characterisation of PABs 142 and 143 by Western immunoblotting.	46
Figure 3.6. Characterisation of the PABs 142 and 143 by Immunoprecipitation.	47
Figure 3.7. Characterisation of the PAB 142 by immunofluorescence.	47
Figure 3.8. Characterisation of PAB143 in immunofluorescence assays.	47
Figure 3.9. Characterisation of MAbs RC9, RC28, RC109 and RC152 by immunoblot.	48
Figure 3.10. Immunoprecipitation of L and Lx by a cocktail of monoclonal antisera.	48
Figure 3.11. Characterisation of MAbs RC9 and RC28 by immunofluorescence.	48
Figure 3.12. Characterisation of MAbs RC 109 and RC152 in immunofluorescence assays.	48
Figure 3.13. Characterisation of MAb 6B1 by Immunoprecipitation of HBsAg.	49
Figure 3.14. Characterisation of MAb 6B1 by immunofluorescence.	49
Figure 3.15. Determination of molecular weights of the purified peptides.	50
Figure 3.16. Epitope mapping of MAbs RC 9, RC28, RC109, RC152 and MAb 18/7 with inhibitory peptides.	51
Figure 3.17 G. Purification of MAb RC28 from serum-free medium.	52
Figure 3.18. Characterisation of proteins used in ligand-binding assays.	53
Figure 4.1 Analysis of expression of cellular markers in COS-7 cells.	62
Figure 4.2 Analysis of expression of cellular markers in HepG2 cells.	62
Figure 4.3 Analysis of expression of cellular markers in H5 cells.	62
Figure 4.4 Analysis of expression of cellular markers in H16 cells.	62
Figure 4.5 Evaluation of novel and established cell lines for the expression of annexin V.	62

Figure 5.1. Characterisation of the intracellular distribution of L protein in HepG2 cells.	66
Figure 5.2. Colocalisation of S and M with intracellular membranes.	66
Figure 5.3 Recognition of HBV surface antigens by MAbs directed against HBsAg.	67
Figure 5.4 Recognition of M and S by MAb 6B1.	68
Figure 5.5 Co-expression of L and S in HepG2 cells.	68
Figure 5.6 Co-expression of L and S in HepG2 cells.	68
Figure 5.7 Co-expression of Lx and S in HepG2 cells.	69
Figure 5.8 Co-expression of L and M in HepG2 cells.	69
Figure 5.9. Co-expression of Lx and M in HepG2 cells.	69
Figure 5.10 MAb 6B1 recognises S but not L or Lx by immunoprecipitation.	70
Figure 6.1 Colocalisation of core and L in HepG2 cells.	76
Figure 6.2 Colocalisation of core in H5 cells expressing core and L.	76
Figure 6.3 Colocalisation of core and L in HeLa cells.	76
Figure 6.4 Intracellular distribution of Core and L in H5 cells.	76
Figure 6.5 Intracellular distribution of Core and L in H5 cells.	76
Figure 6.6 Colocalisation of core and Lx in HepG2 cells.	78
Figure 6.7 Colocalisation of core and Lx in H5 cells.	78
Figure 6.8 Colocalisation of core and Lx in HeLa cells.	78
Figure 6.9 Intracellular distribution of Core and Lx in H5 cells.	78
Figure 6.10. Failure of recognition of L-core with RC28.	78
Figure 6.11 HepG2 cells expressing both core and M.	79
Figure 6.12 HepG2 cells expressing core and vHBsAg.	79
Figure 7.1 HBV preS1 domain binding to HepG2 and BHK cells.	85
Figure 7.2 HBV preS1 domain binding to non-hepatocyte cells.	86
Figure 7.3 Hepagene binding to HepG2, COS-7 and H5 cells.	87
Figure 7.4 Assessment of vLx protein binding to H5 cells.	87
Figure 7.5. Confocal-based assay to assess vLx binding to plasma membranes of HepG2, COS-7 and H5 cells.	88
Figure 7.6. Scanning Electron Microscopy-based assay to assess preS1 domain binding to plasma membranes of COS-7 cells.	88

List of Tables.

Follows page

Table 1. Peptide production, purification and characterisation.	50
Table 2. Summary of results for the expression of markers in novel and established cell lines.	62

Abbreviations

Complementary DNA	cDNA
Deoxyribonucleic acid	DNA
Duck Hepatitis B Virus	DHBV
Dulbecco's Modified Eagle's Medium	DMEM
Endoplasmic Reticulum	ER
Endoplasmic Reticulum-Golgi intermediate compartment	ERGIC
Fetal Calf Serum	FCS
Hepatitis B Virus	HBV
Hepatitis C Virus	HCV
Hepatocellular carcinoma	HCC
Human Immunodeficiency Virus	HIV
Immunoprecipitation	IP
Kilobases	kb
KiloDaltons	kD
Messenger RNA	mRNA
Microgram	ug
Microlitre	uL
Milligram	mg
Millilitre	mL
Molar	M
Nanogram	ng
Open Reading Frame	ORF
Phosphate Buffered Saline	PBS
Polyacrylamide Gel Electrophoresis	PAGE
Polyethylene Glycol	PEG
Polymerase Chain Reaction	PCR
Ribonucleic Acid	RNA
Sodium Dodecyl Sulphate	SDS

Chapter One

Introduction

Human hepatitis B virus (HBV) is the prototypic member of the family *Hepadnaviridae*, which includes avian, primate and rodent hepatitis viruses. All hepadnaviruses share the property of restricted host range, a strong, but not exclusive, tropism for hepatocytes, and the ability to cause liver damage. HBV is a major human pathogen causing a chronic inflammatory liver disease often leading to the development of hepatocellular carcinoma (HCC). The clinical significance of HBV is easily demonstrated by the fact that more than 250 million people throughout the world are chronically infected. The portion of the population that is infected with HBV is exposed to a risk of developing HCC that is 200 times that seen in the uninfected population (Milich *et al.*, 1994). Thus, HCC is one of the most frequently occurring cancers, with peak incidence where HBV infection is endemic. The overall risk of HCC increases with age: Asian patients have an average age of 50, whereas African patients have a shorter life expectancy, due to the higher incidence of HBV carriers in Africa, compounded with other factors such as the presence of aflatoxins in poorly preserved foodstuffs (Milich *et al.*, 1994). Animal models have given useful data on the development of HCC in populations infected with Woodchuck hepatitis virus (WHV), Duck hepatitis B virus (DHBV) and Ground Squirrel hepatitis virus (GSHV). The woodchuck data reported a risk of 100% for development of HCC within three years of WHV infection, and data from ground squirrels has given a risk of 7% for HCC development. Human data has shown that in 80-90% of cases of HCC, HBV DNA is capable of insertion into the host chromosomal DNA (Chen *et al.*, 1986) and is found in the liver tissue of patients (Dejean and de The, 1990). The ability of HBV to integrate its DNA into the host chromosomes is an important factor in the disease pathogenesis. It is not likely, however, that HBV is acutely transforming, due to the large lapse in time between infection and HCC.

1.1 Genome organisation

HBV has a relaxed circular partially double stranded DNA genome of approximately 3.2 kb (Fig. 1.1). The HBV genome consists of a complete long strand (termed the minus strand) of constant length with a free 3' terminus and a 5' terminus linked

covalently to a small protein (TP). The short strand (positive strand) of DNA is incomplete and heterogeneous in length, varying between 15-60% of the length of the long strand (Fig. 1). The 5' ends of both S and L strands are base paired, assuring the relaxed circular form of the genome. There are also 11-base pair direct repeats (5'TTCACCTCTGC) at the 5' ends, known as DR1 and DR2, which serve as a template for the synthesis of pregenomic RNA (Bartenschlager and Schaller, 1993). Important differences exist between the hepadnaviruses infecting different species. In comparison with the HBV, the avian hepadnaviruses possess no X gene, and no preS2 gene. Primate hepadnaviruses have been isolated and found to share similar genomic organisation with HBV (Lanford *et al.*, 1998).

The HBV replication cycle is poorly understood due to the lack of a suitable *in-vitro* culture system for examining the viral replication. However, some major steps have been characterised and these are briefly summarised. Following infection, the HBV genome is transported to the nucleus and converted to covalently closed circular (CCC) DNA to yield a double-stranded genome which serves as a template for transcription by the host cell RNA polymerase II. Transcription of the template gives rise to pregenomic mRNA and three sub-genomic mRNAs. The 3.5 kB pregenomic mRNA is produced with redundant ends and is used for the translation of the core protein and polymerase enzyme. Following transport of the pre-genomic mRNA and translation in the cytoplasm, selective encapsidation of the RNA into the nucleocapsid ensues, along with encapsidation of RNA polymerase. In the immature capsid, the 3.5 kB mRNA is reverse transcribed, to yield the minus strand. The RNA is degraded and the DNA strand is replicated, producing the second, shorter DNA strand. Early in the infection cycle, the cellular burden of viral DNA is amplified following the transportation of the mature nucleocapsid to the nucleus in order for replication to repeat. Viral surface proteins are produced at a later stage of the infection process, where subgenomic mRNAs are produced and translated. Nucleocapsids containing DNA genomes then acquire their outer envelope, probably by budding into the endoplasmic reticulum (ER) in areas where transmembrane HBsAg are inserted. The resulting Dane particles are then transported from the cell by normal pathways of vesicular transport. The particles are assembled and released without cell lysis, with no evidence of injury to host cells (Bruss *et al.*, 1996a; Yen, 1993).

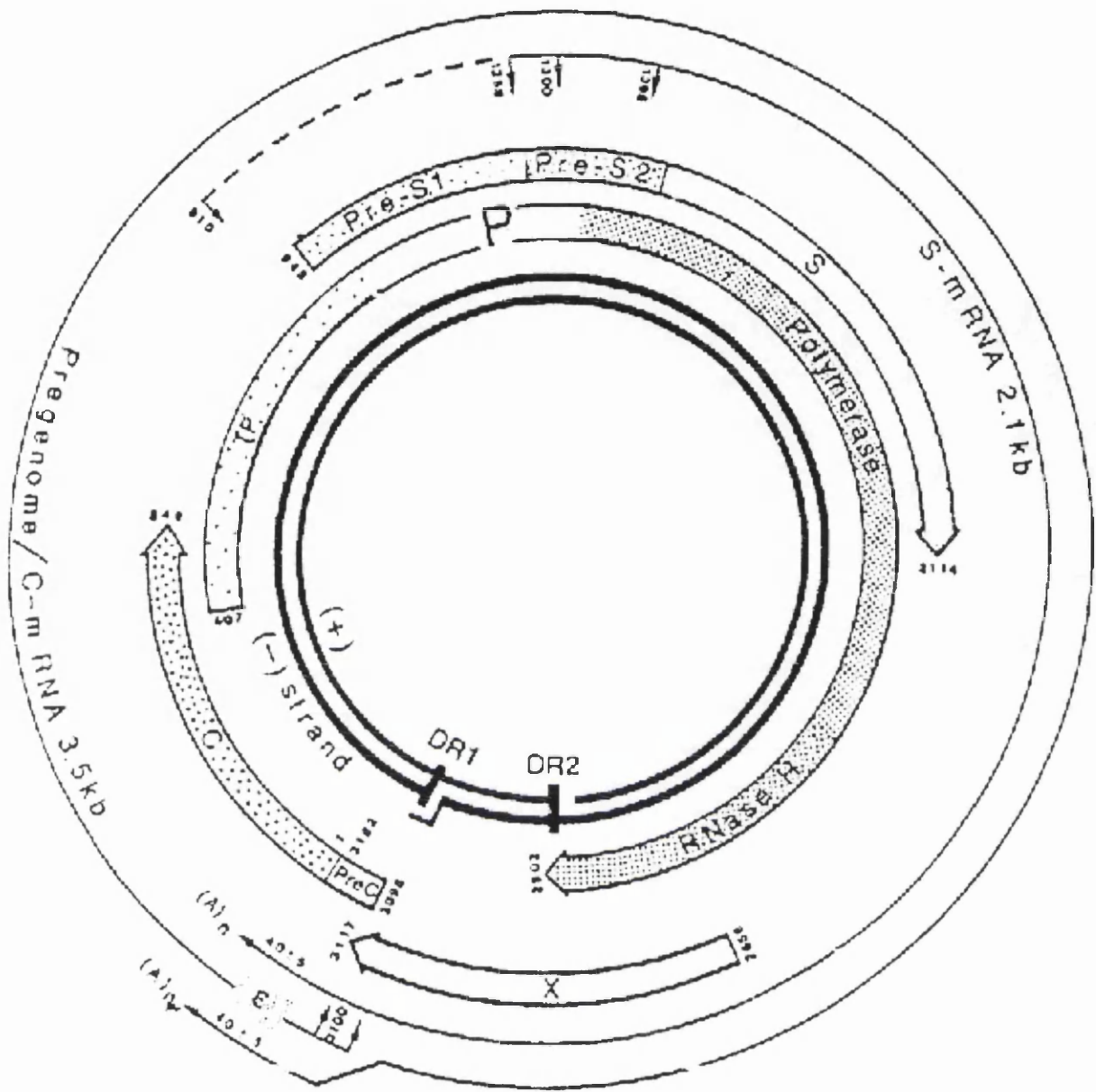


Figure 1.1 Organisation of the HBV genome.

The physical, genetic and transcriptional map of HBV genome. The inner circles represent the viral DNA genome. The terminal redundancy is at the 5' end of the minus strand. The open reading frames are depicted as open arrows. The Pre-S1, Pre-S2 and S regions are for the HBsAg. TP is the terminal protein, followed by the polymerase and RNase H. The X is the transcribed region for the HBx protein, and the Pre-Core and C denote the Precore and Core protein, respectively. DR1 and DR2 are the direct repeats. The encapsidation signal is shown as ϵ (Bartenschlager & Schaller, 1993).

There are two enhancers in HBV that are capable of upregulating transcription. The first enhancer (EnI) is capable of upregulating all four promoters, as shown by studies using plasmids or recircularised genomic DNA, by up to two orders of magnitude. Certain transcription factors found in hepatocytes (e.g. c/EBP, and another factor of unknown identity called HBLF) appear to bind to EnI (Chen *et al.*, 1994; Garcia, *et.al*, 1993). A second enhancer (EnII) has the effect of upregulating the S promoter by approximately one order of magnitude. Identification of multiple transcription factors, HLF, FTF, HNF3 and E4BP4 binding to and controlling hepatitis B virus enhancer II has enhanced our understanding of the control of replication of HBV (Ishida *et al.*, 2000; Li *et al.*, 1995). A clearer understanding of the cellular factors that bind to the enhancers and influence the activity of the enhancer elements of HBV is likely to be of great importance in the delineation of the replicative mechanisms of HBV in the infected patient.

1.2 Polypeptides encoded by HBV

1.2.1 The core and pre-core proteins

Four promoters can be found in the HBV genome, giving rise to four major transcripts (see Fig. 1.1.) The core (C) promoter generates two transcripts, one of which is translated into a secreted protein (the misnamed precore protein, HBeAg) and one which generates the core protein (the nucleocapsid protein, HBcAg). The latter transcript also serves as a template for the translation of the polymerase protein, and as the pregenomic RNA that is packaged, reverse-transcribed and degraded. Thus, all the nucleocapsid components are the product of one RNA species (Yen, 1993). In order to produce these two transcripts from the core ORF, the elongating RNA polymerase II complex must ignore the polyadenylation signal once, but not the second time. The mechanism by which the polyadenylation signal is first ignored is not yet clear.

The hepatitis B virus core antigen (HBcAg) is a 21 kDa phosphoprotein of 183 or 185 residues, depending on subtype, that is capable of self-assembly and forms the capsid that contains the nucleic acids and polymerase protein of HBV. The core particle has been structurally resolved and has been shown to exist in two species, one species exhibiting a triangulation number of T=3 (with 180 copies of HBcAg) the other

Hepatitis B Virus

Hepadnaviridae

HBsAg Particles

HBV-subviral

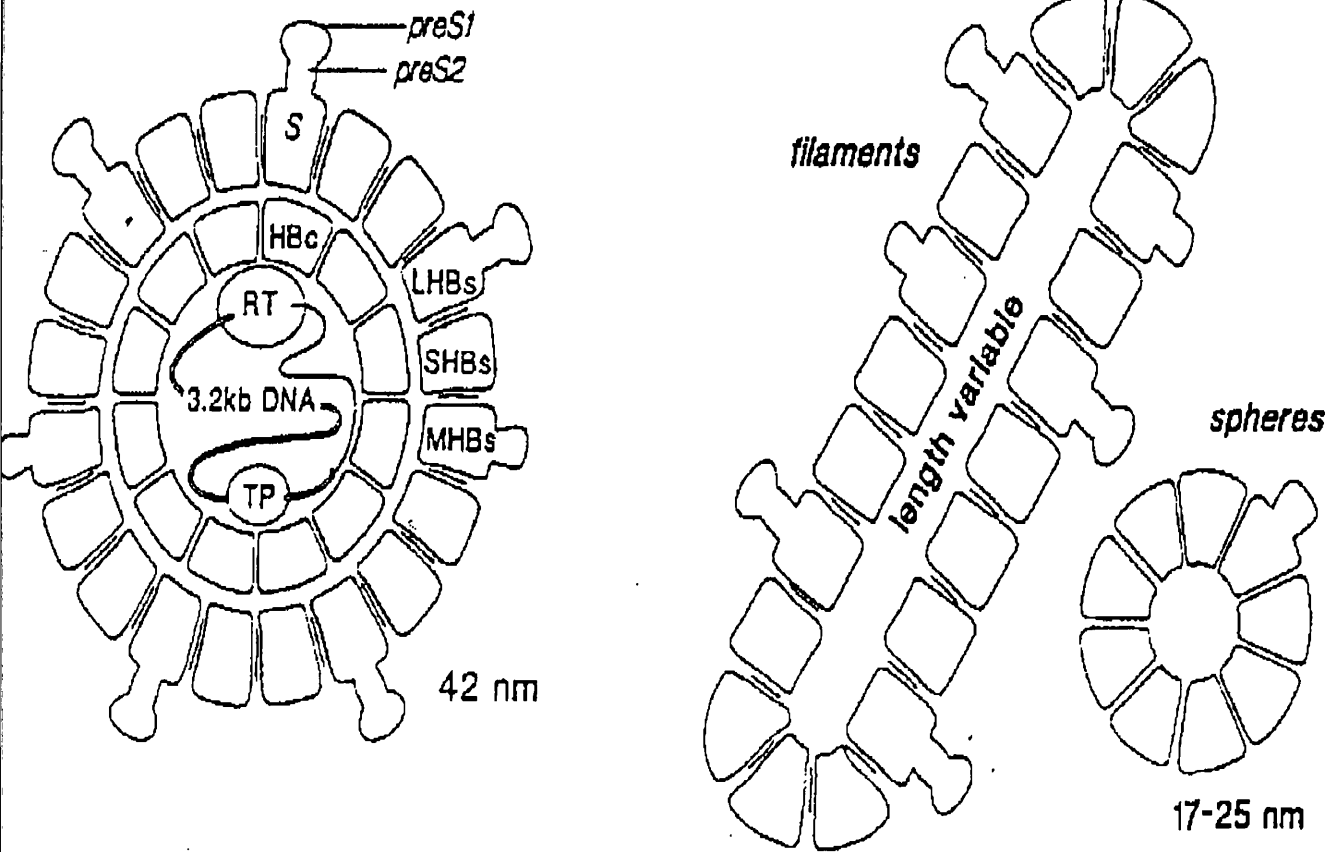


Figure 1.2 Morphology of the virion and sub-viral particles.

The surface antigens are visible on the virion as LHBs (large HBV surface antigen) MHBs and SHBs are medium and small surface antigens, respectively. The core protein is present only in the virion. The sub-viral particles are abundant in patient serum and are composed chiefly of HBsAgs with no other components (Gerlich *et al.*, 1993b). The filaments can be as long as 200 nm.

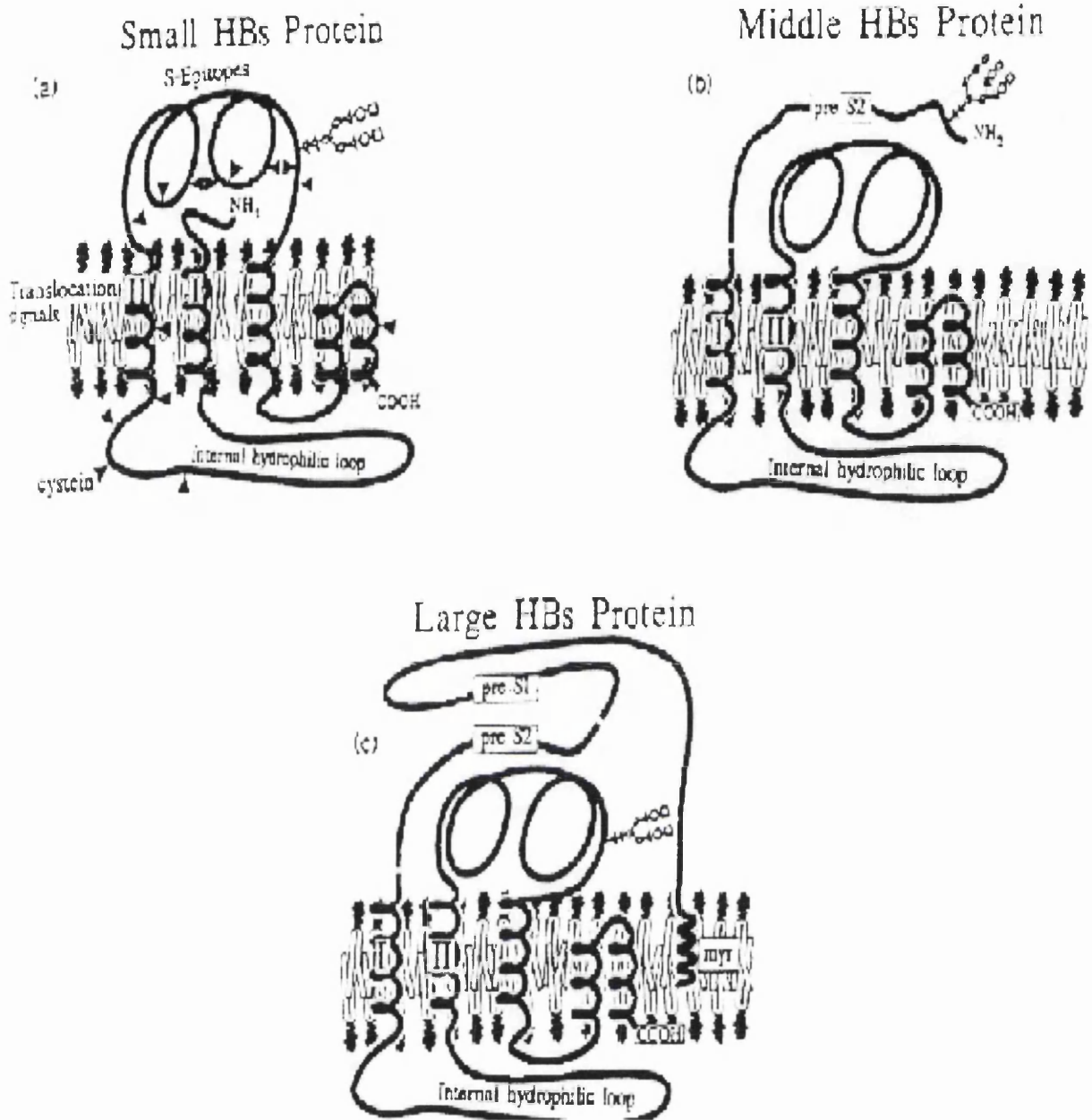


Figure 1.3 Putative model of spatial arrangement of HBsAg envelope proteins.

The nature of the conformation of the proteins is apparent, and the transmembrane regions of the S protein are clearly shown. There are clear differences between the proposed structures of the S protein and the S domain of L protein. The rearrangement of the transmembrane regions at signal sequences I and II is shown with a comparison between S and L (from Gerlich *et. al.*, 1993).

species exhibiting T=4 (240 copies) (Crowther *et al.*, 1994). More recent work has shown, by cryoelectron microscopy, the structure of the core particle to a resolution of 7.5 Angstroms (Conway *et al.*, 1998; Zlotnick *et al.*, 1997). The core protein is known to dimerise and form the subunit component of the core particle. The crystal structure of the core particle has become available (Wynne *et al.*, 1999), showing the assembly of the core homodimers at a resolution of 3.3 Angstroms.

The core protein has been the subject of much study in order to delineate the mechanisms involved in encapsidation and virion morphogenesis. The effect of N-terminal extensions on the behaviour of the core protein was investigated (Hui *et al.*, 1999) and it was shown that an extra 23 amino acids including a polyhistidine tag still enabled nucleocapsid assembly, but abrogated nucleocapsid envelopment. It is feasible that the additional N-terminal residues are interfering with the surface antigen binding residues on the tip of the core spike (residues 78-82). The 149 C-terminal residues of core are capable of self-assembly into nucleocapsids (Nassal, 1992b). The residues 150-183 are involved in binding nucleic acids and are rich in arginine residues (Nassal, 1992a). Furthermore, a C-terminal motif of SPRRR (Ser-Pro-Arg-Arg-Arg), while allowing assembly has been shown to be important in the preservation of competence for replication (Hui *et al.*, 1999).

Structural studies have shown by peptide-difference mapping that the N-terminus of the core protein is visible by cryoelectron microscopy. The incorporation of an octapeptide at the N-terminus enabled the location of the N-terminus at the side of the spike, as the spike protrudes from the circumference of the spherical particle (Conway *et al.*, 1998). The ability of core to assemble and tolerate significant insertions in the region of residues 78-82 has been exploited in efforts to design epitope delivery systems of potentially therapeutic value (Chambers *et al.*, 1996).

The pre-core antigen (HBeAg) shares 149 residues involved in assembly of the core protein, but has an N-terminal extension of ten residues, which form the product from the propeptide which contains an extra 29 N-terminal residues. The pre-core protein is secreted from the cell, in marked contrast to core, and is in an unassembled form. The difference in the states of assembly between the core and pre-core is probably due to

disulphide bonding of the residue cys-7 with cys61 (Nassal and Rieger, 1993). The pre-core protein has no apparent function but affords clinicians with a diagnostic tool.

1.2.3 The X Protein

The X protein (HBxAg) has not been thoroughly investigated yet, and its function remains largely unclear although it is believed to be a viral transactivating protein. The X protein is approximately 17 kDa in size and shares no topological features with other HBV proteins. In cultured cells, the X protein has been shown to exhibit transactivational behaviour on not only HBV promoters, but also class I MHC promoters, the c-myc promoter and the SV40 enhancer/early promoter (Su and Yee, 1992). The X protein has been shown to be essential for the establishment of HBV infection *in vivo* but not for production of virions from cultured cells (Blum *et al.*, 1992). The intracellular degradation of X in infected cells has been shown to be rapid (Hu *et al.*, 1999). Furthermore, it has been shown that X targets the proteasome complex and this represents a possible mechanism by which non-lysosomal protein degradation can be retarded in infected cells (Hu *et al.*, 1999), thus, the X protein may attenuate the proteolytic processes employed by the host cell in the production of viral proteins. Clearly, there remains much to be learnt about the relevance and function of X protein in hepadnaviral infections.

The X protein is reported to perform many other functions including protein kinase activation (Wu *et al.*, 1990), nucleotide diphosphate kinase activity (De-Medina and Shaul, 1994), and ATPase activity (de-Medina *et al.*, 1994). However, the relevance of any of these functions to *in vivo* activity of the X protein remains unclear. It is interesting to note that the X gene is preserved in chromosomally integrated genomes of HBV, perhaps pointing to a role in establishing chronic infections. The X gene appears to support viral replication by transcriptional activation, it is dispensable, *in vitro*, which may suggest that L can overlap its function, with L protein exerting its transactivational effect early in the infection process, prior to the appearance of X (Hildt *et al.*, 1996). Furthermore, the X protein acts on the infected cells by reducing cell proliferation (Sirma *et al.*, 1999). Mutants of HBx are unable to prevent proliferation of infected hepatocytes, they are associated with increased risk of HCC (Sirma *et al.*, 1999).

The X gene is absent from the avian hepadnaviruses, but there are X genes in other mammalian hepadnaviruses such as WHBV and GSHBV, which further confuses the issues concerning the role of the X gene in HBV. The role of X protein remains unclear and is clearly in need of much study to elucidate its function, if any, in hepadnaviral infections.

1.2.3 The surface antigens

There are three envelope proteins in the HBV: Small (S), medium (M) and large (L) proteins, which constitute three forms of the HBsAg (Fig. 1.2). These three proteins are encoded from the *env* ORF. Upstream from *env* is a TATA box which contains a promoter (PS1) which is responsible for directing the transcription of a 2.4 kB subgenomic mRNA (Fig. 1.1). Full translation of the ORF yields the L or preS1 protein (390 amino acids). The start sites for the M and S proteins are contained in-frame in the ORF. PS2, a second promoter is present in the ORF but has no TATA box and directs the transcription of 2.1 kB mRNAs. The 2.1 kB mRNAs possess heterogeneous 5' ends. At the 120th codon (or the 109th depending on subtype) on the slightly longer transcript is an AUG which is used for the production of the M protein (281 amino acids). Some transcripts have the 5' end downstream of this AUG, so the protein S (226 amino acids) is expressed. This S-domain is a polypeptide of 226 amino acids. Close to the N-terminus of the S protein is a signal sequence that inserts into the endoplasmic reticulum (ER) and causes translocation of downstream sequences. The signal sequence has a hydrophobic region at amino acids 8-22, and models (see Fig. 1.3) have predicted this region to be embedded in the membrane because a second signal sequence is found and this is also hydrophobic at amino acids 80-98 (Bruss *et al.*, 1996a). The hydrophilic regions of the S protein remain cytoplasmic but a large proportion of the protein is inserted into the ER. A hydrophilic region is presented at the surface of the virion, and this is presumably stabilised by the disulphide bridges that are present in abundance in the S protein. Posttranslational modification of the S protein is apparent, but this is uniform with respect to all forms of HBsAg. The S protein is only partially N-glycosylated at the Asn 146, thus giving rise to two bands during sodium dodecyl sulphate polyacrylamide gel electrophoresis (SDS-PAGE) corresponding to a protein at 24 kDa and a glycoprotein at 27 kDa. Further studies are necessary in order to obtain a clearer picture concerning the structure and functions of the S protein. The abundance

of cysteine residues in the S protein leads to disulphide bridging: 4 cysteine residues are present in the cytosolic loop, 1 in signal II, 8 in the luminal loop and 1 at the C-terminal (Gerlich, *et.al.*, 1993). The effects of the disulphide bridging on the tertiary structure of the S protein can be seen in the proposed model in Fig. 1.3.

The preS2 domain is 55 amino acids long, and is located upstream of the S protein, forming the M protein. The pre-S2 region of the M protein is presented outside the mature virion (Gerlich, *et. al*, 1993) or in the lumen of the ER (Bruss *et al.*, 1996a). The glycosylated form of M protein migrates as a 34 kDa band in SDS-PAGE. The partial resolution of the structure of the preS2 domain has been undertaken, and this has been examined as a fusion protein with the maltose-binding protein. The residues 14-21 of the preS2 domain contain a B-cell stimulating epitope (Fei *et al.*, 1995). The structure of some regions of the preS2 domain has been investigated (Saul *et al.*, 1997). The M protein has been found to be localised within the ER upon expression in mammalian cells (Hildt *et al.*, 1993), but the function of M in the viral life cycle remains largely enigmatic (Le Seyec *et al.*, 1998).

The preS1 domain has been shown to contain no signal sequences or hydrophobic regions, but the anchorage and translocation of the L protein into the ER is achieved by the signal sequences in the S domain (Gerlich, *et. al*, 1993). The potential glycosylation site in the preS1 domain of L is not used, even though some models suggests its use (Gerlich, *et. al*, 1993). The L protein is myristilated at gly2, and this fatty acid moiety has a profound effect on the *in vitro* infectivity of the virion (Bruss *et al.*, 1996b). The new model of the L protein conformation suggests that half of the preS1 domains are located in the inside of viral particles, interacting with HBcAg and providing a scaffolding function. The remaining proportion of the preS1 are exposed at the surface of the virion (Bruss *et al.*, 1996a). The dual topology of the L protein is a phenomenon that sets a precedent for viral proteins, and represents economical use of the genome for coding sufficient molecules for function with few genes.

The distribution of the surface proteins in the virion and in the sub-viral particles is of great interest and the subject of much study. The subviral particle of about 20 nm (HBsAg) is the most common serum particle and has around 100 surface molecules, of which, two or less are L protein (Fig. 1.2). The M protein is equally distributed

throughout all the forms of particle and is purported to compose 5% of the particles. The L protein is more abundant in the mature virion and the filamentous particle in comparison with the spherical subviral particles. The M protein is not necessary for complete virion formation or virus infectivity, but the S and L proteins are necessary for virion formation and infectivity (Ganem, 1991).

There are several features apparent in the sequence of the L protein in Fig. 1.3 (*adw* subtype). The preS1 domain is contained in the amino acids 1-108, and in the preS1 domain is a sequence 19-23 against which an antibody, MAb 18/7, has been raised (Gerlich, *et. al*, 1993) and this has aided many studies of the surface antigens (Germaschewski and Murray, 1995). The pre-S1 domain carries a sequence of amino acids from residues 21-47 which binds or interacts with a possible receptor on the surface of hepatocytes (Gerlich, *et. al*, 1993). Many studies have implicated various regions of the L protein in attachment to various cell surface components in efforts to determine the receptor or receptors for HBV.

Two protease cleavage sites are found near the start of the S domain: a V8-sensitive site at residue 165 and a chymotrypsin-sensitive site at residue 179. There is a potentially fusogenic peptide sequence at 169-181 and it has been suggested that this region is involved in the fusing of the viral and cellular membranes during the infection process (Lu, *et. al.*, 1996; Rodriguez-Crespo *et al.*, 1999). There are five possible sites for N-linked glycosylation on the L protein at positions 4, 112, 166, 222 and 309. It is unclear whether all the potential sites are glycosylated but it is known that there is at least some degree of glycosylation (Gerlich, *et. al*, 1993).

There are different serotypes of HBV, determined by genetic variability at several positions on S. The group specific determinant, *a*, is present in all S material, along with two sets of usually mutually exclusive determinants, *d* or *y* and *w* or *r*. The *w* determinant has been shown to have several variants, thereby widening the pool of variants of the HBV. Subtypes *ayw*, *ayr*, *adr*, *adw2* etc. are occasionally found in patients. The different subtypes are not known to have any biochemical, clinical or physiological differences attributable them, but they are useful markers for epidemiological studies.

Recent data have uncovered aspects of the functions of the L protein that implicate it in a number of activities besides the putative receptor-binding role. The L protein has been implicated as a transcriptional activator (Hildt *et al.*, 1996). The L protein was investigated for transactivational activity after reports showed that the preS2 region of the M protein was sufficient for generation of a transcriptional activator function, providing evidence that the preS2 domain of both L and M proteins is capable of *in vitro* transactivation (Hildt *et al.*, 1996). A difference in the localisation of the preS2 region was shown to be important for the interaction of the M protein with the cytosolic binding partners. In the M protein, the N-terminal region of the M protein is oriented towards the lumen of the ER, whereas the transcriptionally active M protein has the N-terminus facing the cytoplasm. The authors then reasoned that the L protein might exhibit similar behaviour if the preS2 region was oriented in the direction of the cytoplasm. In cotransfection assays into HepG2 cells it was shown that the L protein elevated the level of the reporter CAT expression by 6 to 7-fold in the presence of M and S (Hildt, *et al.*, 1993; Hildt *et al.*, 1996). The minimal promoters for the NF- κ B and AP-1 genes were also activated by the presence of L protein.

The transcriptional activation ability of the L protein is in turn mediated by c-Raf-1 kinase. The importance of the new information in this study is that the overproduction of L protein is capable of activating several kinase enzymes and activation of these enzymes might contribute to the development of HCC (Hildt and Hofschneider, 1998). Thus, from information gathered so far it seems that in addition to the structural role, the L protein is involved in transcriptional activation leading to changes in host cell gene expression and possibly enhancement of viral replication.

The glycosylation pattern of the HBV surface proteins is typical of other serum proteins produced in the liver. Mass spectra obtained by Liquid Secondary Ion Mass Spectroscopy (LSIMS) have shown that the oligosaccharide structures on the S appear to mimic those found on glycoproteins such as plasma fibronectin, a serum glycoprotein produced by the liver (Gillececastro *et al.*, 1987). It is not surprising that the oligosaccharide residues are similar, as the viral proteins are produced and glycosylated in the liver before release. The relevance of the oligosaccharides to the adsorption of the virus to the target cell is not clear. It is reasonable to assume that if the oligosaccharides were involved in cell attachment, then this process is unlikely to

be restricted to hepatocytes, as many cells endocytose the products of the liver. The specificity of HBV for hepatocytes and very few other types of cells suggest that the oligosaccharides are not likely to be involved in receptor binding.

1.2.4 The polymerase

The polymerase protein of HBV is known to have three functions: DNA-dependent DNA polymerase (DDDP), RNA-dependent DNA polymerase (RDDP) and RNase H. These activities of HBV polymerase are essential for viral replication. HBV polymerase has been successfully expressed in *E. coli* as a fusion protein in frame with maltose-binding protein (Jeong *et al.*, 1996). A protein of 134 kDa was obtained, and was proteolytically cleaved into approximately 73 kDa of active fragment by proteinase K. Two activities of the polymerase were investigated and showed optima under conditions of 1 mM (DDDP) or 0.25 mM (RDDP) of MnCl₂, 400 mM KCl, 37° C (DDDP) or 24° C (RDDP), and pH 7.0-7.7.

The HBV RNase H domain of HBV polymerase has been expressed as a maltose-binding protein-RNase H fusion protein (MBP-RNase H) (Lee *et al.*, 1997). The MBP-RNase H fusion protein (43 kDa MBP plus 17 kDa HBV RNase H domain) was proved to be RNase H by *in vitro* activity assays, inhibitor studies, and mutagenesis. The HBV RNase H domain represented the optimal RNase H activity in the presence of either 8 mM MgCl₂ or 16 mM MnCl₂, with the pH optimum between 7.7 and 8.2. Mutation of highly conserved amino acids in the HBV RNase H domain diminished the RNase H activity. These authors suggest that the RNase H activity is separable from viral HBV polymerase enzymatic activities.

When polymerase is expressed in *Xenopus* oocytes upon injection of polymerase RNA (RT RNA), the polymerase assembles into a higher molecular weight complex with the characteristics of a ribonuclear protein (RNP) complex (Seifer and Standring, 1995). The authors used results from *in vitro* RNA competition-binding experiments to suggest that RT RNA is preferentially packaged into this complex even though it lacks the viral encapsidation signal, epsilon, and viral nucleocapsid. The authors speculate that HBV RNP complexes containing polymerase and viral RNA may play

a role in viral nucleocapsid assembly as the initial stages of virion morphogenesis, and may help to segregate HBV reverse transcription from the cellular environment.

A comprehensive understanding of the properties of the polymerase protein has been hampered by the inability of workers to propagate the virus in tissue culture. Thus, the advent of an *in vitro* propagation system for HBV should facilitate the understanding of the functions of the viral proteins, their relevance to the life cycle, and possibly the identification of suitable targets for therapy.

1.3 Virion Morphogenesis

Many processes are required to facilitate hepadnaviral morphogenesis. The association of the viral pregenomic RNA with the C-terminus (residues 150-183) of the core protein is the means by which the viral genome is encapsidated and held for reverse transcription by the polymerase enzyme (Zlotnick *et al.*, 1997).

Existing models suggest the core and surface antigens associate as the assembled core passes into the lumen of the ER and obtains an envelope of the surface antigens (Bruss and Ganem, 1991; Bruss and Vieluf, 1995). The mechanism of envelopment of the nucleocapsid by the surface antigens has been the subject of much study. Numerous authors using different methods showed the demonstration of the scaffolding function of the L protein. The existence of an interaction between L and core was shown by the use of a random hexapeptide display library to identify the residues involved in binding the core protein (Dyson and Murray, 1995). Binding of the core particle to the L protein implies that the function of the cytoplasmically disposed loop of the L protein is a scaffolding function i.e. is responsible for associating the core particle with the envelope. The existence of a topological change in the L protein bound to core has been documented (Ostapchuk, *et.al.*, 1994). The association of the L protein with the core particle has been studied by electron microscopy and has given useful information regarding the site of the interaction of the core and the L protein (Bottcher *et al.*, 1998). The site of interaction of L and core has been identified as the tip of the core spike corresponding to amino acids 78-82 on the core protein. Furthermore, critical residues involved in the binding of L to core have been identified in the region between Arg 103 and Ser 124. The N-terminal 5 residues of the preS2 domain of L have been implicated in the morphogenetic process

(Le Seyec *et al.*, 1998). These authors found that the deletion of the N-terminal 5 residues did not support viral morphogenesis, however it remains unclear that these residues are absolutely required for assembly.

There has been shown a complex interaction between L and core using synthetic peptides. The association of L and core has been suggested to be mediated by two interaction sites on the L protein: one site on the preS1 domain, and one site on the S domain (Poisson *et al.*, 1997; Tan, *et.al.*, 1999). Furthermore, these authors suggest a synergistic interaction with the two binding sites forming a strong interaction with the core protein. However, it remains unclear whether the presence of S alone is sufficient to recruit the core protein to the ER for encapsidation. It has not been shown in hepatocytes whether or not the relatively weak S-core bond is sufficiently strong to perform the scaffolding process, and allow the envelopment of the core particle with S in the absence of L.

The intracellular distribution of the core and precore proteins in the liver of patients with chronic HBV infections has been the subject of much study. Immunocytochemical studies have shown infected liver tissue cells expressing core antigen in the nucleus, and the pre-core protein was found to be distributed throughout the cytoplasm (Mondelli *et al.*, 1986). Later work showed that it was a distinct possibility that the embedding protocols used in the sample preparation for immunocytochemistry were responsible for at least partial destruction of antigenicity of core in the cytoplasm of liver cells (Sansonno *et al.*, 1988). The demonstration of core in the cytoplasm of transfected cells has also been achieved (Aiba *et al.*, 1997). These authors show strong cytoplasmic staining from constructs expressing core alone, which contrasts well with the constructs expressing core and pre-core, which lead to a nuclear staining pattern. The intracellular interactions of core protein with the host cell have led to the discovery of an interaction of core (and pre-core) with the extreme C-terminal region of human actin-binding protein (Huang, *et. al.*, 2000).

The intracellular distribution of the surface antigens in infected liver cells has been investigated and has been shown to be variable in different patients (Chu and Liaw, 1992). The differences observed by these authors were between the distribution patterns of L and M proteins, with a mixture of membranous and cytoplasmic

distributions. The examination of the intracellular retention of L protein has yielded useful information regarding the processing and the retention of the mature protein. There has been a clear demonstration of the association of L with p53, a component of the anterograde protein transport pathway, the endoplasmic reticulum-golgi intermediate compartment (ERGIC) (Xu, *et. al.*, 1997). Data from Xu, *et. al.* has shown the formation of intracellular particles composed of L in the RER the ERGIC. The authors suggest that the L protein is retained in the ER and ERGIC by virtue of its interaction with calnexin. Furthermore, the retention of L within the ER has been demonstrated to lead to induction of the S promoter (Xu, *et. al.*, 1997) with the effect of S production leading to secretion of the L and S proteins. The removal of the L protein from the ER by S results in lowering the oxidative stress in the ER, which in turn may prevent damage to the cell due to the accumulation of L (Xu, *et. al.*, 1997). It is possible that the induction of physiological changes within infected host cells due to retention of L is one of the mechanisms of induction of hepatocellular carcinoma, as reasoned by many authors

1.4 Existing *in vitro* systems for the propagation of HBV.

Some attempts have been made to produce a productive infection *in vitro* of cell lines with HBV. However, most of these attempts have proven ineffective. Some researchers have infected human adult primary hepatocytes with HBV by using PEG and DMSO to enhance the entry of the virus. The efficiency of infection of the cell lines was measured by the amount of replicated HBV DNA in the cells. The environmental conditions for the maintenance of susceptibility to infection are stringent and involve incubation with 2% DMSO at the time of infection (Gripon, *et. al.*, 1993). In this case, it is unlikely that the *in vivo* conditions of virus attachment and penetration resemble those used in this tissue culture system. Other researchers have found that the primary hepatocytes isolated from adult humans are competent for infection with HBV as determined by the *de novo* synthesis of viral proteins and the appearance of single-stranded viral DNA (a precursor to the mature virion) (Galle *et al.*, 1994). However, with time, these cells lose the ability to produce the virus, and this is probably due to the loss of certain hepatocyte-specific functions. Moreover, only a fraction of the hepatocytes showed a susceptibility for infection, so this propagation system is far from ideal for use as an *in vitro* source of HBV, or for

studying the early replicative steps of HBV. It has been shown that an established hepatoblastoma cell line, HepG2, is capable of supporting viral replication and virus particle synthesis following transfection with cloned HBV DNA (Sells, *et. al.*, 1987). The authors identified 22 nm particles purported to correspond to S by the use of electron microscopy. Particles similar to Dane particles were also identified. However, as with the primary hepatocytes, this system is inefficient and furthermore, HepG2 cells are resistant to infection by the progeny virus. Other reports have suggested that non-hepatocyte cell lines may be used for propagation of hepadnaviruses (Galun *et al.*, 1992), adding confusion to this difficult field.

Reports of the infection of peripheral blood mononucleocytes (PBMCs) have led to many researchers trying to establish *in vitro* HBV infections in PBMCs, but these have remained unfruitful. (Kock *et al.*, 1996) demonstrated that the association of HBV DNA and RNA with PBMCs, however, only the relaxed circular form (RC DNA) of the DNA was seen, and not the CCC DNA that is the replicative intermediate during active infection. The data presented shows clearly there is CCC DNA present and detectable in the liver of infected patients, but not in PBMCs (Kock *et al.*, 1996). The association of HBV RC DNA with the PBMCs is explainable by adsorption and entry of the virus, but not infection. It is possible that the delivery of the viral genome to the nucleus is not facilitated in PBMCs, or it may be possible that the expression of gene products from the HBV genome is hindered by the lack of liver-specific gene expression factors, resulting in the inability of the HBV genome to replicate or synthesise viral products. However, the association of HBV with PBMCs, even in the absence of indications of active replication, suggests that one or more of the mechanisms involved in viral adsorption and entry are employed, but that productive infection remains to be established. The infection of the peripheral blood cells by HBV remains unclear due to difficulties in discerning the adsorbed virus from infection (Kock *et al.*, 1996).

It is likely that the absence of an efficient propagation system for HBV (and Hepatitis C Virus) is due at least in part to the unavailability of cell lines permissive for active replication by these viruses.

1.5 Putative receptors for HBV and mechanisms of uptake.

1.5.1 Receptors for L protein

The L protein has been found to bind to the asialoglycoprotein receptor (ASGPR) on the surface of hepatocytes (Treichel *et al.*, 1994). The ASGPR is responsible for the endocytosis of N-galactose-containing glycoproteins into the hepatocyte. The ASGPR was isolated from plasma membrane preparations derived from fresh human livers by affinity chromatography and desalting, and bound an ¹²⁵I-labelled asialoglycoprotein (asialoorosmucoid), thus demonstrating the biological activity of the isolated protein. Human hepatoma cell lines, HepG2 and Huh7, were also used to express ASGPR. The techniques used to study the interactions of HBV with ASGPR and the plasma membranes were radioimmunoassay and solid phase enzyme immunoassay. The results of radioimmunoassays in which HBV was incubated with the plasma membranes showed binding of HBV to the membranes in the absence of competing ligands. However, in the presence of the competing ligand asialofetuin, the binding was completely inhibited. The HBV interacted with the ASGPR with and without the presence of the competing ligand, but with the competing ligand the binding was reduced by 90%. Moreover, the binding of HBV to the ASGPR was completely inhibited, in a dose dependent manner, by the addition of an anti-preS1 antibody (MA18/7) (Treichel *et al.*, 1994). Interestingly, addition of an anti-preS2 antibody (Q19/10) had no effect on the binding. The blocking of the HBV interaction by the anti-preS1 antibody indicates that the preS1 region is responsible for the binding of HBV to the ASGPR (Treichel *et al.*, 1994). However, the idea that HBV would bind to ASGPR in the presence of other ligands possessing higher affinities due to their greater degree of glycosylation than the relatively low degree of glycosylation of the HBV preS1 is not compelling. The glycosylation of the preS1 region remains a contentious issue and needs further study. The presence of ASGPR is exclusive to hepatocytes and may lend weight to the idea of organotropism, but the picture is still no clearer because other cell types not expressing the ASGPR, such as peripheral blood lymphocytes, can be infected. Generally, the ASGPR component is no longer considered as a cellular receptor for HBV.

The preS1 domain has been strongly implicated in cellular attachment of the virus. (Neurath *et al.*, 1986) examined areas of the preS1 and preS2 domains and found a

region that was recognised by specifically directed antibodies and anti-HBV serum. In this study, a commercially available S was used in preference to natural HBV particles. The authors state that the preliminary results from using natural HBV particles were very similar to the data obtained from the commercial S. This paper gives a great deal of information regarding the potential binding sites on HBV and has led to important developments over the last decade. Interactions of S with hepatocytes were studied by using HepG2 cells and HBsAg supported on cellulose. The HepG2 cells were found to bind to the HBsAg on the cellulose in the absence of competition, whereas the addition of specific antibodies inhibited the cell binding. The authors then treated the HBsAg-cellulose with pepsin to remove the preS sequences and leave the presumably intact S domain exposed for attachment. However, the removal of the preS domains resulted in no attachment of the HepG2 cells. Thus, it was reasonable to conclude that the S domain alone was devoid of attachment sites for the HepG2 cells. Attachment of the HepG2 cells to the HBsAg was inhibited by preparations of the HepG2 plasma membranes containing crudely purified cell receptor. It was found that three monoclonal antibodies recognising epitopes in the amino acids 12-32, 32-53 and 120-145 of the preS reduced virus attachment to HepG2 cells by 70%, 94% and 40% respectively. These findings led the authors to construct a region corresponding to 21-47 of preS1 that overlapped the 12-32 and 32-53 region. Antibodies to the 21-47 region successfully prevented attachment of the HepG2 cells to the HBsAg. Further evidence that the amino acids region 21-47 of preS1 is involved in cell attachment came when a synthetic peptide corresponding to the 21-47, but not the 12-32 and 120-145, block virus attachment to cells. The results give strong evidence for the existence of a dominant binding site for the HepG2 cells on the preS1 region of the HBV surface protein, and that this site is within the region of preS1 (21-47). Furthermore, the binding site is well mimicked by a synthetic peptide analogous to amino acids 21-47 (Neurath *et al.*, 1986).

The insertion of the N-terminus of the preS1 domain into the membrane is modulated by the attachment of myristic acid at glycine 2 (Bruss *et al.*, 1996b). These authors have shown that the myristylation at Gly 2 is essential for the maintenance of infectivity of HBV *in vivo*. The glycine 2 was changed by a point mutation to alanine, and the DNA was then cotransfected into HepG2 cells. This change to alanine resulted in a loss of *in vitro* infectivity of the progeny virus, but the presentation of the

preS1 domain on the virion surface, and the particle morphology were not adversely affected. It is reasonable to assume that the myristate moiety is responsible for anchorage of the preS1 into the membrane and preserving the presentation of the preS1 domain and allowing the receptor binding region to be properly displayed in order to be infective, as illustrated by the putative conformation (Gerlich, *et al.*, 1993), (see Fig.1.3). The non-myristilated protein was still located on the surface of the virion as demonstrated by immunoprecipitation using anti-preS1 monoclonal antibodies. This evidence gives further support for the role of preS1 in the infection process and strongly implicates the preS1 domain as a receptor protein. However, in the absence of any X-ray crystallographic data to support a model of the structure of the L, M and S proteins, the presentation of these proteins at the virion surface remains uncertain.

More recent data has shown that the amino acids 21-47 of the preS1 domain may not be the only region involved in the binding of HBV to the hepatocyte. An 80 kDa protein (p80) has been found to specifically bind to surface proteins of primary hepatocytes and hepG2 cells (Ryu *et al.*, 2000). Using a pull-down assay, the authors showed that the glutathione-S-transferase-(GST)-preS1 domain fusion protein specifically interacted with a 80 kDa protein present in a biotinylated preparation of plasma membranes. This interaction was completely inhibited by the addition of increasing concentrations of free preS1 on the assay. The specificity of the binding of GST-preS1 to p80 was studied to elucidate the regions of the preS1 domain involved in the binding to p80. Truncation and deletion mutants of the preS1 domain were generated and purified from bacterial cell lysate as GST fusion proteins and used in pull-down assays. Interestingly, two regions of the preS1 domain were identified as critical in the binding of p80 in pull-down experiments; these regions were amino acids 12-20 and 82-90. The ability of HBV particles to bind this protein was shown by immunoprecipitation of p80 from cell lysates, giving good evidence that the *in vitro* interaction between the preS1 domain and p80 represents the interactions *in vivo* interactions with the host cell. A most interesting observation concerning the tissue and species specificity of p80 came from pull-down experiments using extrahepatic tissues such as skin, cervical epithelium, kidney and peripheral blood mononucleocytes: p80 could be pulled down from cell lysates of all those tissues. The inability of the GST-preS1 domain to pull-down p80 from lysates of human

fibroblasts was noted, but furthermore, it was shown that a primary rat hepatocyte culture expressed a cell surface protein of 80 kDa that was bound to the preS1 domain. The possibility that p80 could be Hsc70, a chaperone protein, known to interact with L (Loffler-Mary, *et. al.*, 1997), was dismissed by the use of a monoclonal antibody against Hsc70 failing to recognise p80. Given the hepatotropic nature of HBV whether p80 is a “true” receptor for HBV preS1 is debatable as p80 appears to be widely distributed in human tissues and is also found in other species.

1.5.2 Receptors for the M protein.

The preS2 region of the M protein has been implicated in binding in a number of studies. Most of these studies have focused on the interaction of the polymerised human serum albumin (pHSA) with the preS2 region (Dash, *et. al.*, 1990; Michel *et al.*, 1984). The studies are overshadowed by the assumption that the glutaraldehyde-linked pHSA (G-pHSA) used in the studies is similar to the pHSA found *in vivo*. The preS2 component 120-145 has been shown to contain the epitope for pHSA binding (Dash, *et. al.*, 1990). Dash *et al* have shown that there are two classes of binding site for native pHSA on HepG2 cells, with the sites having equilibrium dissociation constants of 16 ± 9.6 pmol/L and 1019 ± 172 pmol/L. The glutaraldehyde-linked pHSA binding sites were not blocked by the introduction of the monomeric HSA suggesting that there are separate sites for the binding of G-pHSA and HSA. However, the introduction of anti-preS antibodies in competition experiments showed that the antibodies block binding of preS2 peptide and HBV to primary hepatocytes by 40% and 70%, respectively. This is reasonable evidence to suggest that there is involvement of the preS2 region in attachment of HBV to the hepatocyte, but is also evidence to show that the preS2 region is not solely and completely responsible for the initial attachment of the HBV to the hepatocyte. Furthermore, preS2 is not essential for virus infectivity, making it an unlikely candidate for cellular attachment.

1.5.3 Receptors for S protein.

There is evidence for the involvement of the S protein in the attachment of HBV to the hepatocyte (de Bruin *et al.*, 1995; de Bruin *et al.*, 1996; Gong *et al.*, 1996; Hertogs *et al.*, 1994; Hertogs *et al.*, 1993). The authors have shown that S bound to endonexin II (also known as annexin V) present in human liver membrane preparations, and that

the immunisation of rabbits with native or recombinant human liver endonexin II results in the production of antibodies that are reactive with S. The development of antibodies that are anti-idiotypic for S is good evidence for suggesting that there is a receptor-ligand relationship between the S and human liver endonexin II. Rabbit antibodies against rat liver endonexin II which is known to have 90% homology with the human liver endonexin II, did not react with S, thus confirming the specificity of the antibodies produced by the immunisation of the rabbits. The authors excluded the possibility of contamination. The anti-idiotypic antibody was found to react only with S and exhibited no reactivity with preS1 or preS2. The authors further investigated the interaction between S and annexin V and proceeded to generate a rat hepatoblastoma cell line expressing human annexin V which has been shown to be infectable by HBV (Gong *et al.*, 1999).

The S was also found to be able to bind to apolipoprotein H (apo H) *in vitro* (Mehdi *et al.*, 1994). Mature apo H is a protein found on plasma membranes and in serum, and consists of 326 residues. The S was able to bind to the apo H which was in an altered form compared with that which is found in the serum of humans (Mehdi, *et al.*, 1996). It was speculated that the apo H was bound to S, and then bound to the hepatocytes via a specific receptor for the apo H, thus allowing the virus entry into the cell. However, HBV from the sera of patients failed to associate with apo H. Thus, faced with no evidence of S associating with apo H in patient serum, it was not a compelling hypothesis that the apo H receptor was responsible for the uptake of the HBV with the apo H molecule into the hepatocyte.

It has been suggested that S may be important in the entry of the virus after attachment has taken place. The cell line HepG2 was used in investigations of a potential fusogenic region of S. Entry of enveloped viruses often requires fusion of the envelope with the cellular membrane, allowing passage of the viral genome into a suitable compartment of the cell. HBV can attach the HepG2 cell surface via preS1 but is unable to enter the cell line and initiate infection. (Lu, *et al.*, 1996) have shown that protease treatment of the HBV virion has profound effects upon its ability to infect HepG2 cells *in vitro*. Cleavage of the M and L proteins with V8 staphylococcal protease has resulted in exposure of a region of the S protein that is capable of fusing with the host cell membrane. Interestingly, another protease, chymotrypsin, cleaves

the S protein at a site close to the V8 site, but does not induce the presentation of the fusogenic region. The removal of the preS regions was confirmed by the failure of antibodies specific to preS1 and preS2 to bind to the protease treated virions. A conformation-dependent antibody C20/02 was used against the S after protease treatment and this showed no difference in binding to the protease treated virion. Thus, it is reasonable to assume that the conformation of S was not adversely affected by the removal of the preS1 and preS2 regions. Upstream of the potentially fusogenic region is a PEST sequence (Lu *et al.*, 1996). The PEST sequence is a region rich in P, E or D, S and T residues. The appearance of a PEST sequence is commonplace in many proteins that are rapidly degraded within the cell (Lu, *et. al.*, 1996). It seems likely that a fusogenic region is involved in the *in vivo* entry of the virus to the host cell, but this is probably only one step of the entry process, and will come after the initial attachment at the cellular receptor site.

Non-specific, pre-S-independent, binding of HBV sub-viral particles to HepG2 cells after treatment of the particles with proteases has been demonstrated (Lu, *et. al.*, 1996). Treatment of the viral particles with staphylococcal V8 or porcine chymotrypsin resulted in infection of the HepG2 cells. The cleavage sites for staphylococcal V8 and porcine chymotrypsin are close to a potentially fusogenic region of the S domain, therefore the authors propose that the removal of the preS1 and preS2 domains results in an exposed or active fusogenic domain that is necessary for the integration of the viral envelope with the plasma membrane of the host cell. This work has shown that the cleavage of the surface antigens of HBV at the protease sensitive site results in the ability of the virus to infect (Lu, *et. al.*, 1996), therefore indicating that the proteolytic cleavage of the surface antigens is an important process in the natural infection pathway.

1.5.4. Receptors for Duck Hepatitis B Virus.

Some workers have made considerable progress on the elucidation of the entry process of the hepadnaviruses by studying the entry processes of DHBV. There are many advantages to using the Duck as a model for the identification of receptors for the hepadnaviruses (such as availability of primary hepatocytes). Early work on the infection process of DBHV has lead to some interesting observations. The infection

process of DHBV involves the endocytosis of the virus, but this endocytic compartment is not an acidic compartment, and therefore no acid-dependent cleavage of proteins is required in the fusion process of the infection (Kock *et al.*, 1996). The authors used lysosomotropic reagents such as sodium azide and 2-Deoxy-D-glucose to reduce the available energy in the normally acidic lysosome, therefore preventing the formation of acidic conditions. Under these conditions, it was still possible for DHBV to infect the cells. The detection of the DHBV DNA by sensitive RT-PCR allowed efficient determination of infection without gene expression; such gene expression would be disrupted by the use of sodium azide and 2-Deoxy-D-glucose.

Receptor-binding experiments have revealed a 120 kDa protein (p120), able to bind the preS protein, which is only expressed in tissues infectable with DHBV (Li, *et al.*, 1996). The authors used preparations of metabolically labelled primary duck hepatocytes and the GST-preS of DHBV for these assays. The association of p120 with the preS is apparent, but interestingly, the binding of preS truncation mutants to p120 revealed a region at residues 98-102 that were critical for the interaction of preS with p120 (Li, *et al.*, 1996). Contained within the 98-102 region is a motif that was found to be the p120-binding motif: the Phe-Arg-Arg motif. The p120 was shown to be available at the surface of the primary hepatocytes by cell surface labelling with biotin and subsequent pull-down using the GST-preS protein and associated truncation mutants. Pull-down experiments with cell lysates from other tissues showed that only liver, kidney and pancreas cells expressed the p120 that bound the preS. This is in keeping with the known tropism of DHBV (Halpern *et al.*, 1983). Li and co-workers postulate that the 120 kDa protein may represent a candidate for the second receptor for the DHBV, and suggest that this may be involved in the restriction of the host range of DHBV (Li, *et al.*, 1999).

Recently, the primary receptor for DHBV has been identified and characterised by work involving a number of groups. A protein of approximately 170 kDa was found to be responsible for the binding of the large surface antigen of DHBV on primary hepatocytes (Tong, *et al.*, 1995). This work showed that there was a likely receptor candidate for the initial stages of the infection process. Further work revealed the identity of a 180 kDa protein (p180) involved in the plasma membrane binding of DHBV. The identity of the preS-binding protein p180, is carboxypeptidase D (CPD),

a golgi-resident protein that is also present on the plasma membrane in small amounts (Urban *et al.*, 1998). The initiation of infection by DHBV preS was studied and there was found to be a region of 85 residues in the preS of DHBV that are critical for the interaction of preS with CPD (Urban *et al.*, 1998). The authors showed that it was possible to inhibit the infection of primary duck hepatocytes with DHBV by competition with free DHBV preS in a dose-dependent manner. Furthermore it was also possible to inhibit the infection with free HHBV preS in a dose-dependent, manner (Breiner, *et al.*, 1998). Further work demonstrated the inhibition of infection of primary duck hepatocytes with DHBV with soluble CPD (Breiner, *et al.*, 1998). However, the overexpression of CPD in non-permissive cell lines did not lead to permissivity of infection (Breiner, *et al.*, 1998). The functional characterisation of CPD was undertaken and three domains of the CPD were found to be present. The domains A and B of CPD were shown to exhibit carboxypeptidase activity, and the C domain contains the preS-binding site (Eng *et al.*, 1998). The process of attachment of the preS to CPD has been investigated and the association constants of the preS-CPD complex have been determined at $2.2 \times 10^7 \text{ M}^{-1}$ at 37°C (Urban, *et al.*, 1999). The association rate of preS and CPD has been determined at $4.0 \times 10^4 \text{ M}^{-1} \text{ S}^{-1}$, and the dissociation rate has been determined to be $1.9 \times 10^{-3} \text{ S}^{-1}$. These constants and rates indicate that there is a very high affinity of preS to CPD. The DHBV preS region found to be responsible for maximal binding of CPD lies within an 85 residue stretch (corresponding to amino acids 30-115) covering about half of the length of the preS domain of DHBV. The authors showed specific dose-dependent inhibition of binding of DHBV by the addition of preS polypeptides produced in *E. coli*. Internal deletions in the amino acids 30-115 region of the preS domain result in a markedly reduced ability of the polypeptides to inhibit infection of the primary hepatocytes with DHBV. Internal deletions in the preS that were located outside of the 30-115 region had little or no effect on the ability of the preS polypeptide mutant to inhibit infection. The authors then proceeded to establish that the affinity of the recombinant preS polypeptides for CPD is similar to the affinity of the DHBV L protein for CPD (Urban *et al.*, 1998). CPD also demonstrated the ability to bind the preS from HHBV, suggesting that the CPD may be involved as a common component of the avian hepadnavirus-receptor complexes. Homologous CPDs from other species have been identified and cloned and this family of proteins are found to be type I transmembrane

proteins located on internal and plasma membranes (McGwire *et al.*, 1997). An obvious avenue of investigation has been the evaluation of human CPD as a potential HBV receptor, and many researchers have investigated this with none reporting interactions between HBV and human CPD.

Project aims.

The overall aims of this project were; (1) to generate reagents such as MAbs, PAbs, cell lines and recombinant viruses to study the expression of these proteins and provide reagents for further research; (2) investigation of the behaviour and structure of the L and S proteins with novel immunological reagents, in order to obtain further information on the conformational nature of the surface antigens; (3) investigation of the interaction of the surface antigens with the core proteins when expressed intracellularly to delineate the mechanisms of hepadnaviral morphogenesis, and ; (4) to investigate the binding of the preS1 domain to the plasma membranes of hepatocytes and other cells in order to provide new information on the specificity of binding and the host range of HBV.

Chapter 2

MATERIALS AND METHODS

Radiochemicals

³⁵S L-methionine was obtained from Amersham at a specific activity of 10 $\mu\text{Ci}/\mu\text{L}$.

Solutions

PBSA: 170 mM NaCl; 3.4 mM KCl; 10 mM Na₂HPO₄; 1.8 mM KH₂PO₄; pH7.2.

PBSC: PBSA with CaCl₂.2H₂O and MgCl₂.6H₂O at 1g/L.

PBST: PBSA plus 0.05% Tween-20.

FPBS: PBSC; 2% FCS; 0.05% sodium azide.

Glycine-SDS buffer: 14.4 g glycine; 3.75 g Tris in 1 L distilled water.

10X TBE: 1.25 M Tris; 0.4 M boric acid; 27 mM EDTA.

TE: 10 mM Tris-HCl; 1 mM EDTA pH 8.0.

Towbin's buffer: 100 mL methanol; 14.4 g glycine; 3.75 g Tris in 1 L water.

Zweig's buffer: 10% glycerol; 0.1 M Tris-HCl; 0.5% NP-40; 0.5% Na-Deoxycholate; protease inhibitors (Complete protease inhibitors Boehringer Mannheim); in distilled water.

Chemicals and reagents

Laboratory chemicals were purchased from Sigma Chemicals or BDH Chemicals, UK unless otherwise stated.

Amersham Life Science: Rainbow protein markers RPN 756

Beecham Research: ampicillin (Penbritin)

Bio-Rad: ammonium persulphate (APS), acrylamide (27.5%) crosslinker, N,N,N',N', tetramethylethylenediamine (TEMED), coomassie brilliant blue.

Boehringer Mannheim: protease inhibitors (EDTA-free).

Gibco BRL: IPTG

Marvel: dried skim milk

Prolabo: ethanol, glycerol, methanol.

UKC Chemical Laboratories: Citifluor.

2.1 Bacterial strains

The *E.coli* strains DH5 α , TG1 and JM109 were employed for the growth and maintenance of plasmid DNA. The growth medium for these bacteria was LB broth (Lauria-Bertani medium, 10 g NaCl, 10 g Bactopectone, 5 g yeast extract in 1 L water at pH 7.5). The *E.coli* strain M15 carrying the plasmid pREP4 (Invitrogen) was used for the expression of recombinant proteins. For expression, these bacteria were grown in 2YT broth (5 g NaCl, 16 g Bactopectone, 10 g yeast extract in 1 L water at pH 7.5). Agar plates were made in 90 mm diameter dishes with the inclusion of about 25 mL LB-agar (LB broth with 1.5% agar). Antibiotic supplementation was as follows: for Amp^r cultures, 50 μ g/ml, for Kan^r cultures 25 μ g/ml.

For the preparation of electrocompetent *E.coli* cells, 100 mL 2YT broth was inoculated with an overnight culture at a dilution of 1:50 and the bacteria allowed to grow until they reached an OD₆₀₀ of about 0.6. The culture was cooled on ice for 30 minutes and centrifuged at 2500 rpm in a Sorval RT6000B centrifuge for 15 minutes. The supernatant was decanted, and the cells were carefully resuspended in distilled water and recentrifuged. The cells were resuspended in water a further two times and finally the cells were resuspended in 2 mL water containing 10% glycerol, and immediately frozen in liquid nitrogen. The cells were stored in 40 μ L aliquots at -70°C.

Transformation of the electrocompetent cells was done by the addition of 5 μ L of a ligation mixture, or 0.5 μ g of DNA, into the 40 μ L aliquot of freshly thawed cells. The cells were mixed with the DNA for 1 minute on ice, then electroporated in a Bio-Rad electroporation cuvette at 200 Volts and immediately transferred into 1 mL of L broth without antibiotics and incubated with shaking for 1 hour at 37°C. The cells were then plated onto LB agar plates containing the appropriate antibiotics and incubated overnight at 37°C. Individual colonies were picked and analysed for the presence of the plasmid.

2.2 Expression and purification of the preS1 domain.

A single colony of *E.coli* M15 (pREP4) cells harbouring the plasmid pQES1 was inoculated into 10 mL 2YT containing amp/kan and incubated with shaking at 37°C overnight. The 10 mL culture was then added to 500 mL of pre-warmed 2YT broth with amp/kan and incubated with shaking at 37°C until the OD₄₅₀ had reached 0.3. To induce expression IPTG was added to a final concentration of 1 mM and the culture was incubated for a further 3 hours. The bacteria were pelleted at 8,000 r.p.m. in a SORVAL RCB centrifuge for 15 minutes at 4°C and the supernatant decanted. The pellets were resuspended in TN buffer (10 mM Tris-HCl, 150 mM NaCl, pH7.5) and freeze-thawed three times in a dry ice/methanol bath. The bacteria were then lysed with a sonic probe for bursts of 15 seconds with immediate incubation on ice. The resultant cell lysate was pelleted in a SS34 rotor at 15,000 r.p.m. in a SORVAL RCB centrifuge for 30 minutes at 4°C. The supernatant carrying soluble proteins was removed and incubated with Ni-NTA resin (equilibrated in TN buffer) for one hour at 4°C. The slurry was then dispensed into a Bio-Rad 5 cm disposable column and washed with 3 column volumes of TN buffer. The column was then washed with 3 column volumes of TN buffer containing 20 mM imidazole (Sigma) to remove proteins bound non-specifically to the resin. The preS1 protein was eluted from the column with 2 column volumes of TN buffer containing 250 mM imidazole. The eluted protein was dialysed against PBSA at 4°C for three changes in DIALYZE-A-SLIDES (Pierce Warriner) with a molecular weight cut-off of 10 kDa. The dialysed protein was further concentrated by centrifugation at 2,500 r.p.m. for 2 hours at 4°C using an Amicon concentrator with a molecular weight cut-off of 10 kDa in a SORVAL bench top centrifuge. Final protein concentration was determined with the Bio-rad protein determination kit. The protein solutions were aliquoted and stored at -20°C until required.

2.3 Nucleic acid manipulations.

Restriction enzyme digestion of DNA was carried out according to the manufacturers instructions. The buffering systems were either the Boehringer Mannheim system (buffers A, B, H, L, M) or the New England Biolabs buffer system (buffers 1, 2, 3, 4). For diagnostic analysis, the reaction volumes of 20 µL generally contained 1 µg DNA

and 1 unit of the restriction enzyme in 1X buffer. For the isolation of specific fragments, the amount of DNA used in the digestion was about 20 µg.

Blunt ending of DNA containing 5' overhangs was achieved with the incubation of the digestion mixture with dNTPs and 2 units Large Klenow fragment of DNA polymerase I. The blunt ending reaction was left for 30 minutes at 37°C.

The removal of 5' phosphate groups from digested vectors was performed using alkaline phosphatase in order to prevent re-circularisation of the vectors with complementary ends. The addition of 1 unit of calf intestinal phosphatase to the digestion mixture ensured the removal of the phosphate groups. The extraction of nucleic acids from reaction mixtures was done by using the nucleic acid extraction kits (Qiagen) according to the manufacturer's instructions. Ligation of appropriately ended insert and vector DNA fragments was done by incubation of a 5:1 respective ratio of target/vector DNA in a reaction volume of 20 µL with 1X ligation buffer and 2 units of T4 DNA ligase at room temperature overnight.

2.4 Electrophoresis of nucleic acids.

Resolution of nucleic acids was achieved by the use of agarose gels at a concentration of 1% w/v, containing 1 µg/mL ethidium bromide (EtBr). Gels approximately 1 cm thick were poured into the gel moulds and, once set, immersed in 1% TBE buffer with EtBr in the Bio-Rad gel tank system. The DNA samples were mixed in DNA loading buffer to make a final volume of 20 µL. The gels were run at 100 V until the dye front had migrated to the end of the gel. DNA fragments were visualised with a short-wave UV light and images captured by The Imager (Appligene). If required, the band of DNA was retrieved from agarose gels by excision of the band of interest and subsequent purification performed using the Gel Extraction kit (Qiagen) according to the manufacturer's instructions.

2.5 Sodium-dodecyl sulphate polyacrylamide gel electrophoresis (SDS-PAGE).

SDS-PAGE was performed with the Mini-Protean II kits from Bio-Rad. Resolving gels were poured to a height of 5 cm between two glass plates and were overlaid with water until polymerisation was complete. After washing with distilled water, the

resolving gels were overlaid with the stacking gels and left to polymerise with a track marker comb inserted in the top of the gel. Samples for electrophoresis were mixed with final sample buffer (FSB) and boiled for 2 minutes before loading. Gels were run in the holding tank in glycine-SDS buffer at 120 V until the FSB dye reached the bottom of the gel. The resolving gels used in this work were at a concentration of 9%, 10% or 12% acrylamide. TEMED and APS were used as the catalysts for the polymerisation of the acrylamide. The fractionated proteins were visualised by staining with coomassie brilliant blue (Bio-Rad), autoradiography, or Western blotting.

2.6 Western blotting.

Electroelution of proteins from SDS-PAGE gels was done by using the Western Blot kit supplied with the Mini-Protean II kits. The nitrocellulose transfer membranes (Hybond ECL) were obtained from Amersham and were cut to size before transfer. Transfer of proteins from the gels was done in Towbin's Buffer at 90 V for one hour with the inclusion of an icepack in the tank to prevent overheating. Following transfer, the ECL membranes were removed from the tank and quickly immersed in a 90 mm Petri dish containing PBST with 5% milk powder, for blocking of non-specific binding sites, for at least 30 minutes followed by a further incubation with a fresh solution of 5% marvel added for a further 30 minutes. The membranes were then washed three times in PBST to remove the milk powder and were the probed with antisera. Primary antibodies were diluted in PBST/BSA (PBST containing 2% BSA) into a total volume of 5 mL and were added to the membranes with gentle agitation for 60-90 minutes. Residual primary antibodies were washed off with three washes of PBST and the appropriately diluted secondary antibodies added in PBST/BSA for one hour with gentle agitation. Three 15 minute washes with PBST were used to remove residual secondary antibodies, and the membranes were incubated for 2 minutes in a mixture of equal volumes of ECL Enhanced Chemiluminescence reagents (Amersham). The membranes were sandwiched between two sheets of transparent film and the chemiluminescence was detected with Kodak X-OMAT film by exposure to the membranes for varying lengths of time.

2.7 Immunoprecipitations.

Cells were grown in 24-well plates to about 60% confluence, and were then infected with the relevant recombinant vaccinia viruses (rVVs). For radiolabelling of proteins, cells were washed with PBSA at 5 hours post-infection and incubated in methionine-free Eagles Medium containing 50 $\mu\text{Ci/mL}$ ^{35}S -Methionine for 18 hours. After 24h, the culture supernatant was aspirated and clarified at 13,000 r.p.m. in a benchtop centrifuge to remove cellular debris. The clarified supernatant was then transferred to an eppendorf tube, added to an equal volume of Zweig's buffer and stored at -20°C . Cell monolayers were washed three times with PBSA and the cells were dislodged and pelleted by brief centrifugation to pellet the cells. The cells were resuspended in 200 μL of Zweig's buffer and incubated on ice for 30 minutes to allow lysis. The cell lysates were centrifuged at 15,000 r.p.m. in a benchtop centrifuge to pellet the nuclei. The lysates were transferred to fresh tubes and stored at -20°C . The cell lysates were used in 50 μL volumes. To immunoprecipitate proteins, 5 μL of rabbit polyclonal antisera, 50 μL of hybridoma supernatant, or 10 μL of ascites fluid were added to the cell lysates or cell medium. The samples were incubated at 4°C overnight with shaking to form the antigen-antibody complexes. Immune complexes formed with rabbit polyclonal antisera were mixed with 50% slurry of protein-A-Sepharose, equilibrated in Zweig's buffer and incubated for 2 hours at 4°C with shaking. The protein-A-Sepharose was washed three times in Zweig's buffer and once in 0.5 M lithium chloride in 20 mM Tris at pH 7.5. The protein-A-Sepharose was resuspended in 50 μL of final sample buffer and boiled for 2 minutes before loading on SDS-PAGE gels.

For immunoprecipitations using mouse monoclonal antibodies, a bridging antisera, rabbit anti-mouse IgG, was added to the protein-A-Sepharose slurry for 30 minutes at 4°C . The use of the bridging antisera enables efficient recruitment of the mouse IgG molecules which have a lower affinity for protein A in comparison with rabbit IgGs. Unbound bridging antisera was removed by washing and 50 μL of 50% slurry was added to the samples for 2 hours at 4°C . The samples were prepared for SDS-PAGE as described above.

2.8 Preparation of samples for Cryo-Electron Microscopy.

Cells were grown in 6-well plates to about 60% confluence and infected at a m.o.i. of 5 p.f.u. per cell for each rVV. The cells were incubated after infection for 24 hours, washed three times with PBSA and removed from the wells by a rubber policeman. The cells were suspended in 400 μ L of PBSA, placed in Beem Capsules, and centrifuged in a benchtop centrifuge at 1,200 r.p.m. for 4 minutes at room temperature (RT) to pellet the cells. The supernatant was removed from the pellet and 500 μ L of 2.5% glutaraldehyde (EM grade, double distilled, TAAB, Aldermaston, UK) was carefully added to the pellet for fixation of the cells. The fixing pellet was stored at 4°C for at least one day. The Glutaraldehyde was carefully removed and the Beem capsule was filled with a 4% w/v solution of gelatin (TAAB) in PBSA at 37°C. The pellet was stored at 37°C for 3 hours to allow the cells to become permeated with the gelatin, and then the samples were transferred to 4°C overnight to solidify the gelatin. The Beem capsules were sectioned with a razor blade to expose the cell pellet. The pellet was carefully removed from the capsule and the excess gelatin was removed from the cell pellet. The pellet was cut into small blocks of about 1 mm² by hand, and placed in a solution of 2.3 M sucrose for two days at 4°C for cryoprotection. Samples were removed from the sucrose and manipulated on aluminium stubs, then plunge-frozen in liquid nitrogen. The stubs were inserted into the chuck of a microtome and sectioned to give 70 nM sections. The microtome components were constantly cooled with liquid nitrogen throughout the sectioning procedure. The sections were transferred to grids (nickel, copper or gold) and floated in water to remove excess sucrose. The grids were incubated in primary antibody by flotation on a drop of PBSA with the appropriately diluted antibodies for 3 hours at RT. Transferring the grids sequentially to three drops of PBSA washed off the residual primary antibodies. Incubation with the secondary antibodies was done by flotation in a drop of PBSA containing 1:50 dilutions of an appropriate anti-IgG-gold conjugate (Nanoprobes Ltd) for one hour at RT. Sequential transfer to three drops of PBSA washed off the residual secondary antibodies. Following washing, the samples were treated with Nanovan (vanadium acetate, Nanoprobes Ltd) to negatively stain the proteins. The use of Nanovan enables enhanced resolution of proteins by transmission EM and gave clearer results than uranium acetate due to the smaller ionic radius of the vanadium.

The stained samples were placed in a specimen holder and analysed in a JEM 100S electron microscope.

2.9 Scanning electron microscopy.

Cells were plated on glass coverslips in 24-well plates and grown in DMEM at 37°C for three days to reach a confluence of 60-70%. The cells were cooled for one hour to 4°C in DMEM. The cells were labelled with approximately 1 µg of ligand (where applicable) in DMEM for 30 minutes at 4°C, followed by three washes with fresh medium. A mixture of MAbs RC9, RC28 and RC152 was diluted in DMEM and the cells were incubated in this mixture for 30 minutes at 4°C, followed by three washes with fresh medium. Secondary antibody (anti-mouse IgG-Gold conjugate with a 10 nm gold particle) was diluted in DMEM and added to the coverslips for 30 minutes at 4°C. The residual secondary antibodies were washed off with three washes with DMEM and the samples were then fixed by the addition of 2.5% glutaraldehyde (EM grade, double distilled, TAAB, Aldermaston, UK) in PBSA to the wells. The samples were stored at 4°C overnight. The glutaraldehyde was removed, and the cells washed twice with distilled water. The cells were then osmicated by the addition of 1 mL 1% osmium tetroxide in distilled water at RT for one hour. The coverslips were washed and dehydrated in 30%, 50%, 70%, 90% and finally 100% ethanol. In order to ensure complete removal of water from the cells the samples were placed in acetone to displace the ethanol and were then inserted into a critical point drying chamber and the acetone displaced with liquid carbon dioxide, which was then volatilised. The samples were degassed overnight at room temperature. Scanning electron microscopy was performed with a JOEL Scanning Electron Microscope.

2.10 Generation of Polyclonal antibodies.

Two female NZW rabbits (numbers 142 and 143) were used to generate polyclonal antisera against the preS1 domain. Pre-immune serum was taken from these rabbits prior to injection with antigen. This serum was clarified by centrifugation at 1000 RPM in a Beckman RT6000B centrifuge, then aliquotted into 1 mL volumes and stored at -20°C. The two rabbits were injected intramuscularly with 100 µg quantities of purified preS1 domain at 14 day intervals. The first injections were augmented with 50% Freund's complete adjuvant, the subsequent injections were augmented

with incomplete Freund's adjuvant. Test bleeds were taken after five injections of antigen had been completed, and the antibody response to preS1 was assessed by ELISA. Test bleeds from both rabbits showed high antibody titres following five single injections. Serum from rabbit 142 was harvested, whereas rabbit 143 was injected with antigen a further five times, and the plasma then harvested and clarified. The resultant sera were aliquoted and stored at -20°C. Sera from 142 and 143 were assayed for activity in Western blotting, immunofluorescence and immunoprecipitations.

2.11 Generation of monoclonal antibodies.

The Author gratefully acknowledges the guidance and supervision of Dr Susan Graham during the generation of the monoclonal antisera described here.

The inbred strain of BALB/c mice (Harlan Orlac Ltd., Oxon. England) was used. Five Balb/C mice were subcutaneously injected with 20 µg of preS1 domain in 50% Freund's complete adjuvant with a final injection volume of 100 µl. Three weeks after the first injection, subsequent injections were of 20 µg of preS1 in incomplete Freund's adjuvant were administered. This procedure was repeated twice more at two-weekly intervals. Test bleeds were taken from all mice and assayed by ELISA against the antigen to establish the degree of response from the mice. Two mice with the highest titre of antisera against the preS1 domain were selected and boosted with a intraperitoneal injection containing 100 µg of preS1 domain. Seven days after boosting, splenectomies were performed and lymphocytes were removed from the spleen by repeated irrigation in PBSA using a G19 sterile needle (Sherwood Medical). The spleen cells were then pelleted at low speed in a 50 mL centrifuge tube, and a viable count was performed. NSO (ECACC 85110503) murine myeloma cells were used as the fusion partner for the generation of hybridoma cell lines. These cells are non-invasive, non-metastatic, non-secreting, non-light chain-synthesising plasmacytoma cells subcloned from the non-metastatic SP2/0 cell line. They were grown in NSO growth medium and were split 1:2 three days before the fusion to ensure that they were in logarithmic phase growth before each fusion. The SP2/0-derived cells were resuspended from the incubation flask by shaking and pelleted in a 50 mL centrifuge tube. A viable count was performed. The pelleted cells were

resuspended in 1 mL of serum-free medium. The spleen-derived lymphocytes were thoroughly mixed with a suspension of the SP2/0-derived cells in a ratio of 1:5 and incubated at 37°C. The fusion of cells was induced by the drop-wise addition of 1 mL of 50% polyethylene glycol (PEG₁₅₀₀). The mixture was mixed by gentle aspiration. After 1 minute of incubation at 37°C, 1 mL of serum-free medium (SFM, DMEM with no added components) was added over a period of 1 minute. A further 1 mL of SFM was added over a one minute period. A further 2 mL was added over 1 minute and, finally, 4 mL was added over a period of 1 min. The cell suspension was made up to 40 mL with SFM and centrifuged at 1,200 r.p.m. for 10 minutes to fuse the cells. The cells were resuspended and diluted into 100 mL of HAT medium and 200 µL aliquots of the suspension were plated in 96-well tissue culture dishes. The 96-well plates were incubated at 37°C in a 5% CO₂ atmosphere and the wells were periodically examined for hybridoma colony growth. Supernatants from wells containing colonies were tested for anti-preS1 antibody by ELISA. Colonies found to be secreting antibodies were subcultured to 24 well plates. Frozen stocks of antibody-secreting hybridomas were generated from the 24 well plates by resuspension of the colony, followed by dilution of the aspirated colony into 1 mL of HAT medium containing 10% DMSO. The cells were then gradually frozen overnight in cryovials (Sarstedt) at -70°C in a controlled-temperature reduction vessel. Long-term storage of cultures was done in Linde racks cooled with liquid nitrogen. Viable colonies were subcultured to T25 flasks for evaluation of the hybridoma supernatants. Hybridoma supernatants from the T25 flasks were assayed for activity of antibodies in Western blots, immunofluorescence and immunoprecipitation. Cultures found to be positive in any of the above assays were cultured in T175 flasks to harvest the supernatant. The resultant antibody preparations were then isotyped with the use of a Mouse Antibody Isotyping Kit (Sigma Chemical Co.) according to the manufacturer's instructions.

2.12 Purification of MAb RC28.

The hybridoma supernatants from MAbs RC9, RC28, RC109, and RC152 were examined for activity in FACS assays. It was noted that RC28 was active in FACS assays, where the others were not, therefore milligram quantities of RC28 were purified. The culture of RC28 was grown in serum free hybridoma medium (Gibco) in T175 flasks until the cells appeared crenated. The medium was aspirated from the

flasks and clarified by centrifugation at 3,000 r.p.m. in a Sorvall RT6000B benchtop centrifuge for 5 minutes at RT. The clarified supernatant was dialysed against 20 mM sodium phosphate, pH7.0 for four changes. The dialysed supernatant (approximately 900 mL) was filtered through 0.22 M membranes and passed through a protein G-Superose column (Pharmacia) connected to a LKB FPLC Akta instrument at a flow rate of 1 mL per minute at RT. The column was washed with 20 mM sodium phosphate for one hour and the antibody was then eluted in 0.5 mL fractions with 200 mM glycine, pH2.7. The eluate was collected in 0.5 mL aliquots in tubes containing 50 μ L of 1M Tris-HCl buffer at pH9.0 in order to ensure neutralisation of the pH. The fractions were stored at 4°C until further use.

2.13 Production of peptides representing the preS1 domain.

Peptides were synthesised using an automated peptide synthesiser. Following synthesis, peptides were eluted from the column matrix and lyophilised. Further purification of the peptides was done by high performance liquid chromatography (HPLC) LKB octadecyl silica HPLC column (Shandon Ltd, UK) coupled to a HPLC system (LKB, UK). The peptides were purified to about 95% purity and were lyophilised, weighed, and then redissolved at a concentration of 1 mg/mL in distilled water. The peptides were dispensed in 1 mg aliquots in glass vials and lyophilised. The peptides were analysed with a Lasermat mass spectrometer to ascertain the molecular weight of the purified species. The use of two standard peptides (kindly supplied by Dr. H. Marsden) of known molecular mass enabled calibration of the Mass Spectrometer for the purposes of molecular mass determination of the peptides described here. Further information pertaining to these peptides is shown in table 1.

2.14 Epitope mapping of monoclonal antibodies.

ELISA plates (96-well Immulon II) were coated overnight at RT with 125 μ g of preS1 domain in 100 μ L of PBSA. The next day the plates were washed three times with PBST and blocked with 200 μ L of 2% BSA in PBSA for one hour at RT. The plates were washed three times with PBST and to each well 90 μ L of a known concentration of a peptide corresponding to a known region of the preS1 domain was added. The peptides were added at 10, 100 and 1000 times the concentration of preS1 used to coat the plate. A blank positive control was used, where 90 μ L of PBSA was

added. Finally, 10 μ L of hybridoma supernatant of each MAb generated here was added to the 90 μ L of inhibitory peptide, and the plates were agitated to ensure mixing. The peptide-MAb mixture was left for 2 hours at RT and then removed by washing three times in PBST. The secondary reagent, anti-mouse-HRP conjugate was used at a dilution of 1:1000 for two hours. Following washing three times with PBST, the colour was developed with ABTS in hydrogen peroxide, and the colour measured at 405 nM after 30 minutes.

2.15 Cell culture.

All cell lines, unless otherwise stated, were cultured in Dulbecco's modified essential medium (DMEM) supplemented with 10% FCS (fetal calf serum, Gibco), 1% non-essential amino acids (Gibco) 100 units/mL penicillin/streptomycin and 10 mM glutamine (Gibco).

Baby Hamster Kidney (BHK-C13) cells were grown in Gibco BHK medium supplemented with 5% new-born calf serum, 10 mM glutamine, 100 units/ml and 1% non-essential amino acids. Hybridoma cells were grown in DMEM supplemented with 10% FCS, 4% HAT (hypoxanthine aminopterin, Gibco), 0.1% Gentamycin (Gibco) and 10mM glutamine (HAT Medium). Tissue culture plastics were obtained from Nunc, Bibby, Costar and Falcon.

2.16 Purification of vLx.

BHK cells were cultured in roller bottles to about 60% confluence, then were infected at a m.o.i. of 0.1 p.f.u./cell with WR or vLx, and the infections were allowed to proceed until complete cytopathic effect (c.p.e.) was observed. The medium from the infected cells was harvested and clarified at 3,000 r.p.m. in a benchtop centrifuge, then the supernatant was overlaid on a 40% w/v sucrose cushion and centrifuged at 18,000 rpm in a AH629 rotor (SORVAL) at 4°C for 4 hours. The pellet was resuspended in PBSA and centrifuged through a 15-30% continuous sucrose gradient for 2 hours at 35,000 rpm in a TST41 rotor (SORVAL). The gradients were fractionated and analysed by Western blot for the presence of Lx. Fractions containing the Lx protein were bulked and stored at -20°C, as were the corresponding

fractions from WR-infected samples. The bulked samples were analysed for the presence of Lx by Western blot with MAb RC28.

2.17 Generation of the hepatocyte-derived cell lines.

The generation of immortalised cell lines with the phenotype of hepatocytes has been an area of much study in recent years. The generation of immortalised cell lines from primary hepatocytes was undertaken in this laboratory in order to study the mechanism of infection and the replication of the hepatotropic viruses, HBV and HCV. Primary human hepatocytes were obtained commercially (from BioWhittaker, UK) in the form of monolayers in a 6-well plate. The transformed hepatocyte cell lines were derived from primary human hepatocytes by transduction with a mouse Moloney Leukaemia virus expressing the E6 and E7 proteins from Human Papilloma virus type 16. Following infection, the cultures were incubated at 37°C in DMEM and subcultured. Frozen stocks of the cell lines were generated and cryopreserved. This work was carried out by Dr. A. Patel and viable cell lines were made available to the author for experimentation. The cultures were grown in DMEM (see section 2.15) or Defined Medium (Runge *et al.*, 2000). These novel cell lines were investigated partially for hepatocyte phenotype by probing the plasma membrane and the intracellular matrix for the presence of cytokeratins 8 and 18. Furthermore, the cell lines were probed with antibodies reactive against human albumin, apolipoprotein 1A, alpha-fetoprotein, antitrypsin, and annexin V (see Chapter 4).

2.18 Cloning of HBV structural genes

The genes encoding the HBV structural proteins were cloned immediately downstream from a strong synthetic late vaccinia virus promoter into the transfer vector pMJ601 (Davison and Moss, 1990) as described below. Plasma from an HBV seropositive patient was donated from the laboratory of Dr. W. F. Carman. The portion of the HBV genome encoding the L protein was amplified by the polymerase chain reaction (PCR) by Dr. A. Owsianka in our lab. The resulting PCR product carrying the L open reading frame (ORF) was cleaved with *AfIII* and *HindIII* and inserted together with an oligonucleotide linker with *SalI* to *HindIII* ends and carrying

sequences encoding a secretory signal sequence of a major secretory protein of vaccinia virus (Patel *et al.*, 1990) (Patel, Subaksharpe, and Stow, 1992) into *SalI* to *HindIII*-cleaved pMJ601. The resulting plasmid, pMJLx, carried the HBV L ORF fused in-frame to the vaccinia virus secretory signal sequence at its 5' end (Fig. 2.1). To construct, pMJL, the L ORF from pMJLx was digested with the restriction enzymes *AflIII* and *HindIII* and cloned into *AflIII* to *HindIII*-cleaved pMJ601. To clone the HBV M gene, the nucleotide sequences encoding M ORF (amino acids 131 to 411) was cleaved from pMJL with *Bsu36I*, the ends made blunt using the Klenow fragment of *E. coli* polymerase I, and cleaved with *HindIII*. This *Bsu36I*/blunt to *HindIII* fragment was extracted from agarose gel and cloned into *SmaI* to *HindIII*-cleaved pMJ601 to form pMJM (Fig.2.1). The S gene was subcloned from plasmid pRK5/HBsAg (obtained from Dr. W. F. Carman's lab) on a *NruI* to *HindIII* fragment into *SmaI* to *HindIII*-cleaved pMJ601 to form pMJHBsAg. The HBV core gene was subcloned from plasmid p5D (obtained from Dr W. F. Carman's lab) on a *NruI* to *HindIII* fragment into *SmaI* to *HindIII*-cleaved pMJ601 to form pMJ5D (Fig.2.1). The HBV preS1 domain encoding amino acids 1 to 108 of the L protein was cloned by PCR amplification using pMJLx as a template. The PCR product was cleaved with *BamHI* to *HindIII* and cloned into the bacterial expression vector pQE30 (Qiagen). The resulting plasmid, pQES1, carries sequences encoding the amino acids MRGSHHHHHHGS followed by residues 1 to 108 representing the HBV preS1 domain. The entire nucleotide sequence encoding the Lx ORF in pMJLx, and the 6 histidine-tagged preS1 domain in pQES1 was determined by the dideoxynucleotide chain termination method (Sanger *et. al.*, 1997) and the nucleotide sequence of the Lx gene is shown in Appendix 2.

All the constructs described were derived following ligation and transformation of appropriate DNA into the *E. coli* DH5 α strain. The transformed bacteria were transferred to 1 mL of 2YT broth and incubated with shaking for 1 hour at 37°C, then were plated onto L broth Agar supplemented with 100 μ g/mL penicillin, and were incubated overnight at 37°C. The plates were examined the next day for colonies and twelve colonies were picked and grown in 2 mL 2YT broth containing 100 μ g/mL penicillin for 5 hours. Bacteria from the twelve cultures were pelleted in a benchtop centrifuge and the plasmid DNA extracted by the alkaline lysis method and restriction

analysis was performed to identify colonies carrying the appropriate construct. Large-scale cultures of the positive colonies were grown to produce plasmids using a commercial plasmid extraction kit (Qiagen, UK). This plasmid DNA was used to generate recombinant vaccinia virus (see below).

It should be noted that the plasmids pMJLx, pMJHBsAg, pMJ5D, and pQES1 were constructed by Dr. A. H. Patel. The plasmids pMJL and pMJM were generated by the author.

2.19 Generation of the recombinant vaccinia viruses.

BHK cells were grown in 50 mm dishes and infected with wild-type (wt) Western Reserve (WR) at a m.o.i. of 0.05 p.f.u. per cell in 300 μ l of maintenance medium. The cells were incubated with the inoculum for 1 hour at 37°C to allow the adsorption of the virus. Following adsorption, the cells were transfected with the appropriate plasmids by lipofection. A mixture of 100 μ L of Optimem (Gibco BRL) and 12 μ L Lipofectase was added to a solution containing 5 μ g of plasmid DNA (vector pMJ601 with the appropriate inserted ORF) in 90 μ L of Optimem, and mixed gently. The solution was incubated at RT for 10 minutes, whereafter a further 2 mL of Optimem was added. The WR-infected monolayer was washed twice in Optimem and the lipofection solution was added to the monolayer and incubated at 37°C for 5 hours. The lipofection solution was aspirated and the cells were incubated in maintenance medium for 2-3 days until the c.p.e. was complete. The cells were harvested, freeze-thawed twice and sonicated to release the progeny virus. Aliquots of the lysate was diluted to give 1X, 10^{-1} , 10^{-2} dilutions, and these were added to a monolayers of HuTK⁻ cells (human thymidine kinase negative) in 50 mm dishes, in a final volume of 300 μ L, for a period of 1 hour at 37°C. The monolayers were overlaid with 2 mL of maintenance medium containing 1% low-melting point agarose and 25 μ g/mL BudR. The medium was set, then overlaid with 1 mL of maintenance medium to prevent dehydration of the agarose. The cells were incubated for 2 days, and then the liquid medium was removed and replaced with 2 mL of maintenance medium (containing 1% low-melting point agarose, 25 μ g/mL BudR and 250 μ g/mL X-gal). The cells were incubated overnight at 37°C and examined the next day for blue plaques. Blue plaques were picked and replated onto BHK monolayers four times to plaque purify

the recombinant virus. Following four rounds of plaque purification of the rVVs, the plaques were added to a T25 culture flask containing BHK cells, and incubated at 37°C until a c.p.e. was observed. Cells were removed and freeze-thawed twice, then sonicated to release the progeny viruses. To generate stocks of rVVs, 6 roller bottles of BHK cells were infected at a m.o.i of 1:300 and incubated at 37°C until c.p.e. was complete. The cells were harvested by disruption with glass beads and were centrifuged at 3,000 r.p.m. in a Sorval RT6000B. The pellet was resuspended in 8 mL of Tris-HCl, pH9.0 on ice and was homogenised by 20 strokes in a Dounce homogeniser. The homogenate was pelleted at 2,000 r.p.m. for 10 minutes at 4°C, and the supernatant was collected. The pellet was resuspended in 8 mL of Tris-HCL, pH9.0 on ice and recentrifuged. The supernatants were combined and incubated with 0.1% trypsin at 37°C for 30 minutes with frequent vortexing. The supernatant was diluted to a final volume of 36 mL and two 18 mL aliquots were layered onto 18 mL of 36% w/v sucrose in 10 mM Tris-HCl pH9.0, in AH629 rotor tubes. The samples were centrifuged at 13,500 r.p.m. for 80 minutes at 4°C, then the pellet was resuspended in 2 mL 1 mM Tris-HCl pH9.0. The titre of the rVVs was determined by plating ten-fold dilutions of the stock onto BHK monolayers, incubating at 37°C for one hour, then overlaying with CMC medium. After three days incubation, 2 mL of Giemsa's stain was overlaid on the monolayer and incubated at RT for 3 hours. The stain was washed off in running water, and the plates left to dry at RT. The plates were examined with an optical microscope for CPE and the titre of the viral stocks was calculated. Stocks of virus were stored at -70°C.

2.20 Confocal microscopy.

Samples for analysis by confocal microscopy were prepared on 13 mm glass coverslips in 24 well plates. Cells were grown on the coverslips to 50-60% confluence prior to experimental procedures. Cells were infected with rVVs at a m.o.i. of 0.5 PFU per cell in 100 µl of DMEM for 1 hour at 37°C with periodic agitation to ensure coverage of the cells by the virus suspension. The cells were then washed with PBSA to remove any unbound virus and were incubated in DMEM at 37°C for 24 hours to allow expression of the proteins. Samples for analysis of plasma membrane-bound proteins were washed in PBS three times and were then fixed in 2% paraformaldehyde and stored at 4°C until further use. Labelling of these samples with

antibodies was done by incubating the cells with the appropriate dilution of primary, then secondary antibodies in PBSA in volumes of 200 μ L. Cells to be analysed for intracellular expression and localisation of proteins were washed on the coverslips three times in PBSA, then stored in ethanol at -20°C for at least 20 minutes, usually overnight. The samples were then washed in PBSA and then permeabilised with PBST for 30 minutes at RT. Labelling of permeabilised samples with antibodies was done in 200 μ L volumes of PBST. The labelled samples were mounted on glass slides with a drop of Citifluor anti-fade reagent, and the slides were sealed with Nail varnish. Confocal analysis was performed using a Zeiss Laser Scanning Microscope with LSM5150 software.

2.21 Fluorescence-Activated Cell Sorting.

Cells were grown to near-confluence in T175 flasks. Cell monolayers were washed three times with PBSA and the monolayers were incubated in 10 mL of dissociation buffer at 37°C for approximately 30 minutes or until the monolayers became loose and the cells were no longer in large clumps. The dissociated cells were washed in PBSC twice and centrifuged at 1,000 r.p.m. at 4°C for 2 minutes. The pelleted cells from each T175 flask were thoroughly resuspended in 2 mL FPBS. Cells were dispensed in 100 μ L aliquots (containing approximately 1×10^6 cells per aliquot) to 12 mL tubes for subsequent labelling with ligands and antisera. Where cells were labelled with ligands, the ligands were typically added in volumes of 20 μ L at a concentration of 1 mg/mL and incubated on ice for 30 minutes. Unbound ligands were removed by filling the tube with FPBS and centrifugation of the suspended cells at 1,000 r.p.m. for 2 minutes in a Sorval RT6000B centrifuge. The FPBS was aspirated and the cells resuspended in fresh FPBS and the washing repeated. The cells were resuspended in 100 μ L of FPBS and labelled with primary antibody. Purified antibody RC28 was used at a concentration of 1 mg/mL, and 1 μ L was added to each aliquot of cells requiring labelling. The cells were incubated in primary antibody for 30 minutes at 4°C and were then washed twice and resuspended in FPBS as previously described. The fluorescent labelling of cells was achieved by addition of 1 μ L of anti-IgG-FITC (Sigma) per aliquot of cells resulting in a 1:100 dilution of the secondary antibody. The cells were incubated in secondary antibody for 30 minutes at 4°C and were washed twice and resuspended in a final volume of 0.7 mL.

Fluorescence quantitation and analysis was achieved by passing the cells through a Becton Dickinson FACScan instrument with CellQuest software.

Chapter 3

Generation and Characterisation of Reagents

The generation of reagents was undertaken as part of this work. There was a paucity of reagents for HBV research in this laboratory prior to the author starting work, therefore the initial stages of the work were centred around creation and characterisation of reagents for Hepatitis B Virus research. Reagents generated here include recombinant vaccinia viruses expressing L, Lx, M, S and core proteins, a bacterially produced 6-histidine tagged (6xHis) preS1 domain, monoclonal and polyclonal antisera directed against L protein and cell lines derived from primary human hepatocytes. Furthermore, some reagents were obtained from other institutes and companies, and were used in this work; a monoclonal antibody 6B1, directed against S (C. McCaughey QUB, Belfast); polyclonal antisera against core protein (DAKO, UK); monoclonal antibody to preS2 (Heermann *et al.*, 1987) antibodies to cellular markers (see appendix 1); and HepB3 protein (Medeva, UK). The generation and characterisation of reagents is described in this chapter. These reagents were used to carry out the aims and objectives of this thesis.

3.1 Expression and purification of the preS1 domain

The gene encoding the preS1 domain of HBV (*adw* subtype) surface antigen was fused in-frame to the nucleotide sequence coding for the amino acids MRGS followed by six histidine residues and two extra amino acids (GS) in the plasmid pQE30 (QIAGEN, UK). The resulting plasmid, pQES1, was transformed into *E.coli* M15 (pREP4) for protein expression. The expressed product was expected to carry the amino acids sequence MRGSHHHHHHGS followed by the N-terminal 108 amino acids of the preS1 domain with an estimated molecular mass of 14 kDa. A single colony each of *E.coli* strain M15 [pREP4] carrying the plasmid pQE30 or pQES1 was grown in 2YT broth in the presence or absence of IPTG. Five hours after addition of IPTG, the cell extracts were analysed by SDS-PAGE either directly or following affinity chromatography on Ni-NTA resin. Figure 3.1 shows the expression of the preS1 domain in *E. Coli* and its subsequent purification. As expected, a 14 kDa band was seen in IPTG-induced, but not in uninduced, culture of cells carrying pQES1 (Fig. 3.1, lanes C and D, respectively). This band was not present in induced or

uninduced cultures of cells carrying the plasmid vector pQE30 (Fig. 3.1, lanes A and B). This indicated that the band in lane C from the induced cells carrying pQES1 may contain the expressed HBV preS1 domain. To test if this protein was expressed in a soluble form, IPTG-induced cultures of cells carrying pQES1 were lysed following two rounds of freeze thawing and sonication. The total lysate was then spun for 30 minutes at 15,000 r.p.m. and the supernatant carrying soluble proteins analysed on SDS-PAGE. As shown in Fig. 3.1 lane G, the clarified lysate indeed contained the 14 kDa protein indicating that at least some of the expressed protein is produced in a soluble form. To purify this protein, the clarified lysate was incubated with Ni-NTA slurry on a mixer for 1 h at RT, following which it was transferred to a 5 mL disposable chromatography column. The column was wash extensively with TN buffer and the bound proteins were eluted from Ni-NTA in 250 mM imidazole in TN buffer. Analysis of the eluted proteins by SDS-PAGE showed the presence of a band at 14 kDa (Fig. 3.1, lanes E and F). The 14 kDa band is the only band visible at the limits of optical detection by coomassie blue staining in SDS-PAGE, indicating that the purification was highly effective.

The identity of the preS1 domain from lane E in Fig. 3.1 was verified by Western immunoblotting of this sample of protein using a monoclonal antibody directed against the MRGS-6xHis tag (Qiagen, UK) or the HBV preS1 domain. As shown in Fig. 3.2A, the anti-his MAb recognised the 14 kDa protein in the total extract of IPTG-induced cells carrying pQES1 (lanes B and C) and in the protein fraction eluted from the Ni-NTA column (lane A). As expected, the anti- his MAb failed to recognise a 14 kDa product in the extracts of pQE30-carrying cells (Fig. 3.2A, lanes D and E). To show that the his-tagged product was the preS1 domain, another Western blot was performed using a monoclonal antibody MAb18/7 that is known to recognise the preS1 domain (Heermann *et al.*, 1984). As seen in Fig. 3.2B, the MAb 18/7 identified the protein of the same molecular weight as the protein recognised by the anti-His MAb. These results, taken together with those shown in Fig. 3.1 show that the preS1 domain is expressed in reasonable quantities in bacteria, that this protein is recoverable in a soluble form, and that it can be purified by single-step affinity chromatography to near homogeneity.

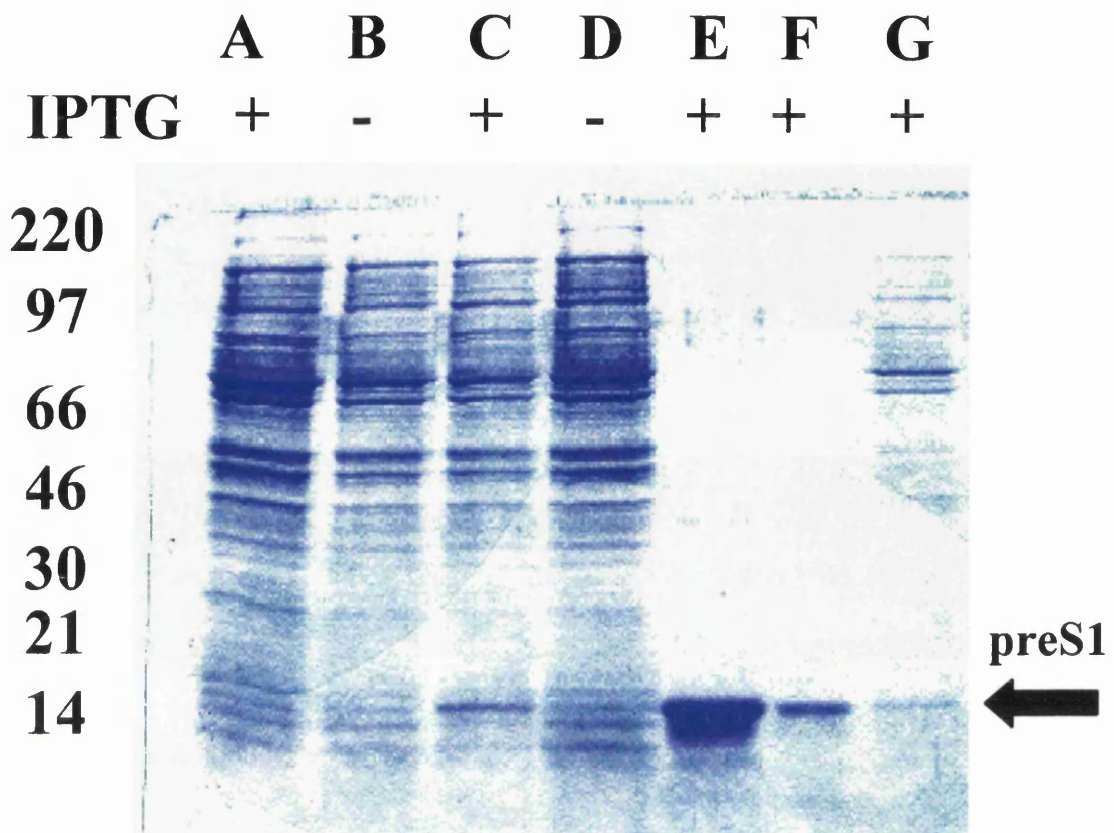


Figure 3.1 Expression and purification of HBV preS1 domain from *E. Coli*.

E.coli strain M15 (pREP4) carrying pQE30 (lanes A and B) or pQES1 (lanes C to G) was grown in the absence (-) or presence (+) of IPTG. Following incubation at 37°C for 5 hours, cells were harvested and analysed on a 12.5% SDS-PAGE either directly (lanes A-D) or after lysis and affinity chromatography (lanes E+F) on a Ni-NTA column. The fractionated proteins were visualised with coomassie brilliant blue.

Lane A+B: Total extract of cells carrying pQE30.

Lane C+D: Total extract of cells carrying pQES1.

Lane E+F: proteins from *E. coli* expressing pQES1 eluted with 250 mM and 20 mM imidazole, respectively.

Lane G: soluble cell lysate from cells expressing pQES1.

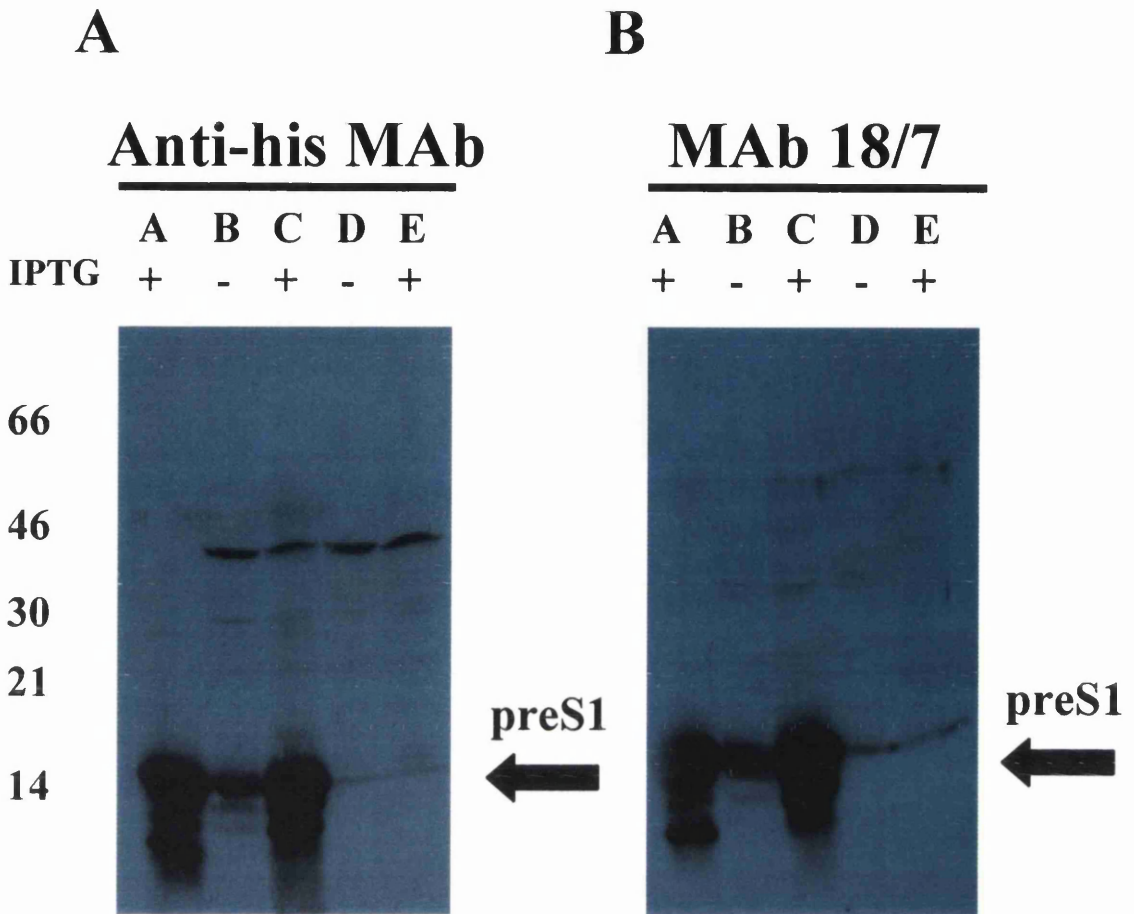


Figure 3.2A and B: Verification of the identity of the purified protein as the preS1 domain fusion protein.

The induction of the bacteria with IPTG leads to the expression of protein species migrating at 14 kDa that are reactive with antisera against known epitopes. The purified protein eluted in 250 mM imidazole (lane A, panels A and B) was probed with anti-MRGS-6xHis MAb (3.2A), or MAb 18/7 (3.2B). The lysate from cells carrying pQES1 (lanes B and C) following induction with IPTG (+) or in the absence of IPTG (-), and the lysate from cells carrying the pQE30 plasmid (lanes 4 and 5) following induction with IPTG (+) or in the absence of IPTG (-) were probed with anti-MRGS 6xHis and Mab 18/7 to confirm the identity of the proteins.

Lane A: purified protein from Ni-NTA eluted in 250 mM imidazole.

Lanes B and C: Total extract of cells carrying pQES1.

Lanes D and E: Total extract of cells carrying pQE30.

3.2 Generation and characterisation of recombinant vaccinia viruses expressing HBV structural proteins.

The genes encoding HBV structural proteins L, M, S, and core were inserted into the thymidine kinase locus of vaccinia virus strain WR (see Materials and Methods). Briefly, the L gene was PCR amplified by Dr A. Owsianka from a patient serum and cloned immediately downstream from a strong synthetic late vaccinia virus promoter into the transfer vector pMJ601 (Davison and Moss, 1990). The nucleotide sequence of the Lx gene was determined and its amino acids sequence deduced and is shown in Appendix 2. As expected, the amino acids sequence of the Lx gene was almost identical to the published sequences of L protein of *adw* subtypes. However, several variant amino acids were present in the Lx sequence (see Appendix 2). It is not clear whether these changes have occurred due to PCR errors or represent the patient serotype. The ORFs encoding L and M and the preS1 domain were subsequently subcloned from the plasmid pMJLx into appropriate vectors as described in the Materials and Methods. The genes encoding S and core were subcloned into pMJ601 from constructs obtained from Dr. W. F. Carman. The pMJ-based constructs were used to generate recombinant vaccinia viruses (rVVs) vL, vLx, vM, vS and v5D (as described in Materials and Methods).

3.2.1 Expression of L, Lx, M, S and core in mammalian cells.

The initial characterisation of the proteins expressed by the rVVs was performed by Western immuno blotting and confocal microscopy using antibodies specific to viral antigens. BHK cells were mock infected or infected with wt vaccinia virus strain WR or the rVVs. At 24 h post-infection, the medium was collected, cells washed twice with PBS and lysed in lysis buffer (see Materials and Methods). The medium and cell lysate of infected cells were then subjected to SDS-PAGE and the fractionated proteins were electrotransferred to Hybond ECL membranes. The membranes were subjected to Western immunoblotting using an anti-preS1 MAb 18/7 or an anti-core MAb 2A23 As shown in Fig. 3.4A, the MAb 18/7 specifically recognised a 42 kDa product in the lysate of cells infected with vL or vLx, but not with strain WR or mock-infected controls. Furthermore, this MAb also recognised the same sized product in the medium of cells infected with vLx, but not with WR, or mock infected control (Fig. 3.4A). These results show both vL and vLx express the L protein of expected molecular weight. Furthermore, in agreement with observation made by

others, the L protein is not secreted into the medium. However, secretion of L protein can be achieved if the protein is fused to a secretory signal peptide (see Fig. 3.3A, lane Lx, SN).

As expected, Western immunoblot using anti-core MAb 2A23 showed that this MAb specifically recognised a 22 kDa core protein in cells infected with v5D, but not with WR-infected or mock-infected cells (Fig. 3.4B). The ECL membranes were also probed with available antibodies to the M and S protein of HBV. Unfortunately, neither of these antibodies recognised the appropriate protein in Western blots (data not shown). However, the expression of M and S by vM and vS, respectively, was confirmed by immunofluorescence assay (see below).

To facilitate confocal analysis of the structural proteins, HepG2 cells were infected with the recombinant vaccinia viruses vL, vLx, vM, vS or v5D on coverslips, incubated for a further 24 hours at 37°C and fixed 24 hours post-infection in methanol at -20°C. After washing, the fixed cells were incubated with anti-preS1 MAb 18/7, anti-M MAb 2-2f12 (kindly supplied by Professor W. H. Gerlich, Institute of Medical Virology, Giessen, Germany; (Heermann *et al.*, 1984), anti-S MAbs H166 and H53 (Abbott Laboratories; obtained from Dr W. F. Carman's lab), or a polyclonal antiserum raised against HBV core (DAKO, UK). Following washing, the cells were then incubated with anti-mouse IgG-FITC or anti-rabbit IgG-TRITC conjugate as appropriate for 1 h at RT. After washing the coverslips were mounted on glass slides and cells examined under confocal microscope. As shown in Fig. 3.4, cells infected with vL and vLx produced a protein that was recognised by MAb 18/7 (panel A and B). Similarly, MAb 2-2f12, MAb H166, or polyclonal anti-core anti-serum recognised the HBV M (panel C), S (panel D), or core (panel E), respectively, in cells infected with appropriate rVVs (Fig. 3.4). All the expression products encoded for by the rVVs reacted with the antisera directed against that particular protein, thus providing evidence that the encoded HBV protein was reactive with antisera known to react specifically with a particular HBV antigen. A detailed characterisation of expressed protein is described in chapters 5, 6 and 7.

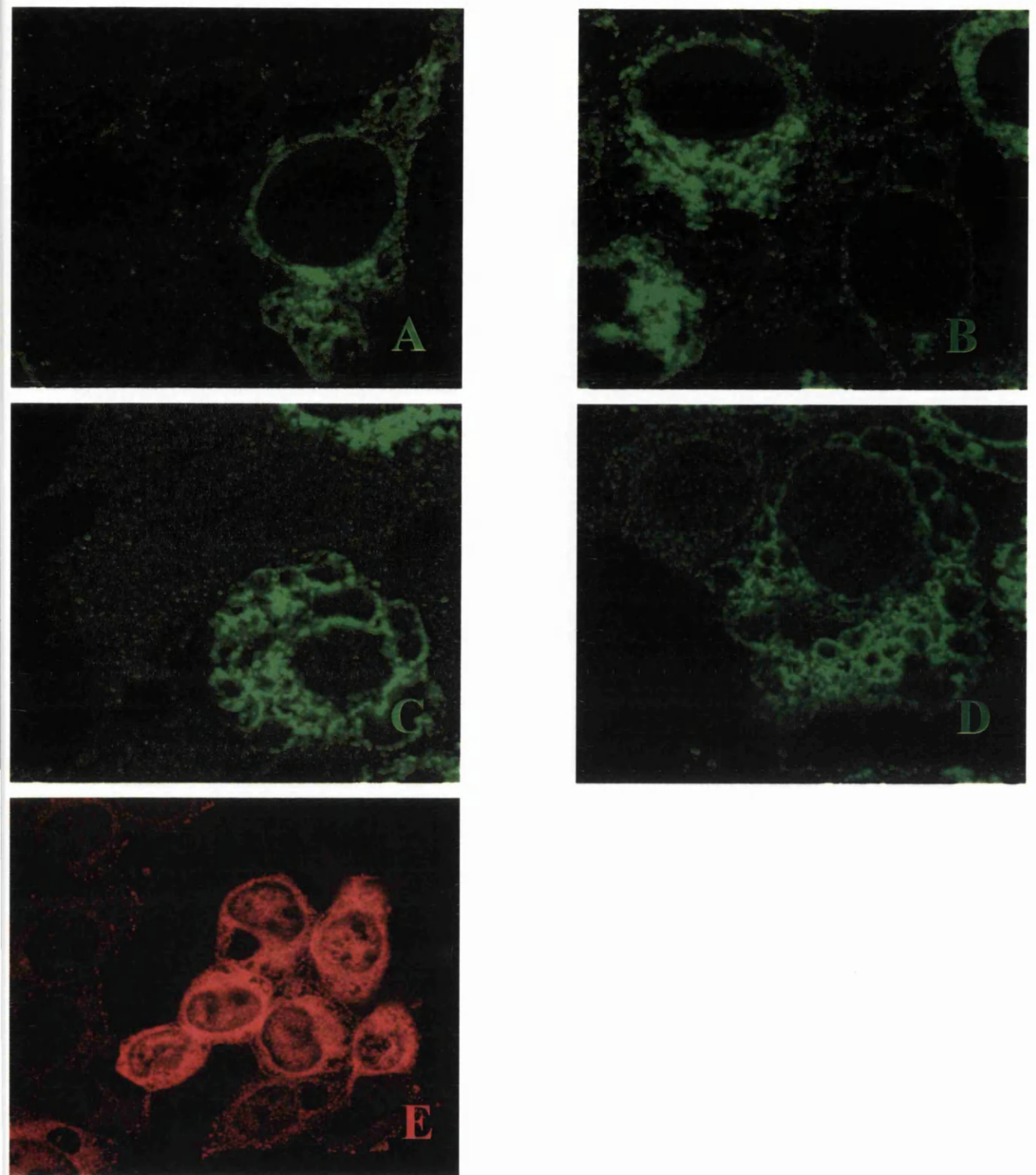


Figure 3.3. Characterisation of HBV structural antigens.

HepG2 cells on glass coverslips in 24-well plates were infected at an m.o.i. of 0.5 p.f.u./cell with vL (Panel A), vLx (panel B), vM (panel C), vHBsAg (panel D), and v5D (panel E). At 24 hours post-infection, the cells were fixed in methanol at -20°C, then permeabilised in PBST. The cells were probed with MAb 18/7 (panels A and B), MAb 2-12f2 (panel C), MAb H166 (panel D) and a polyclonal antiserum against core (DAKO, UK, panel E).

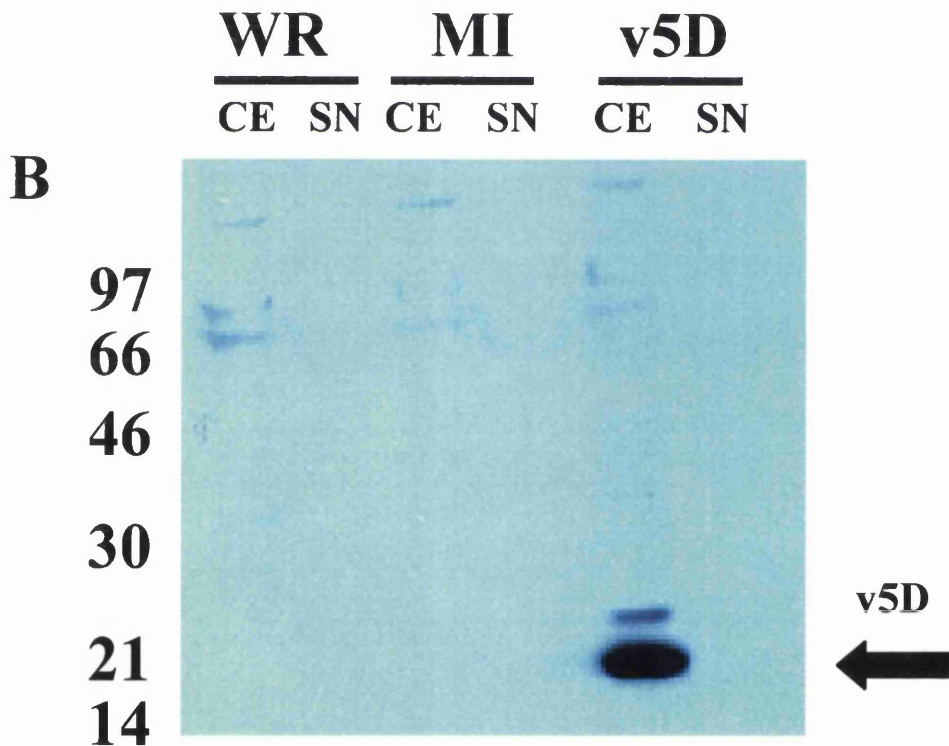
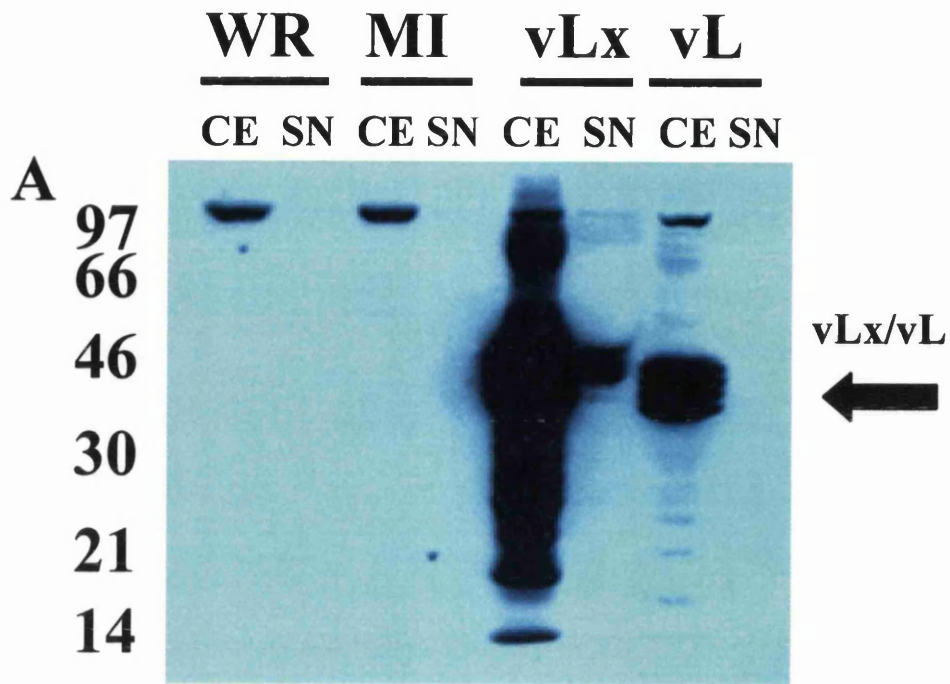


Figure 3.4. Characterisation of HBV structural antigens.

BHK cells were mock-infected, or infected with WR, vLx, vL or v5D at a m.o.i. of 10 p.f.u./cell. At 24 hours post-infection, the supernatants were clarified, and the cells were harvested and lysed with final sample buffer and subjected to 10% SDS-PAGE. The fractionated proteins were transferred to Hybond ECL membranes and probed with MAb 18/7 (panel A) at a 1:1000 dilution, or MAb 2A23 (panel B) at a 1:500 dilution. The bound antibodies were detected with 1:1000 diluted anti-mouse-IgG-HRP followed by chemiluminescence with ECL reagents.

3.3 Generation and Characterisation of Antisera.

Polyclonal and monoclonal antibodies were generated by immunisation of rabbits and mice respectively, with the purified preS1 domain described in section 3.1. The characterisation of the rabbit polyclonal antibodies (PABs) generated here was performed by the author and is described in the following sections.

3.3.1 Polyclonal Antisera 142 and 143.

Two rabbits, numbers 142 and 143, were repeatedly immunised with the preS1 domain in order to obtain polyclonal antisera reactive against the L protein of HBV. Following the immunisation protocol (described in Materials and Methods), the rabbits were exsanguinated and the serum clarified by centrifugation, aliquotted and stored at -20°C.

The rabbit-derived antisera raised against the preS1 domain were evaluated for activity in the following assays: Western blot, immunoprecipitation and immunofluorescence. For Western blotting, HepG2 cells were infected at an m.o.i. of 10 p.f.u./cell with vaccinia virus strain WR or the recombinant vaccinia virus expressing Lx (vLx). At 24 h post infection, the cells were lysed in SDS-PAGE denaturation buffer. The extracts were electroblotted on to Hybond ECL membrane following resolution of proteins by SDS-PAGE, and probed with PAb 142 or 143 as shown in Figs. 3.5A and B. Both antisera reacted specifically to a 46 kDa band in vLx-infected cells but not in cells infected with the wt vaccinia strain WR. The pre-immune sera taken from each rabbit prior to the start of the immunisation (see Materials and Methods) regimes were tested shortly after acquisition and were found to be unable to immunoprecipitate or recognise vLx protein in Western immunoblot (data not shown), thus confirming the specificity of PABs 142 and 143 to HBV L protein.

To test the reactivity of PABs 142 and 143 in immunoprecipitation assay, HepG2 cells were either mock-infected or infected with the wt vaccinia strain WR, or recombinant vaccinia viruses vLx, or vL and the cells radiolabelled with ³⁵S-methionine from 5 h to 18 h post-infection. The infected cells were washed twice with PBS and lysed in Zweig's buffer. The lysates were clarified and the labelled proteins

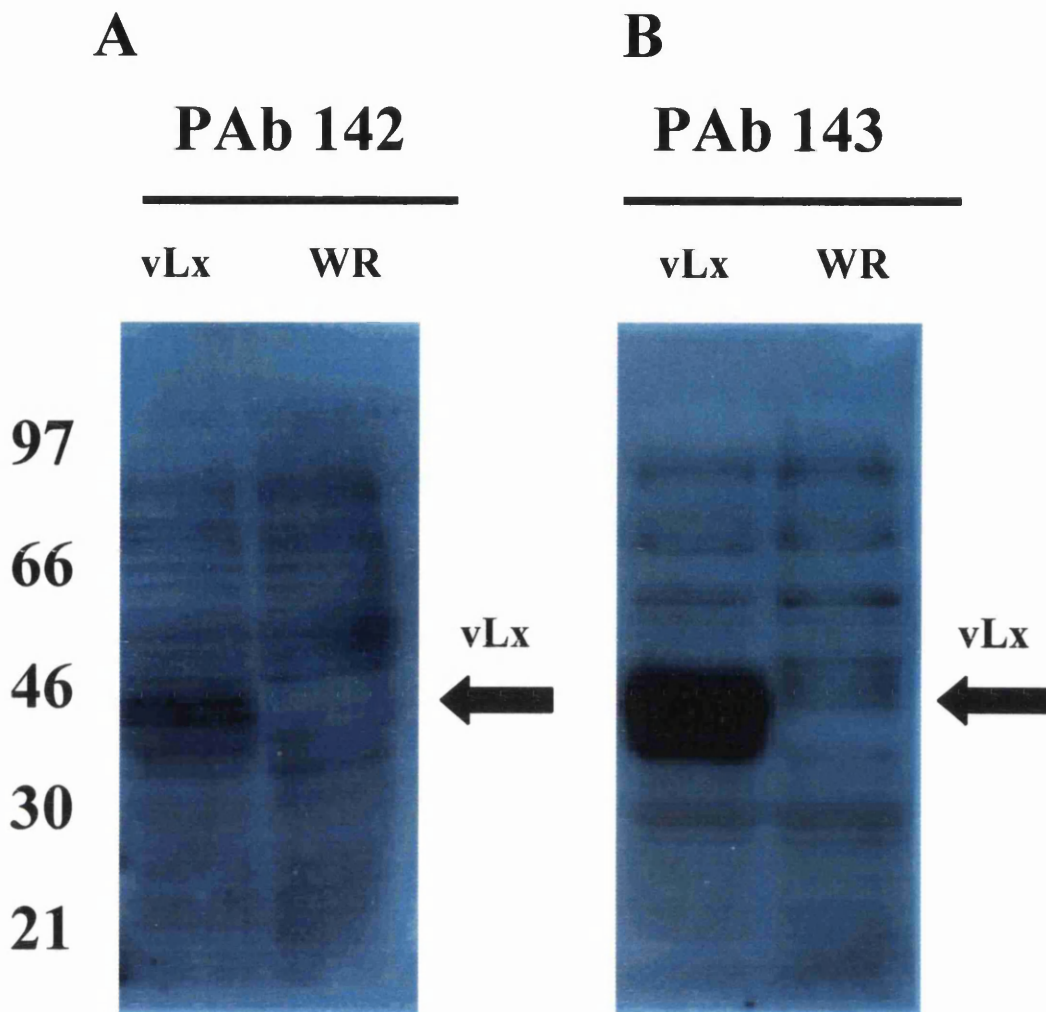


Figure 3.5. Characterisation of the PABs 142 and 143 by Western immunoblotting.

BHK cells were infected with the wild-type vaccinia virus strain WR or the recombinant vaccinia virus expressing the Lx protein (vLx) at a m.o.i. of 10 p.f.u./cell. At 24 hours post-infection, the cells were harvested and lysed with final sample buffer and the lysate subjected to 10% SDS-PAGE. The fractionated proteins were transferred to Hybond ECL membranes and probed with PAb 142 (panel A) or PAb 143 (panel B) at a 1:1000 dilution. The bound antibodies were detected with 1:1000 diluted protein-A-sepharose followed by chemiluminescence with ECL reagents.

immunoprecipitated using PAb 142 or 143. As shown in Fig. 3.6 A and B, both antisera precipitated a protein of approximately 46 kDa from cells infected with vLx and vL. The absence of any significant bands at the appropriate molecular weight in the mock-infected cells or WR-infected cells at around the 46 kDa position on the autoradiograph indicated that these antisera can specifically immunoprecipitate the L protein with minimal reactivity to cellular or vaccinia virus proteins (Fig. 3.6 A and B). To test the reactivity of PABs 142 and 143 in immunofluorescence assays, HepG2 cells, mock-infected or infected with vaccinia strain WR or vLx, were probed with immune or pre-immune PAb 142 and 143. The antisera were evaluated at titres of 1:500, 1:1000, 1:2000 and 1:4000 for these assays. The results shown in Figs. 3.7 and 3.8 were obtained with a titre of 1:1000. This titre offered the best contrast between the infected and non-infected cells in the vLx-infected samples. As shown in Panel A of Figs. 3.7 and 3.8, both polyclonal antisera specifically recognised the vLx protein. The absence of any reactivity in the panels B and C of Figs. 3.7 and 3.8 indicated minimal reactivity to any cellular or vaccinia virus proteins. Furthermore, the respective pre-immune sera from rabbits 142 and 143 failed to react with the vLx-expressing cells (Panel D, Figs. 3.7 and 3.8) again indicating strongly that the reactivity is specific to the L protein.

Taken together, these results indicate that the polyclonal antisera 142 and 143 are capable of specifically recognising the L protein in the described assays, with minimal recognition of cellular or vaccinia proteins.

3.3.2. Monoclonal antibodies

A batch of five Balb/c mice were immunised with the purified preS1 domain described in section 3.1. Following repeated boosting of the mice with antigen, the spleen cells were removed and fused with the sp2/0 cell line as described in Materials and Methods. Following growth of colonies in 96-well plates, the supernatants from the wells were analysed by ELISA to identify colonies producing immunoglobulins reactive to the preS1 domain. Hybridoma supernatants giving ELISA-positive results were screened for reactivity to the bacterially expressed preS1 domain in Western blotting assays. Hybridoma supernatants showing positive reactivity in Western blots against the preS1 domain were screened for reactivity against the vLx protein in Western blotting assays (data not shown). The aim of this discriminatory assay was

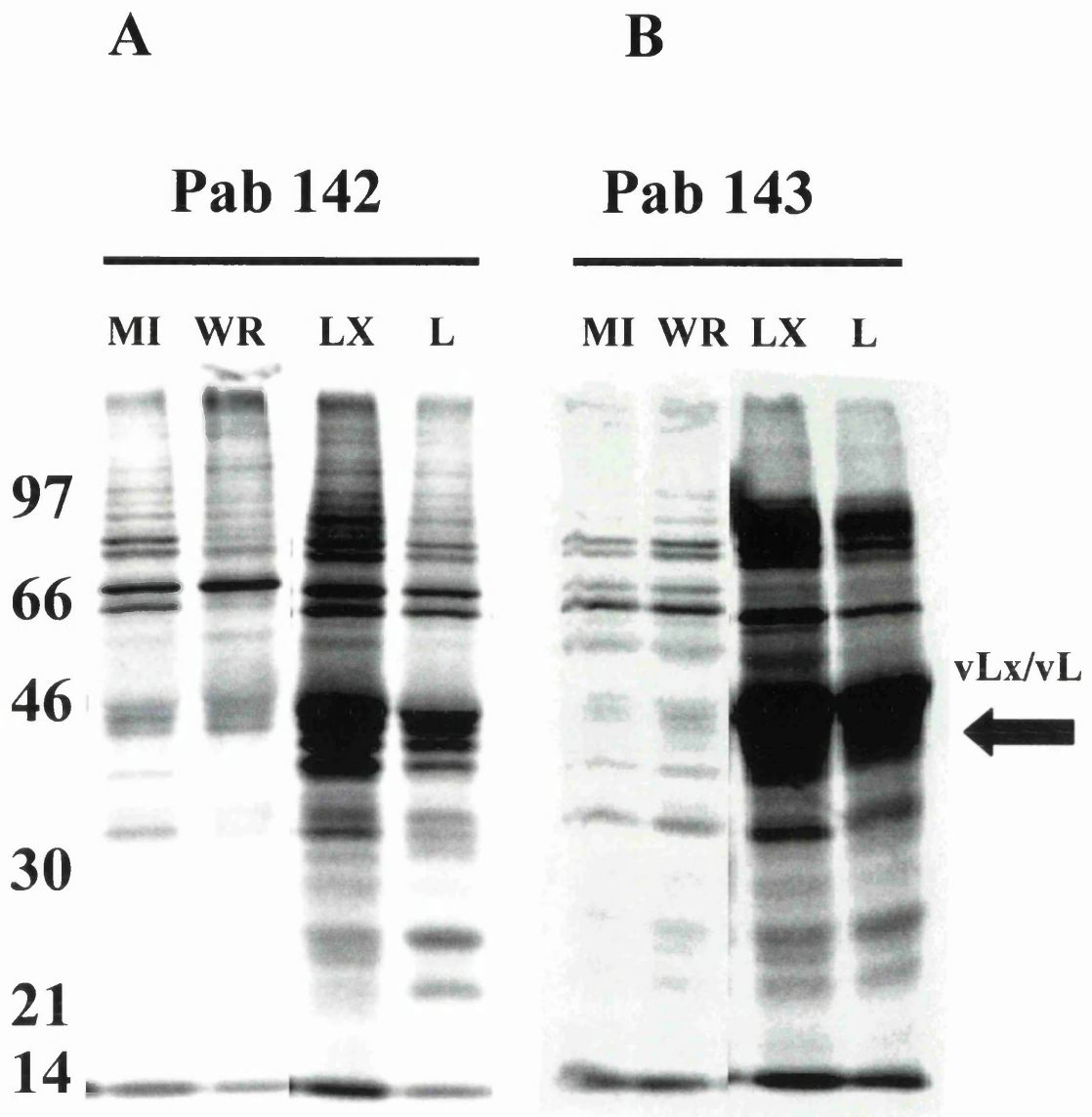


Figure 3.6. Characterisation of the PABs 142 and 143 by Immunoprecipitation.

HepG2 cells were mock-infected, infected with the wild-type WR strain vaccinia virus or the recombinant vaccinia virus expressing the Lx protein (vLx), or vL, at a m.o.i. of 10 p.f.u. per cell. At 5 hours post-infection, the infected cells were radiolabelled with ^{35}S methionine. At 18 hours post-labelling, the cells were lysed, clarified and subjected to immunoprecipitation with PAB 142 (panel A) or PAB 143 (panel B). The immune complexes were subjected to 10% SDS-PAGE and the radiolabelled proteins detected by autoradiography.

Lane MI: Mock-infected cell extract.

Lane WR: WR-infected cell extract.

Lane vLx: vLx-infected cell extract.

Lane vL: vL-infected cell extract.

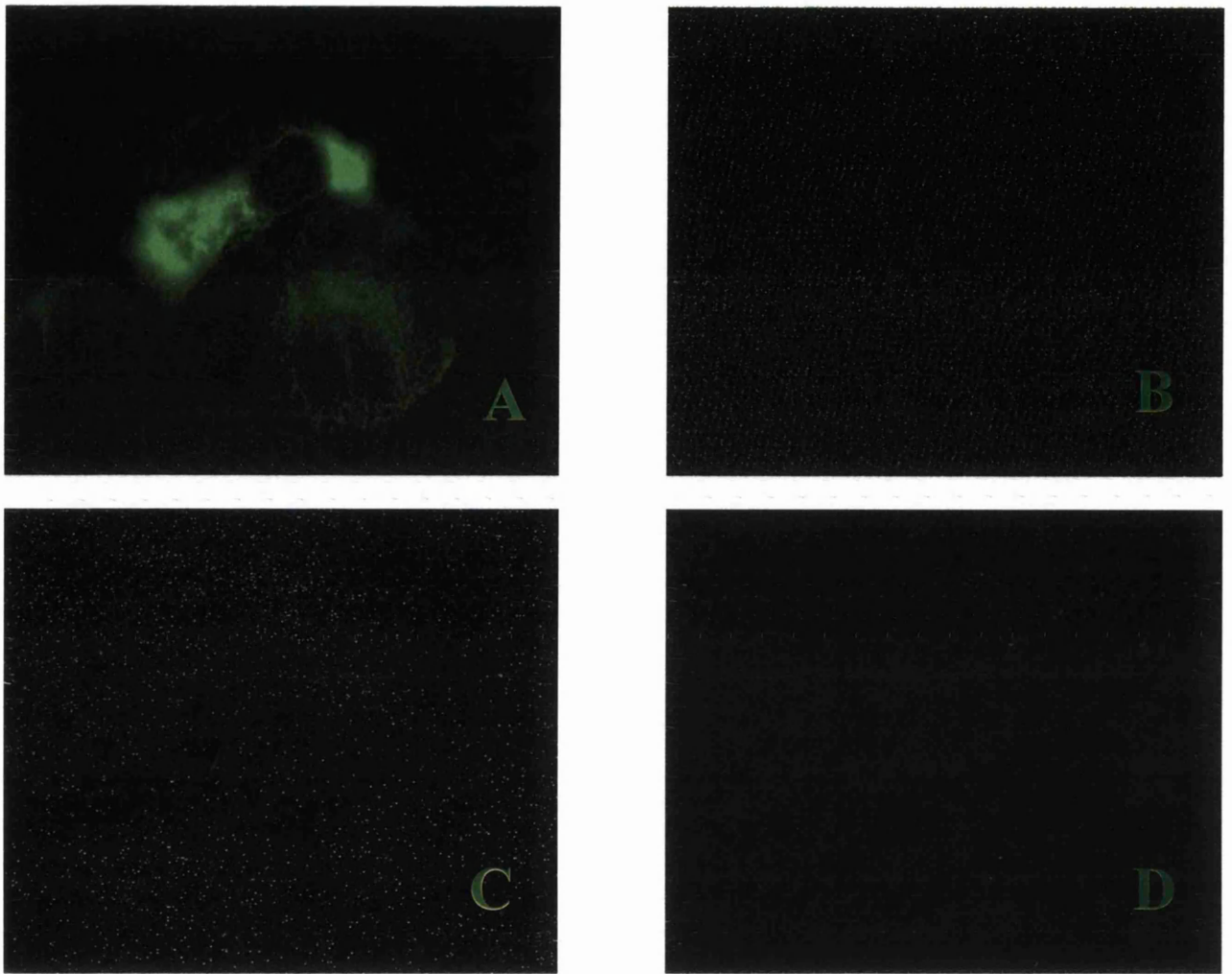


Figure 3.7. Characterisation of the PAb 142 by immunofluorescence.

HepG2 cells on glass coverslips in 24-well plates were infected at a low m.o.i. with the recombinant vaccinia virus expressing the Lx protein (vLx, Panel **A** and **D**) mock-infected (MI, Panel **B**) or wild-type (WR, Panel **C**). At 24 hours post-infection, the cells were fixed in methanol at -20°C , then permeabilised in PBST. The cells were probed with a 1:1000 dilution of PAb 142 (panels **A**, **B** and **C**) or pre-immune serum (panel **D**) from rabbit 142. The immunolabelled cells were detected with a 1:1000 dilution of anti-rabbit-FITC with a NIKON-Microphot microscope.

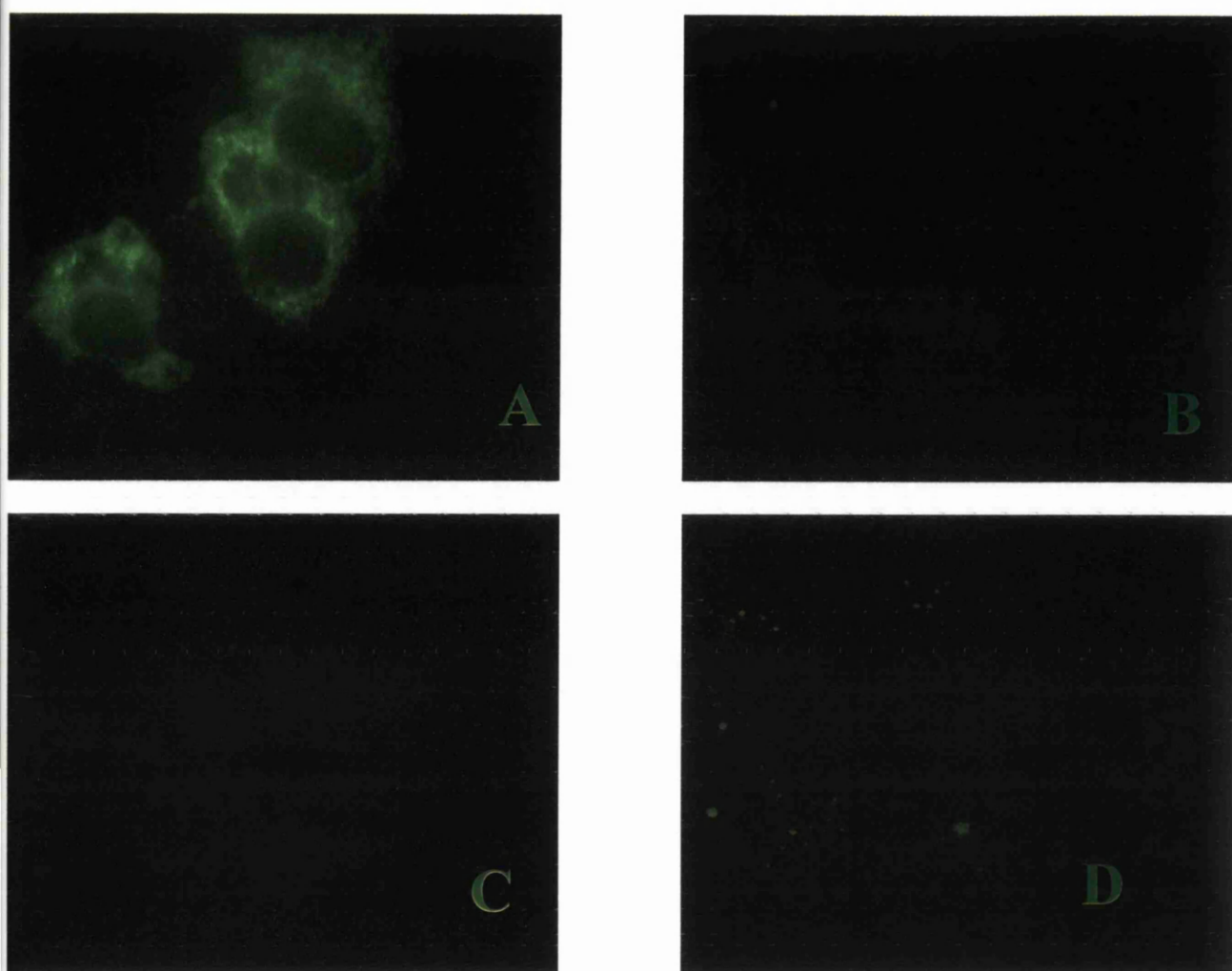


Figure 3.8. Characterisation of PAb143 in immunofluorescence assays.

HepG2 cells on glass coverslips in 24-well plates were infected at a low m.o.i. with the recombinant vaccinia virus expressing the Lx protein (vLx, Panels A and D) mock-infected (MI, Panel B) or wild-type (WR, Panel C). At 24 hours post-infection, the cells were fixed in methanol at -20°C , then permeabilised in PBST. The cells were probed with a 1:1000 dilution of PAb 143 (panels A, B and C) or pre-immune serum (panel D) from rabbit 143. The immunolabelled cells were detected with a 1:1000 dilution of anti-rabbit-FITC with a NIKON-Microphot microscope.

to establish which of the cultures were secreting antibodies that were reactive to the preS1 domain of L, not against the MRGS-6xHis tag. Using this approach, four MAbs were identified which reacted specifically to HBV L protein. The reactivity of these MAbs (RC9, RC28, RC109 and RC152) is shown in Figs. 3.9 A to D, with a negligible background in the WR or mock-infected cells.

The ability of the four monoclonal antibodies RC9, RC28, RC109 and RC152 to immunoprecipitate L protein was examined. Briefly, HeLa cells were infected with WR, vLx, vL viruses, or were mock-infected. The cells were incubated with methionine-deficient medium supplemented with ³⁵S-methionine five hours post infection, and incubated overnight. The next day, the cells were detergent-solubilised and the clarified extract (see Materials and Methods) used in immunoprecipitation assays. In initial experiments, very poor reactivity was observed of the monoclonal antibodies generated here, when tested singly (not shown). However, a cocktail of all four antibodies was able to immunoprecipitate the Lx and the L protein from cells infected with vLx and vL, respectively (Fig. 3.10). There was little reactivity of this mixture of antibodies with proteins in mock- or vaccinia virus strain WR-infected cells (Fig. 3.10) indicating the specificity of these MAbs to HBV L protein. It has been reported that a combination of monoclonal antibodies directed against a particular protein can be used to greater effect in immunoprecipitations than one monoclonal antibody alone (Ehrlich and Moyle, 1986). Certainly, in this case it is evident that a co-operative effect is observable with immunoprecipitation being effectively enabled with a combination of monoclonal antibodies. It is not clear why the MAbs failed to immunoprecipitate the L protein when tested individually. It is possible that the conditions (e.g. lysis buffer) employed for immunoprecipitation assays in this work were not optimal for the individual antibodies to immunoprecipitate the L protein.

Hybridoma supernatants RC9, RC28, RC109, or RC152 were examined in an immunofluorescence assay for reactivity against the Lx protein in vLx-infected HeLa cells. As shown in Figs. 3.11 and 3.12, all four MAbs reacted with the Lx protein in vLx-infected cells (panels A and D), but there was no discernible fluorescence in the WR-infected and mock-infected cells (panels B, C, E, and F) indicating that these antisera are reacting specifically to HBV L in immunofluorescence assays. These

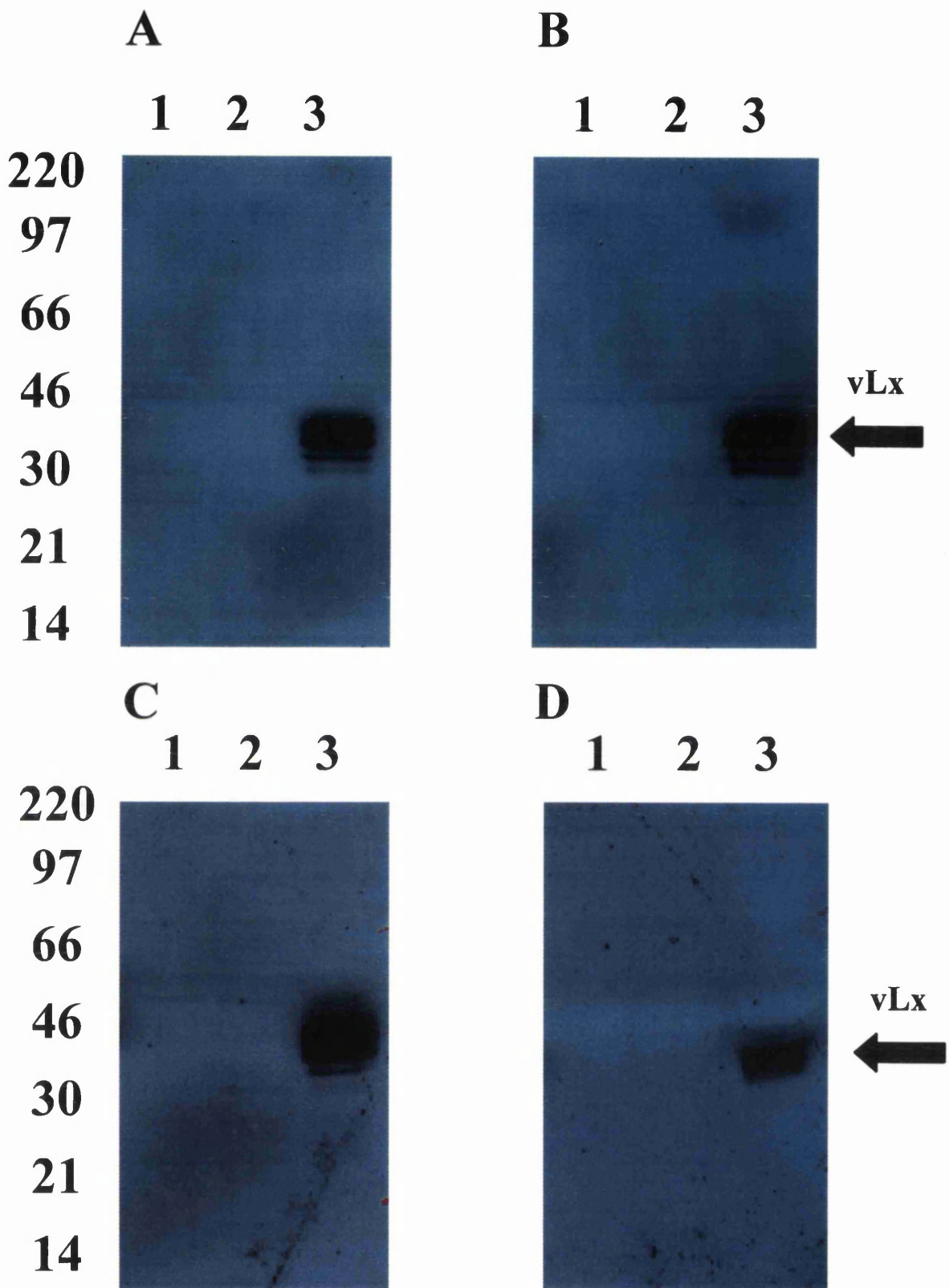


Figure 3.9. Characterisation of MAbs RC9, RC28, RC109 and RC152 by immunoblot. HepG2 cells were infected at a m.o.i. of 10 p.f.u./cell with WR (lane1), vLx (lane 3) or were mock-infected (lane 2). At 24 hours post-infection, the cells were lysed in final sample buffer and the lysate subjected to 12.5% SDS-PAGE. The fractionated proteins were transferred to Hybond ECL membranes and were then probed with 1:1000 dilution of RC9 (panel A), RC28 (panel B), RC109 (panel C) or RC152 (panel D). The bound antibodies were detected by anti-mouse-IgG-HRP followed by chemiluminescence with ECL reagents.

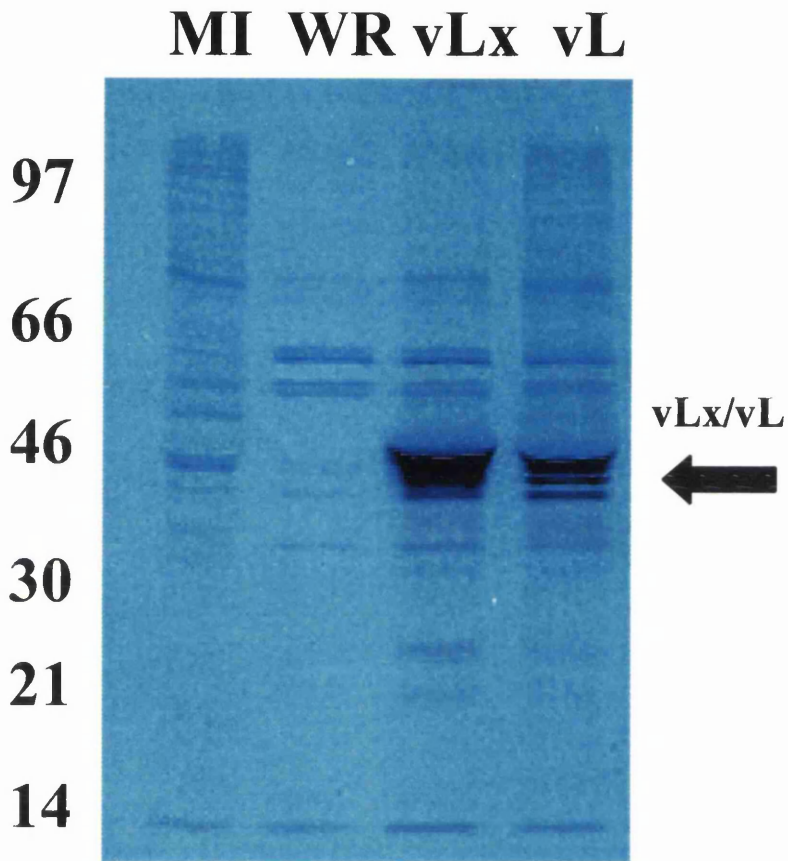


Figure 3.10. Immunoprecipitation of L and Lx by a cocktail of monoclonal antisera. HepG2 cells were mock-infected (lane 1) or infected at m.o.i. of 10 p.f.u./cell with WR (lane 2), vLx (lane 3) or vL (lane 4). At five hours post-infection the cells were labelled with methionine-deficient medium supplemented with ^{35}S -methionine. At 18 hours post-infection, the cells were harvested and lysed. The cell lysate was subjected to immunoprecipitation with a cocktail of hybridoma supernatants from cultures RC9, RC28, RC109 and RC152. The immune complexes were analysed by 10% SDS-PAGE and the radiolabelled proteins were detected by autoradiography. The combination of antibodies results in effective immunoprecipitation of the large surface antigen, with minimal reactivity with cellular or vaccinia proteins.

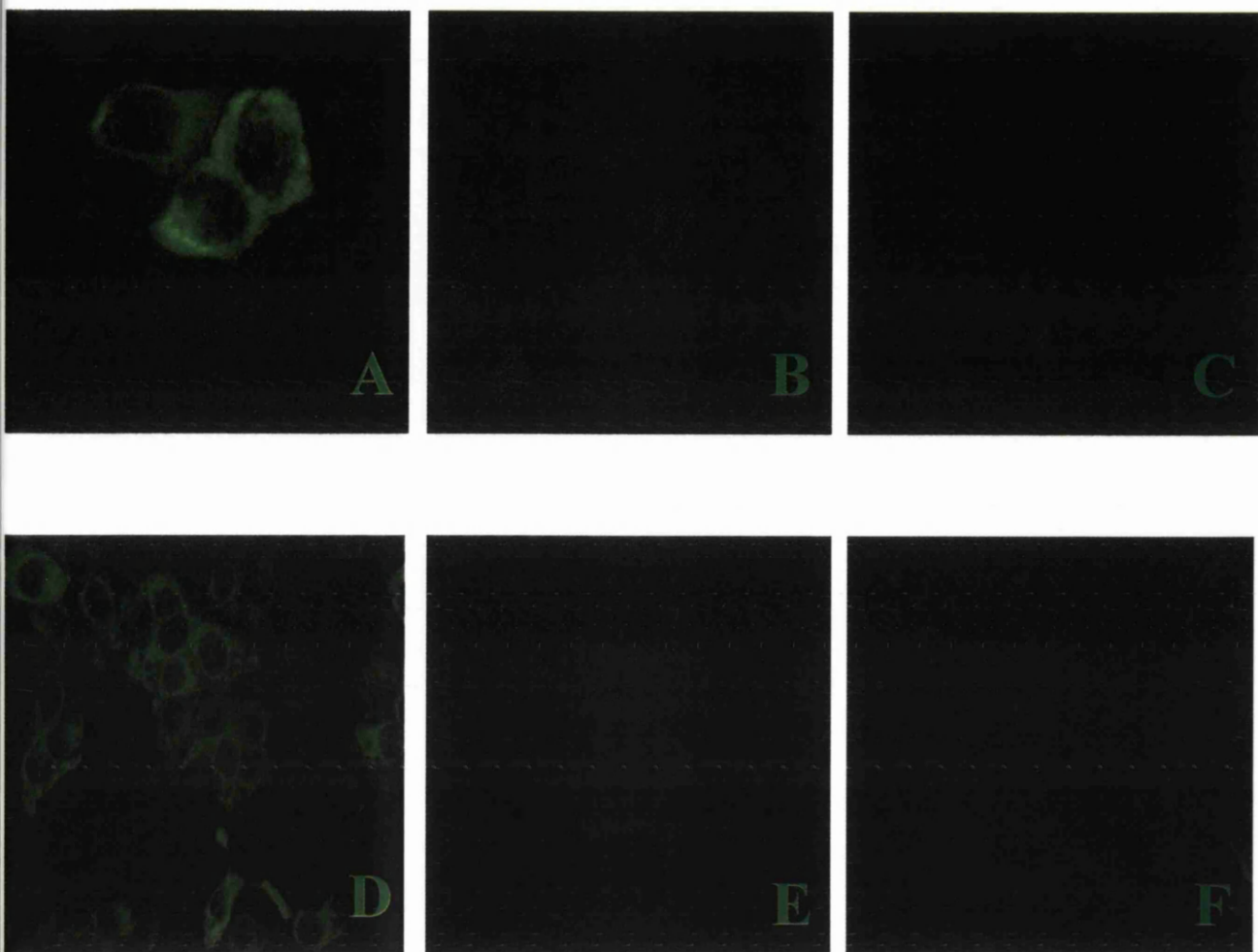


Figure 3.11. Characterisation of MAbs RC9 and RC28 by immunofluorescence. HepG2 cells on glass coverslips in 24-well plates were infected at an m.o.i. of 0.5 p.f.u./cell with the recombinant vaccinia virus expressing the Lx protein (vLx, Panels A and D) mock-infected (MI, Panels B and E) or wild-type (WR, Panels C and F). At 24 hours post-infection, the cells were fixed in methanol at -20°C , then permeablised in PBST. The cells were probed with a 1:1000 dilution of RC9 (panels A, B and C) or RC28 (panels D, E and F). The immunolabelled cells were detected with a 1:1000 dilution of anti-rabbit-FITC with a NIKON-Microphot microscope.

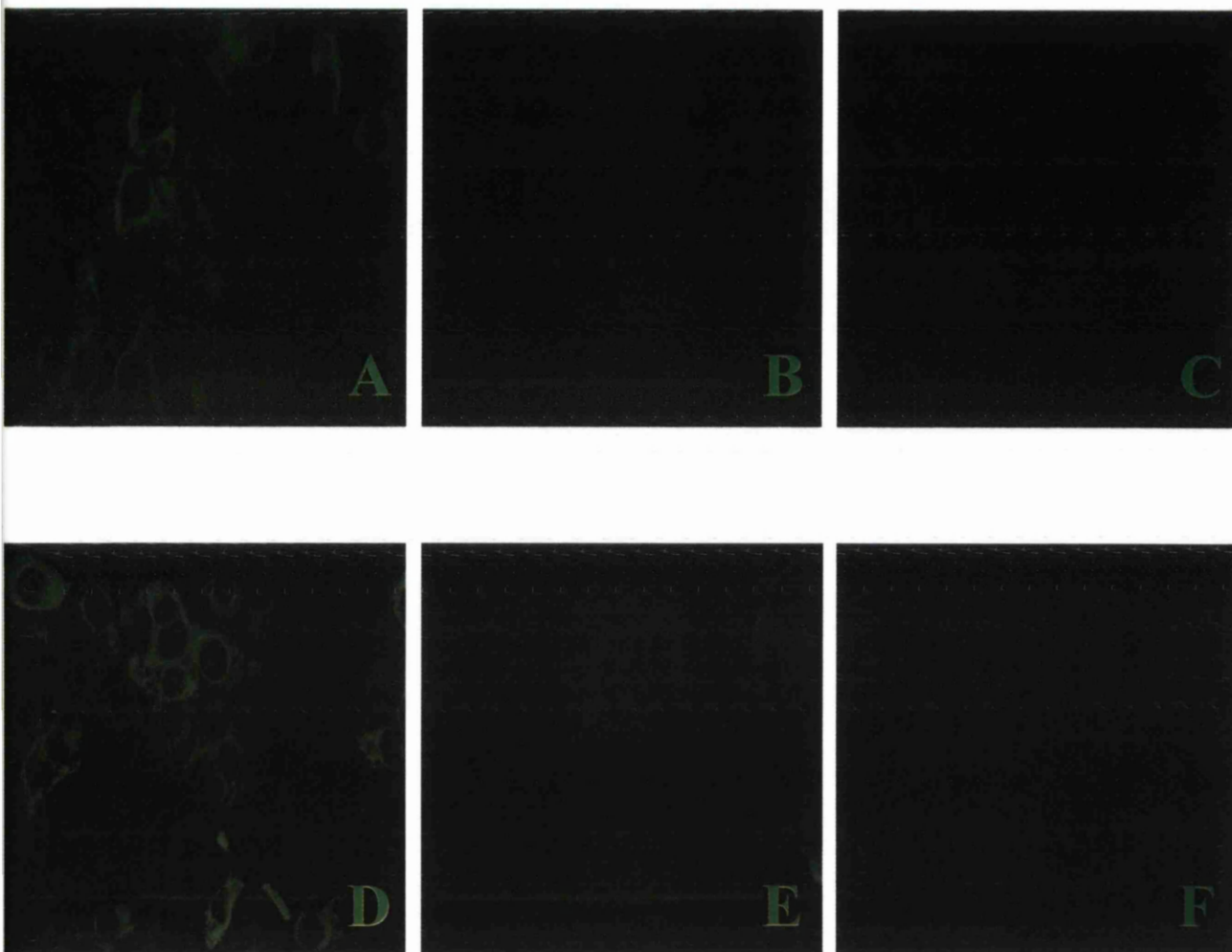


Figure 3.12. Characterisation of MAbs RC 109 and RC152 in immunofluorescence assays. HepG2 cells on glass coverslips in 24-well plates were infected at an m.o.i. of 0.5 p.f.u./cell with the recombinant vaccinia virus expressing the Lx protein (vLx, Panels A and D) mock-infected (MI, Panels B and E) or wild-type (WR, Panels C and F). At 24 hours post-infection, the cells were fixed in methanol at -20°C , then permeabilised in PBST. The cells were probed with a 1:1000 dilution of RC109 (panels A, B and C) or RC152 (panels D, E and F). The immunolabelled cells were detected with a 1:1000 dilution of anti-rabbit-FITC with a NIKON-Microphot microscope.

supernatants were used at a titre of 1:1000 in these assays, and also at 1:1000 for any other immunofluorescence assay during this work. The reactivity of the MAbs RC9, RC28, RC109 and RC152 against the Lx protein (which lacks a MRGS-6x His tag) confirms that these antibodies are directed against the preS1 domain of the L protein.

3.3.4. Monoclonal Antibody 6B1

A previously uncharacterised monoclonal antibody 6B1, raised against the Engeryx™ vaccine consisting of S, was kindly supplied by Dr. C. McCaughey of Queen's University, Belfast, UK. The MAb 6B1 was initially supplied as a hybridoma supernatant, and then as an ascites fluid, and was characterised by the author.

Initially, MAb 6B1 was tested in Western immunoblot for reactivity against S protein from cells infected with vS, but it consistently failed to show recognition (data not shown). This may have been due to amino acid differences between the S present in Engeryx™ preparation and that encoded by vS. Alternatively, it is possible that the MAb 6B1 recognises a conformational epitope in S. To ascertain if that is the case, MAb 6B1 was tested for its ability to specifically immunoprecipitate S. Radiolabelled proteins of HepG2 cells infected with vaccinia virus strain WR or vS were immunoprecipitated with MAb 6B1 and the immune complexes were analysed following SDS-PAGE. As shown in Fig. 3.13, MAb 6B1 specifically immunoprecipitated proteins of the characteristic double band at 25 and 27 kDa corresponding to the glycosylated and non-glycosylated forms of the S. These bands were not seen in the WR- or mock-infected cells, thus demonstrating the ability of MAb 6B1 to specifically immunoprecipitate S from clarified cell extract of S-expressing cells. This result was further confirmed in an immunofluorescence assay where S was clearly recognised by MAb 6B1 in HepG2 cells infected with vS (Fig. 3.14, panel A), but showed little or no discernible fluorescence in the WR or mock-infected samples (panels B and C). Although the fluorescence in this figure seems weak, it should be noted that the immunofluorescent microscope (NIKON Microphot-SA) was used for all of these initial characterisation experiments. Later work done with the Zeiss Laser Scanning Confocal Microscope portrays more accurately the immunofluorescent labelling characteristics of the MAb 6B1.

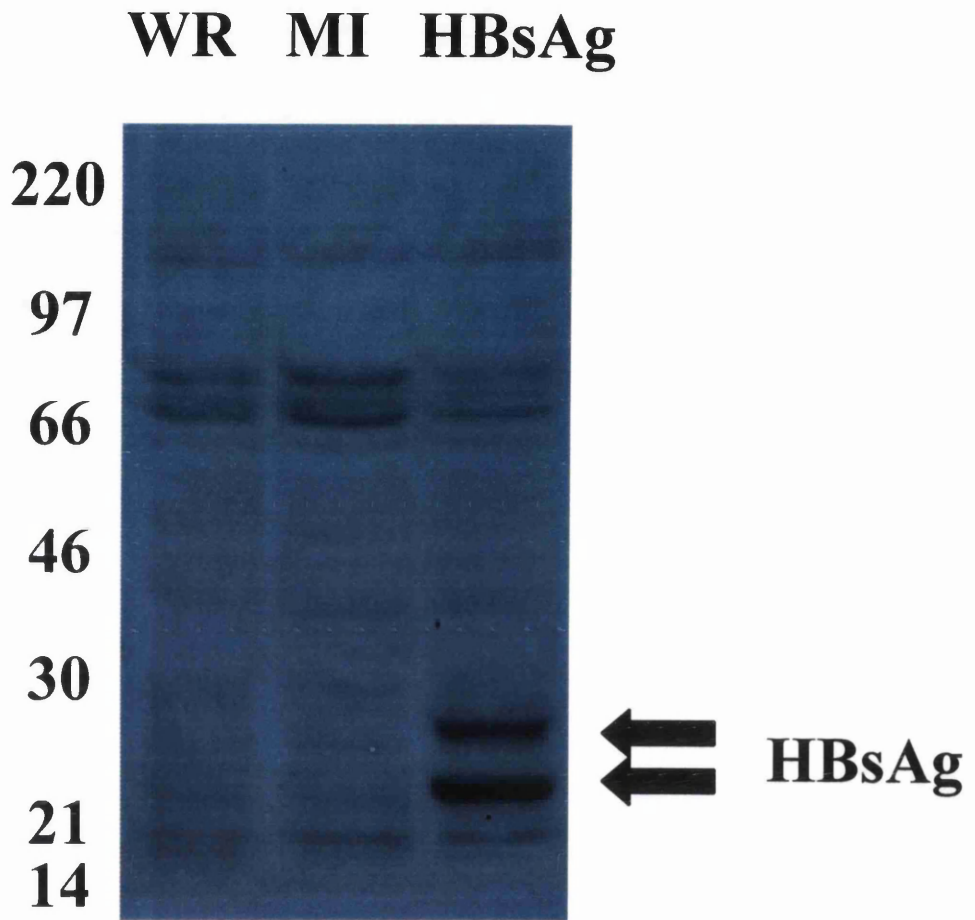


Figure 3.13. Characterisation of MAb 6B1 by Immunoprecipitation of HBsAg.

HepG2 cells were infected at m.o.i. of 10 p.f.u./cell with WR (lane 1), mock infected (lane 2) or vHBsAg (lane 3). At five hours post-infection the cells were labelled with methionine-deficient medium supplemented with ^{35}S -methionine. At 18 hours post-infection, the cells were harvested and lysed. The cell lysate was subjected to immunoprecipitation with the ascites fluid from culture 6B1. The immune complexes were analysed by 10% SDS-PAGE and the radiolabelled proteins were detected by autoradiography. There is clearly effective immunoprecipitation of the glycosylated and non-glycosylated forms of the surface antigen. There is minimal reactivity of the 6B1 ascites fluid with cellular or vaccinia proteins.

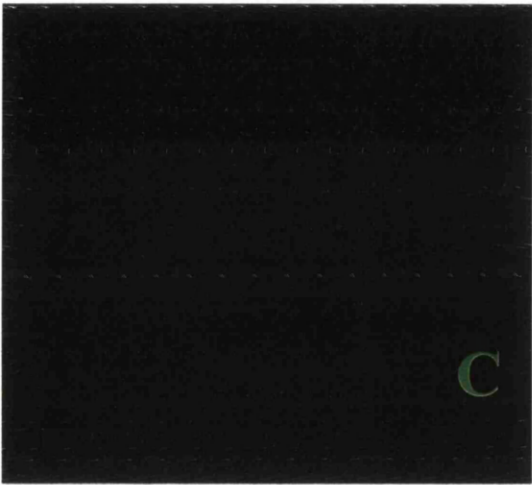
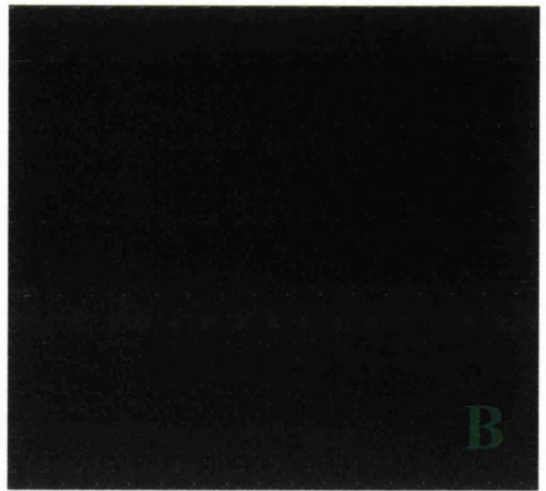
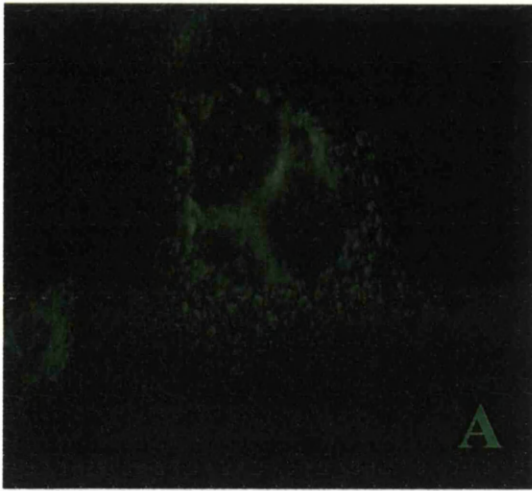


Figure 3.14. Characterisation of MAb 6B1 by immunofluorescence.

HepG2 cells on glass coverslips in 24-well plates were infected at an m.o.i. of 0.5 p.f.u./cell with vHBsAg, (Panel A) mock-infected (panel B) or WR (panel C). At 24 hours post-infection, the cells were fixed in methanol at -20°C , then permeabilised in PBST. The cells were probed with a 1:500 dilution of MAb 6B1. The immunolabelled cells were detected with a 1:1000 dilution of anti-rabbit-FITC with a NIKON-Microphot microscope.

Taken together, the above results show that the inability of MAb 6B1 to recognise S is not due to amino acid difference between the antigen used to immunise mice and that expressed by vS, but rather it recognises a conformation-dependent epitope in S.

3.3.5. Isotype determination

Assessment of the isotype of immunoglobulin expressed by each of MAbs RC9, RC28, RC109 and RC152 was performed using a commercially available mouse antibody testing kit (Sigma, UK), according to the manufacturer's instructions. All of the monoclonal antibodies were found to be of the IgG1a subtype.

3.4 Peptide characterisation

The production of short peptides corresponding to overlapping regions of the preS1 domain was undertaken in order to facilitate epitope mapping of the MAbs generated here. A series of eight peptides, mostly of 20 residues with an overlapping 5 residue region at the C-terminus corresponding to the N-terminal 5 residues of the next peptide in the series were synthesised and purified (see Materials and Methods).

Following purification of the peptides by reverse-phase High Performance Liquid Chromatography, the analysis of the molecular weight of the peptides was undertaken to ensure the correct fractions had been recovered. A typical example of one peptide being analysed in order to establish its molecular weight is portrayed in Fig. 3.15. Two control peptides of known molecular weight, corresponding to segments of the reverse transcriptase of human immunodeficiency virus were included in all samples to enable the calibration of the instrument and also to serve as internal controls throughout the course of the determination of multiple samples. The amino acid sequence of the overlapping peptides is shown in Table 1. The results from the analysis of the molecular weights of the peptides and the comparison of the expected and observed molecular weights are shown in Table 1. All of the peptides synthesised, purified and characterised here were of the expected molecular mass, and were soluble in water.

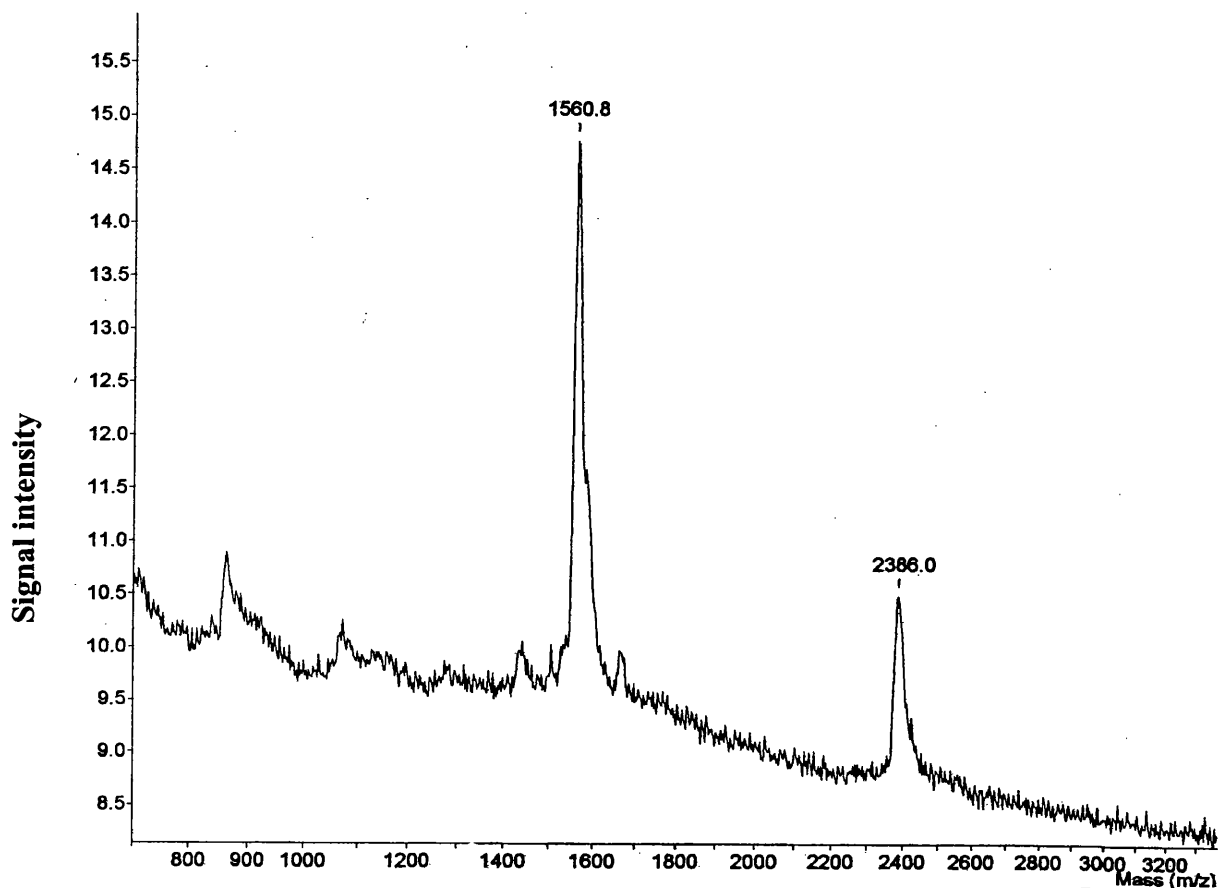


Figure 3.15. Determination of molecular weights of the purified peptides

The molecular weight of purified peptides was assessed by comparison with two peptide standards of known molecular weight by using a Mass Spectrometer. Here, an example of one analysis of a newly synthesised and purified peptide (1123b) shows the observed molecular mass of 2386.0. The peak at 1560.8 mass units is due to the presence of an internal control peptide corresponding to a portion of the reverse transcriptase of HIV-1. The observed molecular weight of peptide 1123b correlated well with the expected molecular mass of 2386.5. The molecular weights determined for the remainder of the series of peptides produced in this work were very close to the expected values (see table 1).

<u>Peptide</u>	<u>aa sequence</u>	<u>M. Wt.</u>	<u>solubility</u>	<u>charge</u>
1123a	MGQNLSTSNPLGFLPDHQLD	2217.6 (2225.8)	+	-1
1123b	DHQLDPAFRANTNNPDWDFN	2386.5 (2386.0)	+	-2
1123c	TNNPDWDFNPKKDPWPEANK	1818.9 (1824.0)	+	-2
1123d	PKKDPWPEANKVGVGAYGPG	2298.5 (2314.5)	+	-1
1123e	AYGPGFTPPHGLLGWSPQS	1880.2 (1882.0)	+	+2
1123f	WSPQSQGTLTTLPADPPAS	1998.2 (2009.8)	+	-1
1123g	PPASTNRQS GRQPTPISPP	2090.3 (2362)	+	+2
1123h	PISPPLRDSHPQA	1953.2 (1952.9)	+	+2
21-47	PLGFLPDHQLDPAFGANSTNPDWDFNPY			

Table 1 Peptide production, purification and characterisation.

The design and characterisation of the peptides is portrayed above. The molecular weights of the peptides obtained after HPLC purification is shown, the first of the figures being the expected molecular weight of the peptide as calculated from the amino acid composition, the figures in parenthesis are the observed molecular weights following determination by mass spectrometry. In most cases, the observed and expected values are within the limitations of the sensitivity of the instrument (10 mass units). The peptides were all soluble in distilled water. It should be noted that peptide 21-47 was produced by Dr. A. Owsianka prior to the commencement of this work. The sequence for peptide 21-47 corresponds to the receptor binding region and is derived from data published by Gerlich *et. al.* 1993.

3.5. Epitope Mapping of MAbs

Epitope mapping of the monoclonal antibodies was performed so that the residues of the preS1 domain each antibody is reactive with could be delineated. An ELISA-based peptide-inhibition-binding assay was used to competitively inhibit the binding of the antibody to the immobilised preS1 domain with the peptide that contains the reactive residues (see Materials and Methods). Briefly, the wells of a 96-well Immulon II microtitre plate were coated with 125 ng of preS1 domain. Unbound preS1 domain was removed by washing with PBST buffer. Peptides 1123A to H were added to the wells in 0, 10, 100 and 1000-fold molar excess in volumes of 100 μ L for the inhibition assays. The MAbs RC9, RC28, RC109 or RC152 were incubated along with the peptides for two hours. The wells were washed with PBST and anti-mouse IgG-HRP was added to the wells for one hour. The unbound secondary antibody was washed away with PBST and the chromogenic substrate was added and the intensity determined in an ELISA plate reader. The inhibition of recognition of preS1 domain by MAbs RC9, RC28, RC109 and RC152 can be seen in Fig. 3.16 A to D. The inhibitory peptide responsible for abrogation of binding of MAbs RC9, RC28, RC109 and RC152 to preS1 domain is identified as 1123B in all cases. The inhibition by 1000x molar concentration of the inhibiting peptide 1123B resulted in almost complete abrogation of binding of the MAbs to the immobilised preS1 domain. Aside from 1123B, no other peptides were capable of an inhibitory effect on the binding of the MAbs to the preS1 domain, therefore, all of the MAbs are found to be reactive to residues contained within the positions 15-35 of the preS1 domain. However, due to the overlapping design of the peptides, it could be suggested that the residues 15-20 are not involved in binding the MAbs, as the peptide 1123A did not inhibit binding, and furthermore, the peptide 1123C (residues 30-45) did not inhibit binding. Thus, it could be suggested that the minimal epitopes for reactivity of the MAbs lie between the residues 20-30. Furthermore, the MAb 18/7 was assessed for reactivity to its epitope (Fig. 3.16E) by the same method of inhibition by increasing concentrations of inhibitory peptide and was also found to be reactive to the region of the preS1 domain represented by the 1123B peptide. This is in agreement with (Heermann *et al.*, 1984) data which mapped MAb 18/7 to the PAFRAN epitope.

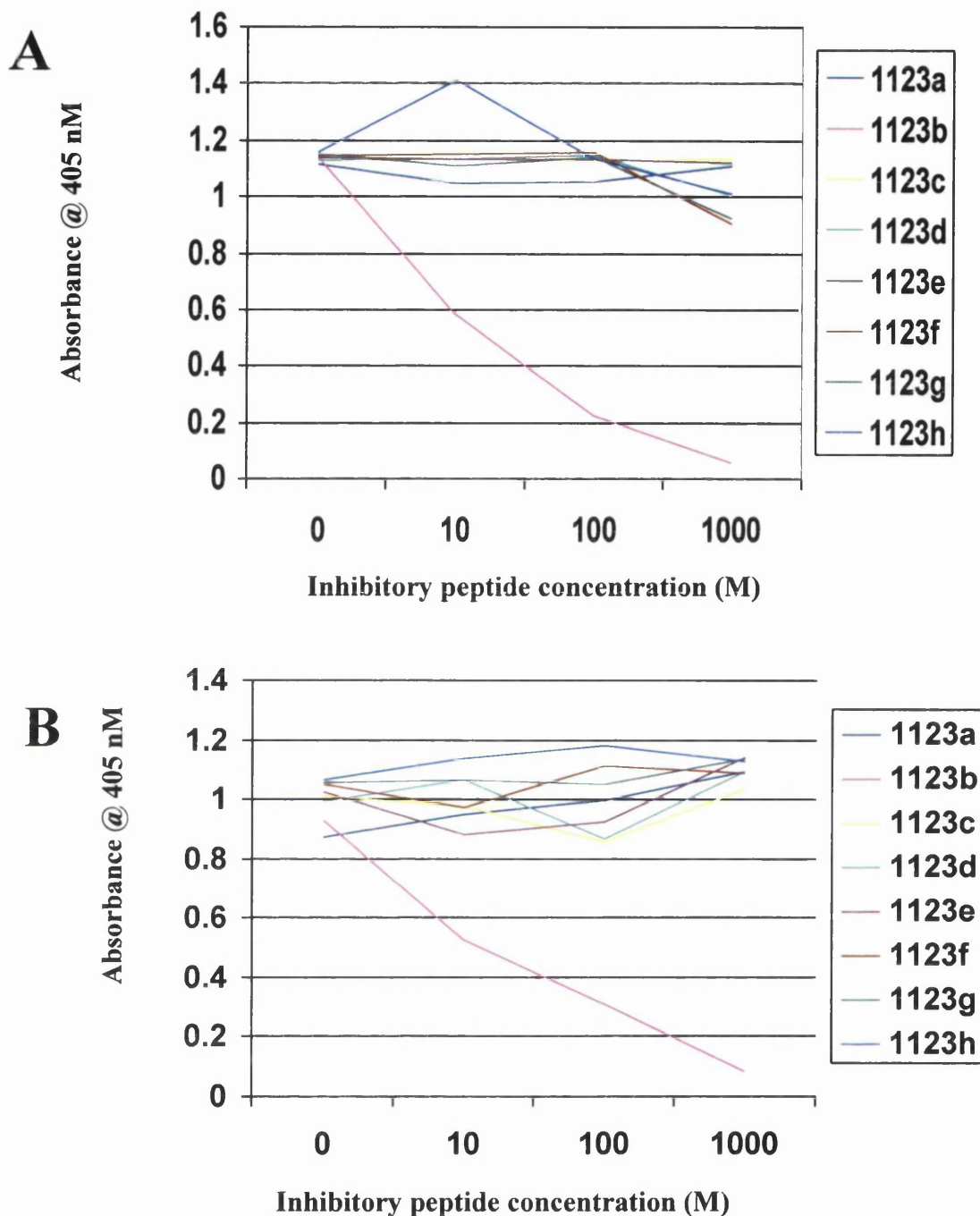


Figure 3.16 A and B. Epitope mapping of MAbs RC 9, RC28, RC109, RC152 and MAb 18/7 with inhibitory peptides.

96-well plates were coated with 125 ng of preS1 domain, overnight at room temp. The next day, the wells were blocked with 2% BSA in PBSA. The monoclonal antisera RC9 (panel A), RC28 (B), RC109 (C), RC152 (D) and MAb 18/7 (E) were added to the wells in the absence of peptides 1123a-h, or in the presence of 10, 100 or 1000x molar excess of peptides 1123a-h. The antisera were also incubate in the presence of 1000x molar excess of peptides corresponding to epitopes not present on the preS1 domain (panel F). The unbound complexes were washed from the plate and the bound antibodies detected by anti-mouse IgG-HRP and the chromogenic substrate ABTS.

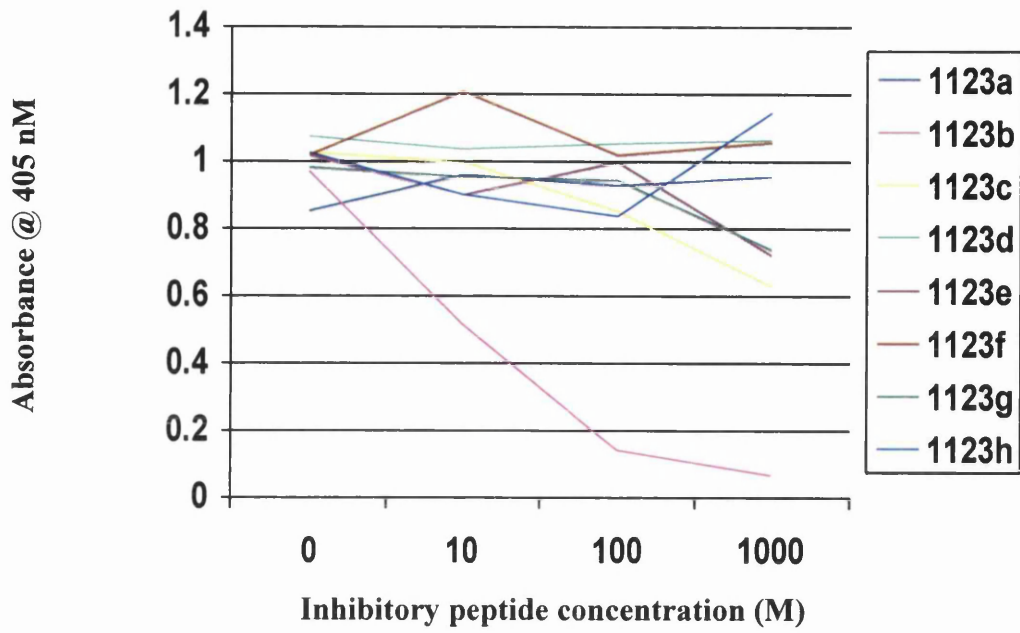
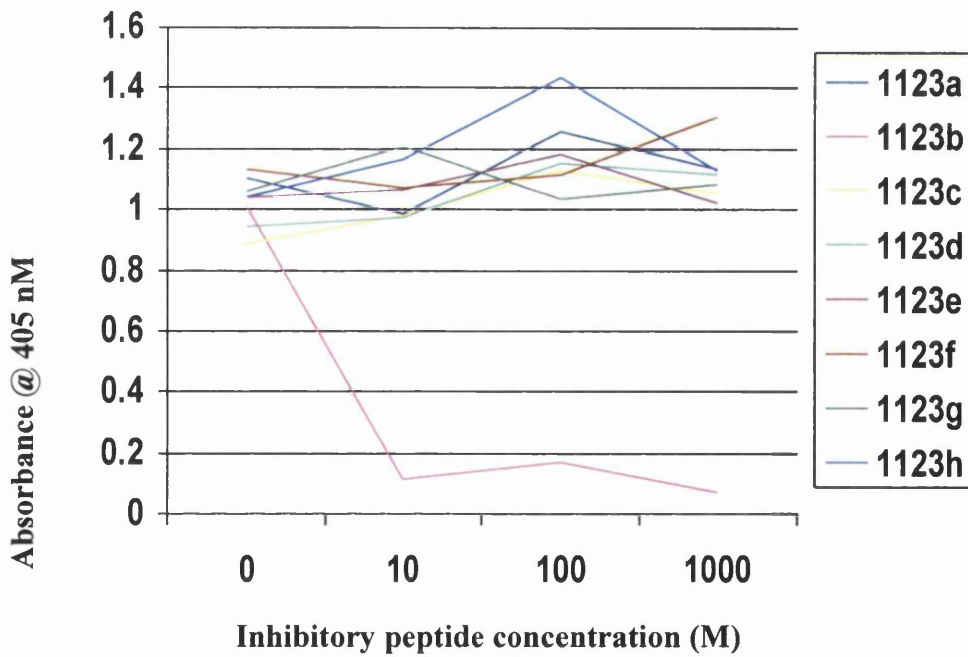
C**D**

Figure 3.16 C and D. Epitope mapping of MAbs RC 9, RC28, RC109, RC152 and MAb 18/7 with inhibitory peptides (continued).

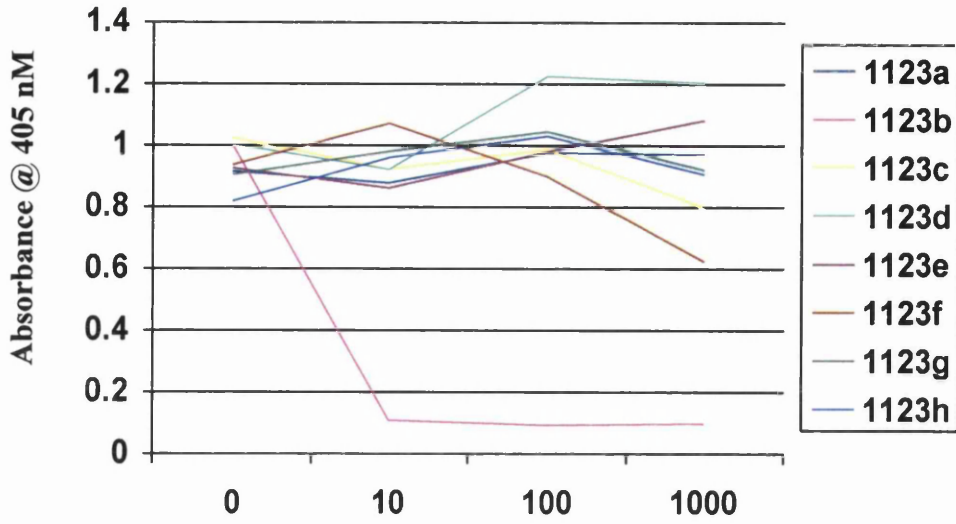
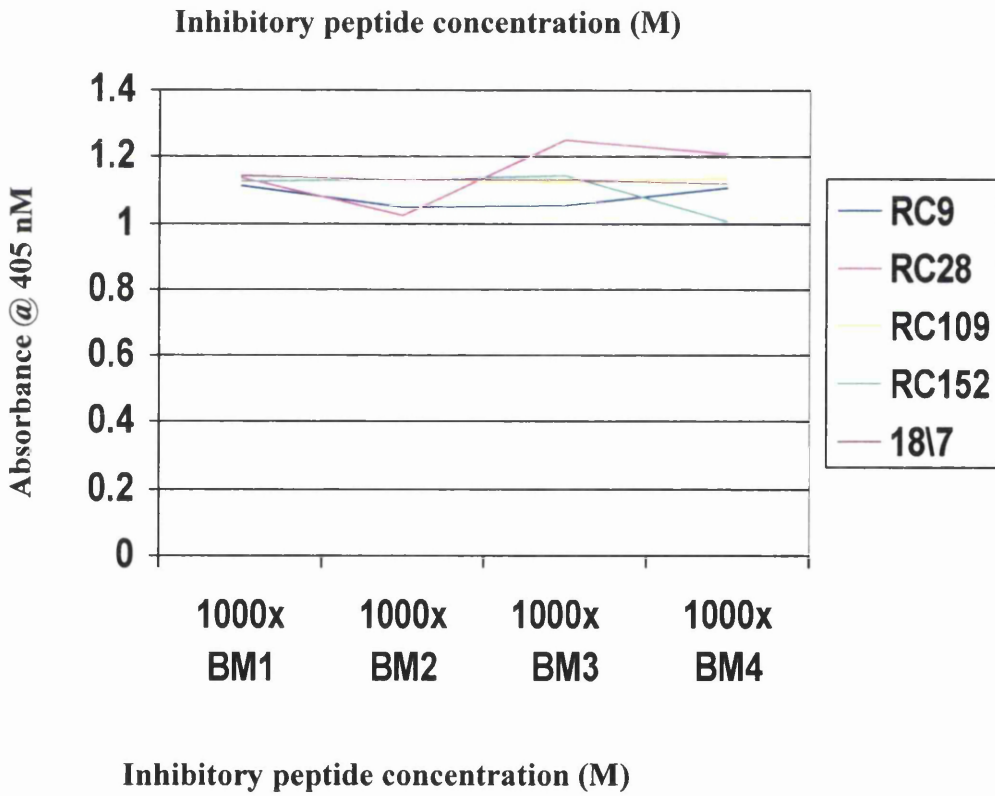
E**F**

Figure 3.16 E and F. Epitope mapping of MAbs RC 9, RC28, RC109, RC152 and MAb 18/7 with inhibitory peptides (continued).

For a further control study, four peptides were obtained from Dr. W. F. Carman's laboratory, corresponding to the hydrophilic regions of the S. Each antibody mixed with a 1000x molar concentration of the S peptides was tested for reactivity to the immobilised preS1 domain. As expected, the peptides failed to block MAb recognition of preS1, indicating that the peptide 1123B-mediated inhibition of preS1 recognition by MAbs RC9, Rc28, RC109, and RC152 not due to non-specific interactions with a peptide not representing a portion of the preS1 domain (Fig. 3.16F).

Taken together, these data show that the four MAbs generated and characterised here are reactive to regions in the preS1 domain that are represented by the 1123B peptide. Thus, the four anti-preS1 MAbs used in this study are reactive to linear epitopes of the preS1 domain.

3.6 Purification of MAb RC28.

The MAb RC28 was purified in order to obtain a preparation of antibody that was free from contaminants such as bovine IgG. It was considered desirable to purify RC28 in order to obtain a pure monoclonal antibody to use in ligand-binding assays. It should be noted that the co-purification of bovine IgG with mouse IgG would possibly interfere in binding assays where the sensitivity of the assays could be crucial, therefore purification of RC28 from serum-free medium was undertaken.

Large-scale purification of the MAb RC28 from serum-free hybridoma medium (Gibco) was undertaken, and the purification profile is depicted in Fig. 3.17. Briefly, the serum-free supernatant was dialysed against 20 mM phosphate buffer then filtered before pumping onto a protein-G Superose column (Pharmacia), washing in phosphate buffer, and fractional elution by Glycine at pH 2.7 into tubes containing neutralisation buffer (see Materials and Methods). The elution of the MAb RC28 is apparent from the UV absorbency at 280 nm, at position C on Fig. 3.17. This antibody was dialysed against PBSA after neutralisation of the glycine with Tris-HCl buffer in order to minimise pH-dependent degradation of the immunoglobulin over time. This purified antibody preparation was used chiefly for flow cytometry-based ligand binding assays to investigate the binding of the preS1 domain to plasma membranes (See chapter 7).

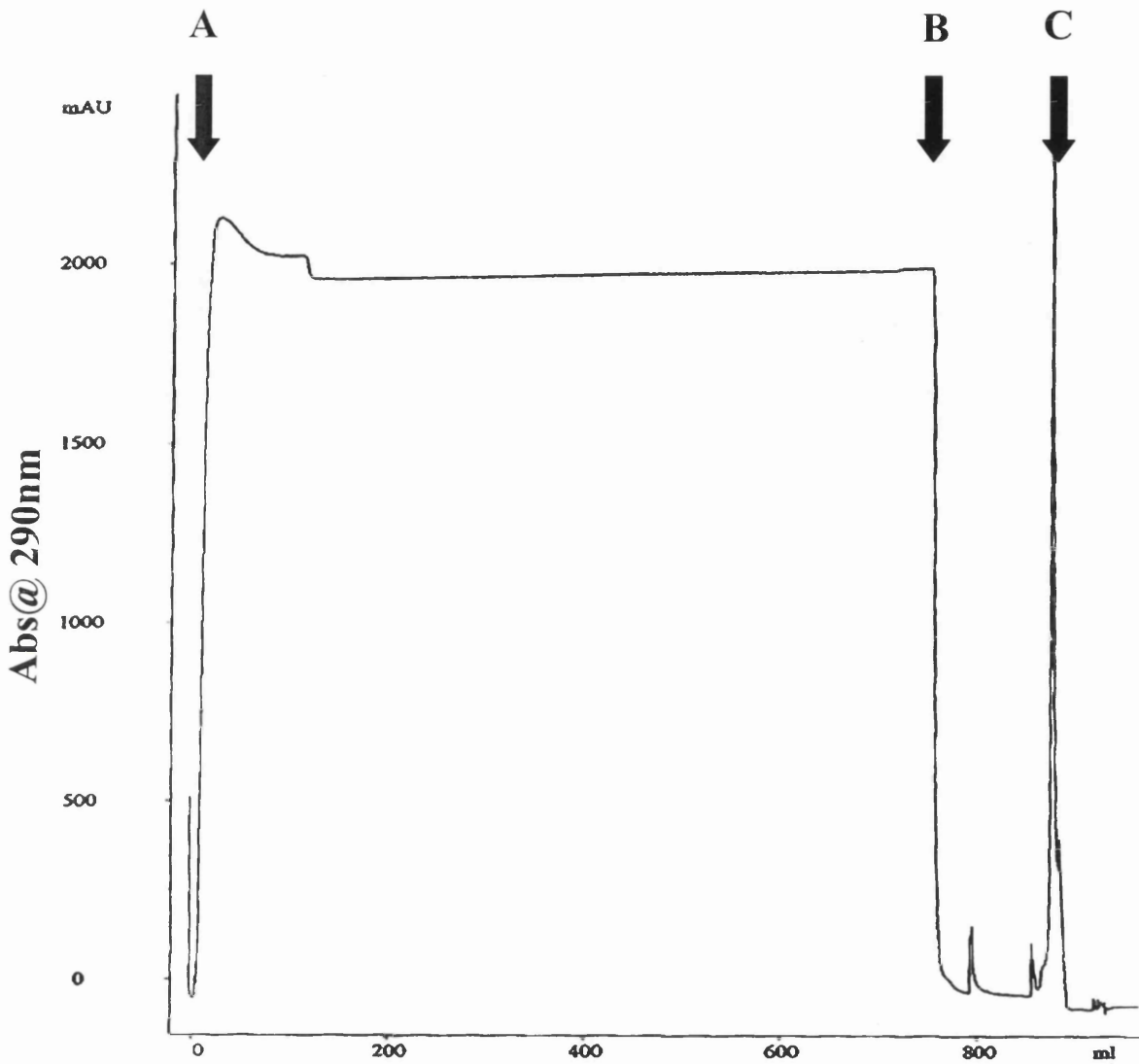


Figure 3.17. Purification of MAb RC28 from serum-free medium.

Hybridoma cells of culture RC28 were grown in T175 flasks in serum-free medium. After 10-14 days of incubation, the medium was harvested and clarified, then dialysed against 20 mM phosphate buffer at pH7.0 then was pumped on to a protein G column (Sigma) starting at point A, the column was washed in 20 mM phosphate buffer (point B) and the antibody was eluted in glycine at pH2.7 (point C). The MAb was eluted in 1 mL aliquots and added to Tris-HCl at pH9.0 and mixed thoroughly. The eluted MAb was dialysed against three changes of PBSA at 4° C, and stored in 1 mL aliquots at 4°C.

3.7 Preparation and Characterisation of Proteins for Ligand-Binding Assays.

The use of ligands representing the surface proteins of viruses has been employed successfully by many researchers to elucidate mechanisms of viral entry and also in the identification of cellular receptors for viruses (Flint *et al.*, 1999; Higginbottom *et al.*, 2000). This section describes the preparation and characterisation of various proteins that were used later in binding assays. The preparation of a variety of ligands was undertaken in order to assess the binding of each ligand to the plasma membranes of cells, but also to provide more than one means of examining the ligand-cell interaction for HBV surface antigens. The ligand most often used in this work was the preS1 domain described in section 3.1. This ligand was purified in milligram amounts and used in flow cytometry and other assays (see Chapter seven) to investigate the binding to cells. Another ligand, HepB3, was a kind gift from Medeva, UK. The HepB3 preparation consists of recombinant S particles carrying the amino acid 21-47 region of the preS1 domain into one of the hydrophilic loops. The HepB3 is intended for vaccine use, but was evaluated here as a ligand in flow-cytometry assays.

The surface iodination using ^{125}I of the preS1 domain and the HepB3 preparation was undertaken in order to provide radiolabelled ligands for use in cell binding assays, and the autoradiograph profile of the labelled proteins was examined. This was to ensure that the iodination has worked and that the proteins had remained intact during this procedure. As shown in Fig. 3.18A, a major band of 21 kDa or 14 kDa of HepB3 particle or preS1 domain was seen, and there was no indication of apparent degradation of the proteins. The HepB3 preparation was used for iodination as supplied by the manufacturer, and is seen here in Fig. 3.18A to be composed of a number of proteins, two of which resemble the S dual bands thought to be the glycosylated and non-glycosylated form. The higher bands at around 40 kDa in Fig. 3.18A are presumably the preS1 21-47-region-containing versions of the recombinant S that form part of the particle. The HepB3 preparation is expected to contain particles consisting of S alone or S carrying the preS1 21-47 amino acid region (personal communication, Medeva Plc).

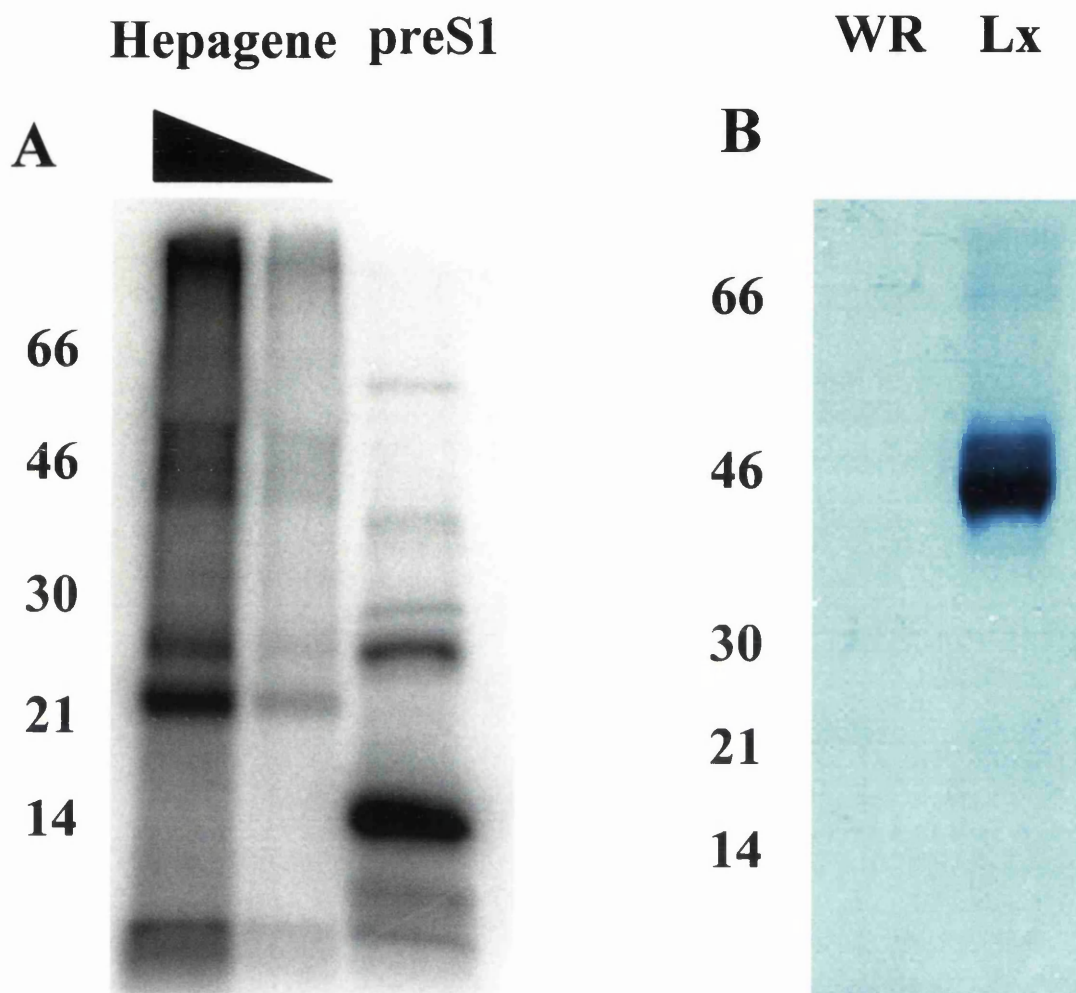


Figure 3.18. Characterisation of proteins used in ligand-binding assays.

Samples of the Hepagene protein (Medeva, UK) and the preS1 domain were radiolabelled with ^{125}I (see Chapter 2) and subjected to 10% SDS-PAGE to examine the integrity of the proteins (panel A). BHK cells were cultured in roller bottles to about 60% confluence, then were infected at a m.o.i. of 0.1 p.f.u./cell with WR or vLx, and the infections were allowed to proceed until complete c.p.e. was observed. The medium from the infected cells was harvested and clarified, then overlaid on a 40% w/v sucrose cushion and centrifuged at 18000 rpm in a AH629 rotor (SORVAL) at 4°C for 4 hours. The pellet was resuspended in PBSA and centrifuged through a 15-30% continuous sucrose gradient for 2 hours at 35000 rpm in a TST41 rotor (SORVAL). The gradients were fractionated and analysed by Western blot for the presence of Lx. Fractions containing the Lx protein were bulked and stored at -20°C, as were the corresponding fractions from WR-infected samples. The bulked samples were analysed for the presence of Lx by Western blot with MAb RC28 (panel B).

In addition to having radiolabelled ligand described above, it was also desirable to have a relatively pure form of the Lx protein. In order to obtain this preparation of the Lx protein, roller bottles containing BHK cells were infected at a high m.o.i. with Lx or WR and incubated until all cells exhibited c.p.e. The medium from the infected cells containing the secreted Lx protein was clarified and the secreted proteins centrifuged at 18,000 r.p.m. in a AH629 rotor onto a cushion of 40% w/v sucrose. The pelleted material was then centrifuged through a continuous gradient of 15-30% w/v sucrose and removed in 1 mL aliquots (see Materials and Methods) and analysed by Western blot for the presence of vLx. The demonstration of this protein by Western blot is necessary due to the low concentration of Lx in the preparation, and the relatively high amount of co-purifying proteins. The enriched preparation of vLx obtained for infected cell supernatant was shown to contain a protein reactive with the MAb RC28 at a molecular weight of 42 kDa (Fig. 3.18B). The centrifugation procedure provided a means of enrichment for Lx, but could not be described as an effective purification. The medium from cells infected with WR was treated in the same way as the vLx-infected cell medium in order to provide negative controls for binding experiments.

3.8 Discussion.

In order to achieve the aims and objectives of this project, several important reagents were generated. The structural components of HBV were expressed in bacterial and recombinant vaccinia virus system. The preS1 domain was produced from a bacterial expression system, and was purified to near homogeneity by single-step affinity chromatography. The authenticity of the bacterially expressed preS1 domain was confirmed in Western blot assay using a well-characterised monoclonal antibody, MAb 18/7. The purified preS1 domain was used to (1) raise both polyclonal and monoclonal antibodies to the HBV L protein, and (2) map the epitopes recognised by the anti-preS1 MAbs.

Both polyclonal antibodies generated reacted specifically to HBV L protein in Western blot, immunoprecipitation, and immunofluorescence assays. Similarly, the four anti-preS1 monoclonal antibodies generated reacted specifically to L in both Western blot and immunofluorescence assays. However, the reactivity of the monoclonal antibodies in immunoprecipitation assays when used singly was

disappointingly poor. In contrast, when used as a cocktail, they efficiently immunoprecipitated the L and Lx proteins with minimal reactivity with other cellular or viral proteins from cells infected with the appropriate recombinant vaccinia virus. To map the epitopes recognised by the anti-preS1 MAbs, a series of eight peptides representing overlapping regions of the preS1 domain were synthesised, purified and characterised. All four monoclonal antibodies were found to be of isotype IgG1, and the reactivity of all to the pre-S1 domain was blocked by the synthetic peptide 1123B representing amino acids 15-35. The peptides generated here were also tested for their ability to block preS1 binding to putative cell surface receptor(s) (see Chapter 6).

The structural antigens (L, M, S, and core) of HBV were expressed in their full-length form using a recombinant vaccinia virus system. The recombinant vaccinia viruses were initially characterised for expression of appropriate HBV proteins using specific antibodies in both Western blot and immunofluorescence assays. The vaccinia virus-expressed structural antigens were also analysed with the anti-preS1, -preS2, -S and anti-core monoclonal and polyclonal antisera generated here (for L and Lx) and/or those obtained from elsewhere. The molecular masses of the L, Lx, S, and core proteins were in agreement with those observed by others using similar expression systems (Xu, *et. al.*, 1997). In contrast to L, the Lx protein was shown to be secreted from expressing cells (see Fig. 3.3A). This is due to the gene encoding Lx carrying a heterologous secretion signal sequence. The monoclonal antibody, MAb 6B1, although generated elsewhere (Connal McCaughey, Queen's University, Belfast) was characterised for the first time for reactivity against the small surface antigen. Interestingly, this MAb was found to be reactive with a conformational-specific epitope on S. To the author's knowledge, there are no other conformation-dependent monoclonal antibodies in existence that are capable of distinguishing between the surface antigens of HBV. This novel reagent represents a valuable tool by which the structures of the surface antigens can be investigated. Further detailed characterisation of intracellular behaviour of these proteins using the antibodies described here is presented in Chapter 6. Taken together, the characterisation data prove that the reagents generated here are reactive to the HBV structural proteins. Furthermore, as shown in the following Chapters, they have proven extremely useful tools for pursuing the aims of this project.

Chapter 4

Generation and partial characterisation of novel hepatocyte-derived cell lines

Hepatitis viruses such as HBV and HCV are refractory to growth in tissue culture, which has hampered advances in understanding virus-host interaction, replication, and pathogenesis. The generation of immortal cell lines that retain hepatocyte phenotype has remained an important aim not only for virologists, but also for cell biologists and toxicologists. There is an enormous scope for the use of cell lines that closely resemble the hepatocyte phenotype, as such cell lines could be considered as a proper host for carrying out functional analysis of HBV proteins, and moreover, they may support efficient replication of the virus.

Primary hepatocytes do not divide in culture, but they can be maintained for several weeks in maintenance medium in which it is necessary to include a number of reagents to retain the hepatocyte phenotype (Runge *et al.*, 1999). The inclusion of certain growth factors, hormones (e.g. epidermal growth factor and hepatocyte growth factor) and dimethyl sulphoxide (DMSO) has been reported to assist in the retention of the hepatocyte phenotype, and withdrawal of DMSO from the medium has been documented to result in the appearance of a fibroblastic phenotype. Clearly, for hepatitis virologists interested in delineating the mechanisms involved in hepatocellular tropism, the retention of the hepatocyte phenotype in cultured cells is important: it is likely that fibroblasts will not express the liver-specific genes whose products are involved in the hepatocyte-specific processes. Furthermore, the omission of culture medium components that could interfere with viral entry (such as DMSO and polyethylene glycol) is desirable (Gripon *et al.*, 1988). Therefore, the immortalisation of hepatocytes could be employed as a means of retaining the hepatocyte phenotype without the use of DMSO, and enabling the establishment of cultures from non-tumour cells. The hepatocyte cell lines HepG2, Huh7 and WRL68 are derived from hepatoblastoma, hepatocellular carcinoma and fetal liver cancer, respectively. Thus, the expression of liver-specific genes in those tumour cell lines could be greatly different to that observed in cell lines derived from healthy

hepatocytes. These cell lines have been shown to replicate HBV and produce progeny virus when infected with HBV (Bchini *et al.*, 1990) and/or when transfected with infectious viral DNA (Mabit *et al.*, 1994), however, the efficiency of infection remains low and is subject to considerable variation.

Primary hepatocytes derived from normal human liver were immortalised by retrovirus-mediated transduction of human papilloma virus type 16 E6 and E7 transforming proteins (A. Patel, unpublished). Several cell lines were established which were able to grow both in serum-free, defined medium (see Materials and Methods) as well as serum containing medium. The cell lines were initially grown in defined medium lacking serum for ten passages and cryopreserved stocks were generated. It was found necessary to coat culture vessels with a preparation of collagen under serum-free conditions in order to provide the cells with an acceptable matrix for growth. However, when DMEM was used as the culture medium, there was no requirement for collagen coating of the growth surfaces of the culture vessels, and the coating step was omitted. The culture medium for the growth and maintenance of the novel hepatocytes during the studies performed here was changed from the defined medium to DMEM and the cultures propagated in the same manner as established cell lines HepG2 and COS-7. Two immortalised hepatocyte cell lines, H5 and H16, which were among the cell lines that were viable after many passages, were used in this study. These cell lines were assayed for some markers of hepatocyte phenotype, and were compared with the established hepatocyte cell line HepG2, and also compared with a non-human, non-hepatocyte cell line COS-7 (African Green Monkey kidney). Here, the generation and initial characterisation of the cell lines by immunofluorescent analysis with specific antisera to certain cell proteins is described. The antisera used for testing the cell lines are as follows: monoclonal antibodies to Cytokeratins 8 and 18, annexin V, albumin, alpha-fetoprotein, alpha-1-antitrypsin and apo-lipoprotein 1a. These were used as part of the initial characterisation of the cell lines because they were readily available to us, but it is important to point out that these markers are only a small proportion of the markers that are routinely used by hepatologists to characterise hepatocyte-specific gene expression.

4.1 Analysis of novel and established cell lines for expression of hepatocyte-specific proteins.

4.1.1. Cytokeratins 8 and 18.

The expression of cytokeratin 8 and 18 has been shown to be specific to a number of cell types, particularly liver and liver-derived tumours (Blaheta *et al.*, 1998), however, there is an absence of cytokeratin 8 and 18 from fibroblasts (Tsuji *et al.*, 1999). Therefore, the analysis of expression of the cytokeratins 8 and 18 affords a means of distinction between fibroblasts and hepatocytes. All the cell lines used in this study were evaluated for the expression of human cytokeratin 8 and cytokeratin 18. As shown in panels A, B, C and D, of Figs. 4.1, 4.2, and 4.3, monoclonal antibodies against human cytokeratin 8 and 18 show clearly the plasma membrane distribution and cytoplasmic expression of cytokeratins 8 and 18 in HepG2, H5 and H16 cell lines. The fluorescence from the H5 and H16 cell lines compares well with the positive controls for the hepatocytes (HepG2). There is a small degree of plasma membrane fluorescence in some of the hepatocyte-derived cell lines. That the presence of both cytokeratins 8 and 18 is evident in the H5 and H16 cell lines suggests that these cell lines have not reverted back to the fibroblast phenotype that occurs commonly in hepatocyte-derived cell lines (Gripon, *et al.*, 1993). As expected in COS-7 cells, no intracellular expression of cytokeratin 8 or 18 was seen, however, both antibodies reacted very weakly with plasma membrane proteins (Fig. 4.1, Panels A to D). It is not clear whether the antibodies were recognising COS-7-specific cytokeratin 8 and 18 or they were binding non-specifically to cell membrane proteins (Fig. 4.4, Panels A to D). It is also possible that this weak signal may be due to autofluorescence.

4.1.2 Albumin.

HepG2, H5, H16, and COS-7 cells were tested for albumin expression by confocal microscopy. Cells grown on glass coverslips were fixed, permeabilised, probed with anti-human albumin MAb followed by FITC-conjugated anti-mouse IgG, and analysed by confocal microscopy. As shown in panel F of each of Figs. 4.1 to 4.4, no albumin expression on any of the cells tested, including HepG2 which are known to express albumin, (Molina *et al.*, 1997) was detected. Given that HepG2 cells were negative for albumin expression, it would appear that the anti-albumin MAb or the

assay chosen here to detect the expression of the albumin might be inappropriate. Therefore, the immunofluorescence results shown in panel F of Figs. 4.1, 4.2, 4.3 and 4.4 are inconclusive. Further examination, of these cells is necessary, probably by analysis of albumin-mRNA to establish the absence or expression of albumin.

4.1.3. Alpha-fetoprotein.

Alpha-fetoprotein (AFP) is a useful clinical marker of HCC. It is known that 75% of HCC patients have serum levels of AFP in excess of 10 ng/mL (Johnson, 1999). The association of AFP with induction of the apoptotic pathway has been established in HepG2 cells (Semenkova *et al.*, 1997). The HepG2 culture is known to be positive for AFP (Semenkova *et al.*, 1997), and the location of AFP in the liver cell has been identified as the endoplasmic reticulum (Sato *et al.*, 1998). It has been shown that there is a relationship between the effect of tumour necrosis factor (TNF) and the presence of AFP in HepG2 cells (Semenkova *et al.*, 1997). The relationship between AFP and TNF seems complex in tissue culture: HepG2 cells are resistant to the effects of TNF while AFP is present in the culture medium. The possibility exists that the AFP is used by the cell to circumvent the cytotoxic effect of TNF, allowing tumour growth to proceed. Furthermore, it has been shown that *in vitro* addition of AFP results in promotion of growth of hepatoma cell lines (Wang and Xie, 1998), strongly indicating a role for AFP in cell proliferation/tumourogenicity. The differentiation between AFP produced in normal tissues and AFP produced in tumours of hepatic tissues is achievable by the exploitation of the differences in the carbohydrate side groups on the AFP (Johnson *et al.*, 1999). The expression of AFP was examined by immunofluorescence assay in the cell lines HepG2, H5, H16, and COS-7. As shown in panel G of Figs. 4.1, 4.2, 4.3, and 4.4 each, AFP was found to be expressed in HepG2 cells, but not in H5, H16, and COS-7 cells. The AFP expression in HepG2 cells is in agreement with previously published results (Semenkova *et al.*, 1997).

4.1.4. Alpha (1)-antitrypsin.

Alpha (1)-Antitrypsin (A-1-AT) is a 54 kDa plasma glycoprotein that constitutes the principal inhibitor of neutrophil elastase in tissue fluids (Molmenti, *et al.*, 1993). Neutrophil elastase is a serine protease that is responsible for tissue degradation at sites of inflammation in infected tissues. A-1-AT has been considered a prototype for

liver-derived acute phase proteins in that its concentration in plasma increases three- to fourfold during the host response to inflammation/tissue injury (Hafeez *et al.*, 1992). Acute-phase proteins are associated with the host response to viral infection and are part of a response to the induction of inflammatory cytokines. The presence of A-1-AT correlated well with HBV infection in one study (Ohmachi *et al.*, 1994), where 81% of HBV-infected patients had A-1-AT in their liver as opposed to only 11% of HCV patients. Expression of A-1-AT has been detected in other tissues besides the liver such as enterocytes and the colon-derived cell line Caco2 (Molmenti *et al.*, 1993).

In the panels labelled H in Figs. 4.1, 4.2, 4.3 and 4.4, the immunofluorescent analysis of the expression of A-1-AT in all of the cell lines studied here is shown. The fluorescence was strongest in the HepG2 cells (Fig.4.1, panel H) presumably because the HepG2 cells are derived from a hepatic tumour. The presence of A-1-AT in HepG2 cells is in agreement with published data (Hafeez *et al.*, 1992), and A-1-AT expression in inflamed and injured tissues is documented (Busachi *et al.*, 1986), as is the existence of A-1-AT in cell lines derived from HCC (He *et al.*, 1984). In comparison with the HepG2 cell line, both H5 and H16 (panel H of Figs. 4.2 and 4.3, respectively) were negative for A-1-AT as determined by the immunofluorescence assay performed here.

4.1.5. Apolipoprotein-1a.

Levels of plasma apolipoprotein-1a (Apo-1a) vary greatly in humans. More than one hundred different alleles of Apo-1a have been identified so far, possibly resulting in proteins with different folding characteristics or different levels of carbohydrate trimming in the near-mature protein (White *et al.*, 1997). It has been suggested that these differences in folding or glycan composition may account for the wide differences in levels of plasma Apo-1a observed in humans (White *et al.*, 1997). Apolipoprotein 1a is involved in the regulation of lipid metabolism, an important function of the liver. The interaction of the C-terminal domains of Apo 1a with lipids has been recently analysed (Laccotripe *et al.*, 1997) and has given useful information regarding the structure-function relationship between the numerous alpha helices of the protein and its lipid ligands. The interactions of Apo-1a with lipopolysaccharide have also been studied (Massamiri *et al.*, 1997), enabling the elucidation of some of

the steps in the metabolism of lipids and other processes, such as the egress of cholesterol from the cell. The association of Apo-1a with phosphatidylcholine enables the formation of lipid disks. The structure of these lipid disks is purported to aid in the protection of the hydrophobic lipid tails of Apo-1a from the aquatic environment (Phillips *et al.*, 1997). The localisation of Apo-1a, and Apo-B has been examined in hepatocytes (Panin *et al.*, 1997), and these proteins are found in highest concentrations in the nucleus. The localisation of radiolabelled high-density lipid (HDL) and low-density lipid (LDL) with the Apo-1a, Apo-B and Apo-E would suggest that these proteins are involved in the import of lipids into the cell nucleus (Panin *et al.*, 1997).

The immunofluorescence results from HepG2 cells (Fig. 4.1, panel I) were strongly positive for the presence of Apo-1a. This is not unexpected as Apo-1a expression in HepG2 cells has been shown previously (Cianflone *et al.*, 1994). Both our hepatocyte cell lines, H5 and H16, also expressed Apo-1a as shown by strong fluorescence when probed with anti-apo-1a MAb (Fig. 4.2 and 4.3, panel I, respectively). In comparison, the COS-7 cells probed with the anti-human Apo-1a MAb (Fig. 4.4, panel I) showed a very weak level of fluorescence that is probably due to autofluorescence.

4.1.2. Annexin V.

Annexin V is a 32 kDa calcium-binding protein that is anchored in lipid membranes. The presence of annexin V has been reported in many cell types such as human foreskin fibroblasts (Barwise and Walker, 1996), chondrocytes (vonderMark and Mollenhauer, 1997), cardiac cells (Luckcuck *et al.*, 1997) and hepatocytes (Hertogs *et al.*, 1993). Annexin V has also been reported to reside within the cytoplasm and nuclei of cultured cells (Sun *et al.*, 1992). An important role of annexin V is to facilitate the Ca²⁺ influx into cytoplasmic vesicles, therefore allowing mineralisation of structures requiring calcium, such as bone. Annexin V has been purported to be a receptor for HBV S protein (Gong *et al.*, 1999). To test for annexin V expression, cells were fixed, permeabilised, and analysed by confocal microscopy using an anti-human annexin MAb. As shown in panel E each of Figs. 4.1 to 4.4, a weak fluorescence was observed in H5 and H7, but not on HepG2 and COS-7 cells. Flow cytometry was used to facilitate quantitative analysis of the expression of annexin V on the plasma membrane of these cells. As shown in Fig. 4.5, panel A, the HepG2

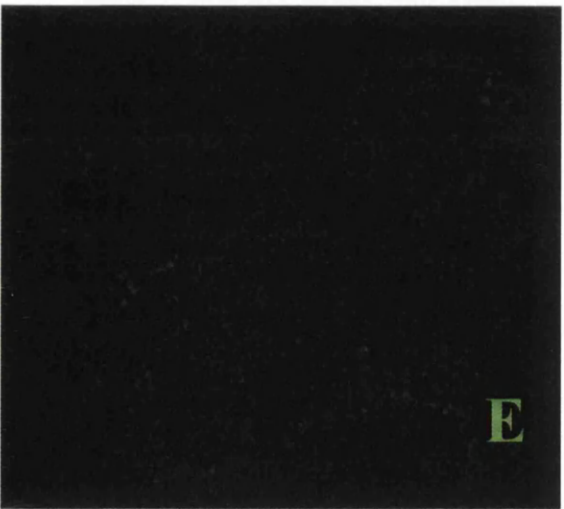
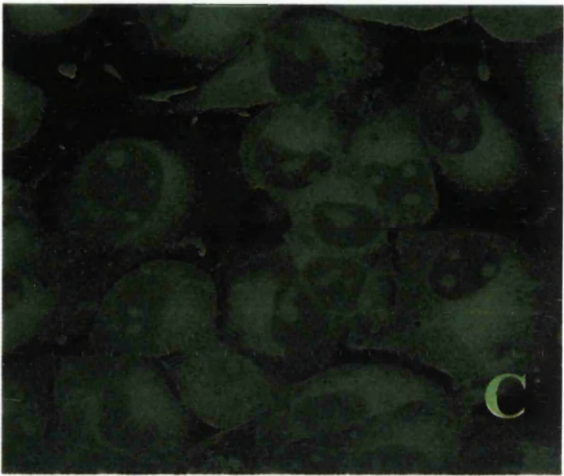
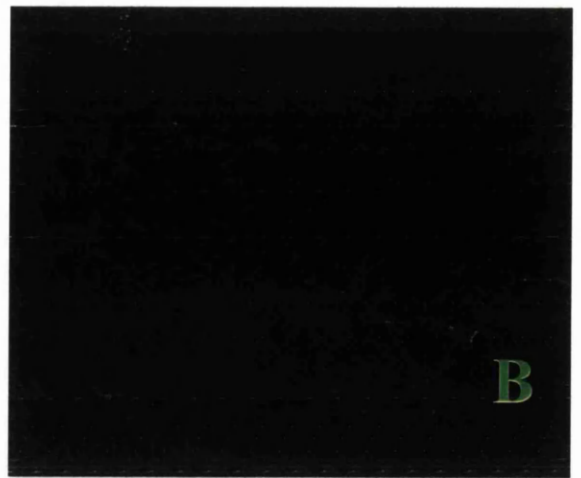
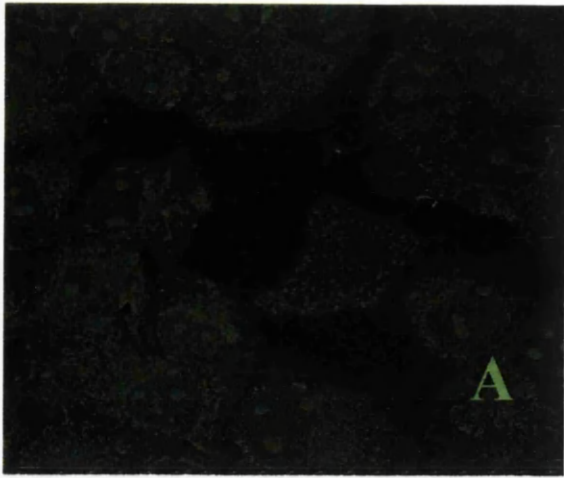


Figure 4.1 Analysis of expression of cellular markers in COS-7 cells. COS-7 cells were grown on glass coverslips in DMEM for 3 days, then were fixed with 2% paraformaldehyde for plasma membrane staining, or permeabilised with methanol at -20°C for intracellular staining. The coverslips were incubated with appropriate antisera as follows: **A:** anti-cyokeratin 8 in non-permeabilised cells. **B:** anti-cyokeratin 8 in permeabilised cells. **C:** anti-cyokeratin 18 in non-permeabilised cells. **D:** anti-cyokeratin 18 in permeabilised cells. **E:** anti-annexin V in permeabilised cells. **F:** anti-human albumin in permeabilised cells.

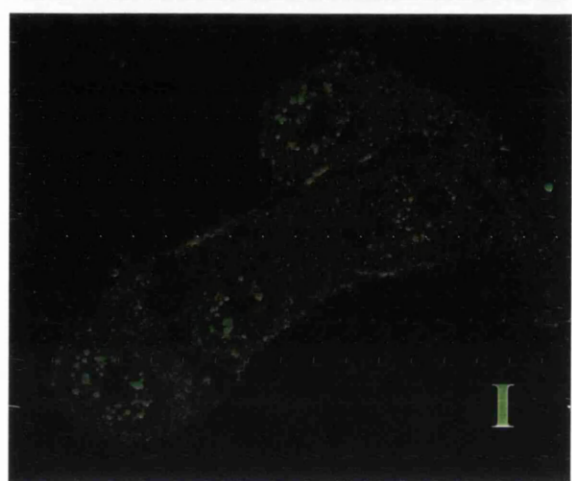
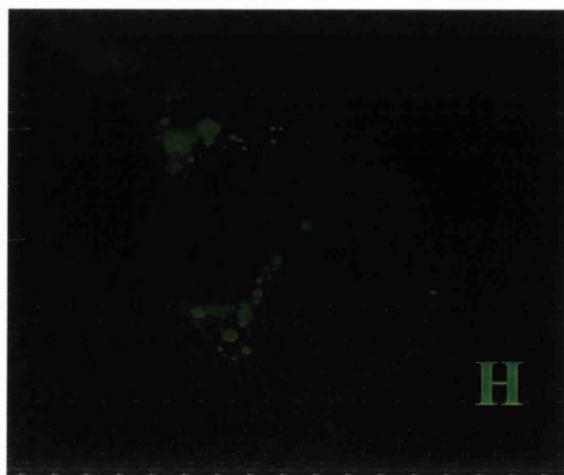
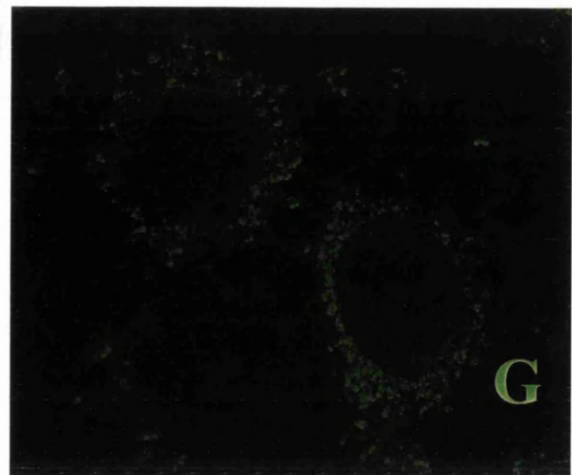


Figure 4.1 Continued. Analysis of expression of cellular markers in COS-7 cells .

G: anti-alpha-fetoprotein in permeabilised cells. **H:** anti-human antitrypsin in permeabilised cells

I: anti- apo-lipoprotein A1 in permeabilised cells.

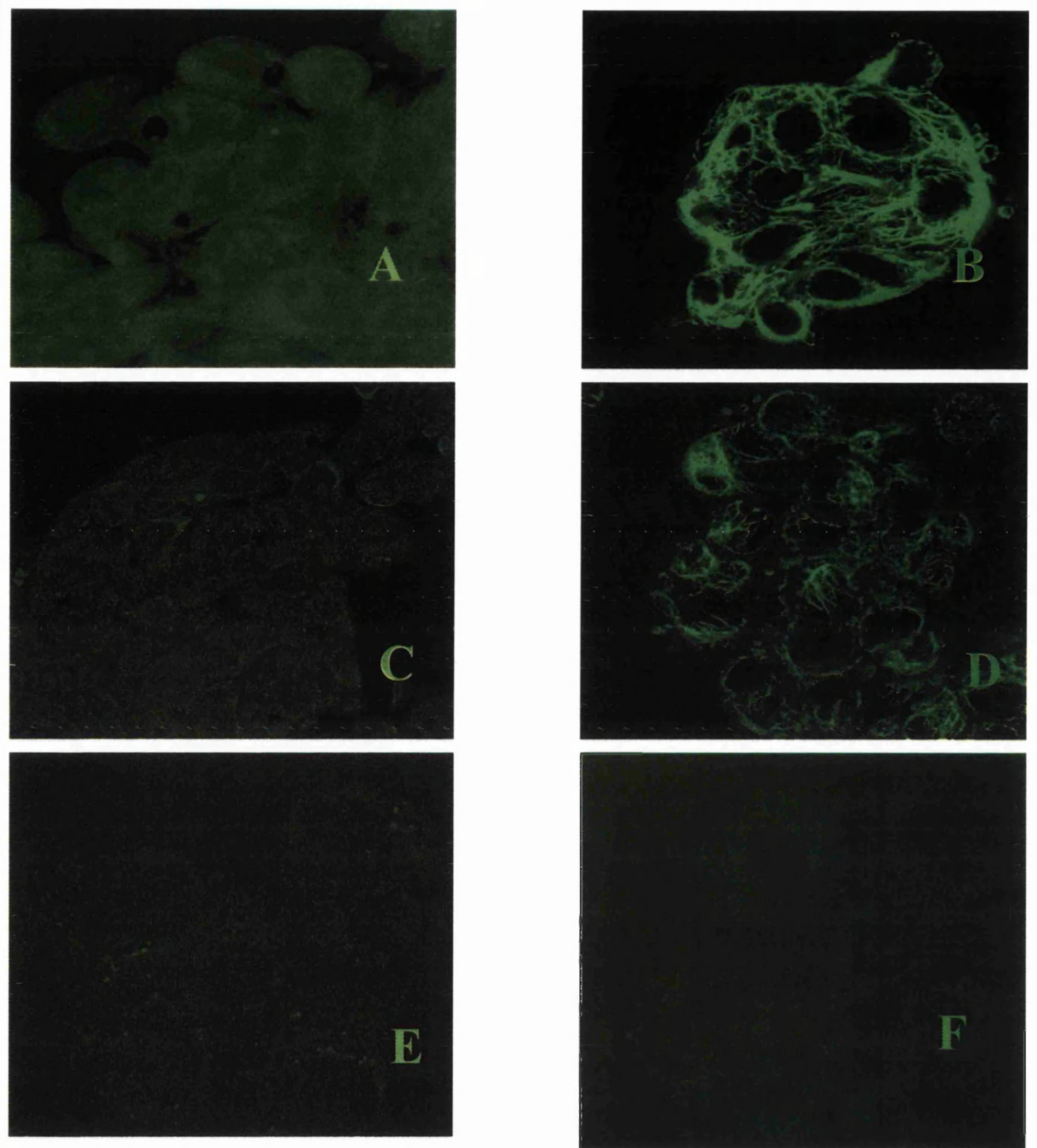


Figure 4.2 Analysis of expression of cellular markers in HepG2 cells. HepG2 cells were grown on glass coverslips in DMEM for 3 days, then were fixed with 2% paraformaldehyde for plasma membrane staining, or permeabilised with methanol at -20°C for intracellular staining. The coverslips were incubated with appropriate antisera as follows: **A:** anti-cytokeratin 8 in non-permeabilised cells. **B:** anti-cytokeratin 8 in permeabilised cells. **C:** anti-cytokeratin 18 in non permeabilised cells. **D:** anti-cytokeratin 18 in permeabilised cells. **E:** anti-annexin V in permeabilised cells. **F:** anti-human albumin in permeabilised cells.

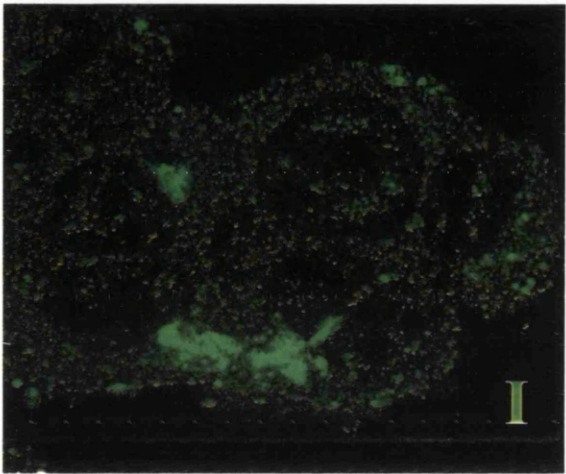
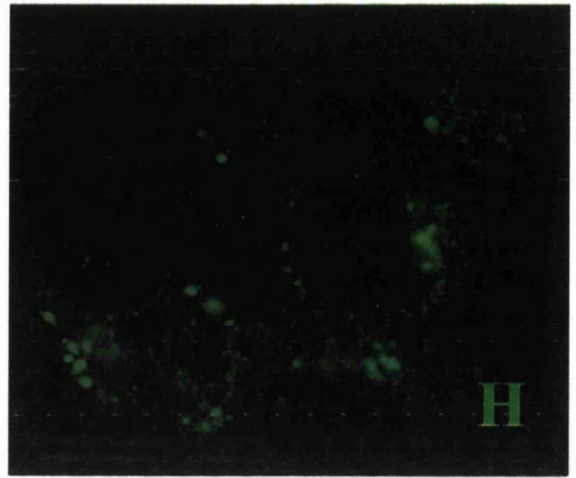
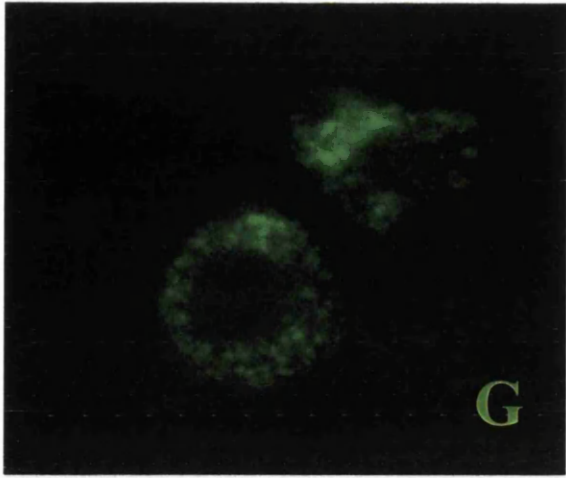


Figure 4.2 Continued. Analysis of expression of cellular markers in HepG2 cells .

G: Alpha-fetoprotein in permeabilised cells

H: Antitrypsin in permeabilised cells

I: Apo-lipoprotein A1 in permeabilised cells.

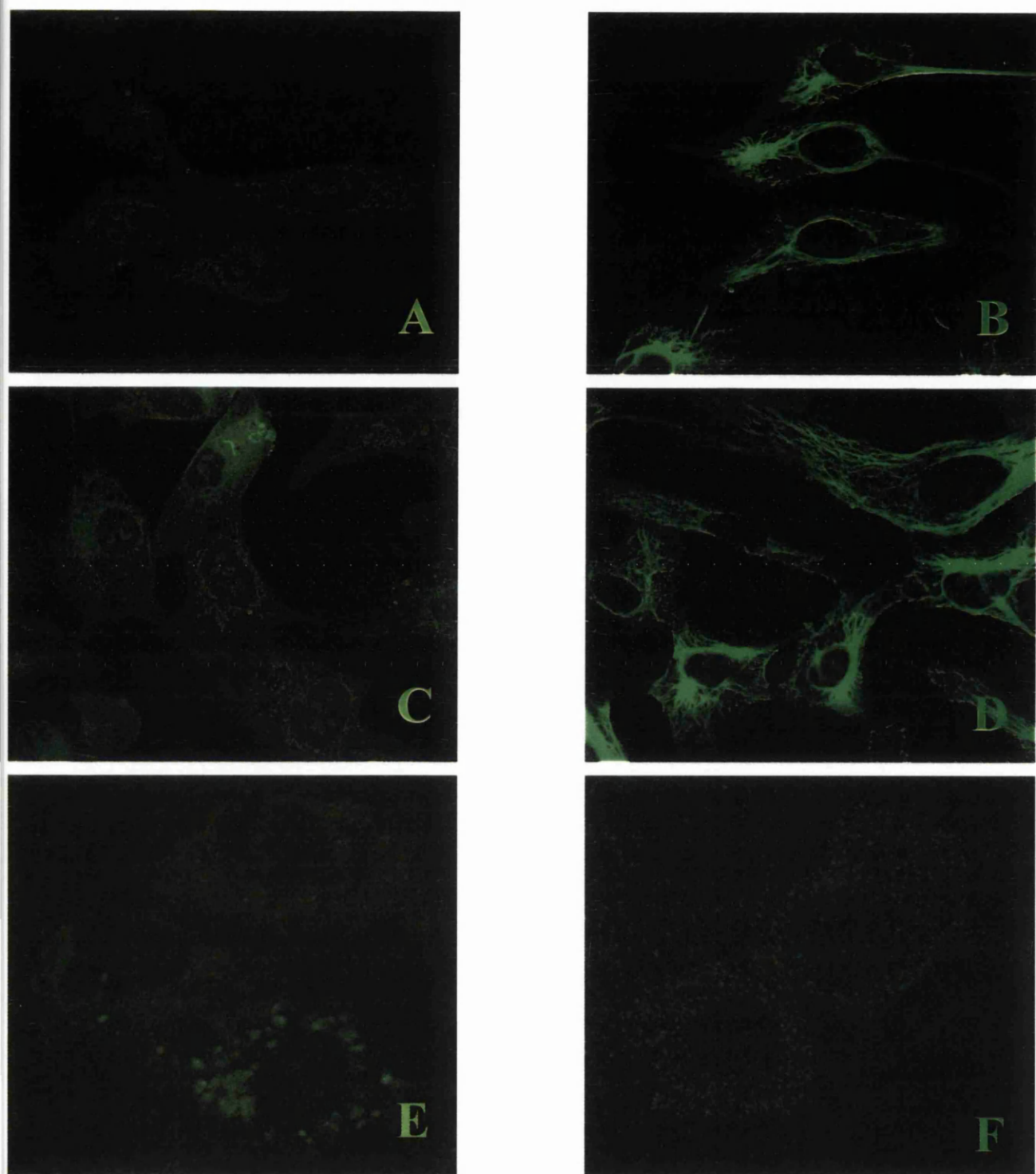


Figure 4.3 Analysis of expression of cellular markers in H5 cells.

H5 cells were grown on glass coverslips in DMEM for 3 days, then were fixed with 2% paraformaldehyde for plasma membrane staining, or permeabilised with methanol at -20°C for intracellular staining. The coverslips were incubated with appropriate antisera as follows: **A:** anti-cytokeratin 8 in non-permeabilised cells. **B:** anti-cytokeratin 8 in permeabilised cells. **C:** anti-cytokeratin 18 in non permeabilised cells. **D:** anti-cytokeratin 18 in permeabilised cells. **E:** anti-annexin V in permeabilised cells. **F:** anti-human albumin in permeabilised cells.

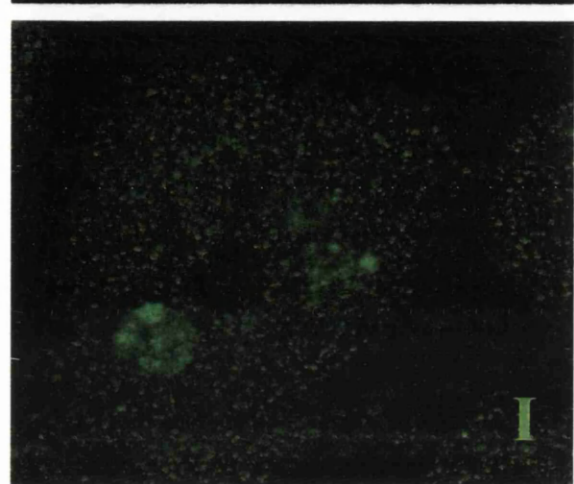
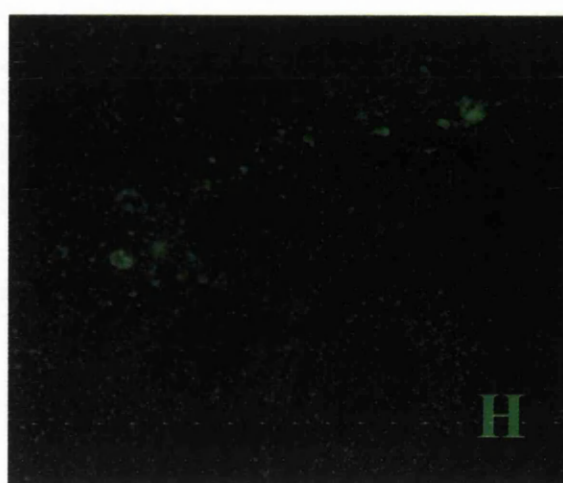
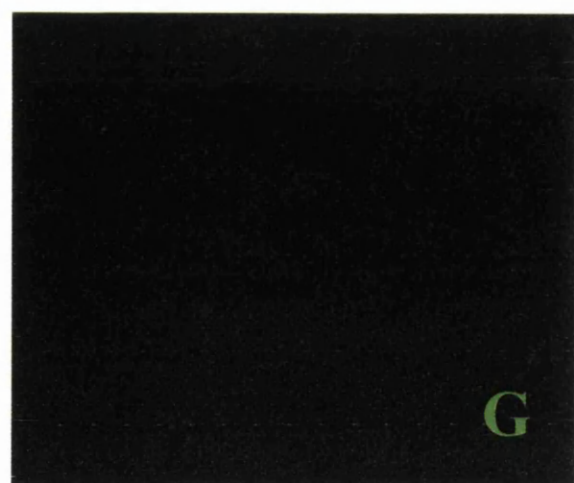


Figure 4.3 Continued. Analysis of expression of cellular markers in H5 cells .

G: anti-alpha-fetoprotein in permeabilised cells.

H: anti-human antitrypsin in permeabilised cells

I: anti- apo-lipoprotein A1 in permeabilised cells.

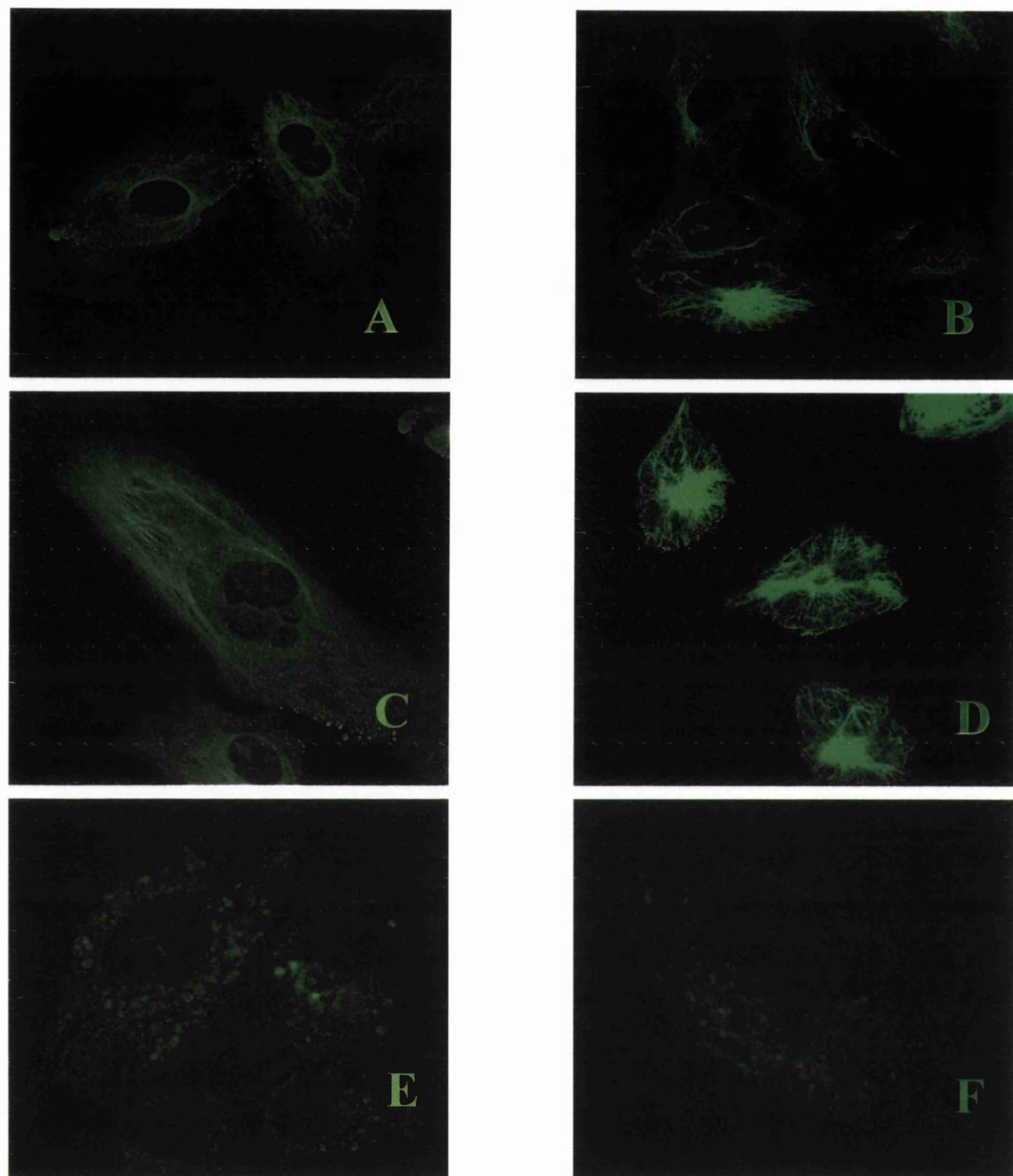


Figure 4.4 Analysis of expression of cellular markers in H16 cells.

H16 cells were grown on glass coverslips in DMEM for 3 days, then were fixed with 2% paraformaldehyde for plasma membrane staining, or permeablised with methanol at -20°C for intracellular staining. The coverslips were incubated with appropriate antisera as follows: **A:** anti-cytokeratin 8 in non permeablised cells. **B:** anti-cytokeratin 8 in permeablised cells. **C:** anti-cytokeratin 18 in non-permeablised cells. **D:** anti-cytokeratin 18 in permeablised cells. **E:** anti-annexin V in permeablised cells. **F:** anti-human albumin in permeablised cells.

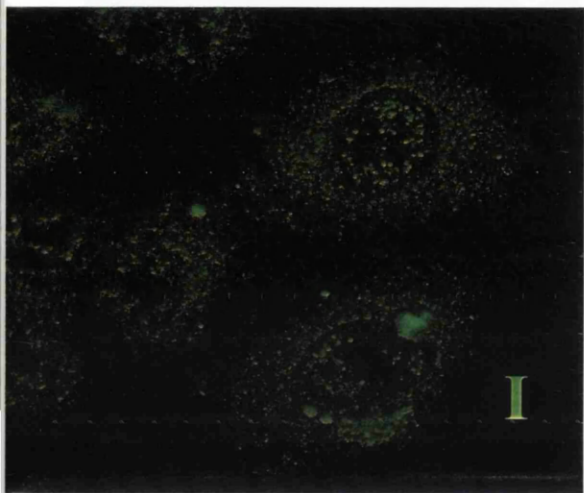


Figure 4.4 Continued. Analysis of expression of cellular markers in H16 cells .

G: Alpha-fetoprotein in permeabilised cells

H: Antitrypsin in permeabilised cells

I: Apo-lipoprotein A1 in permeabilised cells.

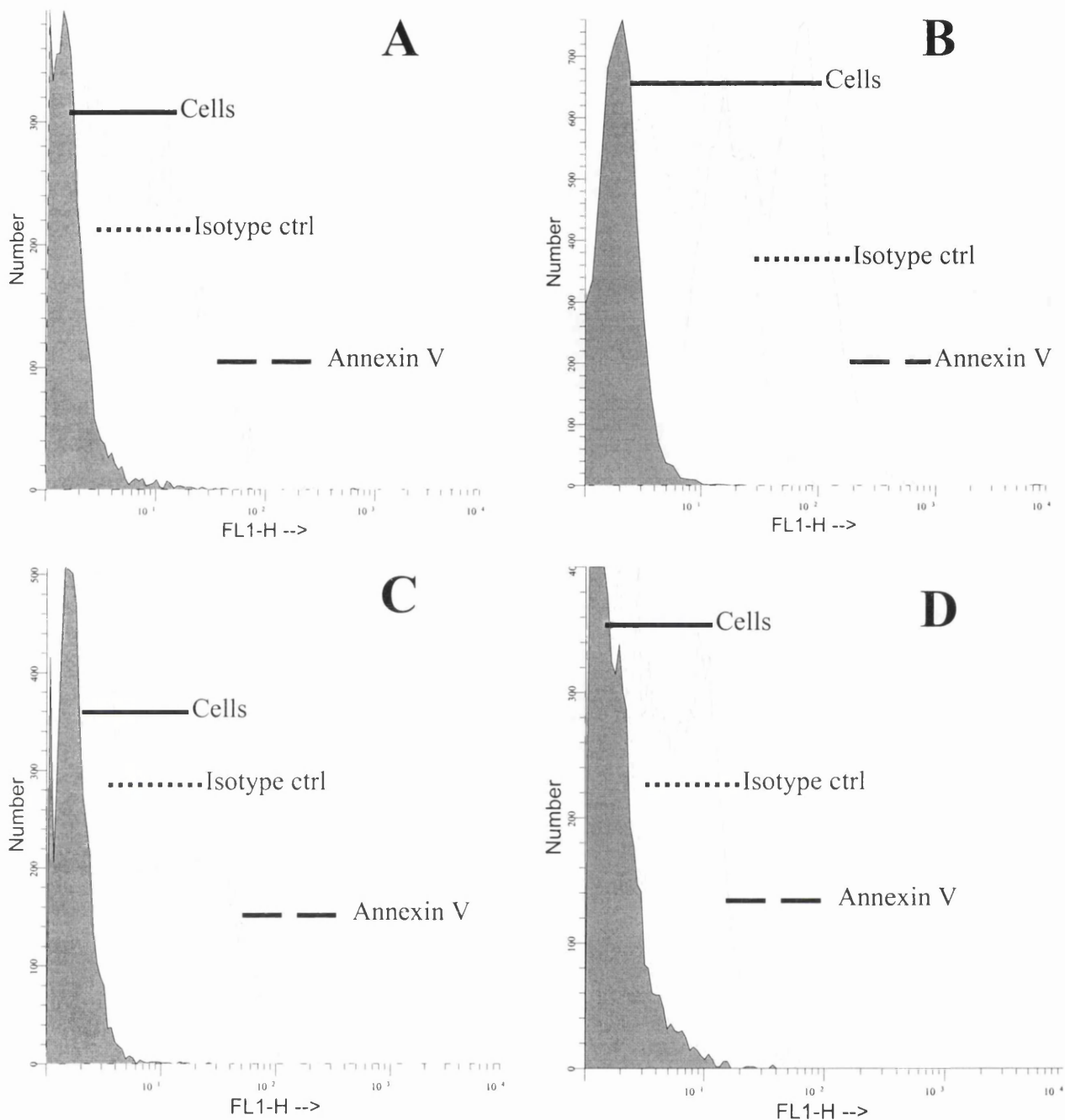


Figure 4.5 Evaluation of novel and established cell lines for the expression of annexin V HepG2, H5, H16 and COS-7 cells were analysed for the plasma membrane expression of annexin V by flow cytometry. The cells were grown in T175 flasks to near confluence and were then dissociated from monolayers. Following washing, the cells were incubated with isotype control MAb, the anti-human annexin V MAb, or no MAb. The bound antibodies were then detected using anti-mouse-IgG-FITC in a BD FACScan.

Panel A: HepG2 cells.

Panel B: H5 cells.

Panel C: H16 cells.

Panel D: COS-7 cells.

Table 2 Summary of results for the expression of markers in novel and established cell lines

	<u>COS-7</u>	<u>HepG2</u>	<u>H5</u>	<u>H16</u>
Cytokeratin 8	-	+++	+++	+++
Cytokeratin 18	-	+++	+++	+++
Annexin V	+	++	++	++
Albumin	-	-	-	-
Apolipoprotein A	-	+	++	++
Antitrypsin	-	++	-	-
Alpha-fetoprotein	-	++	-	-

Cell lines were tested for expression of marker proteins by immunofluorescence and flow cytometry. This table summarises the results obtained. It should be noted that the results obtained from the Anti-Albumin antibody are inconclusive due to the absence of fluorescence in the positive control, HepG2.

cells expressed Annexin V on the plasma membranes. There was a large increase in fluorescence in the majority of the cells (shown as the long broken line) in comparison with the isotype control (shown as the punctate line). There was minimal uptake of the isotype MAb control on the plasma membrane of the HepG2 cells, as can be seen by the very small increase in fluorescent intensity of the isotype MAb control in comparison with the unstained cells. This small difference in fluorescent intensity indicated that the binding of the IgG1 molecule directed against Annexin V is not an artefact due to the presence of IgG receptors on the plasma membrane of the HepG2 cells. Unlike HepG2 cells, there was a significant shift in fluorescence on H5 cells and to a lesser extent on H16 cells due to the isotype MAb control, indicating that the isotype control or the anti-mouse IgG-FITC conjugate binds to the plasma membrane (Fig. 4.5, panels B and C, respectively). However, like HepG2 cells, both H5 and H16 cells exhibited a distinct increase in fluorescence (in comparison with the isotype control) when probed with the anti-annexin V MAb indicating expression of this protein on the cell surface (Fig. 4.5 panels B and C). The binding of the isotype control MAb to the plasma membrane of the cells is probably due to the presence of receptors for the Fc region of IgG molecules, on the plasma membrane. Interestingly, the COS-7 cells used as a supposedly negative control for these experiments showed an increase in fluorescence when probed with the anti-annexin V MAb (Fig. 4.5, panel D). However, the increase in fluorescence due to anti-annexin V MAb did not appear as great as that obtained from the other cell lines studied here.

4.2 Discussion.

The cell lines partially characterised here have been generated as part of an ongoing programme of reagent generation to obtain suitable systems for the study of the mechanisms of hepatotropism exhibited by HBV (and HCV). Although the data presented in this chapter do not fulfil the requirements of a comprehensive characterisation for these cell lines, they do offer some insights into the nature of these cells and indicates that they may be worthwhile reagents for the study of HBV (and HCV) replication and tropism.

The results discussed here have been summarised in Table 4.1. The demonstration of the expression of the cytokeratins 8 and 18 in the novel cell lines indicated that the reversion of these hepatocyte-derived cell lines to fibroblasts has not occurred. This

evidence, while no guarantee of hepatocytic phenotype, suggests that the cell lines H5 and H16 may have retained hepatocytic characteristics. Furthermore, these cell lines were analysed for expression of the products assayed here after about 30 passages in DMEM in normal tissue culture conditions. The retention of the expression of cytokeratins 8 and 18 after this time is encouraging and leads the author to suggest that these cell lines may be of use in work where the phenotype of the cells used should be as close as possible to that of a primary hepatocyte, with the added advantage of being a stable and proliferative cell line.

The expression of Annexin V on these hepatocytes is worthy of study when seen in the context of the literature concerning the binding of the small surface antigen of HBV to hepatocytes. The association of Annexin V with S has been documented (Hertogs *et al.*, 1994). Furthermore, the presence of Annexin V has been suggested as a determining factor for infection of cells by HBV (Gong *et al.*, 1996). Clearly, in the primary characterisation of these novel cell lines that are intended to be used for viral entry studies, the demonstration of expression of Annexin V is of great importance.

The absence of AFP in the H5 and H16 cell lines in comparison with HepG2 is in keeping with the origin of these cell lines: the primary hepatocytes from which these cells were derived were negative for HBV, HCV, HIV1, HIV2 and HCMV, and were taken from a recently deceased but healthy individual. The absence of AFP from H5 and H16 indicates the cells are from uninjured tissue and would imply the cells are unlikely to be expressing acute-phase proteins due to infection or injury. Likewise, the absence of A-1-AT from the novel cell lines provides further evidence for the healthy state of the liver tissue from which the primary hepatocytes were isolated.

The expression of Apo-1a in the novel cell lines is evidence to suggest that these cells have retained at least some of the hepatocytic phenotype. Taken together, the data obtained here provides a good basis to suggest that these cell lines are stable in the short term, are immortalised, express some liver-specific proteins and have not reverted to a fibroblast-like phenotype. That H5 and H16 are growing in DMEM with minimal supplementation, with the absence of factors such as DMSO and dexamethasone, and still retain markers such as these cytokeratins, indicates that these cell lines may be useful tools in the delineation of the infection process of

hepatotropic viruses. The infection of established cell lines with HBV, in many cases, has required the presence of polyethylene glycol (PEG) and DMSO in the culture medium (Gripon *et al.*, 1993). The inclusion of PEG and DMSO in the culture medium is unwanted, as it would complicate the interpretation of results from the point of view of studying the mechanisms of virus attachment and entry into the target cells. The presence of PEG and DMSO could result in disruption of the plasma membrane of the hepatocytes allowing viral entry which does not necessarily mimic the process occurring *in vivo* (Gripon *et al.*, 1993).

It is recognised by the author that the analysis carried out here for marker proteins in these novel cell lines is only a small portion of the required characterisation for novel cell lines. A more comprehensive analysis would include examination of the mRNA transcripts for all of the proteins analysed here, and for other proteins such as cytokeratin 19, cytochrome p450, albumin, hepatocyte nuclear factors one, two, three and four (HNF -I, -II -III and -IV), phosphoenolpyruvate carboxykinase-2 (PCK2) and other serum proteins in cell lines grown both in serum-free and normal growth medium. It is intended, as part of the future work of this laboratory, to characterise these and other novel cell lines for expression of these liver specific marker proteins, and to examine the ability of these cell lines to support the *in vitro* infection processes and replication of HBV (and HCV).

Chapter 5

Investigations into the structure of the surface antigens of HBV

The intracellular behaviour of the surface antigens of HBV is of interest to HBV virologists, because by associating with the nucleocapsid they play a crucial role in the hepadnaviral morphogenesis process, and also in the morphogenesis of sub-viral particles. The ability to distinguish between the surface antigens when co-expressed in the same cell would be a valuable tool for studying the intracellular behaviour of the surface antigens. For example, reagents that could identify M and/or S proteins without detecting the respective domains on the L protein in co-expressing cells would be of great value in evaluating the role of these protein in viral particle assembly and morphogenesis. Additionally, the structure of the surface antigens remains unresolved. The work described in this chapter was undertaken as a study of the structure and intracellular behaviour of the surface antigens.

There is little information available concerning the structure of the HBV surface antigens. There are difficulties associated with the determination of structures of proteins that are embedded in a lipid bilayer which prevent crystallisation of the proteins and therefore X-ray crystallography can not be utilised to resolve the structure. Another way to gain insight into the tertiary structure of proteins embedded in a lipid bilayer is to probe the proteins with monoclonal antibodies that are directed against linear and conformational epitopes. The ability of the antibodies to recognise linear or conformational epitopes of the protein can be exploited to yield information concerning the folding and maturation of proteins.

Computer-generated models have been generated for the structure of S (Peterson, 1987; Sonveaux *et al*, 1995; Stirk *et al* 1992), but there is very little information regarding the prediction of the structure of the L protein. The are features of the L protein which are likely to have influence on the structure of L such as insertion of the PreS1 region into the lipid membrane (Ou and Rutter, 1987; Persing *et al*, 1987; Prange *et al*, 1991), but there remains little biochemical or immunological information regarding the arrangement of the transmembrane helices, and the packing of the surface antigens when oligomerised.

Here, the behaviour of the surface antigens when expressed singly or upon co-expression was examined using both polyclonal and monoclonal antibodies to various HBV surface antigens described in Chapter 3. The antibodies were tested for their ability to distinguish between the surface antigens, and to study the antigenicity of these proteins.

5.1 Intracellular localisation of HBV surface antigens.

Recent work has shown that L protein, when expressed in a heterologous system, is retained in the ER, and co-localising with p53, a protein known to be enriched in the ER-Golgi intermediate compartment or ERGIC (Xu *et al.*, 1997). Therefore the evaluation of the L encoded by rVV vL and vLx was undertaken by confocal microscopy in order to assess its intracellular distribution and to afford comparison with previously published data. HepG2 cells were infected with rVV vL or vLx and fixed after 24 h. The cells were probed with anti-preS1 antiserum PAb143 and anti-p53 MAb and the bound primary antibodies detected by appropriate secondary reagents described in the legend to Fig. 5.1A and B. The L protein was found to localise predominantly in the perinuclear compartment (Fig. 5.1A, panel A), whereas the p53 protein appeared to be localised as large spots again in the perinuclear area, although some weak staining was also seen throughout the cytoplasm (panel B). Superimposition of the two images showed that the spot of p53 colocalised or co-compartmentalisation with the L protein (visible as the yellow colour in panel C), which is consistent with the findings of others (Xu *et al.*, 1997).

In contrast to L, the distribution of Lx is markedly different to that of L in cells infected with vLx in that it was spread evenly throughout the cytoplasm possibly in keeping with its secretory nature (Fig. 5.1B, panel A). As shown in Fig. 5.1A (Panel B), the p53 protein localised as mainly as spots in the perinuclear region, and this localisation was co-incident with at least a portion of Lx (Fig. 5.1B, panel C). This intracellular distribution of Lx and its co-localisation with p53 is in agreement with previously published data obtained using a secretory form of L similar to Lx (Xu *et al.*, 1997).

The intracellular distribution of M or S was analysed by double immunofluorescent staining and confocal microscopy. HepG2 cells were infected with rVV vM or vS, and fixed after 24 h. Anti-M MAb 2-12F2 or anti-S MAb 6B1 were used as primary antibodies in conjunction with the lectin concanavalin A (ConA) conjugated to FITC. Con A is used as a marker for intracellular membranes. As shown in Fig. 5.2, the staining for both S and M was distributed throughout the cytoplasm (panels A and D, respectively), as was that for ConA (panels B and E). The localisations of ConA and S or ConA and M were coincident when the respective images were merged (panel C and F), indicating that these proteins are associated with intracellular membranes. These proteins are known to be secreted but do not bud through the plasma membrane, rather, they are secreted through the exocytic pathway. It is important to note that such a distribution of L or Lx was not evident – L was retained in the ER/ERGIC, whereas Lx was more evenly distributed in the cytoplasm of cells (Fig. 5.1 A and B).

5.2 Evaluation of anti-S MAbs for antigen recognition.

HepG2 cells were infected with rVV expressing L, Lx, M, and S. Following incubation for 24 h, the cells were fixed, permeabilised and probed with a panel of monoclonal antibodies directed against S. As shown in Fig. 5.3 A to D, all the MAbs tested recognised not only S, but also M, L, and Lx proteins. In all cases, the reactivity of the MAbs to the mock-infected and WR-infected negative controls was minimal. It is important to note that the intracellular distribution of M and S was quite distinct from that of L and Lx when probed with all the anti-S MAbs tested here (Fig. 5.3 A to D, panels C to F). Both M and S localised in a matrix-like pattern with internal membranes (as confirmed in Fig. 5.2) in the cytoplasm of the cell, as opposed to L or Lx which have a more even cytoplasmic distribution. The observation that the anti-S MAbs tested here are capable of recognising the M, L and Lx proteins when expressed in this recombinant vaccinia virus system confirms the difficulty in distinguishing between the surface antigens in co-expressing cells. Whereas it is possible to distinguish the L protein from the M or S proteins by the use of antisera directed against the preS1 domain (see Fig. 5.5), it is difficult to discriminate the S protein from the L protein due to the inclusion of the S domain in the L protein. The anti-S MAbs H35, H166, H10 and RF7 are all directed against linear epitopes found on the S protein (for data on H35 and H166 see Chen *et. al*, 1996). The epitopes on S

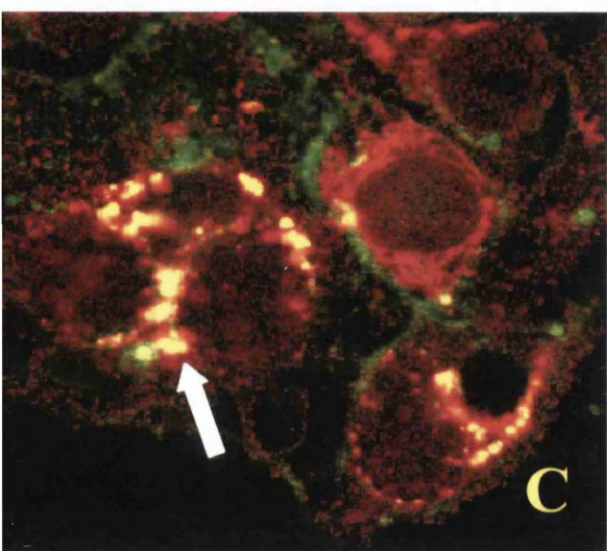
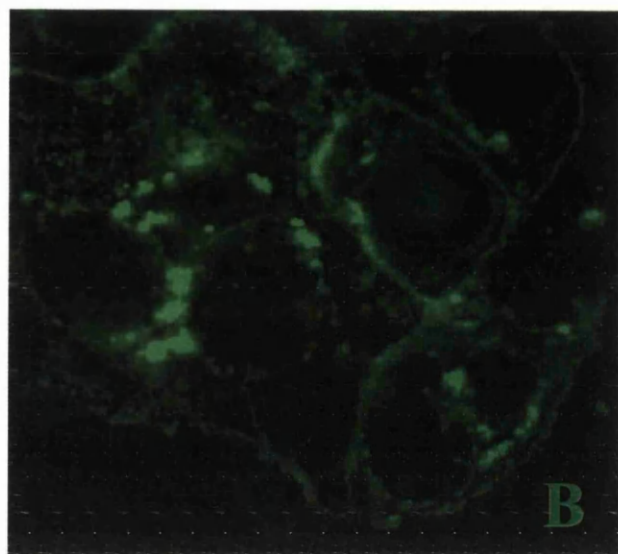
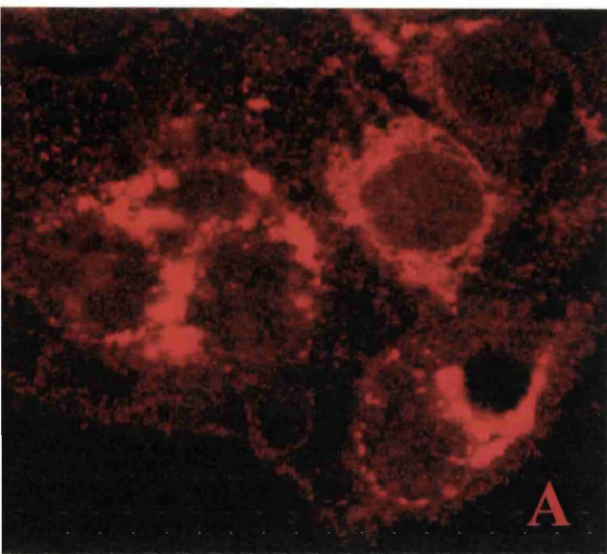


Fig. 5.1A Characterisation of the intracellular distribution of L protein in HepG2 cells.

HepG2 cells on glass coverslips in 24-well plates were infected at a low m.o.i. with vL. At 24 hours post-infection, the cells were fixed in methanol at -20°C , then permeabilised in PBST. The cells were probed with PAb 143 (anti-L) and MAb (anti-ERGIC p53) for two hours at room temperature, then were washed in PBST. The coverslips were incubated with anti-mouse FITC and Anti-Rabbit Cy5, and the coverslips were mounted and examined by Confocal microscopy.

Panel A: Cells expressing vL stained with Pab 143 and anti-rabbit IgG-cy5, coloured red.

Panel B: p53 protein stained with anti-p53 MAb and anti-mouse IgG-FITC.

Panel C: Merge. White arrow indicates area of colocalisation of L and p53.

The intracellular distribution of the L protein is reasonably well associated with the p53 marker for the ERGIC compartment when expressed in HepG2 cells.

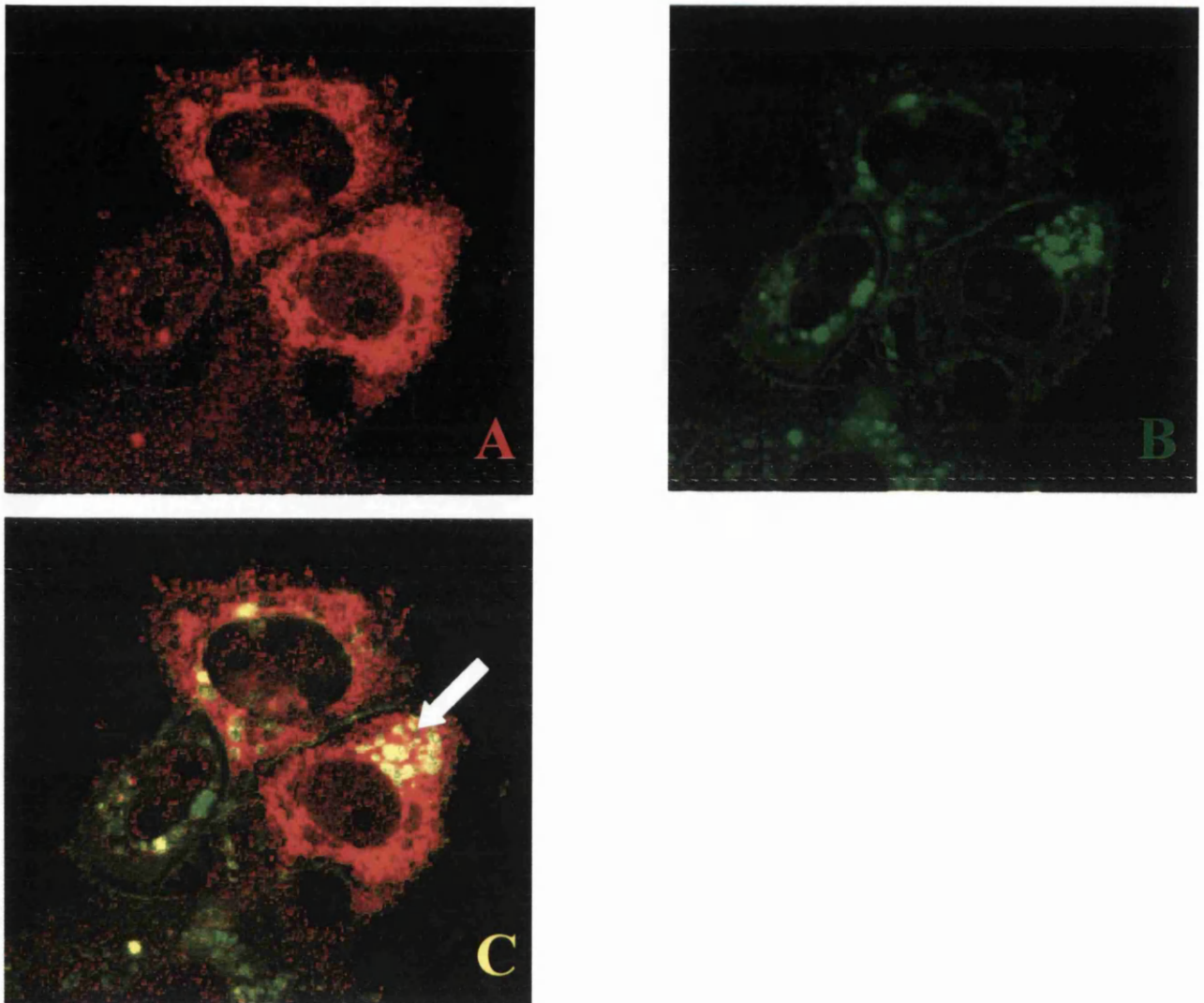


Fig. 5.1B Characterisation of the intracellular distribution of the Lx protein in HepG2 cells.

HepG2 cells on glass coverslips in 24-well plates were infected at an m.o.i. of 0.5 p.f.u./cell with vLx. At 24 hours post-infection, the cells were fixed in methanol at -20°C , then permeabilised in PBST. The cells were probed with PAb 143 (anti-L) and MAb (anti-ERGIC p53) for two hours at room temperature, then were washed in PBST. The coverslips were incubated with anti-mouse FITC and Anti-Rabbit Cy5, and the coverslips were mounted and examined with by confocal microscopy.

Panel A: Cells expressing vLx stained with PAb 143 and anti-rabbit IgG-cy5, coloured red.

Panel B: p53 protein stained with anti-p53 MAb and anti-mouse IgG-FITC.

Panel C: Merge. White arrow indicates area of colocalisation of Lx and p53.

The intracellular distribution of the Lx protein is more widespread than that observed with vL.

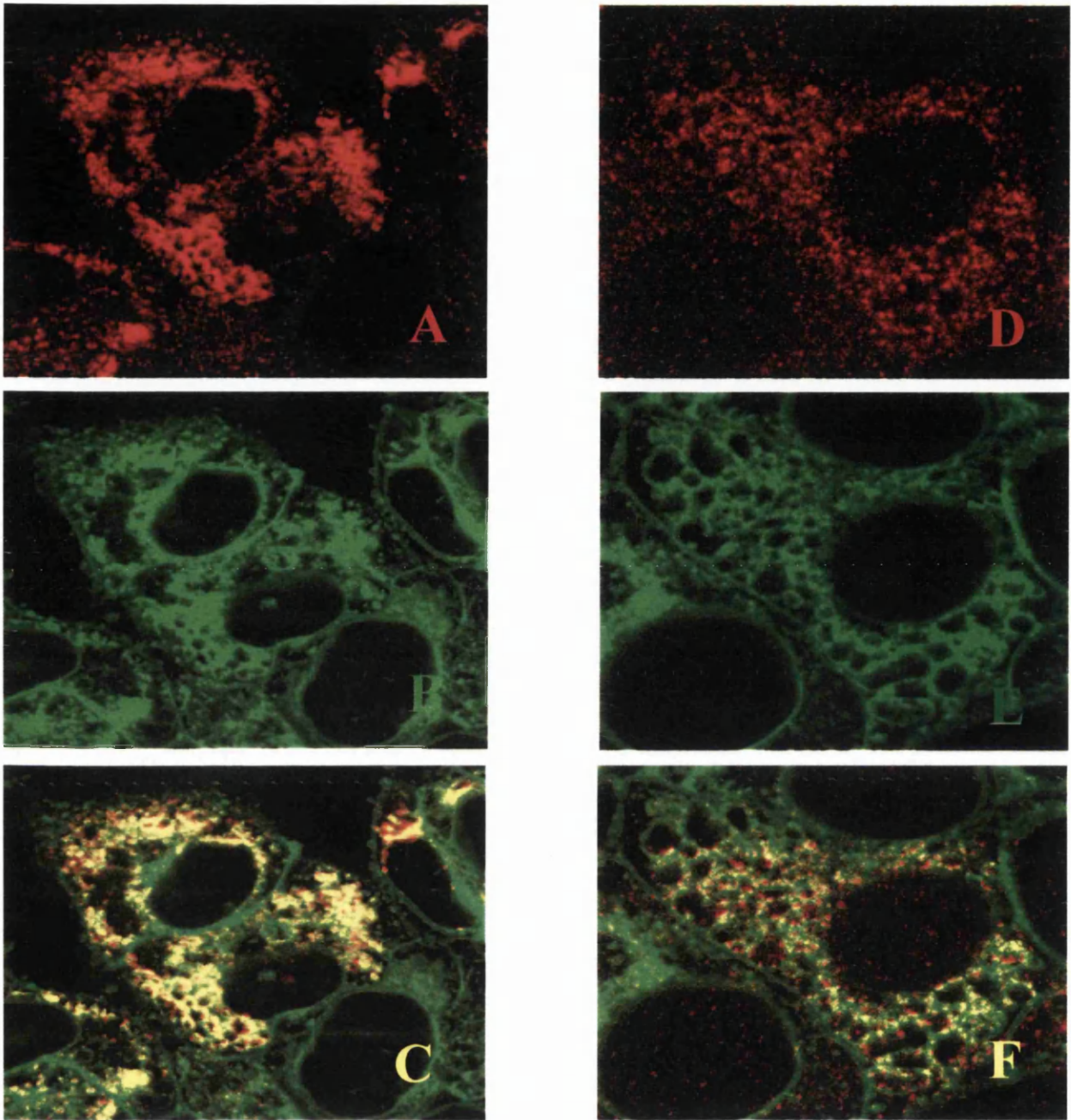


Fig. 5.2 Colocalisation of S and M with intracellular membranes in HepG2 cells.

HepG2 cells on glass coverslips in 24-well plates were infected at an m.o.i. of 0.5 p.f.u./cell with vHBsAg (panels A, B and C) or vM (panels D, E and F). At 24 hours post-infection, the cells were fixed in methanol at -20°C , then permeabilised in PBST. The vHBsAg-infected cells were probed with MAb 6B1, and the vM-infected cells were probed with MAb 2-12F2, and then incubated with anti-mouse-Cy5. All cells were also probed with concanavalin-A-FITC.

Panel A: vHBsAg infected cells stained with 6B1/1 and coloured red.

Panel B: Concanavalin-A-FITC conjugate coloured green.

Panel C: Merge.

Panel D: vM infected cells stained with MAb 2-12F2 and coloured red.

Panel E: Concanavalin-A-FITC conjugate coloured green.

Panel F: Merge.

Fig. 5.3 Recognition of HBV surface antigens by MAbs directed against HBsAg.

Hepg2 cells were grown on glass coverslips in 24-well plates to about 60% confluence. The cells were infected at a m.o.i. of 0.5 p.f.u per cell with vL, vLx, vM, vS, WR, or were mock-infected. At one hour post-infection, the cells were washed and incubated in DMEM for 24 hours. The coverslips were washed three times in PBSA and fixed in methanol at -20°C overnight. After fixing, the coverslips were washed twice with PBSA, then were permeabilised by incubation with PBST for at least 30 minutes. The coverslips were incubated with one of four monoclonal antibodies directed against HBsAg for two hours in a volume of 200 µL. Unbound antibodies were removed by washing, and the coverslips were incubated in anti-mouse IgG-FITC for two hours. The unbound secondary antibodies were removed by washing and the coverslips were mounted and analysed with a Zeiss Laser Scanning Confocal microscope.

Figure 5.3A: Anti-HBsAg MAb H53 at a dilution of 1:100.

Panel A: Mock-infected cells.

Panel B: WR-infected cells.

Panel C: vL-infected cells.

Panel D: vLx-infected cells.

Panel E: vM-infected cells.

Panel F: vS-infected cells.

Fig. 5.3B: Anti-HBsAg MAb H166 at a dilution of 1:100.

Legend as for Figure 5.3A

Fig. 5.3C: Anti-HBsAg MAb H10 at a dilution of 1:100.

Legend as for Figure 5.3A

Fig. 5.3D: Anti-HBsAg MAb RF7 at a dilution of 1:100.

Legend as for Figure 5.3A

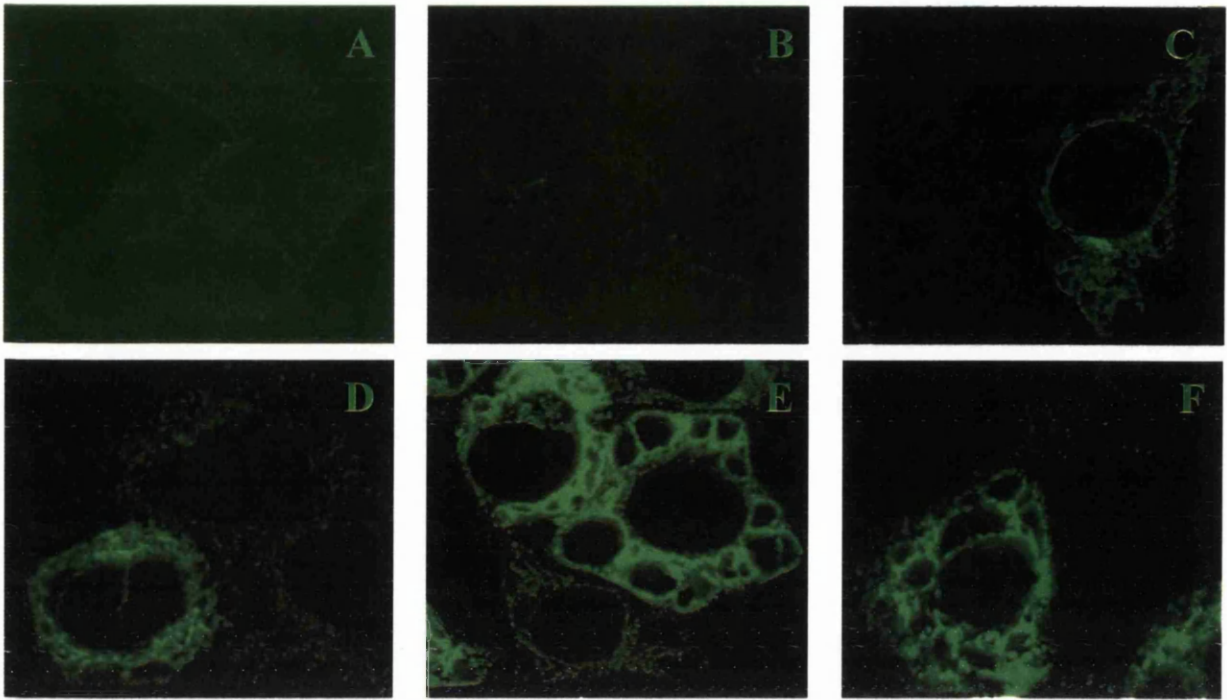


Fig 5.3A MAb H53 recognises all the HBV surface antigens.

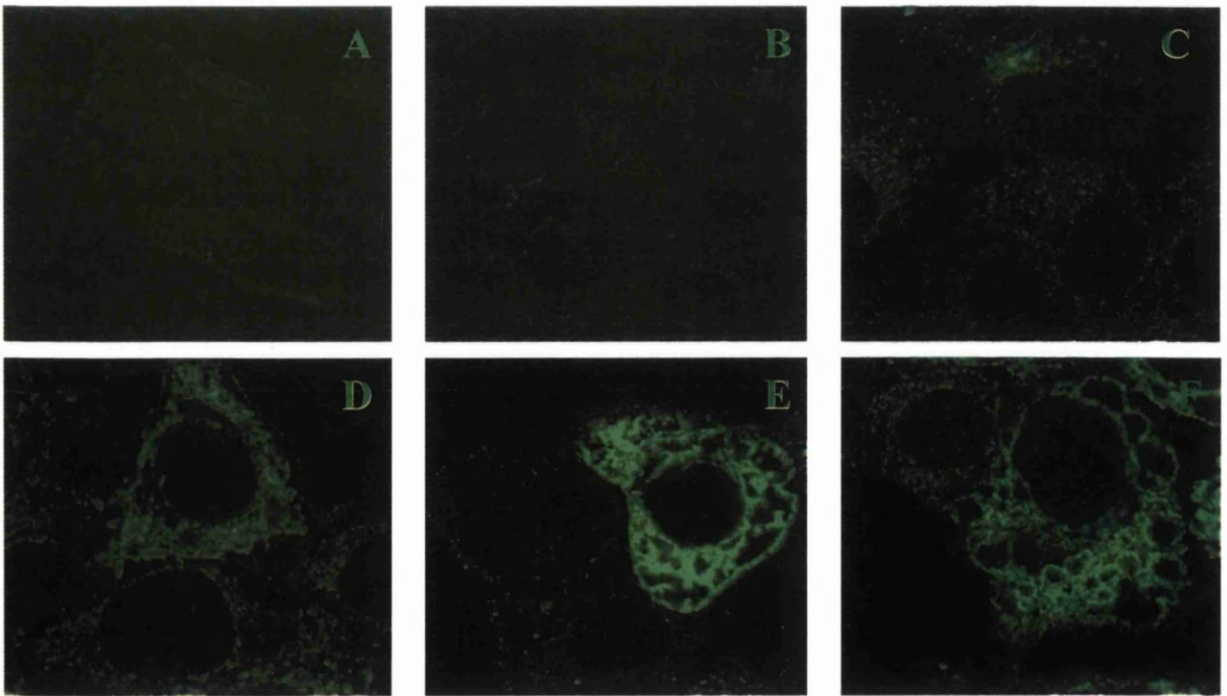


Fig. 5.3B MAb H166 recognises all the HBV surface antigens.

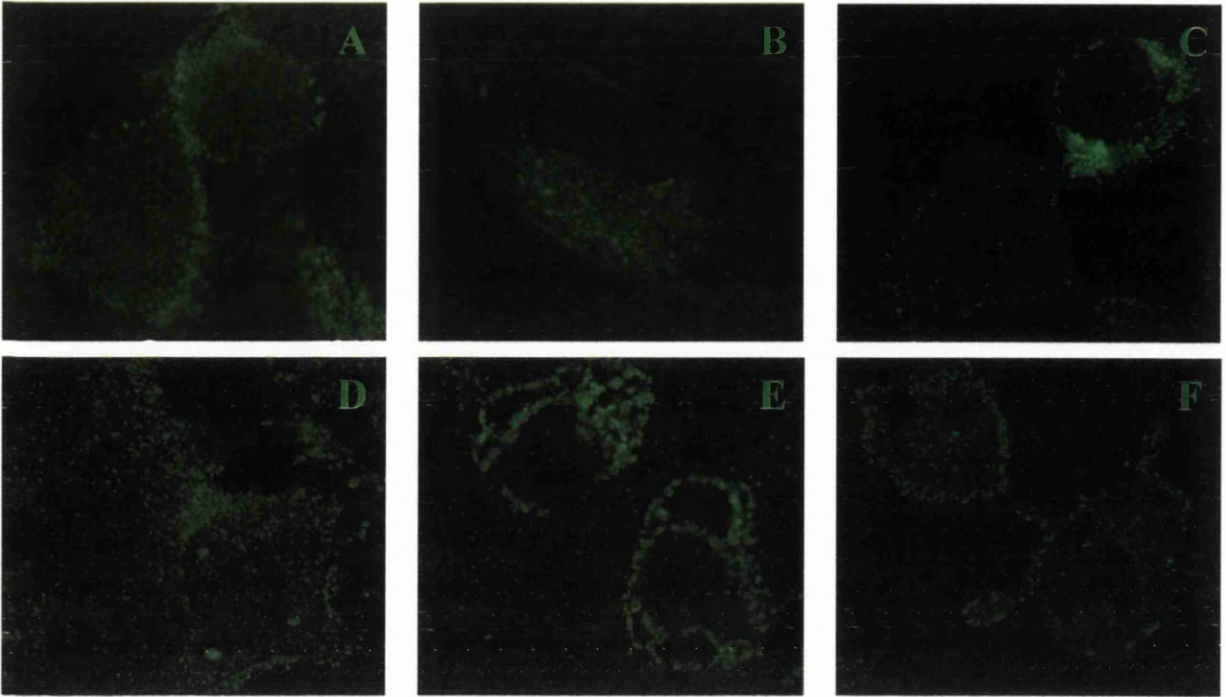


Figure 5.3C MAb H10 recognises all the HBV surface antigens.

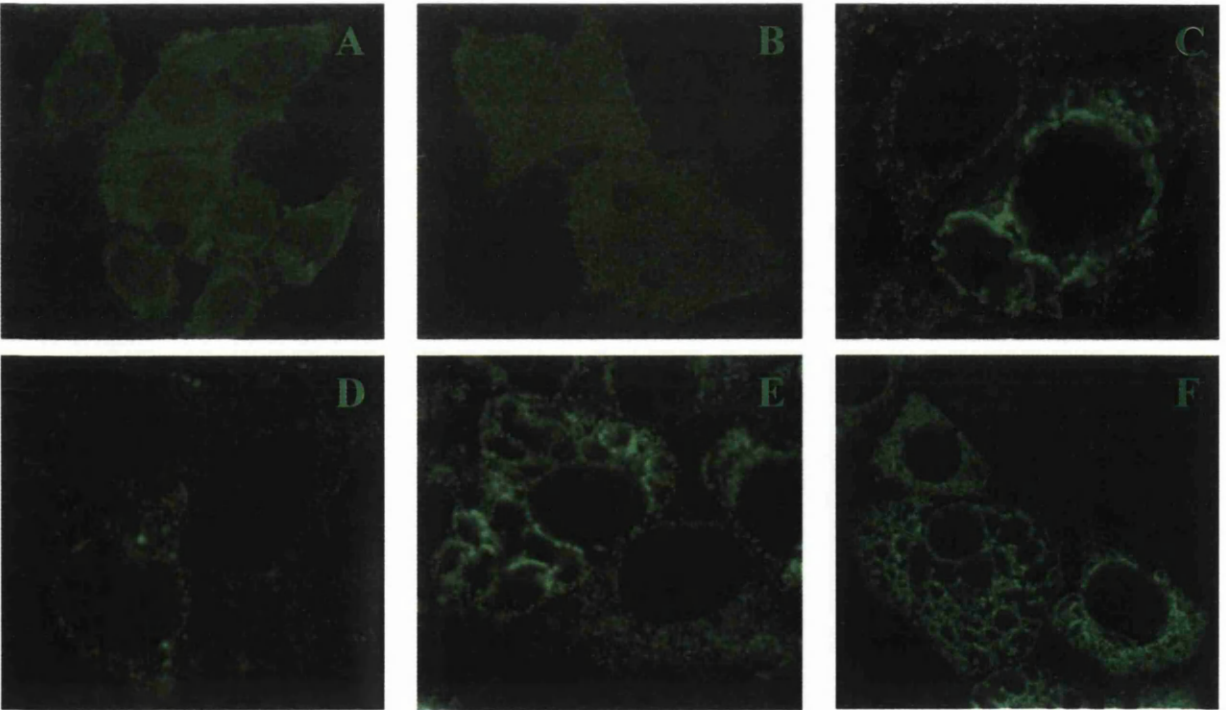


Fig. 5.3D MAb RF7 recognises all the HBV surface antigens.

to which the RF7 and H10 MAbs are reactive remain unknown to the author. The use of the above antisera to study the behaviour of S in the presence of L or Lx would be inappropriate, due to the inability of any of these antisera to differentiate between the surface antigens. This work demonstrated the difficulty of examining the behaviour of these two proteins upon co-expression.

Another anti-S monoclonal antibody, MAb 6B1 was shown in Chapter 3 to be specific for a conformation-sensitive epitope on the S protein. This antibody was tested here for its ability to recognise L, Lx, M, as well as S proteins of HBV. HepG2 cells were infected with vL, vLx, vM or vS and fixed after 24 h. The cells were then probed with MAb 6B1 and analysed by confocal microscopy. As shown in Fig.5.4, this MAb recognised the S protein and the S domain of M (panels B and C), but interestingly, failed to recognise the S moiety on Lx (panel D) It was clear that MAb 6B1 is able to distinguish between the S protein and S domain present in L, and therefore it constitutes a valuable immunological reagent to study the properties of these proteins in expressing cells.

5.3 Co-expression of L and S

As shown in Fig. 5.1A, the HBV L protein is co-localised with the ERGIC marker p53 indicating retention of this protein in the ER compartment of the cell. Since in MAb 6B1 we have a monoclonal antibody that discriminates between L and S, it was thought interesting to examine the intracellular behaviour of these proteins in co-expressing cells. HepG2 cells were co-infected at low m.o.i. with vL and vS, fixed after 24 h, double immunolabelled with anti-preS1 PAb 143 and anti-S MAb 6B1, and analysed by confocal microscopy. Figure 5.5 panel A, shows two cells infected with the rVVs; one of which had an even cytoplasmic distribution of L whereas in the other, it is akin to that seen in S-expressing cells (see Fig. 5.3, panels C to F). The later cell could also be stained by the anti-S MAb 6B1 (Fig. 5.5, panel B), indicating that this cells is co-infected with vL and vS. In contrast the S staining was not seen in the cell carrying an even cytoplasmic fluorescence shown in panel A, indicating that this cells is only infected with vL. This is confirmed by the inability of MAb 6B1 to recognise L in this cell. Superimposition of the two images showed that L and S co-localised in the doubly infected cells (panel C). Also interestingly, the intracellular distribution of L when co-expressed with S changed dramatically - from the ERGIC

compartment to the matrix-like membrane-associated localisation observed with S (Fig. 5.5). The clear difference in the fluorescent labelling of L and S was apparent in Fig. 5.5; the anti-preS1 PAb labelled the L protein (coloured red) and the 6B1-labelled S protein, but not L (coloured green). The inability of the 6B1 antibody to recognise the L protein is also readily apparent in Fig. 5.5. Furthermore, the inability of the anti-preS1 PAb 142 to recognise S is also apparent from the cell only expressing S showing no fluorescence. An attempt was made to triple-label samples showing the L, S and concanavalin-A fluorescent. However, satisfactory images could not be obtained due to both the unavailability of the appropriate antisera and fluorescent conjugates, and also due to channel overlap from fluorochromes with emission spectra overlapping that of other fluorochromes, resulting in areas of false positive colocalisation. However, it is reasonable to assume that the association of the S protein with the intracellular membranes is also present in the cells co-expressing the S and L proteins. The characteristic lattice distribution of S observed in the S-expressing cells is preserved upon coexpression of S and L, with the distribution of L conforming to that of S. To preclude the possibility that the expression of S was causing multinucleation in the cells, samples similar to that shown in Fig. 5.5 were analysed with the same antisera, with the inclusion of a propidium iodide-labelling step to allow identification of the nuclei of the cells. As shown in Fig. 5.6, S and L are distributed in a matrix-like pattern and they co-localise, thus confirming the above observations (panel A, C and D). Furthermore, there was no evidence of multinucleation as staining with propidium iodide showed the presence of a single, intact nucleus in the co-infected cell (panel D).

Similar observations were made in cells co-infected with vLx and vS. The association of the secretable form of the L protein (Lx) with the ERGIC marker and a widespread cytoplasmic distribution of Lx is shown in Fig. 5.1B. There was no marked change in the distribution of Lx in the cell co-infected with vLx and vS (Fig. 5.7, panel A, cell on the top left corner) from that seen in vLx-infected cell. However, as with L, Lx also co-localised with S (panel C) although the association of the S and Lx differed in comparison with L and S proteins seen in Figs. 5.5 and 5.6. Here, the Lx and S formed bodies throughout the cytoplasm, but did not appear to be conforming to the membrane association as seen in the S-Concanavalin-A (Fig. 5.2). The effect of the signal sequence located at the N-terminus of the Lx protein may be sufficient to

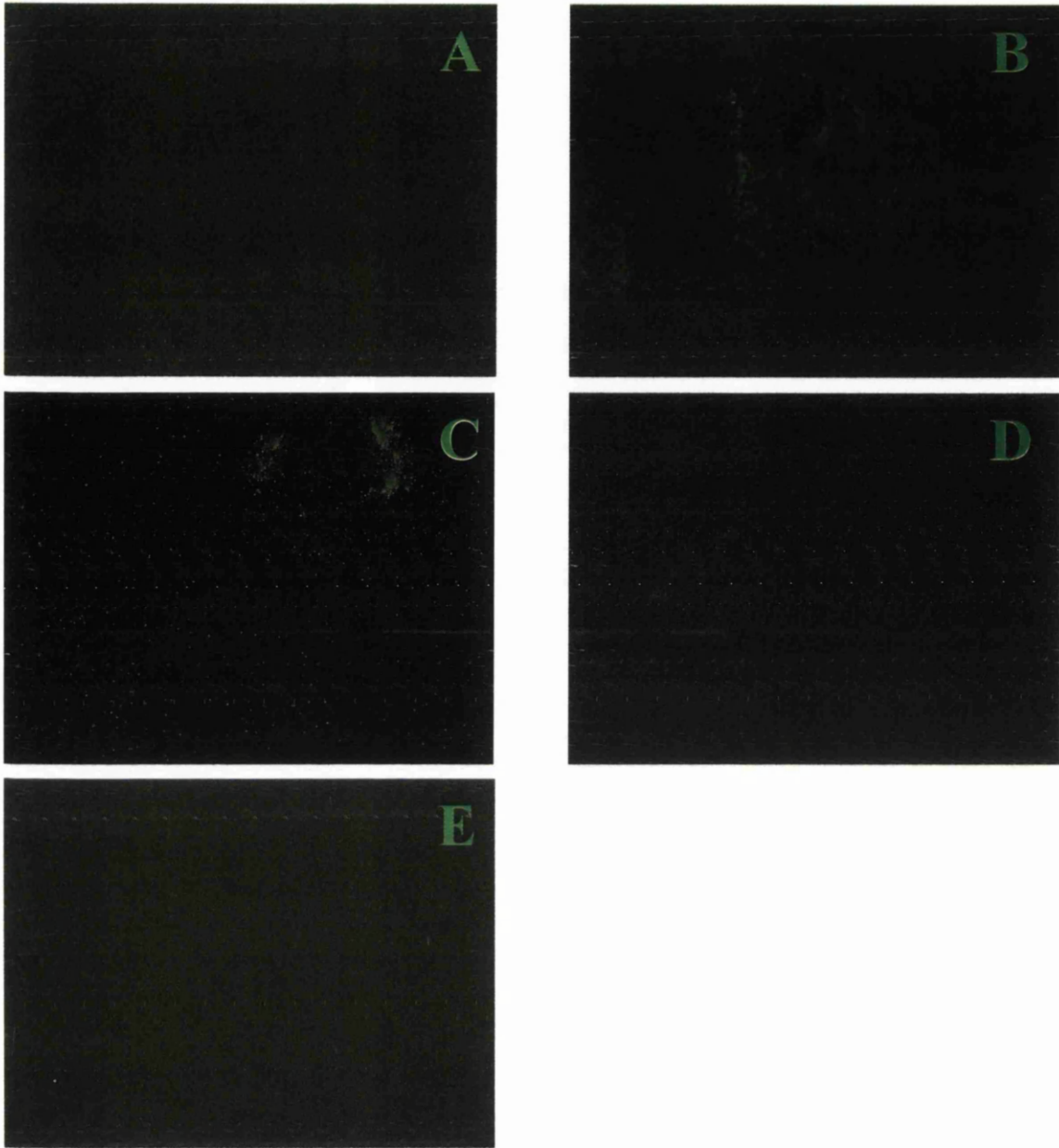


Fig. 5.4 Recognition of vM and vS by MAb 6B1.

Hepg2 cells were infected at a m.o.i. of 0.5 p.f.u per cell with, vLx, vM, vS, WR, or were mock-infected. At one hour post-infection, the cells were washed and incubated in DMEM for 24 hours. The coverslips were washed three times in PBSA and fixed in methanol at -20°C overnight. After fixing, the coverslips were washed twice with PBSA, then were permeablised by incubation with PBST for at least 30 minutes. The coverslips were incubated with MAb 6B1 for two hours in a volume of $200\ \mu\text{L}$. Unbound antibodies were removed by washing, and the coverslips were incubated in anti-mouse IgG-FITC for two hours. The coverslips were mounted and analysed with a NIKON Microphot immunofluorescent microscope.

Panel A: Wr-infected cells

Panel B: vS-infected cells

Panel C: vM-infected cells

Panel D: vLx-infected cells

Panel E: mock-infected cells

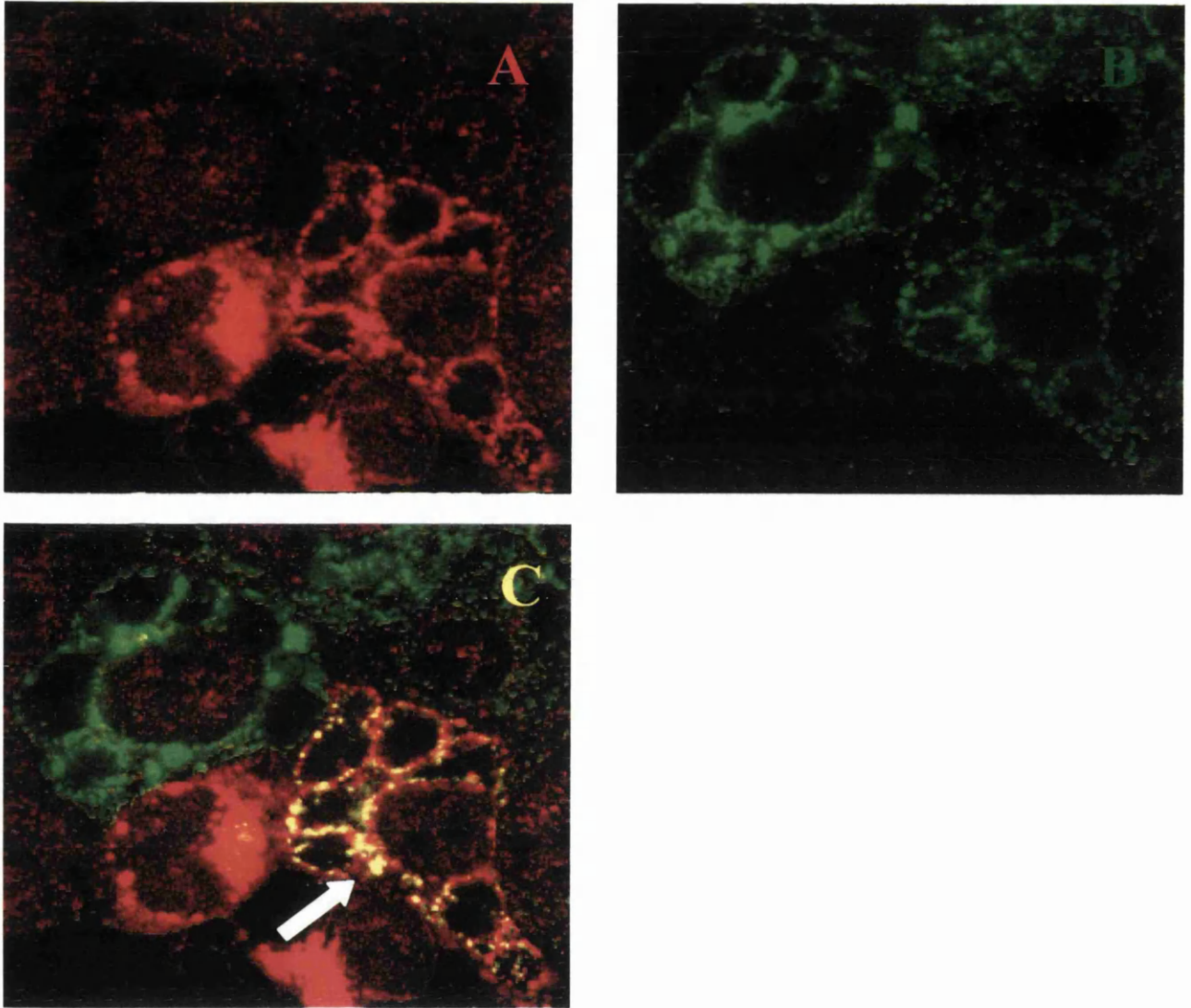


Fig. 5.5 Co-expression of L and S in HepG2 cells.

HepG2 cells were grown on glass coverslips in 24-well plates to about 60% confluence. The cells were coinfecting with vL and vS at a m.o.i. of 0.5 p.f.u per cell. At 24 h post-infection, the coverslips were washed three times in PBSA and fixed in methanol at -20°C overnight. After fixing, the coverslips were washed twice with PBSA, then were permeabilised by incubation with PBST for at least 30 minutes. The coverslips were incubated with a mixture of PAb 143 (at a dilution of 1:1000) and MAb 6B1 (at a dilution of 1:500) for two hours in a volume of $200\ \mu\text{L}$. Unbound antibodies were removed by washing, and the coverslips were incubated in a mixture of anti-mouse IgG-FITC and anti-rabbit Cy5 for two hours. The unbound secondary antibodies were removed by washing and the coverslips were mounted and analysed with a Zeiss Laser Scanning Confocal microscope.

Panel A: Cy5 fluorescence showing the intracellular distribution of vL.

Panel B: FITC fluorescence showing the intracellular distribution of vS.

Panel C: Merge. White arrow indicates areas where L and S are colocalised.

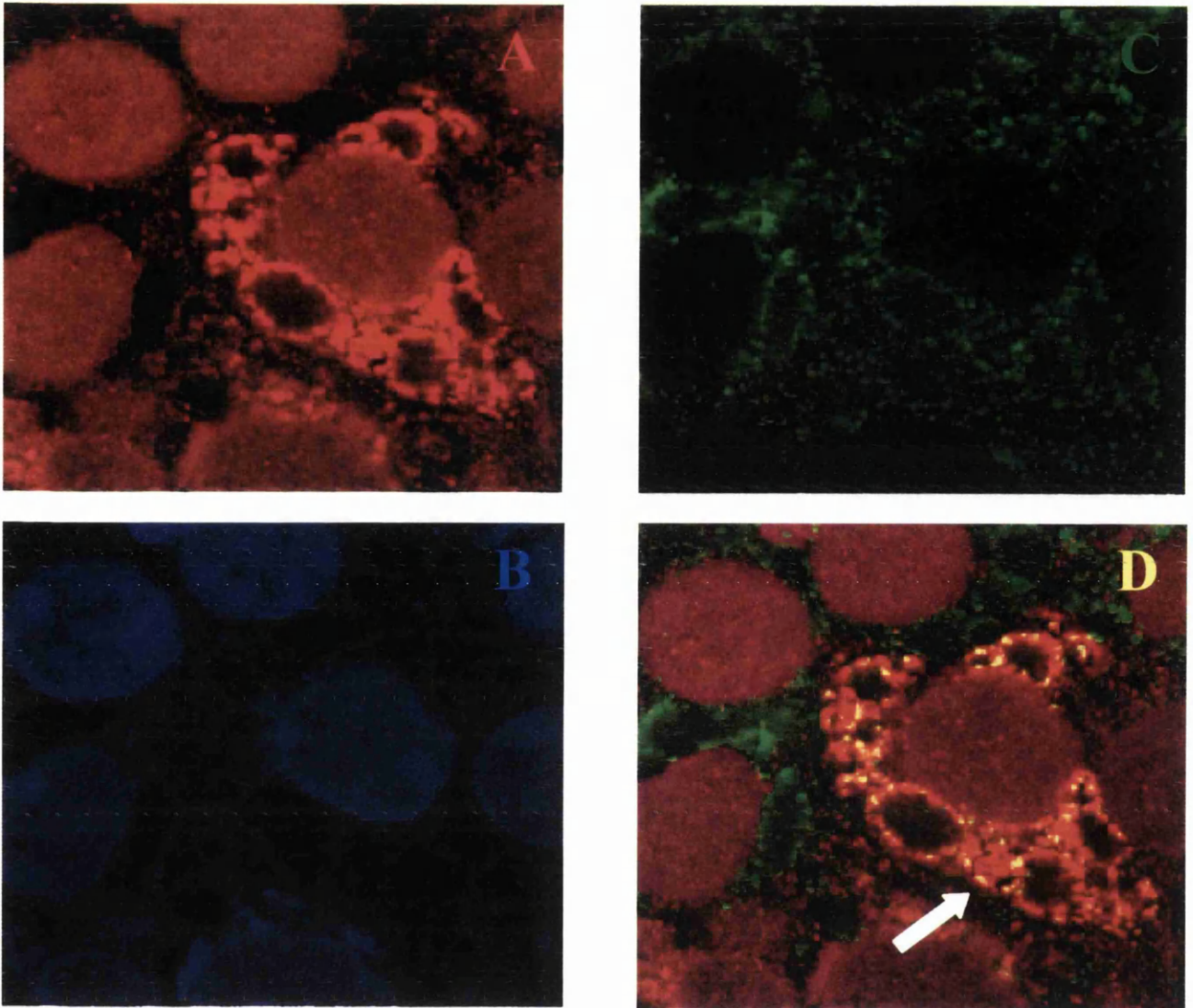


Fig. 5.6 Co-expression of L and S in HepG2 cells.

HepG2 cells were grown on glass coverslips in 24-well plates to about 60% confluence. The cells were coinfecting with vL and vS at a m.o.i. of 0.5 p.f.u per cell. At one hour post-infection, the cells were washed and incubated in DMEM for 24 hours. The coverslips were washed three times in PBSA and fixed in methanol at -20°C overnight. After fixing, the coverslips were washed twice with PBSA, then were permeabilised by incubation with PBST for at least 30 minutes. The coverslips were incubated with a mixture of PAb 143 (at a dilution of 1:1000) and MAb 6B1 (at a dilution of 1:500) for two hours in a volume of $200\ \mu\text{L}$. Unbound antibodies were removed by washing, and the coverslips were incubated in a mixture of anti-mouse IgG-FITC and anti-rabbit Cy5 for two hours. The unbound secondary antibodies were removed by washing. The coverslips were incubated with propidium iodide ($1\ \text{mg}/\text{mL}$) for one minute to stain the nuclei, and were then washed three times in PBSA. The coverslips were mounted and analysed with a Zeiss Laser Scanning Confocal microscope.

Panel A: Cy5 fluorescence showing the intracellular distribution of vL.

Panel B: Propidium iodide staining the nucleus by intercalation with DNA, coloured blue.

Panel C: FITC fluorescence showing the intracellular distribution of vS.

Panel D: Merge. White arrow indicates areas where L and S are colocalised.

could not be obtained due to both the unavailability of the appropriate antisera and fluorescent conjugates, and also due to channel overlap from fluorochromes with emission spectra overlapping that of other fluorochromes, resulting in areas of false positive colocalisation. However, it is reasonable to assume that the association of the S protein with the intracellular membranes is also present in the cells co-expressing the S and L proteins. The characteristic lattice distribution of S observed in the S-expressing cells is preserved upon coexpression of S and L, with the distribution of L conforming to that of S. To preclude the possibility that the expression of S was causing multinucleation in the cells, samples similar to that shown in Fig. 5.5 were analysed with the same antisera, with the inclusion of a propidium iodide-labelling step to allow identification of the nuclei of the cells. As shown in Fig. 5.6, S and L are distributed in a matrix-like pattern and they co-localise, thus confirming the above observations (panel A, C and D). Furthermore, there was no evidence of multinucleation as staining with propidium iodide showed the presence of a single, intact nucleus in the co-infected cell (panel D).

Similar observations were made in cells co-infected with vLx and vS. The association of the secretable form of the L protein (Lx) with the ERGIC marker and a widespread cytoplasmic distribution of Lx is shown in Fig. 5.1B. There was no marked change in the distribution of Lx in the cell co-infected with vLx and vS (Fig. 5.7, panel A, cell on the top left corner) from that seen in vLx-infected cell. However, as with L, Lx also co-localised with S (panel C) although the association of the S and Lx differed in comparison with L and S proteins seen in Figs. 5.5 and 5.6. Here, the Lx and S formed bodies throughout the cytoplasm, but did not appear to be conforming to the membrane association as seen in the S-Concanavalin-A (Fig. 5.2). The effect of the signal sequence located at the N-terminus of the Lx protein may be sufficient to encourage the recruitment of S from the ER or the intracellular membranes and subsequent transport into the cytoplasm. As shown before, the anti-S MAb 6B1 failed to recognise vLx (Fig. 5.7, compare panel A and B cell on the bottom left).

Having established that L and S co-localised to the same compartment in co-expressing cells, it was interesting to see if similar interaction between L or Lx and M existed. To examine this, HepG2 cells were co-infected with vL and vM or vLx and vM, fixed after 24 h, probed with anti-preS1 PAb 143 and the anti S MAb 6B1, and

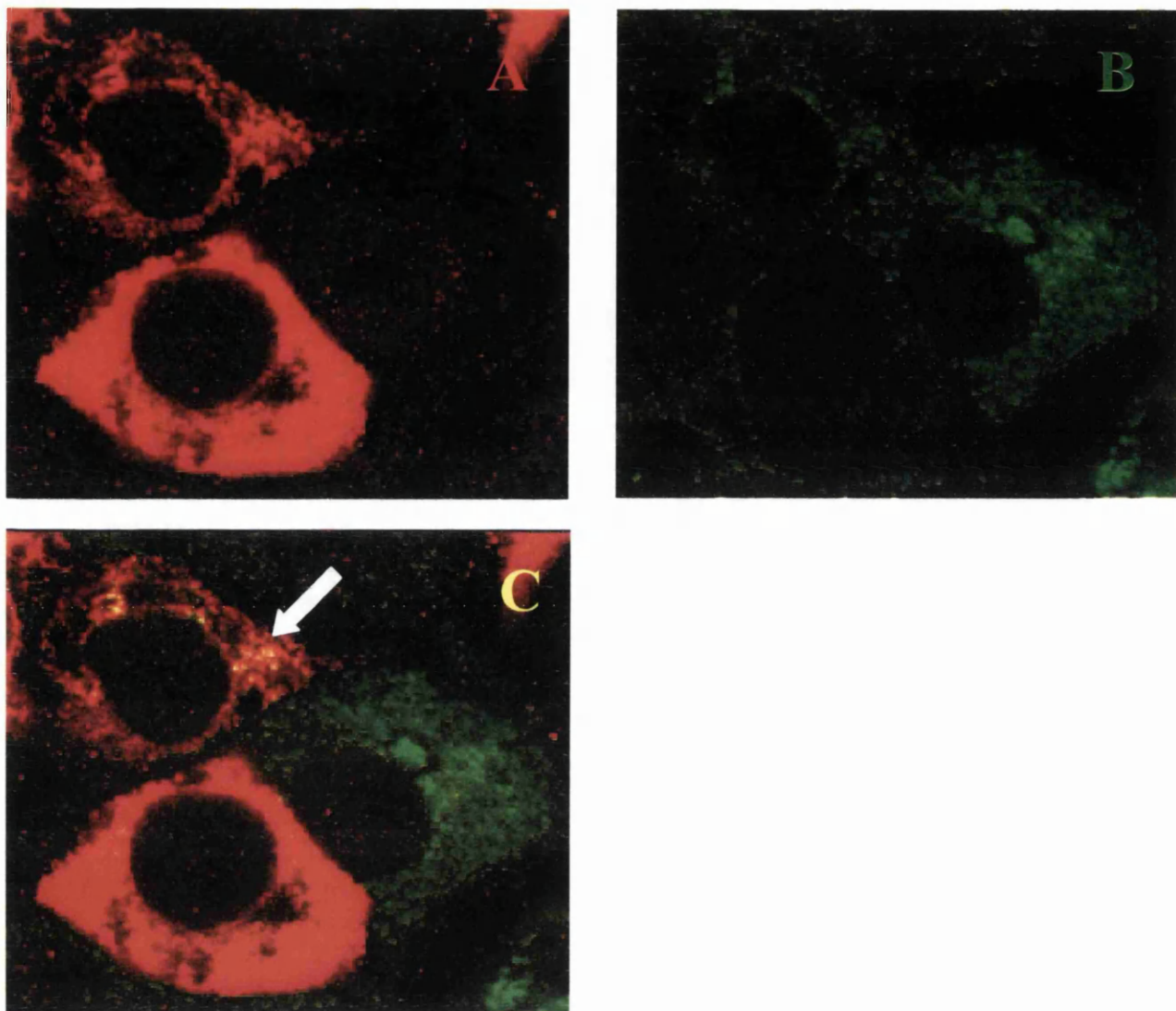


Fig. 5.7 Co-expression of Lx and S in HepG2 cells.

HepG2 cells were grown on glass coverslips in 24-well plates to about 60% confluence. The cells were infected with both vLx and vS at a m.o.i. of 0.5 p.f.u per cell. At 24 h, post-infection, the coverslips were washed three times in PBSA and fixed in methanol at -20°C overnight. After fixing, the coverslips were washed twice with PBSA, then were permeabilised by incubation with PBST for at least 30 minutes. The coverslips were incubated with a mixture of PAb 143 (at a dilution of 1:1000) and MAb 6B1 (at a dilution of 1:500) for two hours in a volume of $200\ \mu\text{L}$. Unbound antibodies were removed by washing, and the coverslips were incubated in a mixture of anti-mouse IgG-FITC and anti-rabbit Cy5 for two hours. The unbound secondary antibodies were removed by washing and the coverslips were mounted and analysed with a Zeiss Laser Scanning Confocal microscope.

Panel A: Cy5 fluorescence showing the intracellular distribution of vLx.

Panel B: FITC fluorescence showing the intracellular distribution of vS.

Panel C: Merge. White arrow indicates areas where Lx and S are colocalised.

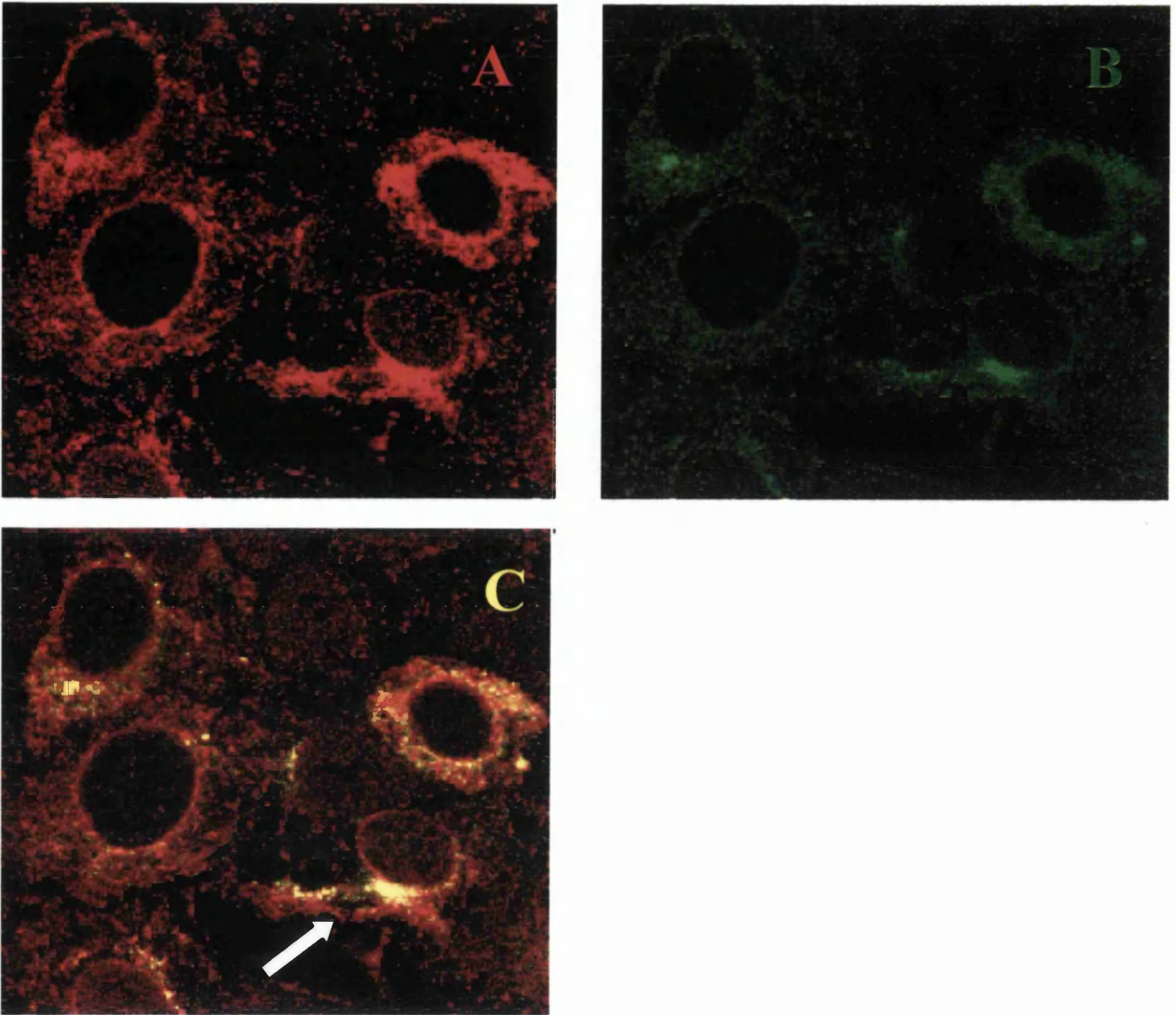


Fig. 5.8 Co-expression of L and M in HepG2 cells.

HepG2 cells were grown on glass coverslips in 24-well plates to about 60% confluence. The cells were infected with both vL and vM at a m.o.i. of 0.5 p.f.u per cell. At 24 h, post-infection, the coverslips were washed three times in PBSA and fixed in methanol at -20°C overnight. After fixing, the coverslips were washed twice with PBSA, then were permeabilised by incubation with PBST for at least 30 minutes. The coverslips were incubated with a mixture of PAb 143 (at a dilution of 1:1000) and MAb 6B1 (at a dilution of 1:500) for two hours in a volume of 200 μ L. Unbound antibodies were removed by washing, and the coverslips were incubated in a mixture of anti-mouse IgG-FITC and anti-rabbit Cy5 for two hours. The unbound secondary antibodies were removed by washing and the coverslips were mounted and analysed with a Zeiss Laser Scanning Confocal microscope.

Panel A: Cy5 fluorescence showing the intracellular distribution of vL.

Panel B: FITC fluorescence showing the intracellular distribution of vM.

Panel C: Merge. White arrow indicates areas where L and M are colocalised.

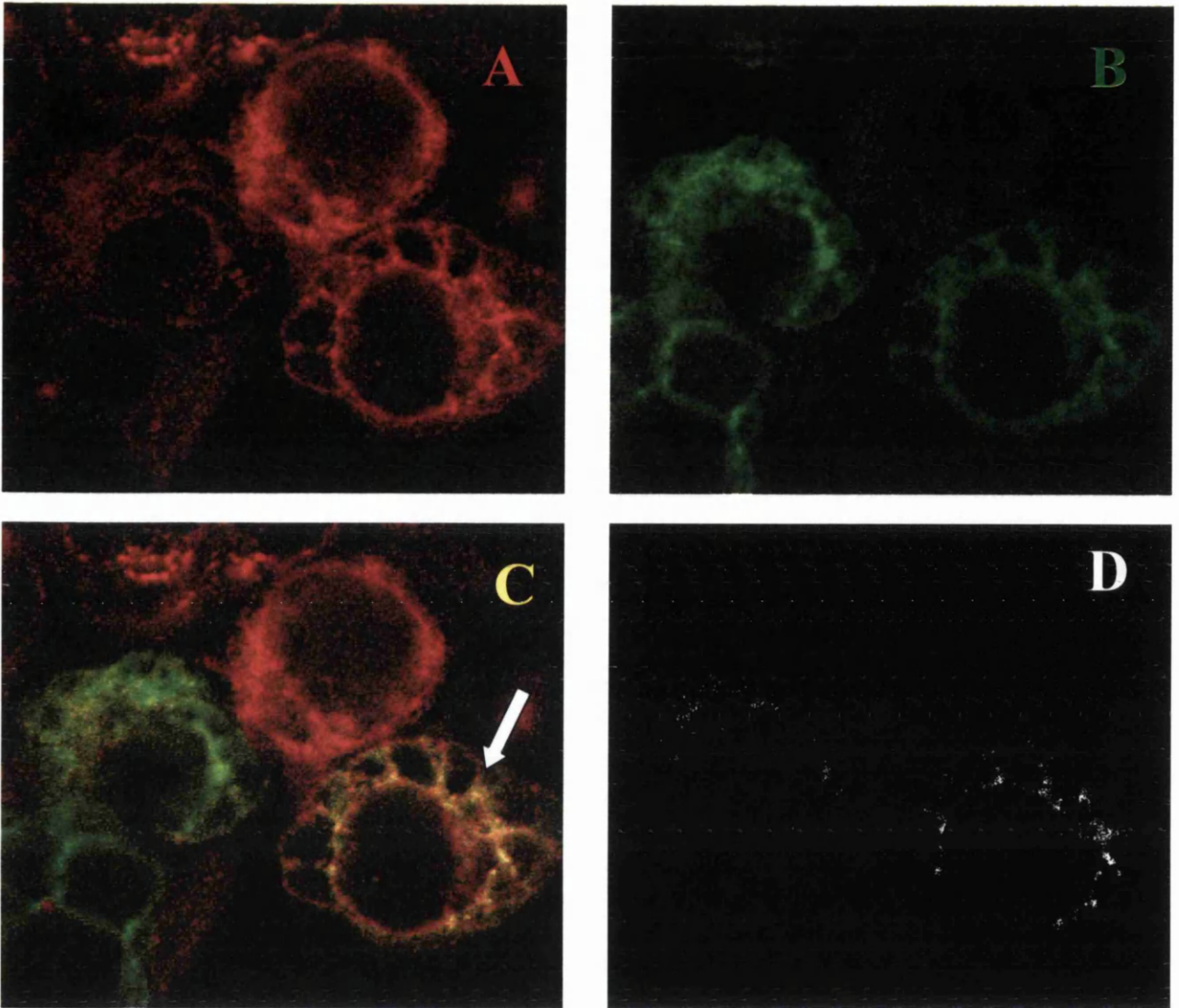


Fig. 5.9 Co-expression of Lx and M in HepG2 cells.

HepG2 cells were grown on glass coverslips in 24-well plates to about 60% confluence. The cells were infected with both vLx and vM at a m.o.i. of 0.5 p.f.u per cell. At 24 h, post-infection, the coverslips were washed three times in PBSA and fixed in methanol at -20°C overnight. After fixing, the coverslips were washed twice with PBSA, then were permeabilised by incubation with PBST for at least 30 minutes. The coverslips were incubated with a mixture of PAb 143 (at a dilution of 1:1000) and MAb 6B1 (at a dilution of 1:500) for two hours in a volume of 200 µL. Unbound antibodies were removed by washing, and the coverslips were incubated in a mixture of anti-mouse IgG-FITC and anti-rabbit Cy5 for two hours. The unbound secondary antibodies were removed by washing and the coverslips were mounted and analysed with a Zeiss Laser Scanning Confocal microscope.

Panel A: Cy5 fluorescence showing the intracellular distribution of vLx.

Panel B: FITC fluorescence showing the intracellular distribution of vS.

Panel C: Merge. White arrow indicates areas where Lx and M are colocalised.

Panel D: the subtraction of fluorescent areas containing a single label results in the localised areas being demonstrable as a black-on-white image, with the white pixels indicating the presence of both fluors at similar intensities.

encourage the recruitment of S from the ER or the intracellular membranes and subsequent transport into the cytoplasm. As shown before, the anti-S MAb 6B1 failed to recognise vLx (Fig. 5.7, compare panel A and B cell on the bottom left).

Having established that L and S co-localised to the same compartment in co-expressing cells, it was interesting to see if similar interaction between L or Lx and M existed. To examine this, HepG2 cells were co-infected with vL and vM or vLx and vM, fixed after 24 h, probed with anti-preS1 PAb 143 and the anti S MAb 6B1, and analysed by confocal analysis. Consistent with the data shown in Fig. 5.4, MAb 6B1 recognised M (Fig. 5.8, panel B), but not L (Fig. 5.8, panel A) or Lx (Fig. 5.9, panel A). The L protein as shown before was distributed evenly throughout the cytoplasm (Fig. 5.8, panel A), and in cells expressing L and M, it co-localised with the M protein (panel C). There was no major change in the distribution of either L or M in these cells. In cells infected with vLx only, the Lx protein showed the characteristic cytoplasmic distribution (Fig. 5.9, panel A). However, in the cell co-expressing Lx and M, both proteins colocalised, resulting in a dramatic change in the distribution of Lx (panels A and C). This distribution was similar to that seen in L- and S-expressing cells (Fig. 5.5) in that the proteins appeared to form a matrix-like pattern associated with internal membranes (Fig. 5.9, panels A and C). That the Lx and M proteins interact in co-expressing cells was further confirmed when fluorescence corresponding to single labels were subtracted resulting in apparent visualisation of the co-localised areas (Fig. 5.9, panel D).

5.4 Analysis of the interactions between L, Lx, M and S by immunoprecipitation.

Confocal microscopy is a powerful technique used in the analysis of the intracellular distribution of proteins to gain valuable information on the localisation and colocalisation of the studied proteins with cellular compartments and/or other proteins. Whereas data obtained by confocal microscopy may indicate colocalisation of proteins on account of two or more fluorochromes localised in similar positions intracellularly, they do not necessarily constitute evidence of a direct interaction between the studied proteins. It may simply be that the studied proteins are co-compartmentalised in the cell. To prove a direct physical interaction between two proteins, an assay to confirm the interaction must be employed. In this study,

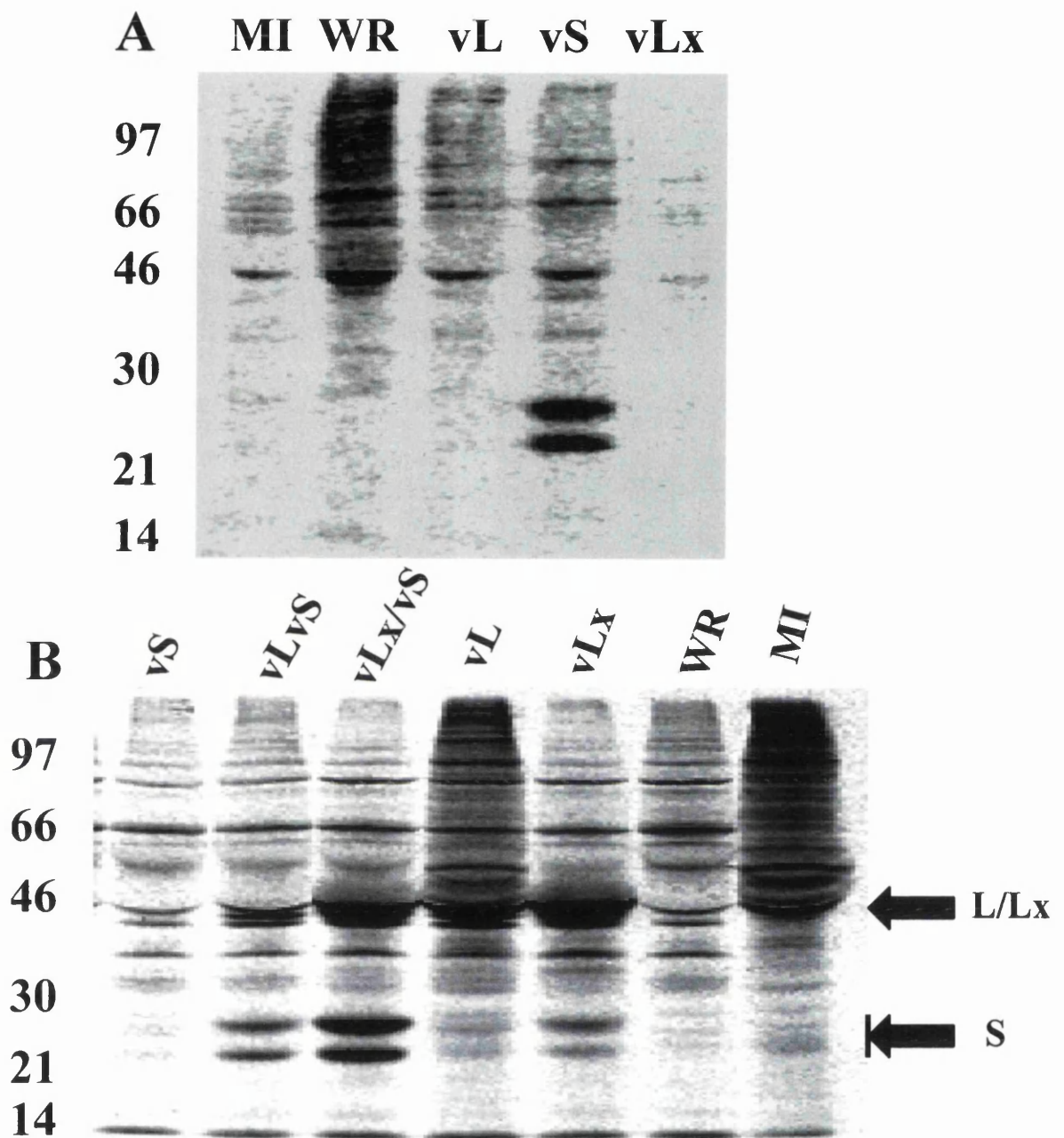


Fig. 5.10 MAb 6B1 recognises S but not L or Lx by immunoprecipitation.

HepG2 cells were grown in 60mm dishes and infected at a m.o.i. of 10 p.f.u. per cell with vL, vLx, vS, a mixture of vL and vS, a mixture of vLx and vS, WR or were mock-infected. At five hours post-infection, the cells were washed twice with PBSA and were radiolabelled with ^{35}S -methionine. At 18 hours post-labelling, the cells were lysed, clarified and subjected to immunoprecipitation with MAb 6B1 (panel A) or PAb 143 (panel B). The immune complexes were subjected to 10% SDS-PAGE and the radiolabelled proteins detected by autoradiography.

immunoprecipitation and co-immunoprecipitation techniques were used to explore the interaction between the surface antigens.

Radiolabelled proteins from HepG2 cells infected with the wild type vaccinia virus WR or rVV vL, vLx, or vS or co-infected with vL + vS or vLx + vS were immunoprecipitated with the anti-S MAb 6B1 or anti-preS1 PAb143, and the immune complexes were analysed by SDS-PAGE. As shown in Fig. 5.10A, MAb 6B1 specifically immunoprecipitated the two characteristic S bands of 26 and 28 kDa, from cells infected with vS. However, MAb 6B1 failed to precipitate L or Lx proteins from cells infected with vL or vLx. This result is consistent with the observation made in confocal microscopy analysis (Figs. 5.4 to 5.7), thus confirming that this conformation-sensitive anti-S MAb is unable to recognise the S domain of the L (or Lx) protein. This strongly indicates that S adopts a different conformation to the S domain of the L protein. There was relatively little reactivity of MAb 6B1 with either cellular (MI) or vaccinia virus proteins (WR) (Fig. 5.10A). As expected, the anti-preS1 PAb143 specifically immunoprecipitated both L and Lx proteins of approximately 42 kDa from cells infected with vL and vLx, respectively (Fig. 5.10B). A small amount of the 26 and 28 kDa S protein bands were also co-precipitated by PAb143 from these cells. This is not unexpected as transcription and translation of the S gene is known to occur from the L ORF in heterologous expression systems as well as from the viral genome. Furthermore, the anti-preS1 antiserum PAb143 also co-immunoprecipitated both S products from cells co-infected with vL + vS or vLx + vS (Fig. 5.10B). The relatively larger quantities of S bands seen in the co-infected cells strongly indicated that S produced *in trans* as well as that supplied *in cis* can directly interact with the L and Lx proteins. The co-immunoprecipitation of S with L is consistent with the confocal microscopy data shown in Figs. 5.5 to 5.7, and is in agreement with previously published results (Bruss and Ganem, 1991). These data suggest that the surface antigens, while over-expressed, are correctly folded and capable of intermolecular interactions, presumably mediated by the disulphide linkages in the transmembrane regions of the S domains.

5.5 Discussion

The HBV surface antigens and core play a pivotal role in virus/subvirus assembly, morphogenesis, and secretion. The structures of the surface antigens remain poorly

characterised due to the complex nature of conformation and transmembrane topology of these proteins. Understanding the biosynthesis, intracellular localisation, and maturation of these proteins in expressing cells should help shed light on the mechanisms involved in viral particle assembly. In this chapter, a detailed antigenic characterisation of the various HBV surface antigens was carried out using the immunological reagents described in Chapter 3.

To date, the biogenesis of HBV surface antigens has been studied largely by biochemical means. Surprisingly, very little information on the immunofluorescence-based direct visualisation of the intracellular distributions of these proteins exists. In this study, confocal microscopy was used to perform such an analysis. The results showed that L protein localised predominantly to the ERGIC compartment. The Western blot data presented in Chapter 3 showed that the L protein is not secreted. Taken together, these results are in agreement with the previously published observations that the L protein is retained in the ER (Cheng *et al.*, 1986; Chisari *et al.*, 1987; Persing *et al.*, 1986; Xu *et al.*, 1997). The L protein has been shown to bud into the ER and is retained in this compartment as 20 nm intracellular particles, possibly by association with calnexin and other ER quality control proteins (Xu *et al.*, 1997). In contrast, when forced through the secretory pathway by addition of a heterologous signal sequence at its N-terminus, the L protein is secreted as particles (Bruss and Vieluf, 1995; Gallina *et al.*, 1995). Consistent with these observations, our Lx protein, which carries a vaccinia virus signal sequence, is efficiently secreted (Fig. 3.3A). In keeping with its secretory characteristic, the intracellular distribution of Lx was markedly different from that of L. In contrast to L, the Lx protein was present throughout the cytoplasm.

The intracellular distribution of the M and S proteins was distinct from the L and Lx proteins in that both of these proteins co-localised with intracellular membranes, as defined by co-staining with ConA. The lectin Con A has a highly specific affinity for carbohydrates with terminal α -D-mannosyl and α -D-glucosyl residues present on glycoproteins. Thus, ConA specifically stains the glycoproteins present in internal membranes (mainly the ER) which have such sugar residues. Both M and S are synthesized as transmembrane proteins, and their translocation across the ER is

mediated by signals of hydrophobic amino acids within the S domain (Eble *et al.*, 1986; Eble *et al.*, 1990; Eble *et al.*, 1987; Sheu and Lo, 1994). Both M and S are known to be secreted from expressing cells. It is not clear why the intracellular distribution pattern of M and S differs from that of Lx, but it is possible that Lx is secreted through a different secretion pathway.

In addition to examining the intracellular distribution of the HBV surface antigens, several anti-S MAbs were tested for antigen recognition. One set of MAbs, H166, H10, and RF7 all recognised S but also L, Lx, and M proteins in confocal assays. MAb H166 is known to recognise a linear epitope (amino acids 121-124) in S, whereas MAb H35 recognises a discontinuous epitope (amino acids 122 – 130 and 166 – 175; (Chen *et al.*, 1996). In contrast with these MAbs, MAb 6B1 which is specific for a conformation-sensitive epitope in S recognised S and M, but not L (or Lx) in an immunofluorescence and immunoprecipitation assays, indicating structural differences in the S moiety of L from that in M and S. It is important to point out here that although all the surface antigens used here have been derived from the *adw* subtype of HBV, the S was obtained from a different patient serum. The M gene was subcloned from that encoding L and therefore originates from the same patient sample. Furthermore, amino acid sequence comparison has identified several variant amino acids between the S domain in L and S (see Appendix 2). However, the inability of MAb 6B1 to recognise the S domain in L or Lx is highly unlikely to be due to the presence of the variant amino acids in L because this MAb clearly recognised the M protein. Rather the data strongly indicate that there are discernible structural differences between the S domain of L, and that of M and S. Interestingly, in cells co-expressing L and S there was a dramatic change in the distribution of L. The L protein appeared to co-localise with S to intracellular membranes, indicating that it is no longer retained in the ER. The behaviour of the L protein when co-expressed depends on the relative amounts of other surface antigens, however, a small portion of it is secreted (Cheng *et al.*, 1986; Chisari *et al.*, 1987; Molnar-Kimber *et al.*, 1988). In these confocal assays the S protein also co-localised with M and Lx proteins.

That there is a specific interaction between L (or Lx) and S was shown by immunoprecipitation assay where an anti-preS1 PAb specifically co-precipitated the S

proteins from cells infected with vL (or vLx) and vS. Other authors have shown immunoprecipitation and SDS-PAGE analysis that the surface antigens form heteromultimeric complexes upon co-expression (Cheng *et al.*, 1986; Chisari *et al.*, 1987; Molnar-Kimber *et al.*, 1988; Wunderlich and Bruss, 1996). A small amount of S synthesised by internal initiation from the L ORF encoded by vL was co-immunoprecipitated by the anti-preS1 PAb. The failure of MAb 6B1 to recognise these S products in both immunoprecipitation and immunofluorescence is likely due to their very low levels of expression in cells.

It is possible the S domain in L protein has a dramatically different topology to the S protein, but presumably, the ability to interact with S must be conserved in order to retain the ability to form virions. It is also worth considering that the insertion of the preS1 domain into the lipid bilayer at Gly2 via the myristic acid moiety, which is necessary for infectivity (Bruss *et al.*, 1996b) may affect the spatial arrangement of the transmembrane regions, therefore contributing to a difference in the conformation of S and L. It is also feasible that the arrangement of the alpha helices in S and L differs, but the association of the disulphide linkages forming the intermolecular bonds remains conserved to allow oligomerisation of the envelope proteins. The observation of Lx interacting with S may indicate that the structure of the Lx protein is similar to that of the L protein, although it may be possible that the extra-luminal domains of the Lx protein whilst undergoing processing in the ER are less abundant than those in the L protein. Furthermore, it can be seen from the Figs. 5.2 and 5.4 that the recognition of S by MAb 6B1 occurs even when the S and L proteins are interacting. This indicates that the binding site of the MAb 6B1, even though unidentified, remains exposed and intact when the S protein is interacting with the L or Lx proteins.

To my knowledge, this is the first report which describes an immunological reagent capable of selectively discriminating S, and the S domain of M, from that of the L protein. Numerous studies on the biosynthesis and maturation of HBV surface antigens have been performed over the years, leading researchers to propose topology models of these proteins. However, several important aspects are unclear. The availability of MAb 6B1 with its unique/novel characteristics should further facilitate the study of the conformational nature of these proteins, without the use of potentially

disruptive techniques such as tagging with heterologous epitopes or fluorescent protein domains into the surface antigens.

Chapter 6

Investigation of the interaction between HBV core and L proteins.

The encapsidation of hepadnavirus pregenomic RNA depends on the formation of a ribonucleoprotein (RNP) complex with the viral polymerase and certain cellular factors that include the heat shock protein 90 (Hsp90) (Hu and Seeger, 1996). This multi-component complex assembles together with HBV core to form nucleocapsids which in turn are enveloped at the ER by docking to the preS regions of viral surface antigen (Bruss and Ganem, 1991; Dyson and Murray, 1995; Ostapchuk *et al.*, 1994; Prange and Streeck, 1995). However, the process of hepadnaviral morphogenesis remains poorly understood, and in particular there is little data concerning the *in vivo* interactions of the structural proteins in the processes of morphogenesis. Previous data based on observations from *in vitro* studies has suggested an interaction of the core protein with the L protein (see Introduction), but there is very little *in vivo* information to support the validity of these observations. Studies of the *in vitro* L-core interaction have suggested a synergistic interaction of core with both the preS1 domain and the S domain of the L protein (Tan *et al.*, 1999). Using deletion analysis, and short peptide mimotopes corresponding to the L protein in an *in vitro* core-binding assay, Tan *et al.* (1999) identified two peptides that were capable of binding the core protein. One of the peptides corresponded to a region within (amino acids 24-119) of the L and the second to a region (amino acids 191-322) in the S domain. Furthermore, the dissociation constants of these peptides to the core protein were different, with the preS1-specific peptide binding strongly, where the S-specific peptide bound relatively weakly to the core. Furthermore, Tan *et al.* suggest that both the preS1 peptide region and the S peptide region bind to the core protein a stronger bond and this is the evidence of a synergistic interaction. Whether the peptide in the S domain of HBsAg and M protein is capable of binding to the core protein *in vivo* remains unclear.

Although considerable benefit can be derived from data obtained from *in vitro* studies, *in vivo* analysis often results in data more likely to reflect the nature of the interactions within the infected cell. This work was undertaken as part of a study of the localisation of the HBV surface antigens within the cell, when expressed

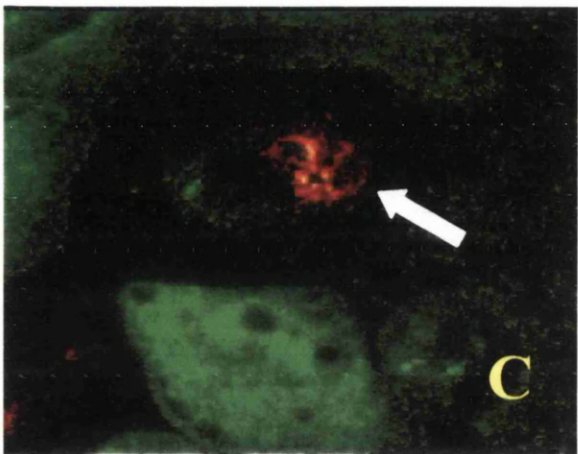
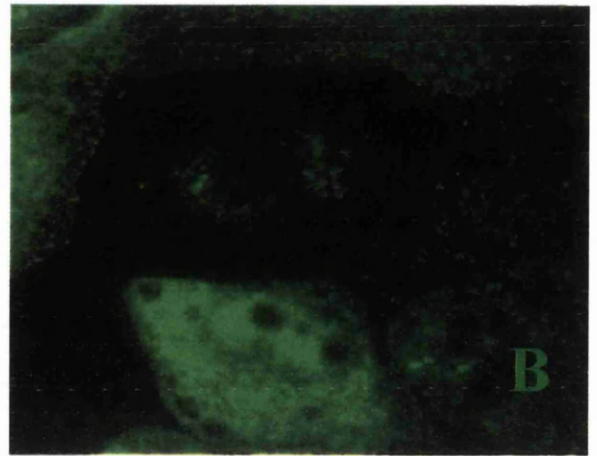
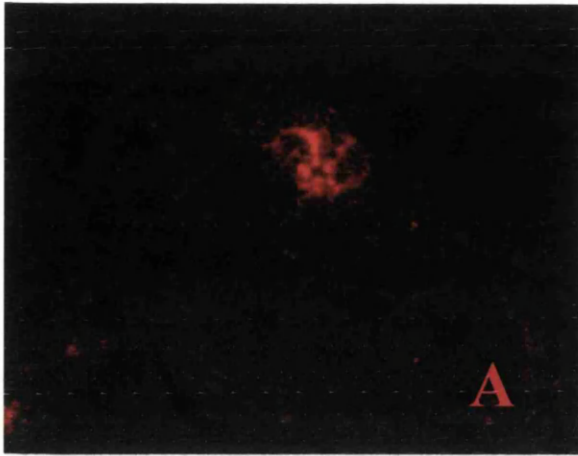


Figure 6.1 Colocalisation of core and L in HepG2 cells.

HepG2 cells on glass coverslips in 24-well plates were coinfectd at an m.o.i. of 0.5 p.f.u./cell with rVVs vL and v5D. At 24 hours post-infection, the cells were fixed in methanol at -20°C, then permeablised in PBST. The cells were probed with MAb RC109 (anti-L) and PAb anti-core for two hours at room temperature, then were washed in PBST. The coverslips were incubated with anti-mouse FITC and anti-rabbit IgG-Cy5, and the coverslips were mounted and examined by confocal microscopy.

Panel A: cells expressing vL stained with MAb RC109 and anti-mouse IgG-FITC.

Panel B: cells expressing core stained with PAb anti-core and anti-rabbit IgG-cy5, coloured red

Panel C: merge. White arrow shows colocalised areas of core and L.

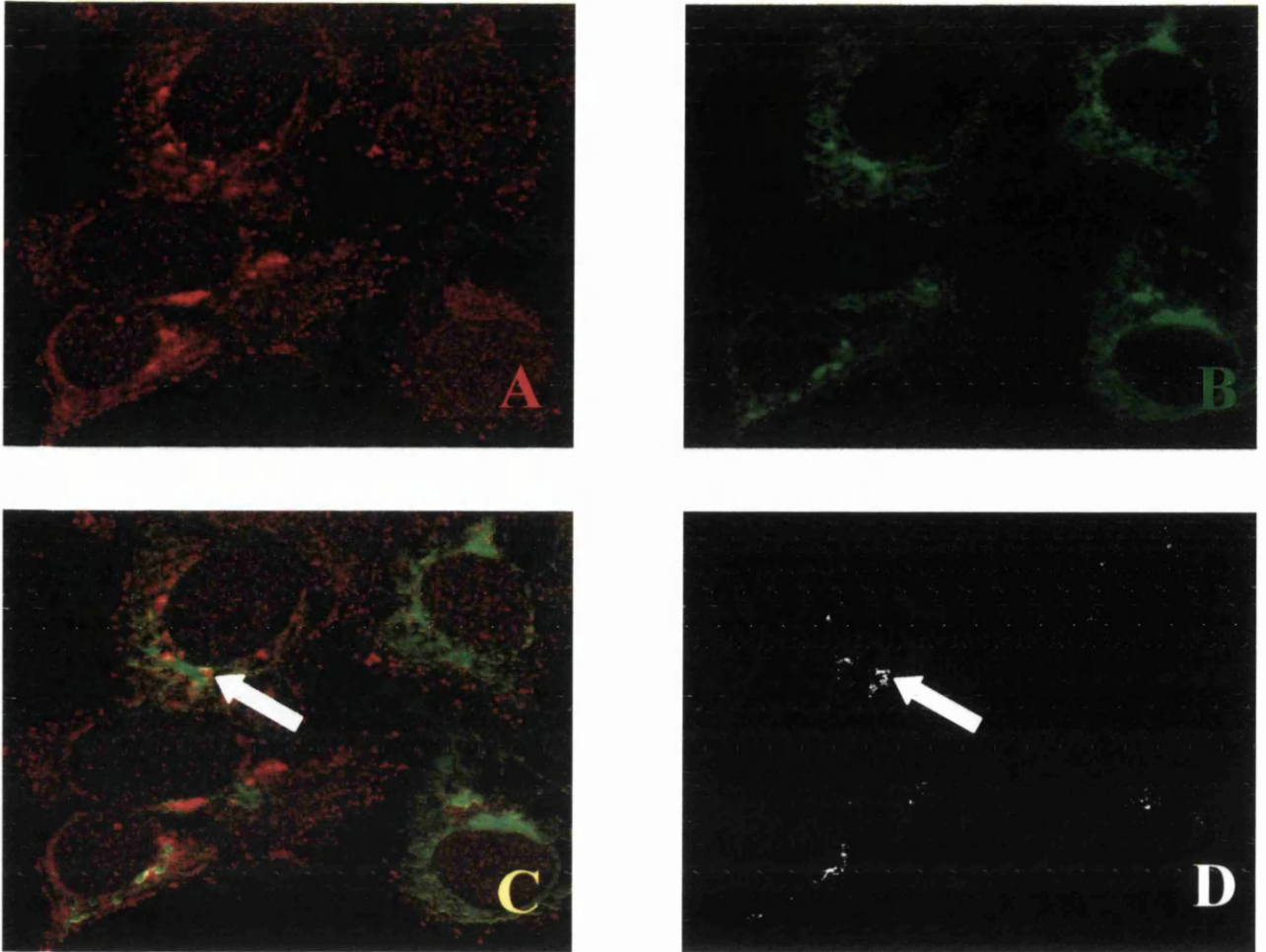


Figure 6.2 Colocalisation of core in H5 cells expressing core and L.

H5 cells on glass coverslips in 24-well plates were coinfectd at an m.o.i. of 0.5 p.f.u./cell with vL and v5D. At 24 hours post-infection, the cells were fixed in methanol at -20°C , then permeablised in PBST. The cells were probed with MAb RC109 (anti-L) and PAb anti-core for two hours at room temperature, then were washed in PBST. The coverslips were incubated with anti-mouse FITC and anti-rabbit IgG-Cy5, and the coverslips were mounted and examined by confocal microscopy.

Panel A: cells expressing core stained with PAb anti-core and anti-rabbit IgG-cy5, coloured red.

Panel B: cells expressing vL stained with MAb RC109 and anti-mouse IgG-FITC.

Panel C: merge. White arrow shows colocalised areas of core and L.

Panel D: the subtraction of fluorescent areas containing a single label results in the localised areas being demonstrable as a black-on-white image, with the white pixels indicating the presence of both fluors at similar intensities.

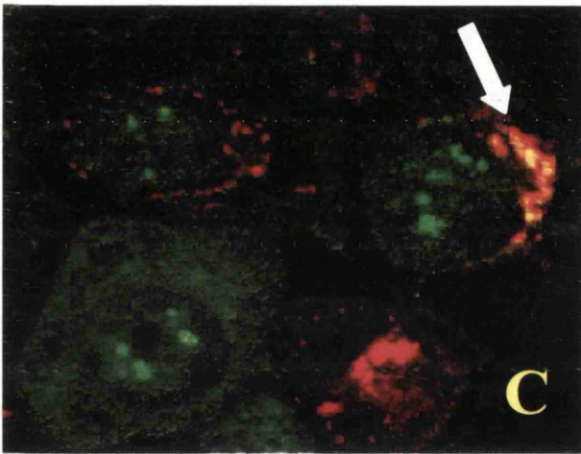
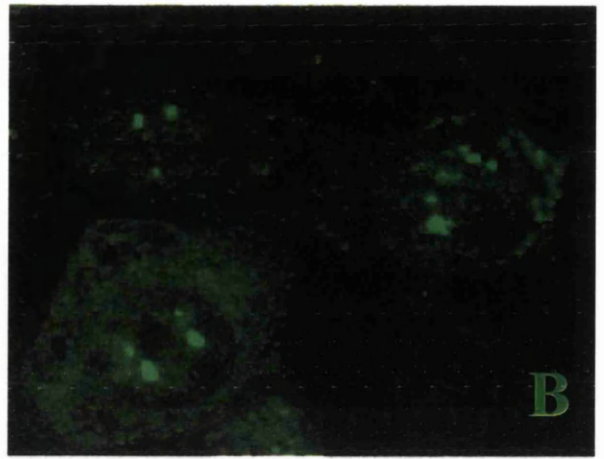
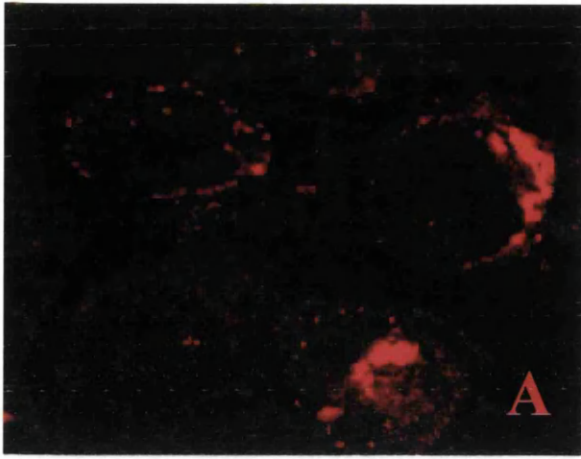


Figure 6.3 Colocalisation of core and L in HeLa cells.

HeLa cells on glass coverslips in 24-well plates were coinfectd at an m.o.i. of 0.5 p.f.u./cell with vL and v5D. At 24 hours post-infection, the cells were fixed in methanol at -20°C , then permeablised in PBST. The cells were probed with PAb 143 (anti-L) and MAb 2A23 anti-core for two hours at room temperature, then were washed in PBST. The coverslips were incubated with anti-mouse FITC and anti-rabbit Cy5, and the coverslips were mounted and examined by confocal microscopy.

Panel A: cells expressing vL stained with PAb 143 and anti-mouse IgG-FITC, coloured red.

Panel B: cells expressing core stained with MAb 2A23 and anti-rabbit IgG-cy5 coloured green

Panel C: merge. White arrow shows colocalised areas of core and L.

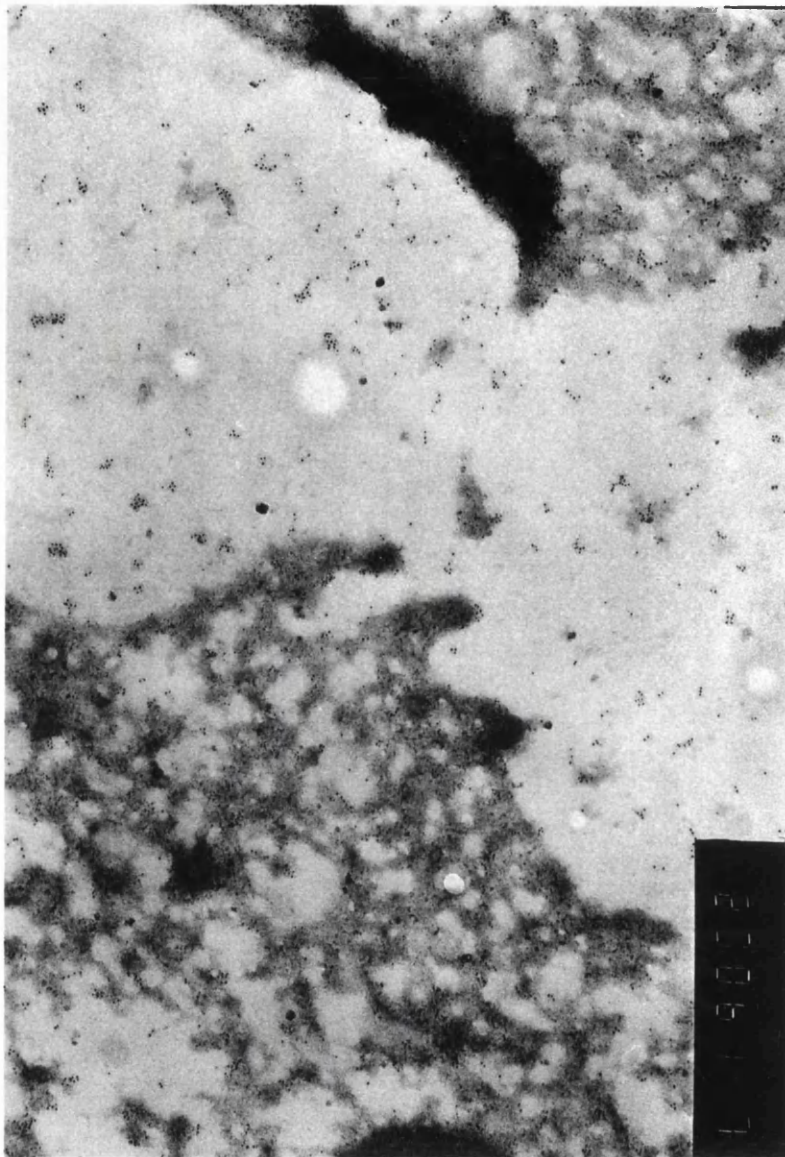


Figure 6.4 Intracellular distribution of Core and L in H5 cells.

H5 cells in 6-well plates were coinfectd with wild-type vaccinia strain WR at a m.o.i of 5 p.f.u./cell and incubated for 18 hours at 37°C. The cells were washed three times with PBSA and scraped into Beem capsules and centrifuged at 400 r.p.m. in a Beckman benchtop centrifuge. The supernatant was discarded, and the cell pellet was fixed by the addition of 400 μ L of 2.5 % glutaraldehyde and then embedded and permeated in 4% gelatin at 37°C. The cell pellets were removed from the capsules and cryo-sectioned into 100 μ M sections, were transferred onto Nickel grids and labelled with primary antibodies (PAb 143 anti-L, and MAb 2A23 anti-core), and secondary antibody-gold conjugates anti-mouse IgG-5nm gold, and anti-rabbit IgG-15nm gold. The samples were visualised with a JOEL 100S electron microscope.

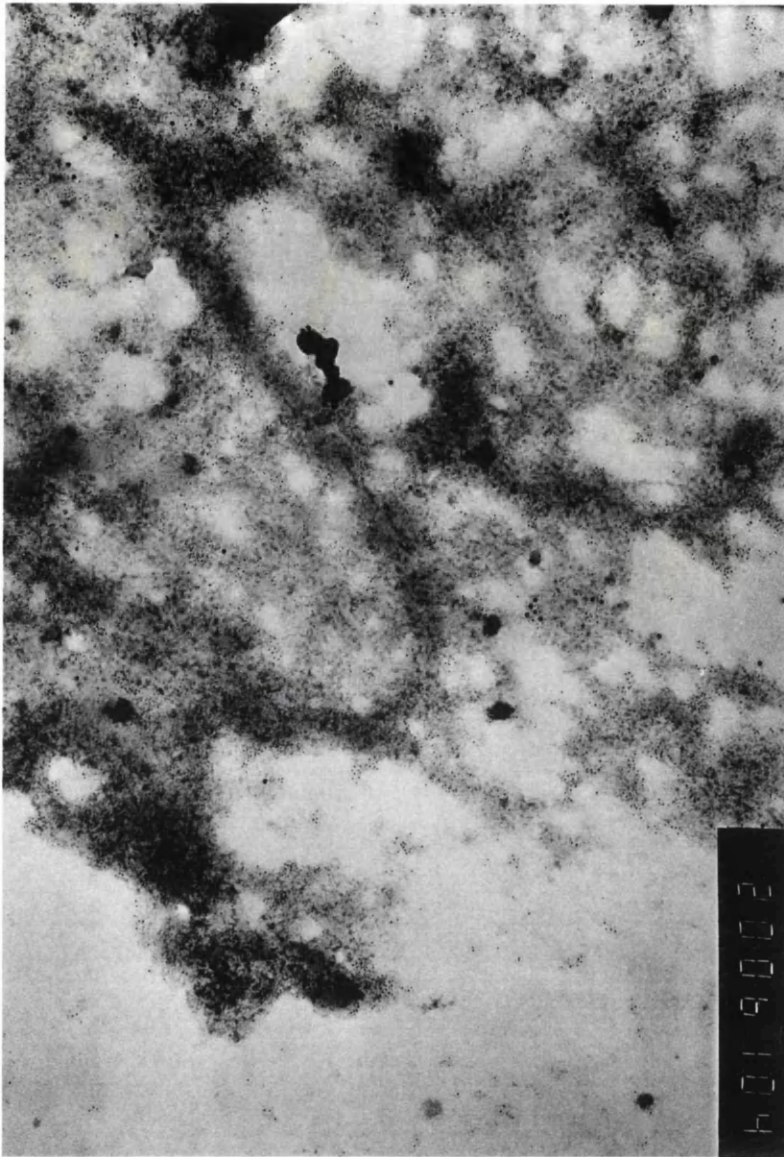


Figure 6.5 Intracellular distribution of Core and L in H5 cells.

H5 cells in 6-well plates were coinfectd with vL and v5D virus at a m.o.i of 5 p.f.u/cell and incubated for 18 hours at 37°C. The cells were washed three times with PBSA and scraped into Beem capsules and centrifuged at 400 r.p.m. in a Beckman benchtop centrifuge. The supernatant was discarded, and the cell pellet was fixed by the addition of 400 μ L of 2.5 % glutaraldehyde and then embedded and permeated in 4% gelatin at 37°C. The cell pellets were removed from the capsules and cryo-sectioned into 100 μ M sections, were transferred onto Nickel grids and labelled with primary antibodies (PAb 143 anti-L, and MAb 2A23 anti-core), and secondary antibody-gold conjugates anti-mouse IgG-5nm gold, and anti-rabbit IgG-15nm gold. The samples were visualised with a JOEL 100S electron microscope.

singularly and upon co-expression with HBV core. Here, a detailed intracellular analysis of the interactions of the surface antigens with core protein has been performed.

6.1 Intracellular localisation of HBV core protein

The distribution of HBcAg produced in HepG2 cells infected with v5D was assessed and compared with reported data. The core protein from v5D can be seen stained with a polyclonal antibody in cells in Fig. 3.3 panel E, and appears ubiquitously distributed throughout the cytoplasm and nucleus, with weaker staining present in the latter, but no staining of the nucleoli. This behaviour of core is in agreement with that observed by others (Aiba *et al.*, 1997).

6.2 Coexpression of L and core.

As reported in Chapter 5, the HBV L protein when expressed using recombinant vaccinia virus in mammalian cells is retained in the ERGIC compartment. The intracellular localisation characteristics of HBV L and core proteins when co-expressed or expressed individually were examined by confocal microscopy using appropriate antibodies. HepG2 cells were co-infected with recombinant vaccinia virus vL and v5D expressing HBV L and core proteins, respectively. The cells were fixed and analysed by indirect immunofluorescence confocal microscopy using anti-L MAb RC109 and anti-core polyclonal antibodies. As shown in Fig. 6.1 (panel B), in cells infected with v5D alone, the core was distributed throughout the cytoplasm and the nucleus with roughly equal intensity. In co-infected cells, the distribution pattern of L was similar to that seen previously (see above) it co-localised with the ERGIC compartment. In contrast, in co-infected cells the intracellular distribution of core had changed; it was not present in the nucleus but it co-localised with L (Fig. 6.1, panels B and C). These results indicate that L influences the intracellular localisation of core such that it co-localises with L in co-expressing cells, and this may occur due to a direct interaction between the two proteins. This redistribution of the core protein when co-expressed with the L protein was evident not only in HepG2 cells as shown above (Fig. 6.1), but also in the other human hepatocyte cell line H5, and in HeLa cells (Figs. 6.2 and 6.3, respectively). This indicated that the redistribution of core in the presence of L is not restricted to a particular cell type.

Whereas the confocal data shows the colocalisation of the core and L protein clearly, this observation alone is insufficient to confirm the existence of the L-core protein-protein interaction. In order to clarify the presence of the interaction *in vivo*, a different method was employed, which would allow immunological detection by electron microscopy (EM) of the proteins in cryo-sectioned. Briefly, the H5 cells were infected with the wild type vaccinia virus strain WR or co-infected with the recombinant viruses vL and v5D in 6-well plates at a m.o.i of 5 p.f.u./cell and incubated for 18 hours at 37°C. The cells were washed three times with PBSA and scraped into Beem capsules and centrifuged at 400 rpm in a Beckman benchtop centrifuge. The supernatant was discarded, and the cell pellet was fixed by the addition of 400 µL of 2.5 % glutaraldehyde (EM grade, double distilled, TAAB, Amersham, UK), and stored at 4°C prior to processing. The cell pellet was then embedded and permeated in 4% gelatin (TAAB, Amersham, UK) at 37°C. The cell pellets were removed from the capsules and sectioned into 100 µM sections, transferred onto Nickel, Copper or gold grids, and labelled with primary antibodies (PAb 143 anti-L, and MAb 2A23 anti-core) followed by secondary antibody conjugated to gold particles of 10 or 15 nm. The samples were stained with vanadium and visualised in a JOEL 100S electron microscope. As shown in Fig. 6.4, both the anti-L PAb 143 and the anti-core MAb 2A23 bound to proteins in the cytoplasm of cells infected with the WR virus. The use of the WR-infected cells as a negative control was essential to exclude the possibility of misinterpretation of binding specificities of the primary or secondary antibodies. The electron micrograph in Fig. 6.4 clearly shows a large amount of non-specific binding as evident by the areas of gold labelling. Similar pattern of gold distribution was also seen in cells co-infected with vL and v5D (Fig. 6.5). A close comparison of electron micrographs shown in Figs. 6.4 and 6.5 showed that there is little discernible difference between them. During the course of this series of experiments, a large number of experimental conditions were employed; antibodies were titred for optimal signal to background ratio, and a variety of embedding techniques were used. The experiments shown in Figs. 6.4 and 6.5 represent the optimal results obtainable in this system. The relatively similar distributions of the gold particles seen in these figures unfortunately prevent any conclusions being reached.

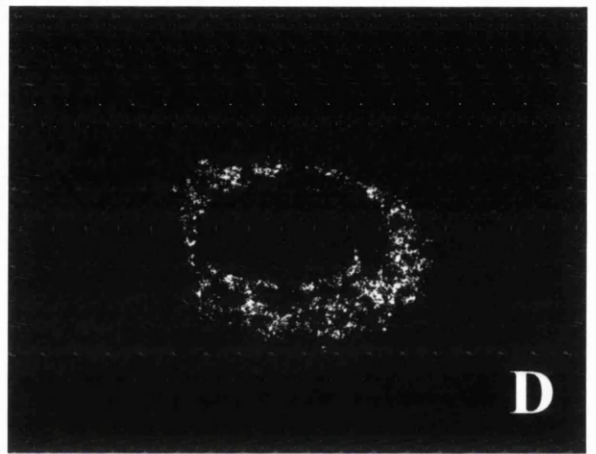
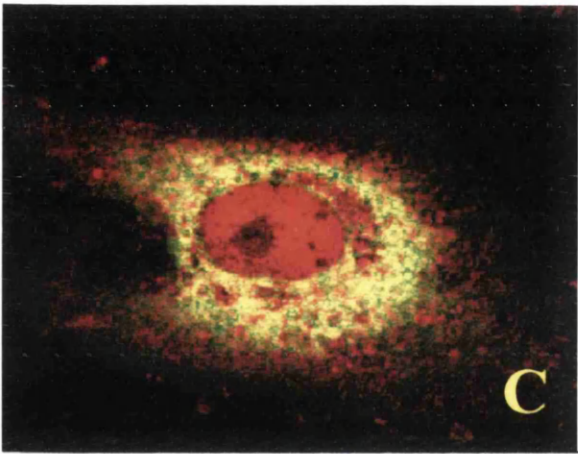
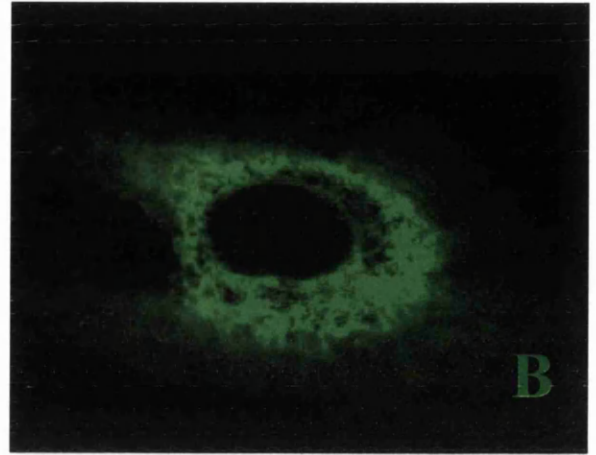
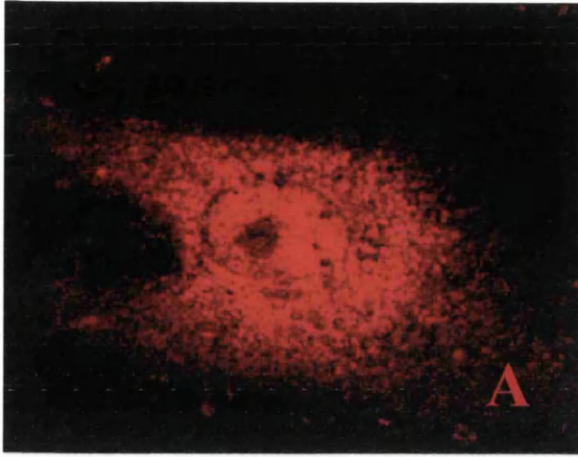


Figure 6.6 Colocalisation of core and Lx in HepG2 cells.

HepG2 cells on glass coverslips in 24-well plates were coinfectd at an m.o.i. of 0.5 p.f.u./cell with vLx and v5D. At 24 hours post-infection, the cells were fixed in methanol at -20°C , then permeabilised in PBST. The cells were probed with MAb 109 (anti-L) and Pab anti-core for two hours at room temperature, then were washed in PBST. The coverslips were incubated with anti-mouse FITC and Anti-Rabbit Cy5, and the coverslips were mounted and examined by confocal microscopy.

Panel A: cells expressing v5D stained with PAb anti-core and anti-rabbit IgG-cy5, coloured red.

Panel B: cells expressing vLx stained with MAb 109 and anti-mouse IgG-FITC.

Panel C: merge.

Panel D: the subtraction of fluorescent areas containing a single label results in the localised areas being demonstrable as a black-on-white image, with the white pixels indicating the presence of both fluors at similar intensities.

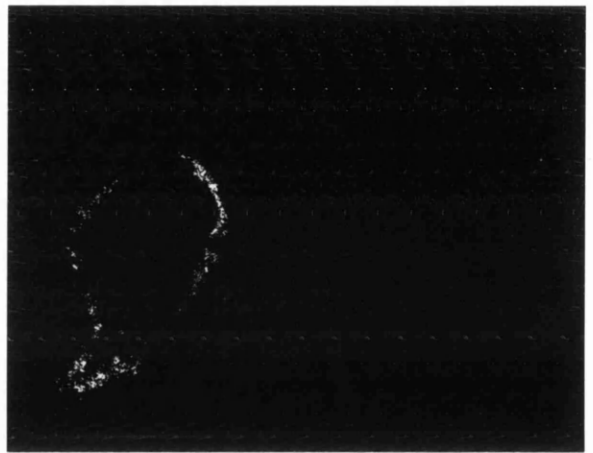
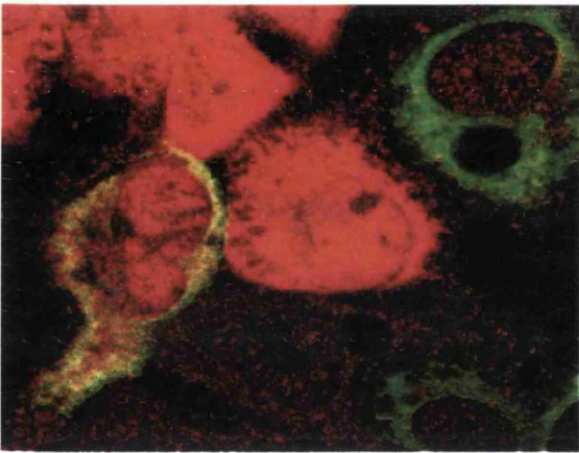
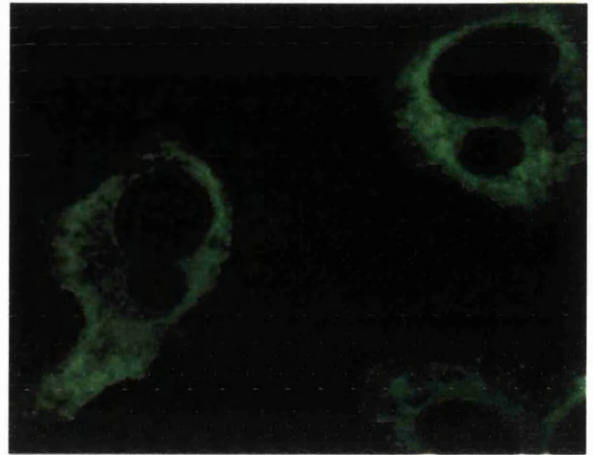
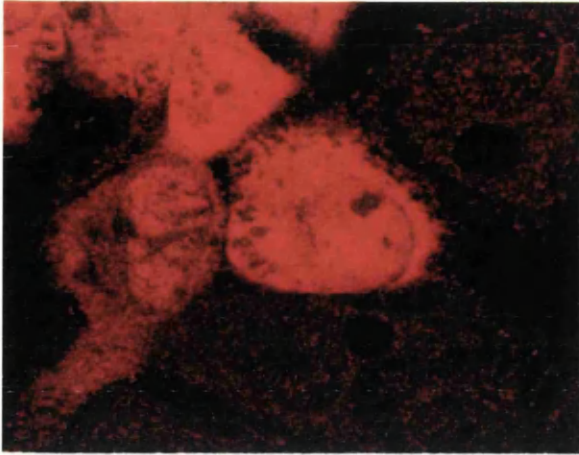


Figure 6.7 Colocalisation of core and Lx in H5 cells.

H5 cells on glass coverslips in 24-well plates were coinfectd at an m.o.i. of 0.5 p.f.u./cell with vLx and v5D. At 24 hours post-infection, the cells were fixed in methanol at -20°C, then permeablised in PBST. The cells were probed with MAb RC109 and PAb anti-core for two hours at room temperature, then were washed in PBST. The coverslips were incubated with anti-mouse FITC and anti-rabbit Cy5, and the coverslips were mounted and examined by confocal microscopy.

Panel A: cells expressing v5D stained with PAb anti-core and anti-rabbit IgG-cy5, coloured red.

Panel B: cells expressing vLx stained with MAb 109 and anti-mouse IgG-FITC

Panel C: merge.

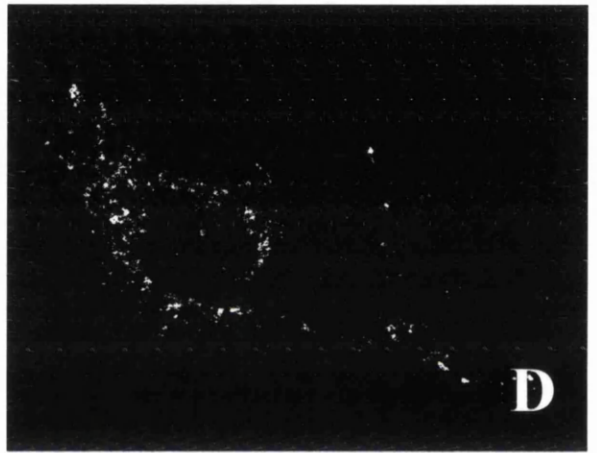
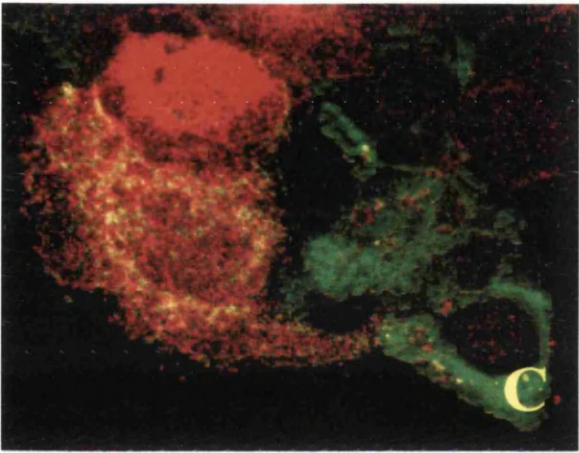
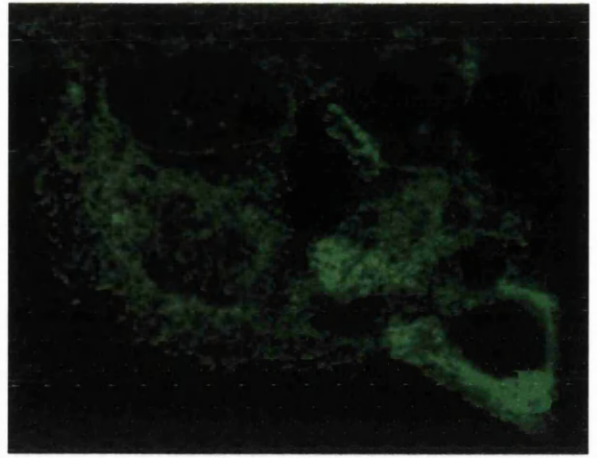
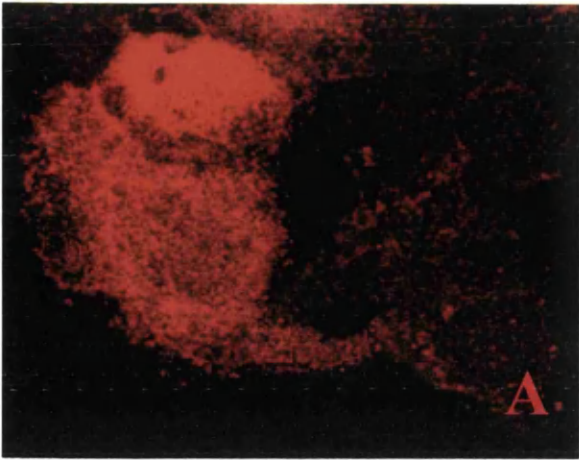


Figure 6.8 Colocalisation of core and Lx in HeLa cells.

HeLa cells on glass coverslips in 24-well plates were coinfectd at an m.o.i. of 0.5 p.f.u./cell with vLx and v5D. At 24 hours post-infection, the cells were fixed in methanol at -20°C , then permeablised in PBST. The cells were probed with MAb RC109 and PAb anti-core for two hours at room temperature, then were washed in PBST. The coverslips were incubated with anti-mouse FITC and anti-rabbit Cy5, and the coverslips were mounted and examined by confocal microscopy.

Panel A: cells expressing v5D stained with PAb anti-core and anti-rabbit IgG-cy5, coloured red.

Panel B: cells expressing vLx stained with MAb 109 and anti-mouse IgG-FITC.

Panel C: merge.

Panel D: the subtraction of fluorescent areas containing a single label results in the localised areas being demonstrable as a black-on-white image, with the white pixels indicating the presence of both fluors at similar intensities.

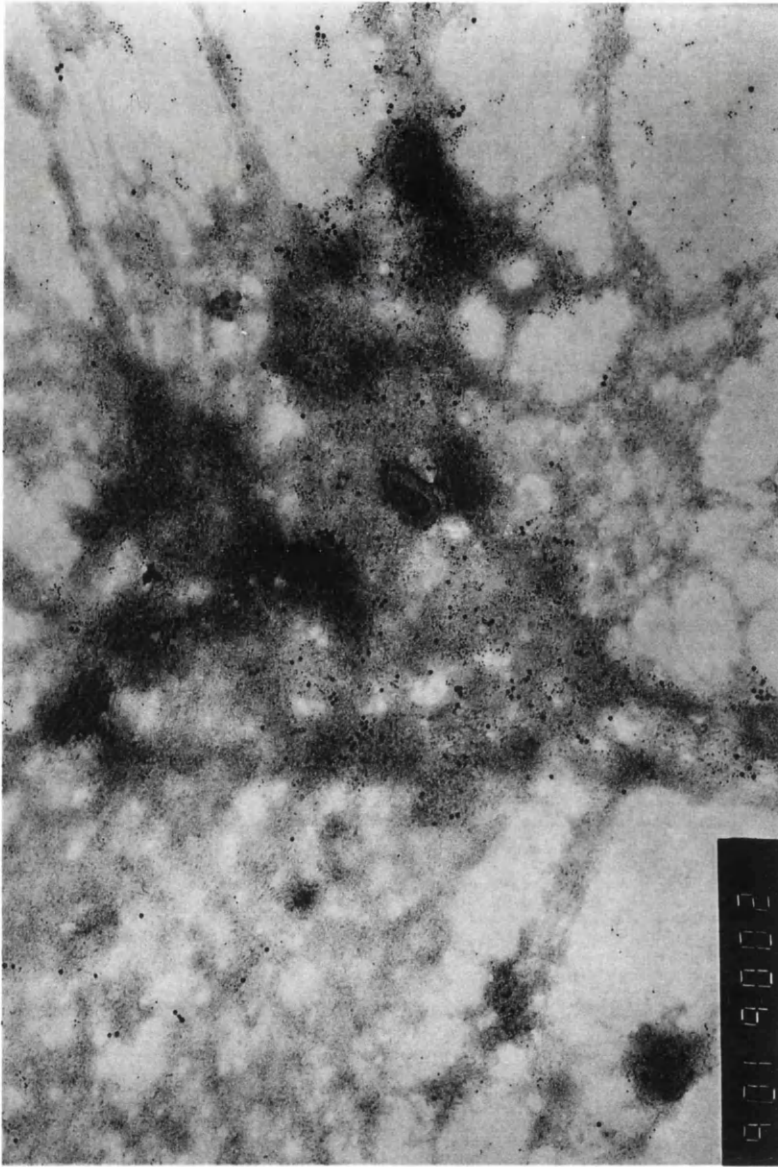


Figure 6.9 Intracellular distribution of Core and Lx in H5 cells.

H5 cells in 6-well plates were coinfecting with vLx and v5D virus at a m.o.i of 5 p.f.u./cell and incubated for 18 hours at 37°C. The cells were washed three times with PBSA and scraped into Beem capsules and centrifuged at 400 r.p.m. in a Beckman benchtop centrifuge. The supernatant was discarded, and the cell pellet was fixed by the addition of 400 μ L of 2.5 % glutaraldehyde and then embedded and permeated in 4% gelatin at 37°C. The cell pellets were removed from the capsules and cryo-sectioned into 100 μ M sections, were transferred onto Nickel grids and labelled with primary antibodies (PAb 143 anti-L, and MAb 2A23 anti-core), and secondary antibody-gold conjugates anti-mouse IgG-5nm gold, and anti-rabbit IgG-15nm gold. The samples were visualised with a JOEL 100S electron microscope.

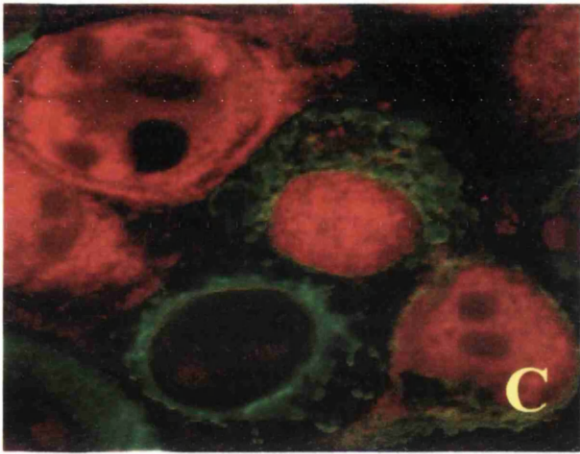
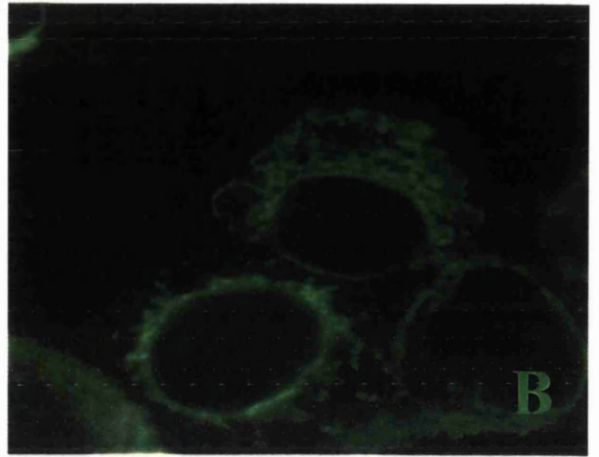
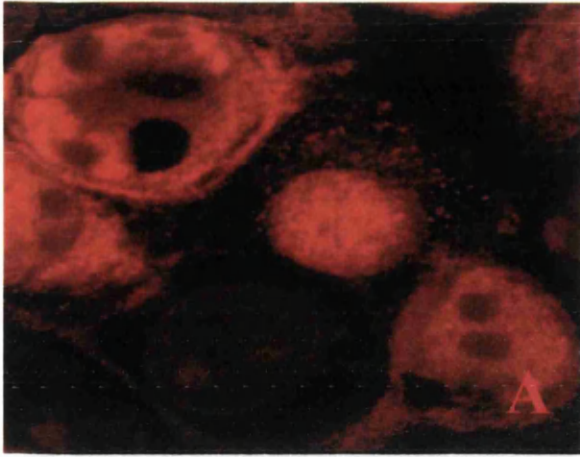


Figure 6.10A Failure of recognition of L-core with RC28.

HepG2 cells on glass coverslips in 24-well plates were coinfectd at an m.o.i. of 0.5 p.f.u./cell with vL and v5D. At 24 hours post-infection, the cells were fixed in methanol at -20°C , then permeablised in PBST. The cells were probed with MAb RC28 (anti-L) and PAb (anti-core) for two hours at room temperature, then were washed in PBST. The coverslips were incubated with anti-mouse FITC and anti-rabbit Cy5, and the coverslips were mounted and examined by confocal microscopy.

Panel A: cells expressing v5D stained with PAb anti-core and anti-rabbit IgG-cy5, coloured red.

Panel B: cells expressing vL stained with MAb RC28 and anti-mouse IgG-FITC.

Panel C: merge.

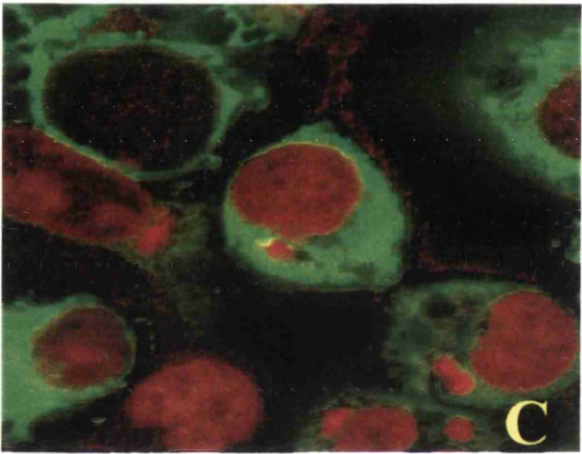
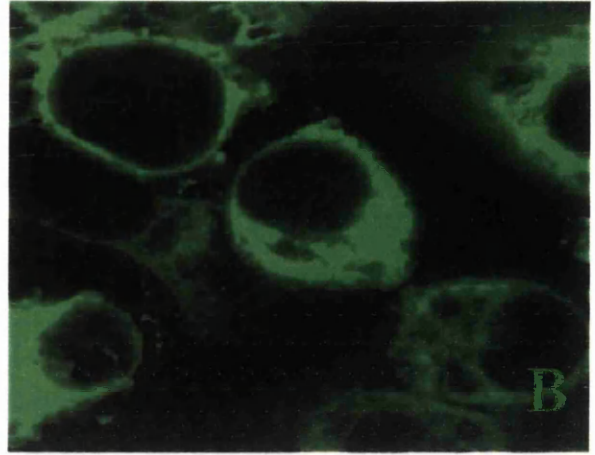
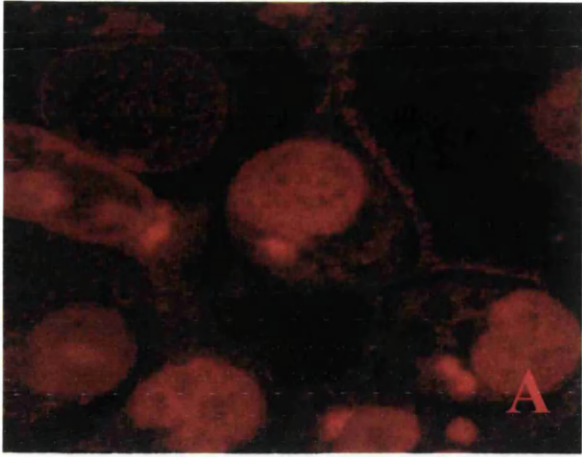


Figure 6.10B Failure of recognition of Lx-core with RC28.

HepG2 cells on glass coverslips in 24-well plates were coinfectd at an m.o.i. of 0.5 p.f.u./cell with vLx and v5D. At 24 hours post-infection, the cells were fixed in methanol at -20°C, then permeablised in PBST. The cells were probed with MAb RC28 (anti-L) and PAb (anti-core) for two hours at room temperature, then were washed in PBST. The coverslips were incubated with anti-mouse FITC and anti-rabbit Cy5, and the coverslips were mounted and examined by confocal microscopy.

Panel A: cells expressing v5D stained with PAb anti-core and anti-rabbit IgG-cy5, coloured red.

Panel B: cells expressing vLx stained with MAb RC28 and anti-mouse IgG-FITC.

Panel C: merge.

6.3 Co-expression of Lx and core.

The immuno-staining of the cells expressing the secretory form of L (Lx) with the ERGIC MAb p53 showed a distribution of Lx clearly contrasting with that of L protein as described in Chapter 5. To examine the intracellular distribution of core when co-expressed with Lx, HepG2 cells were co-infected with recombinant vaccinia viruses, vLx and v5D. The infected cells were probed with the anti-core polyclonal antisera and the anti-L MAb RC28 or the MAb RC109, or anti-L PAb 143 and an anti-core MAb-2A23 (see figure legends for details of antisera, and appendix 1). The distribution of Lx appeared similar to that observed in cells expressing Lx alone, whereas the localisation of core changed to a punctate appearance in comparison with that found with vL and core (see Fig. 6.1, 6.2 and 6.3), but was also found to be in the nucleus of co-expressing cells (Fig. 6.6). It was found necessary to analyse the confocal images with an algorithm (Zeiss) that can be used to exclude dissimilar fluorescent intensities from images, therefore allowing viewing of similar intensities, represented here in this work as panel D (Fig. 6.6). The white areas in the panels labelled correspond to areas of similar fluorescent intensity for both the FITC channel and the Cy5 channel, enabling small areas of fluorescence to be depicted against a suitably contrasting background. The small nature of these bodies found upon the coexpression of the core and Lx proteins is clearly visible in panel D of Fig. 6.6. The punctate distribution of core in the Lx and core-expressing cells differs markedly from the distribution of core when expressed singularly. In these images it has been possible, by using a carefully controlled multiplicity of infection, to obtain images that have unstained cells, singularly expressing cells and co-expressing cells in one or more cell types in Figs. 6.1, 6.2, 6.3 and 6.7. Thus, a comparison of the intracellular distribution of the proteins is possible for each of the protein combinations studied, as is the comparison with mock-infected cells in the images. Identical results were obtained in H5 and HeLa cells, indicating that the changes in the distribution of core in the presence of Lx is not cell-type dependent (Figs. 6.7 and 6.8, respectively). The observation that core co-localises with Lx (and L, see Figs. 6.1 to 6.3) again indicates an existence of a direct protein-protein interaction. As before, an attempt was made to confirm this interaction by immune-labelling cryo-sectioned cells and EM. H5 cells were co-infected with recombinant vaccinia viruses vLx and v5D, cryo-sectioned, probed with anti-L PAb 143 and anti-core MAb 2A23, and analysed by EM as

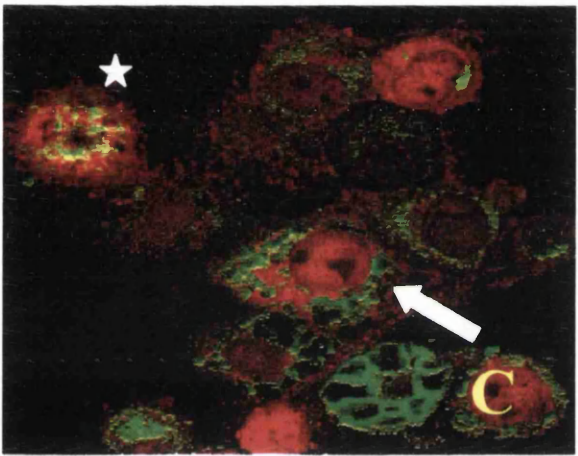
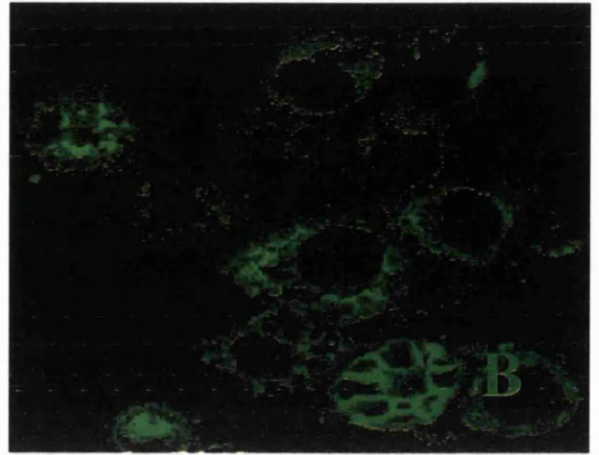
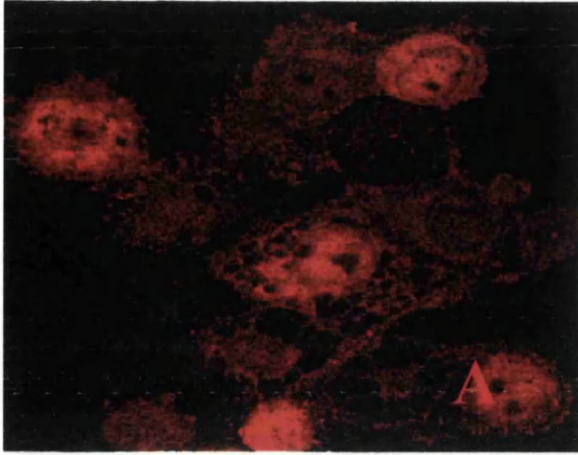


Figure 6.11 HepG2 cells expressing both core and M.

HepG2 cells on glass coverslips in 24-well plates were coinfectd at an m.o.i. of 0.5 p.f.u./cell with vM and v5D. At 24 hours post-infection, the cells were fixed in methanol at -20°C , then permeablised in PBST. The cells were probed with MAb 2-F2-12 (anti-M) and PAb anti-core for two hours at room temperature, then were washed in PBST. The coverslips were incubated with anti-mouse FITC and anti-rabbit Cy5, and the coverslips were mounted and examined by confocal microscopy.

Panel A: staining of core with PAb anti-core, with anti-rabbit-IgG-cy5 fluor.

Panel B: staining of M protein with MAb 2F2-12, with anti-mouse-IgG-FITC.

Panel C: merge. White arrow shows cell expressing core and M, with no colocalised areas. White star is situated next to a cell exhibiting CPE due to the rVV infections.

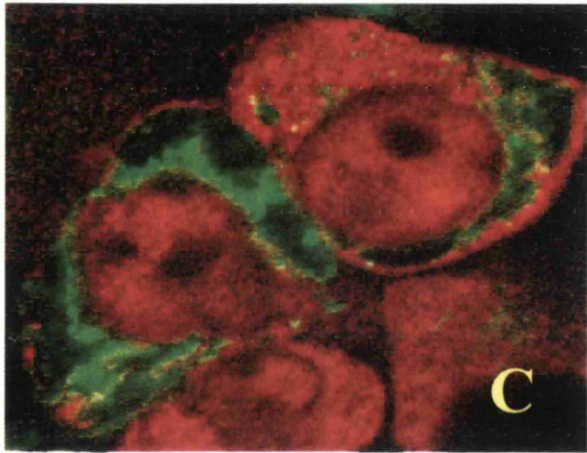
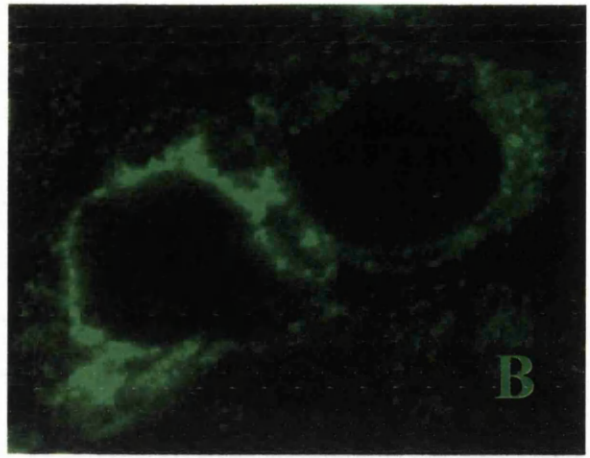


Figure 6.12 HepG2 cells expressing core and vHBsAg.

HepG2 cells on glass coverslips in 24-well plates were coinfectd at an m.o.i. of 0.5 p.f.u./cell with vHBsAg and v5D. At 24 hours post-infection, the cells were fixed in methanol at -20°C, then permeablised in PBST. The cells were probed with MAb 6B1 (anti-HBsAg) and PAb anti-core for two hours at room temperature, then were washed in PBST. The coverslips were incubated with anti-mouse FITC and anti-rabbit Cy5, and the coverslips were mounted and examined by confocal microscopy.

Panel A: staining of core with PAb anti-core, with anti-rabbit IgG-cy5.

Panel B: staining of S protein with MAb 6B1, with anti-mouse IgG-FITC.

Panel C: merge.

described in Figs. 6.4 and 6.5. Gold particles of both sizes were found throughout the cytoplasm of cells (Fig. 6.9). As this pattern of gold distribution is similar to that found in wild type WR-infected cells (Fig. 6.4), it was concluded that the high levels of non-specific binding to proteins by antibodies preclude any firm interpretations of the data.

HepG2 cells co-infected with (A) vL and v5D, and (B) vLx and v5D were also probed with anti-L MAb RC28 and anti-core PAb and the bound antibodies were detected using appropriate secondary antibody conjugates which were then analysed by confocal microscopy. As expected, both MAb RC28 and the anti-core PAb recognised the respective proteins with their characteristic distribution in cells (Fig. 6.10A and 6.10B). Interestingly, MAb RC28 failed to recognise the portion of L or Lx that had co-localised with core – in fact, as opposed to the data shown in Figs. 6.6 to 6.8 where the anti-L MAb RC109 was used to detect Lx, there was a complete absence of any colocalisation of the two fluorochromes when probed with MAb RC28 (Fig. 6.10C). This effect was evident only with MAb RC28, as RC109 (and the other anti-L MAbs RC9 and RC152) were able to recognise the L or Lx protein co-localised with core.

6.4 Co-expression of Core with M and S.

It was previously shown that both HBV antigens M and S associate with cytoplasmic membranes (see Chapter 5). Here, the intracellular distribution of core and M or core and S in co-expressing cells was examined. HepG2 cells were co-infected with rVVs vM and v5D or vS and v5D, immunolabelled with appropriate primary and secondary antibodies, and analysed by confocal microscopy. As shown in Figs. 6.11 and 6.12, the distribution of core protein throughout the cells expressing core alone was comparable with those observed in cells co-expressing core and either M or S. There was no colocalisation of core with either the M or S protein.

6.5 Discussion

The association of the viral envelope with the nucleocapsid is an area of much study in many laboratories, and the mechanisms governing viral assembly and morphogenesis still remain unclear. In the work described in this chapter, the intracellular distribution of core when co-expressed with the surface antigens has been

analysed. This was undertaken to enhance our understanding of the processes involved in hepadnaviral assembly and morphogenesis.

Existing models of hepadnaviral morphogenesis suggest the core and surface antigens associate as the assembled core passes in to the lumen of the ER and obtains an envelope of the surface antigens (Bottcher *et al.*, 1998; Bruss and Ganem, 1991; Bruss and Vieluf, 1995). An *in vitro* binding assay using synthetic peptides was used to identify two interaction sites on the L protein: one site on the preS1 domain, and one site on the S domain (Poisson *et al.*, 1997; Tan *et al.*, 1999). Tan *et al.* suggested a synergistic interaction with the two binding sites forming a strong interaction with the core protein. Also, it has been shown that the N-terminal 5/6 of the preS1 domain of L is dispensable for virion assembly (Bruss and Thomssen, 1994), and that the extraluminal preS1 domains of L when embedded in the ER are capable of binding the pre-formed nucleocapsid (Ostapchuk *et al.*, 1994); (Bruss and Vieluf, 1995).

The data presented here show that the expression of L with core results in the redistribution of core from the nucleus and most of the cytoplasm, and colocalisation with the L protein. As the intracellular distribution pattern of L in co-expressing cells remained the same as that found in cells expressing L alone and as L is known to reside in the ERGIC compartment (Xu *et al.*, 1997), it is reasonable to conclude that core is co-localised with L in the ERGIC compartment.

The preS1 domain has been reported to interact with core (Bruss and Thomssen, 1994; Bruss and Vieluf, 1995; Poisson *et al.*, 1997), and the data presented here is in agreement with these findings. Furthermore, there is evidence from *in vitro* studies that shows there is a region of S that is involved in binding to core (Poisson *et al.*, 1997); (Tan *et al.*, 1999). There remains uncertainty regarding the minimal requirements for an interaction between the viral envelope proteins and the core. Although the intracellular distribution of L upon co-expression with core cannot be proven to be residing in the ERGIC in these images, due to the unavailability of suitable antisera for triple-labelling of these samples, it is reasonable to assume that the localisation of L to the perinuclear compartment in these samples is similar to that observed earlier as part of the characterisation of the L expression system, and from the results of others. The apparent effect of L on the distribution of core can be seen

readily from the confocal images, but there is no indication of the minimal requirements for this effect. The association of Lx with core remains unclear. The data presented here clearly shows that core, when co-expressed with Lx, has a widespread cytoplasmic and punctate appearance, with a large proportion of core still residing in the nucleus. The appearance of the co-localised core-Lx is similar to that of the Lx protein alone, thus, it could be possible that Lx is influencing the distribution of core. The results from the electron microscopic analysis of the infected cells are insufficiently clear to enable any firm conclusions about the precise location of the proteins, and whether the proteins are directly interacting, to be drawn from this work.

During the course of this work, extensive efforts were made to co-immunoprecipitate core and L or Lx from the cytoplasm of infected cells, and from the medium of infected cells. Although it is clear that L and Lx proteins can be readily immunoprecipitated by the specific antisera generated in this work (see Chapter 3), it proved impossible to co-immunoprecipitate core with any of the surface antigens from co-expressing cells.

It was observed that both L and its secretory form of L (Lx) is localised in the cytoplasm and in seemingly punctate bodies, and that core colocalised with these proteins in co-expressing cells (Figs. 6.1 to 6.3 and 6.6, to 6.8). Interestingly, that both L and Lx co-localised with core was detectable with anti-L MAbs RC9, RC109, and RC152, but not RC28. The failure of RC28 to recognise Lx when complexed with core may be explained by the Lx-core complex having different properties in comparison with the L-core, further strengthening the argument for the chief interaction between the two proteins being between the preS1 domain and the core. On account of it being forced through the secretory pathway, the Lx protein is likely to be different from the L protein in terms of its tertiary structure and/or post-translational processing, e.g. glycosylation. Moreover, it is possible that both L and Lx undergo conformational change when bound to core and this together with the possible differences in the tertiary structure and/or glycosylation may mask or impede the binding of RC28 to the preS1 domain of Lx. It is possible that studying the interaction of the preS1 domain, in the presence and absence of RC28, with the core particle could enhance our understanding of the hepadnaviral assembly process.

Delineation of the structural arrangement of the preS1 domain bound to core may give insights into the scaffolding function of the L protein, and possibly allow the evaluation of the RC28 MAb as a means by which the hepadnaviral assembly process could be impeded.

It is interesting to note that the epitopes recognised by our anti-L MAbs RC9, RC28, RC109, and RC152 all map to similar regions (amino acid residues 15 to 35) of the preS1 domain (see Fig. 3.15). The inability of RC28 to recognise Lx-core complex (at least in this immunofluorescence assay) indicates that the amino acid residues in this region of the preS1 domain may play a critical role in L-core interaction. Furthermore, it is impossible to tell the orientation on the preS1 domain the RC28 MAb binds. The preS1 domain must be considered as a three-dimensional molecule, and it remains possible that the MAb RC28 binds to the preS21 domain in a different orientation in comparison with the other MAbs generated here.

Having established a change in the intracellular distribution of core when co-expressed with L or Lx, it was therefore of interest to investigate the ability of M and S to bind and influence the behaviour of the core protein in the absence of L. In Figs. 6.11 and 6.12 it is clear that the core protein did not colocalise with the M or S protein in our expression systems, leading to the suggestion that the chief requirement for the interaction of the envelope proteins with the core is the presence of the preS1 domain. The presence of the second, weaker binding site on the S domain of M and S as described by Tan *et al.* appears to be insufficient for recruitment of core protein to the site of localisation of the smaller surface antigens at least in immunofluorescence assay.

The requirement of HBV M for virion morphogenesis and infectivity has yet to be proven (Le Seyec *et al.*, 1998), and therefore it is of no surprise that there seems to be no effect on core due to the presence of M. The functional relevance of M to the life cycle, infectivity and morphogenesis of the human Hepadnaviruses remains unclear.

The failure of S and M to influence the localisation of core is interesting when considering the evidence from *in vitro* studies. Recently, Tan *et al.* have shown two components of the surface antigen are involved in binding to the core protein. The

two interaction sites are purported to act synergistically in the association of the core and large surface antigen. Here we have explored the potential of the small surface antigen alone to affect the intracellular retention and localisation of the core protein, and we find there is insufficient interaction between the S and core proteins to result in any change in intracellular retention or localisation. This observation may be explainable by the binding site in the S domain responsible for binding core being insufficiently avid to bind to the core protein in the absence of the preS1 domain. Alternatively, the interaction site of S may not be in the appropriate orientation or conformation due to the established topological differences between the L and S proteins (Ostapchuk *et al.*, 1994). It is also possible that the structure of S is different to the structure of the S domain of L (see Chapter 6) and that the synergistic interaction of the two domains of L is dependant on the conformation of the L protein in exposing the available binding epitopes in a manner which may enable efficient binding of core.

Chapter 7

Ligand binding assays

The mechanisms of HBV attachment and entry into the target cell are poorly understood. The delineation of this initial step in infection process remains a goal common to many laboratories. As with other viruses, infection with HBV is thought to initiate by specific binding to cell surface structures via one or more viral envelope proteins. There is no effective *in vitro* cell culture systems for propagation of HBV and this has hampered studies on understanding the mechanisms involved in this process.

The identification of cellular receptors for the L protein of HBV has so far been difficult to achieve. Although there is a body of literature that contains some putative receptor identities (Alberti *et al.*, 1987; Atkins *et al.*, 1997; Budkowska *et al.*, 1993; Dash *et al.*, 1992; Franco *et al.*, 1992; Itoh *et al.*, 1992; Leenders *et al.*, 1990), there remains little evidence to support the role of these proteins in the natural infection.

More recently, progress has been made with the identities of putative cellular receptors and the possible mechanisms of entry utilised by the Hepadnaviruses (Harvey *et al.*, 1999; Klingmuller and Schaller, 1993; Qiao *et al.*, 1994). However, there remains sparse evidence that the proteins identified in the literature are involved in hepadnaviral tropism, therefore workers in the field remain engaged in endeavours to identify the cellular receptors for HBV. As a starting point in the study of the interaction of the virion with the host cell, the author chose to investigate the binding of the preS1 domain of HBV to cultured cells. The preS1 domain was chosen, because this protein is the region of the L protein which is purported to be involved in the initial binding of the virus to the hepatocyte (Mabit *et al.*, 1996; Neurath *et al.*, 1988; Petit *et al.*, 1992). Thus, a series of experiments were designed and executed to explore the binding events of the L protein.

7.1. Binding of preS1 domain to hepatocytes.

Flow cytometry was used as a tool by which the interaction of the preS1 domain with the cell surface could be explored. The assay involved incubation of hepatocytes with

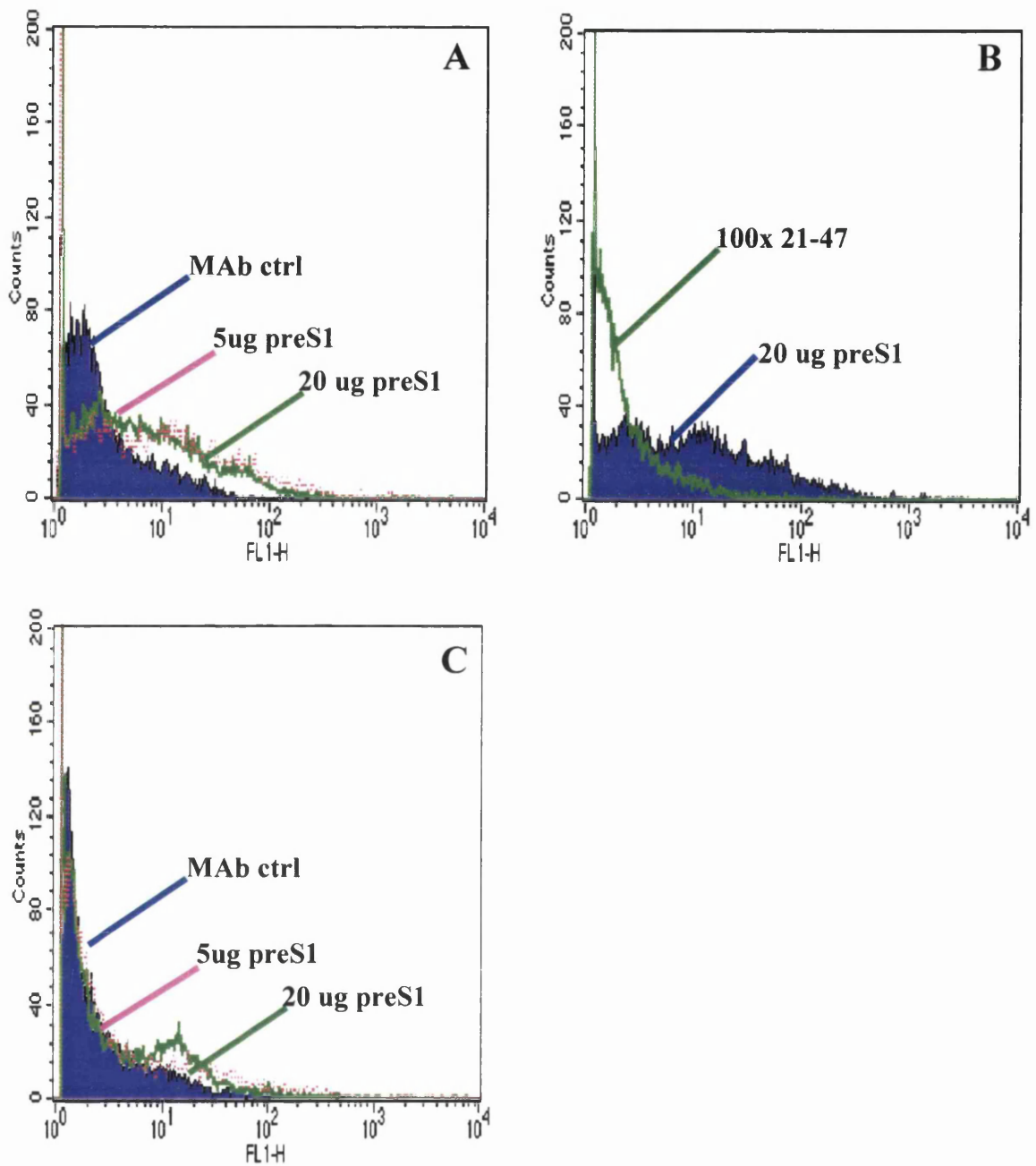


Figure 7.1 HBV preS1 domain binding to HepG2 and BHK cells

HepG2 cells and BHK cells at near confluence were dissociated from the monolayers, washed in FPBS and incubated with the preS1 domain in the presence and absence of a potentially inhibiting peptide 21-47. Unbound ligand was removed by washing, the cells were then incubated with primary antibody RC28, washed, then incubated with anti-mouse IgG-FITC. The cells were analysed for fluorescence in FL1 in a BD FACScan.

Panel A: HepG2 cells incubated with 5 and 20 ug of preS1 domain.

Panel B: HepG2 cells incubated with 20 ug of preS1 domain and 100x molar excess of peptide 21-47.

Panel C: BHK cells incubated with 5 and 20 ug of preS1 domain.

purified preS1 domain for 1 h at room temperature. Following washing, cells were then incubated with MAbs to preS1 again for 1 h at room temperature. Cells were washed, incubated with an anti-mouse IgG-FITC conjugate as above, washed and the bound fluorochrome detected by Fluorescent Activated Cell Sorting (FACS). In order to establish which of the monoclonal antibodies generated in this work were active in FACS assays, they were evaluated as hybridoma supernatants in a pilot experiment. The use of MAbs in the form of hybridoma supernatant in these assays resulted in unwanted background reactivity in some of the samples, and necessitated the production of one monoclonal in serum-free conditions and subsequent affinity purification to obtain an antibody giving rise to negligible background in these assays. The supernatants from RC9, RC109 and RC152 showed little reactivity in these assays and it was therefore decided to use a purified preparation of RC28 (chapter 3) in FACS assays.

To test if the bacterially produced and purified preS1 domain bound to the plasma membrane, HepG2 or BHK cells were incubated with 5 and 20 μg of preS1 and the bound ligand detected using MAb RC28 as described above. As shown in Fig. 7.1, panel A, there was a shift in population of fluorescing cells that were incubated with preS1; the fluorescence intensity obtained at two different concentration of the ligand remained the same. In contrast, the preS1 domain failed to bind BHK cells (Fig. 7.1, panel C), indicating binding of the ligand to the human cells used here. The level of autofluorescence in these cells is low and was used to set the operating parameters for this cell line in the FACScan instrument. Cells treated with a control antibody exhibited a low level of fluorescence due to the presence of fluorescent molecules normally present within living cells (autofluorescence). The level of fluorescence of cells incubated with the anti-mouse IgG-FITC in the absence of ligand, and with a non-specific primary antibody (MAb H53 directed against the S protein of HBV) of the IgG 1a subtype was low, and can be seen in the samples labelled 'MAb ctrl' in Fig. 7.1, panel A. Clearly, there is little fluorescence due to the binding of IgG 1a molecules (which is the same subtype as MAb RC28) on the plasma membrane. The specificity of preS1 binding to HepG2 was demonstrated by pre-incubating the cells with a 100-fold molar excess of a synthetic peptide (peptide 21-47) corresponding to the amino acids 21 to 47 of preS1. As shown in Fig. 7.1 panel B, the binding of the

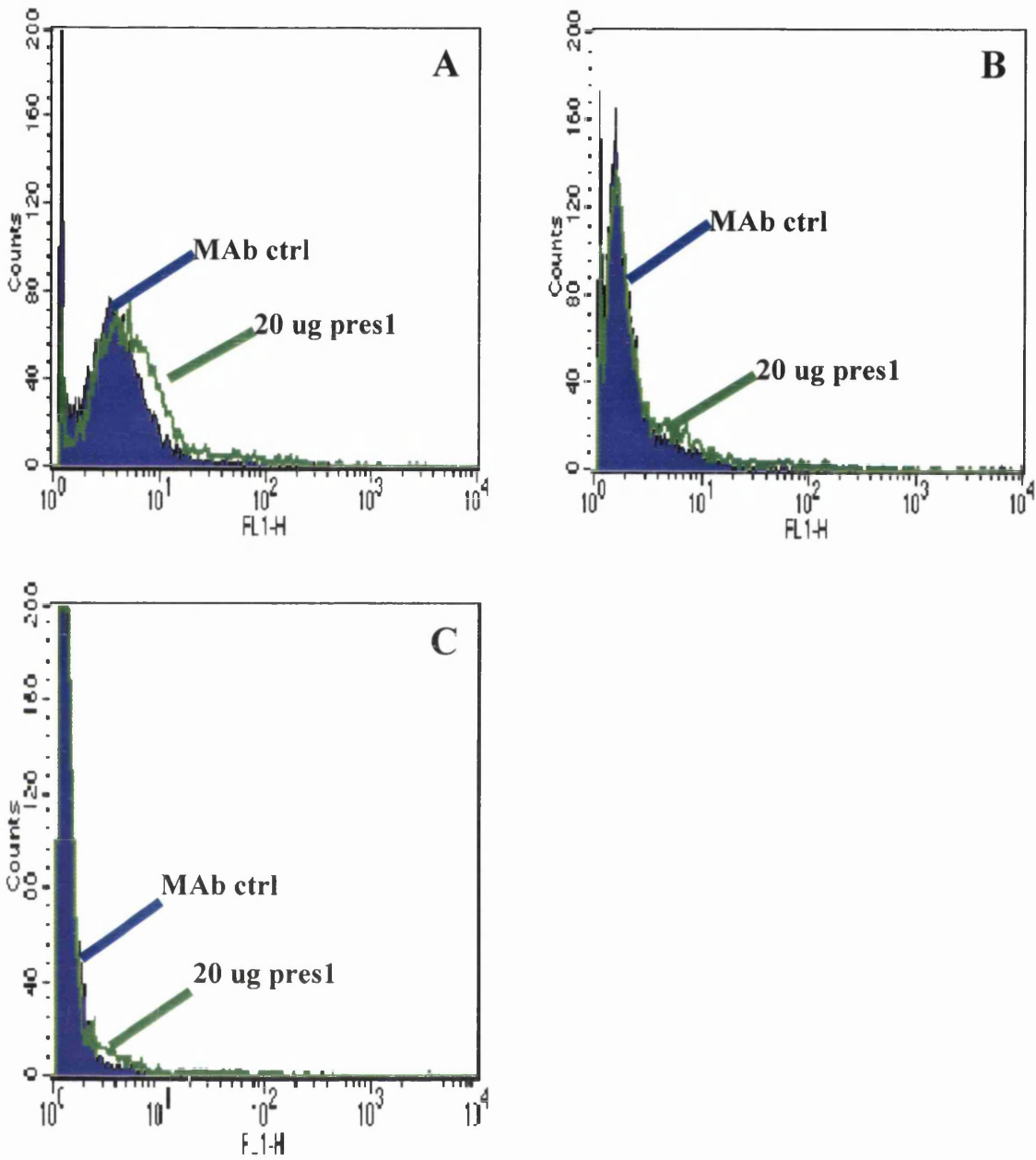


Figure 7.2A-C HBV preS1 domain binding to non-hepatocyte cells

COS7 cells at near confluence were dissociated from the monolayers, washed in FPBS and incubated with the preS1 domain. CEM4 and CCRF-CEM4 cells were taken from suspension culture, washed in FPBS and incubated with the preS1 domain. Unbound ligand was removed by washing, the cells were then incubated with primary antibody RC28, washed, then incubated with anti-mouse IgG-FITC. The cells were analysed for fluorescence in FL1 in a BD FACScan.

Panel A: COS7 cells incubated with 20 ug of preS1 domain.

Panel B: CEM4 cells incubated with 20 ug of preS1 domain.

Panel C: CCRF-CEM4 cells incubated with 20 ug of preS1 domain.

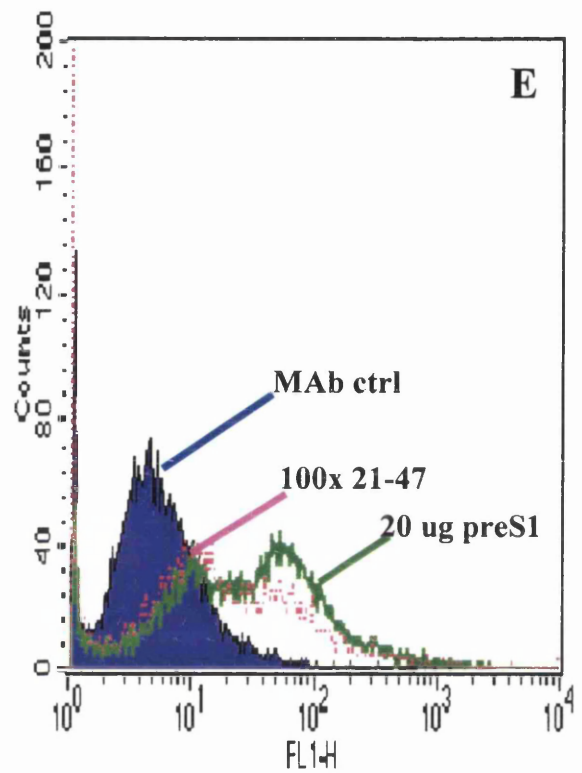
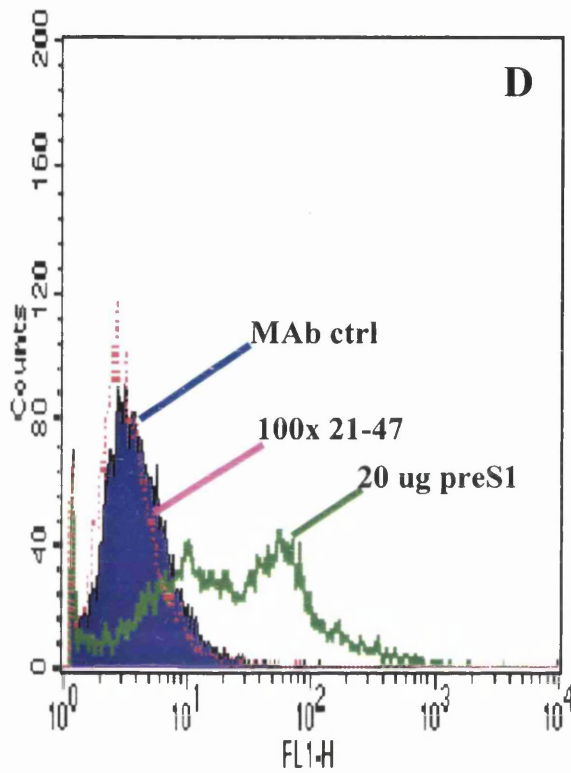


Figure 7.2D-E HBV preS1 domain binding to hepatocyte-derived cell lines.

H5 and H16 cells at near confluence were dissociated from the monolayers, washed in FPBS and incubated with the preS1 domain in the absence or presence of 100x molar excess of peptide 21-47. Unbound ligand was removed by washing, the cells were then incubated with primary antibody RC28, washed, then incubated with anti-mouse IgG-FITC. The cells were analysed for fluorescence in FL1 in a flow cytometer.

Panel D: H5 cells incubated with 20 ug of preS1 domain in the presence or absence of peptide 21-47.

Panel E: H16 cells incubated with 20 ug of preS1 domain in the presence or absence of peptide 21-47.

ligand to cells was completely abrogated in the presence of peptide, indicating that preS1 bound specifically to a receptor(s) on HepG2 cells. The amino 21 to 47 of preS1 has previously been shown to be the region involved in receptor recognition (Gerlich *et al.*, 1993).

Having established that the preS1 domain bound to HepG2 and not BHK cells, experiments were conducted in order to assess the binding of this ligand to a variety of cell lines of human hepatocyte origin, human non-hepatocyte origin, and non-human origin. COS-7 (African green monkey kidney cell line), CCRF-CEM4 and CEM4 (both of human lymphocyte origin and phenotypically similar), and H5 and H16 (both derived from primary human hepatocyte and described in Chapter 4) were used to examine the plasma membrane binding of the preS1 domain in FACS assays. From comparison of the fluorescence intensities in the cells incubated with ligand, primary and secondary antibodies with the cells incubated with the control H53 MAb (Fig. 7.2, panels A-C), it was clear that there was no binding of the preS1 domain to the plasma membranes of the COS-7, CEM-4 and CCRF-CEM4 cell lines. However, there was clearly preS1 binding demonstrable on the plasma membranes of the H5 and H16 cell lines, represented by an order of magnitude increase in fluorescence in the samples incubated with 20 μ g of the preS1 domain (green line) (Fig. 7.2, panels D and E). The affinity of the preS1 domain to H5 and H16 cells was higher than that on HepG2 cells, as judged by the relative shift in fluorescence peaks seen in these samples (compare Fig. 7.1 panels A and B to Fig. 7.2 panels D and E). As in Fig. 7.1, inhibition of preS1 binding to H5 and H16 cells was attempted by pre-incubating the cells with the peptide 21-47 prior to incubation with the preS1 domain. In Fig. 7.2 panel D, it was observed that the fluorescent intensity of the cells pre-incubated with the peptide 21-47 is similar to that of the MAb control (ctrl) cells, indicating that the preS1 interaction of preS1 with cell surface protein(s) on H5 cells occurs via amino acids 21-47. However, when H16 cells are used in similar experiments, (Fig. 7.2, panel E) there is no comparable inhibition of the binding of the preS1 domain to the plasma membrane by pre-incubation with the 21-47 peptide. The control experiments show low levels of autofluorescence and non-specific binding of the MAb RC28 for these assays (Fig. 7.2 panels A to E, samples labelled MAb ctrl) which is in keeping with the results depicted in Fig. 7.1. The results presented in Figs. 7.1 and 7.2

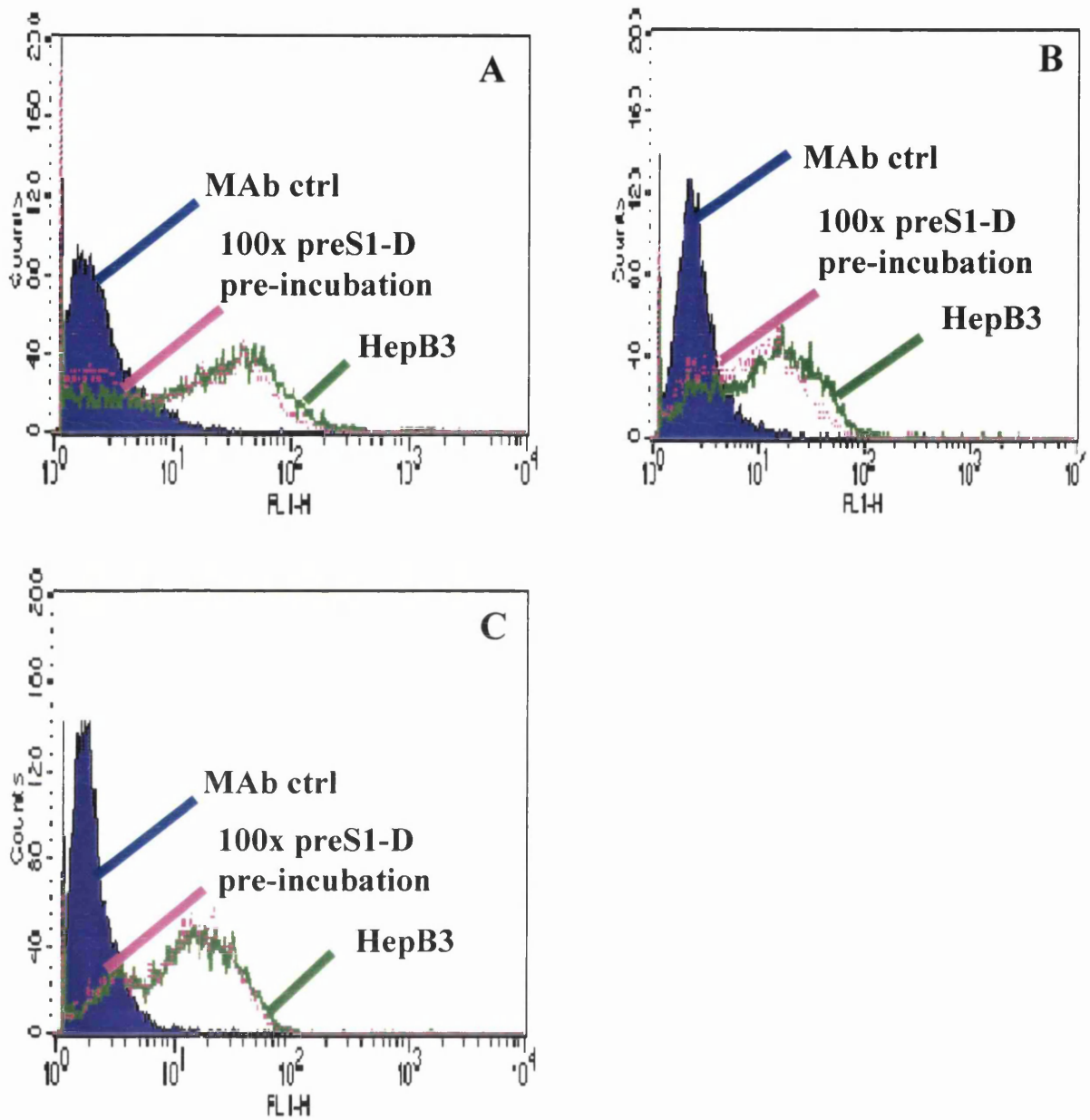


Figure 7.3 HepB3 binding to HepG2, COS7 and H5 cells.

HepG2, COS7 and H5 cells at near confluence were dissociated from the monolayers, washed in FPBS and incubated with the Hepagene protein in the presence and absence of the preS1 domain for inhibition. Unbound ligand was removed by washing, the cells were then incubated with primary antibody H53, washed, then incubated with anti-mouse IgG-FITC. The cells were analysed for fluorescence in FL1 in a flow cytometer.

Panel A: HepG2 cells incubated with HepB3 and preS1 domain.

Panel B: COS7 cells incubated with HepB3 and preS1 domain.

Panel C: H5 cells incubated with HepB3 and preS1 domain.

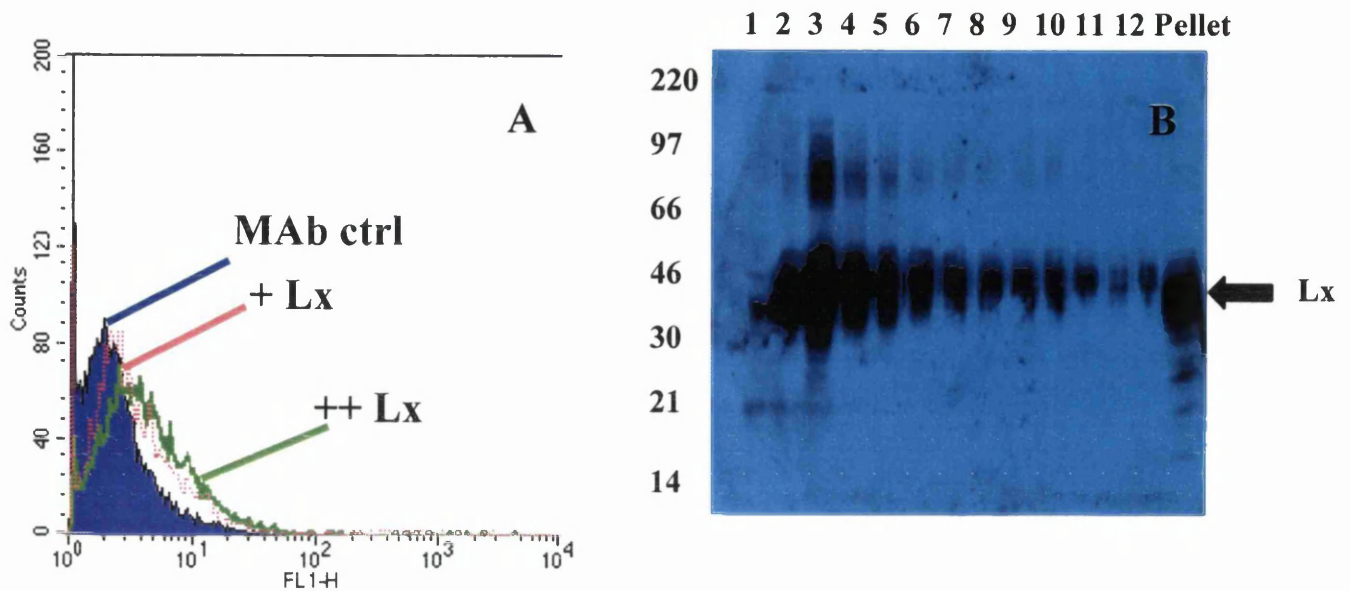


Figure 7.4A-B Assessment of vLx protein binding to H5 cells.

Panel A: To assess the level of binding of the Lx preparation the cell line H5 was grown to near confluence, dissociated from the monolayer, washed in FPBS and incubated with increasing amounts of the vLx-enriched preparation. The unbound ligand was removed by washing and the cells were then incubated with MAb RC28. The unbound RC28 was removed by washing and the bound complexes labelled with anti-mouse-IgG-FITC.

Panel B: The preparation of the Lx protein from the medium of vLx-infected BHK cells. The infected cell supernatant was clarified and overlaid onto a 20% sucrose cushion in a SW28 rotor, at 28K r.p.m. for 4 hours. The pellet was resuspended, overlaid on a 15-45% sucrose gradient, centrifuged a TST41 rotor at 40K r.p.m. for four hours and then fractionated from the top in 1 mL fractions. The fractions were then analysed by SDS-PAGE on a 10% acrylamide gel, followed by western blotting with MAb RC28 and the immune complexes were visualised by chemiluminescence. It should be noted that the proteins visible by the western blot in this figure were indiscernible by coomassie blue staining of the fractions analysed by SDS-PAGE, hence the use of western blotting to demonstrate the presence of Lx proteins.

demonstrated that the preS1 domain is capable of binding specifically to cells of human hepatic origin.

7.2. Binding of HepB3 and Lx protein to hepatocytes.

In addition to the preS1 domain, two other ligands in the form of HepB3 particle preparation (kindly donated by Medeva, UK) and a partially purified Lx protein were also tested for their ability to bind cells in FACS assay. The HepB3 preparation contains a mixture of particles composed of the S protein with an inserted region of the preS1 domain. HepG2, COS-7, or H5 cells were incubated with HepB3 particles alone or with the preS1 domain, and the bound particles were detected using anti-S MAb H53. As shown in Fig. 7.3 panels A to C, the particles bound to all the cell lines tested. Furthermore, the preS1 domain failed to block binding of HepB3 particles to cells. These results are in contrast to the preS1 domain, which was shown to bind specifically to human hepatocytes and not COS-7 cells (Figs. 7.1 and 7.2). It should be noted that the shift in the fluorescing cells seen in Fig. 7.3 is not due MAb 53 binding non-specifically to cells, as this MAb does not produce background fluorescence (Figs. 7.1 and 7.2). Thus, it would appear that the shift in fluorescence seen in Fig. 7.3 is due to recognition by MAb H53 of cell-bound HepB3 articles. The conclusions that can be drawn from the failure of the preS1 domain to inhibit the binding of the HepB3 particles are that either the HepB3 particles are binding non-specifically to the plasma membranes of cells, or that the binding is specific and is mediated through the S domain of the particles. In either case, the HepB3 particle is unsuitable for investigation of the binding of the preS1 domain to cells.

To test the ability of the Lx protein to bind to H5 cells, it was first partially purified as described in Fig. 7.4 (panel B). However, the yield of the protein was very low suggesting that a major effort outside the author's remit was required to produce the Lx protein in large quantities and to develop appropriate purification protocols. However, the small quantities of the partially pure Lx generated as described in Fig. 7.4 (panel B) was used in FACS assays which showed that there was a small increase in fluorescent intensity of the H5 cells when incubated with increasing amounts of the

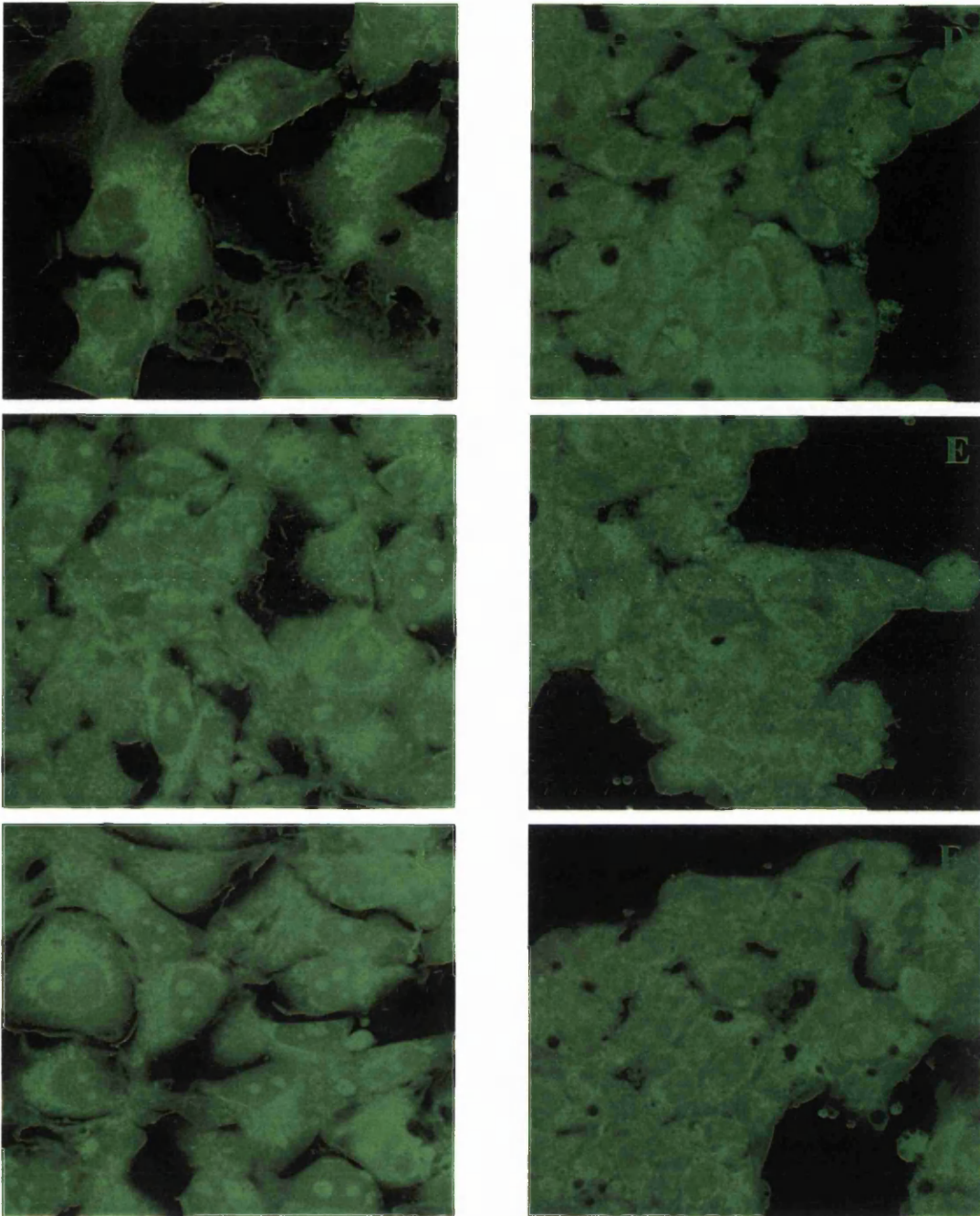


Figure 7.5. Confocal-based assay to assess Lx binding to plasma membranes of HepG2, COS7 and H5 cells.

HepG2, COS7 and H5 cells were grown in 24-well plates on glass coverslips for three days, then were incubated with the Lx preparation, a WR-derived preparation, or mock antigen, in DMEM for one hour at 4°C. The unbound antigens were washed with DMEM and the cells were incubated with MAb RC28 for one hour. After washing, the cells were labelled with anti-mouse-IgG-FITC and were examined for fluorescence with a Zeiss Laser Scanning Confocal microscope.

Panels A and D: COS7, and HepG2 cells, respectively, with WR-derived purified protein.

Panels B and E: COS7, and HepG2 cells, respectively, with mock antigen.

Panels C and F: COS7, and HepG2 cells, respectively, with purified Lx protein.

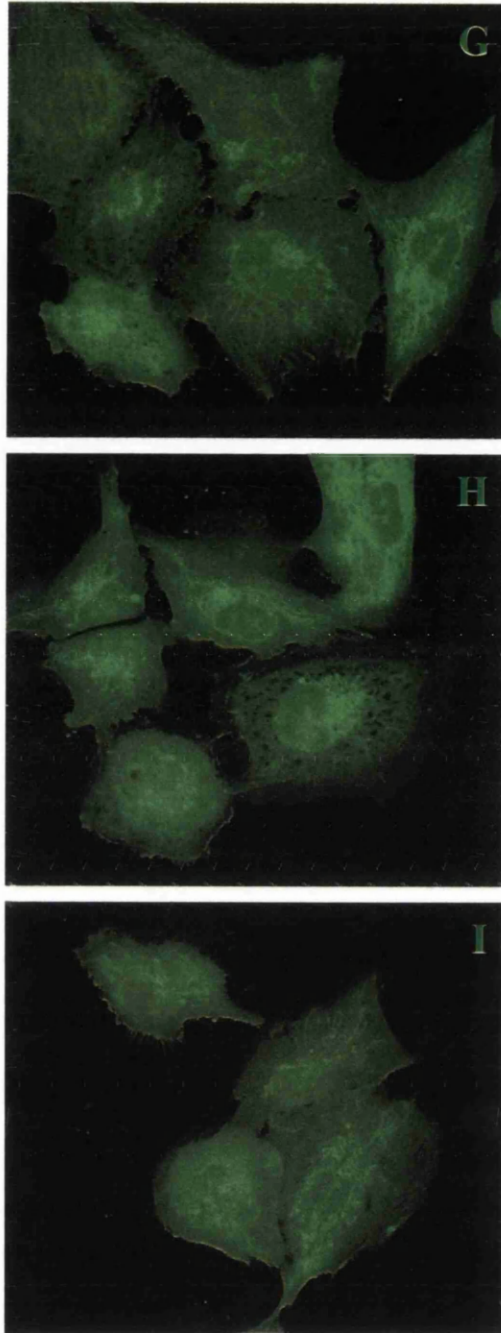


Figure 7.5. Confocal-based assay to assess Lx binding to plasma membranes of HepG2, COS7 and H5 cells (continued).

G: H5 cells, with WR-derived purified protein.

H: H5 cells, and HepG2 cells, with mock antigen.

I: H5 cells, and HepG2 cells, with purified Lx protein.

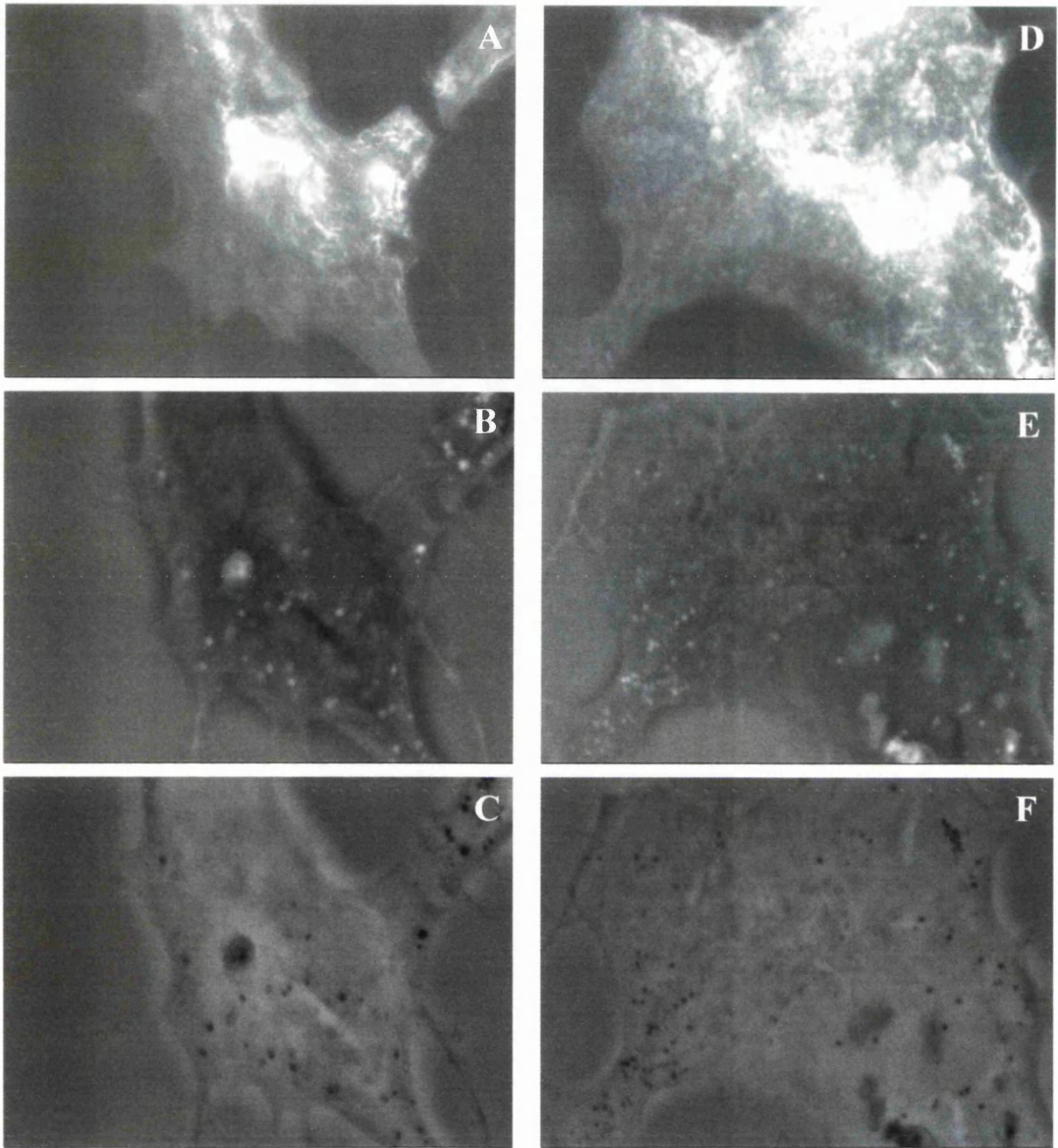


Figure 7.6A. Scanning Electron Microscopy-based assay to assess preS1 domain binding to plasma membranes of COS7 cells.

COS7 cells were grown in 24-well plates on glass coverslips for three days, then were incubated with preS1 domain, or mock antigen, in DMEM for one hour at 4°C. The unbound antigens were washed with DMEM and the cells were incubated with MAb RC28 for one hour. After washing, the cells were incubated with anti-mouse-IgG-30 nm. gold conjugate, washed and fixed in 2.5% glutaraldehyde. The cells were dehydrated in ethanol, dried by critical-point displacement with CO² and coated with carbon. The samples were analysed by secondary electron detection (panels **A** and **D**), by back-scatter analysis (panels **B** and **E**) and by reverse back-scatter (panels **C** and **F**).

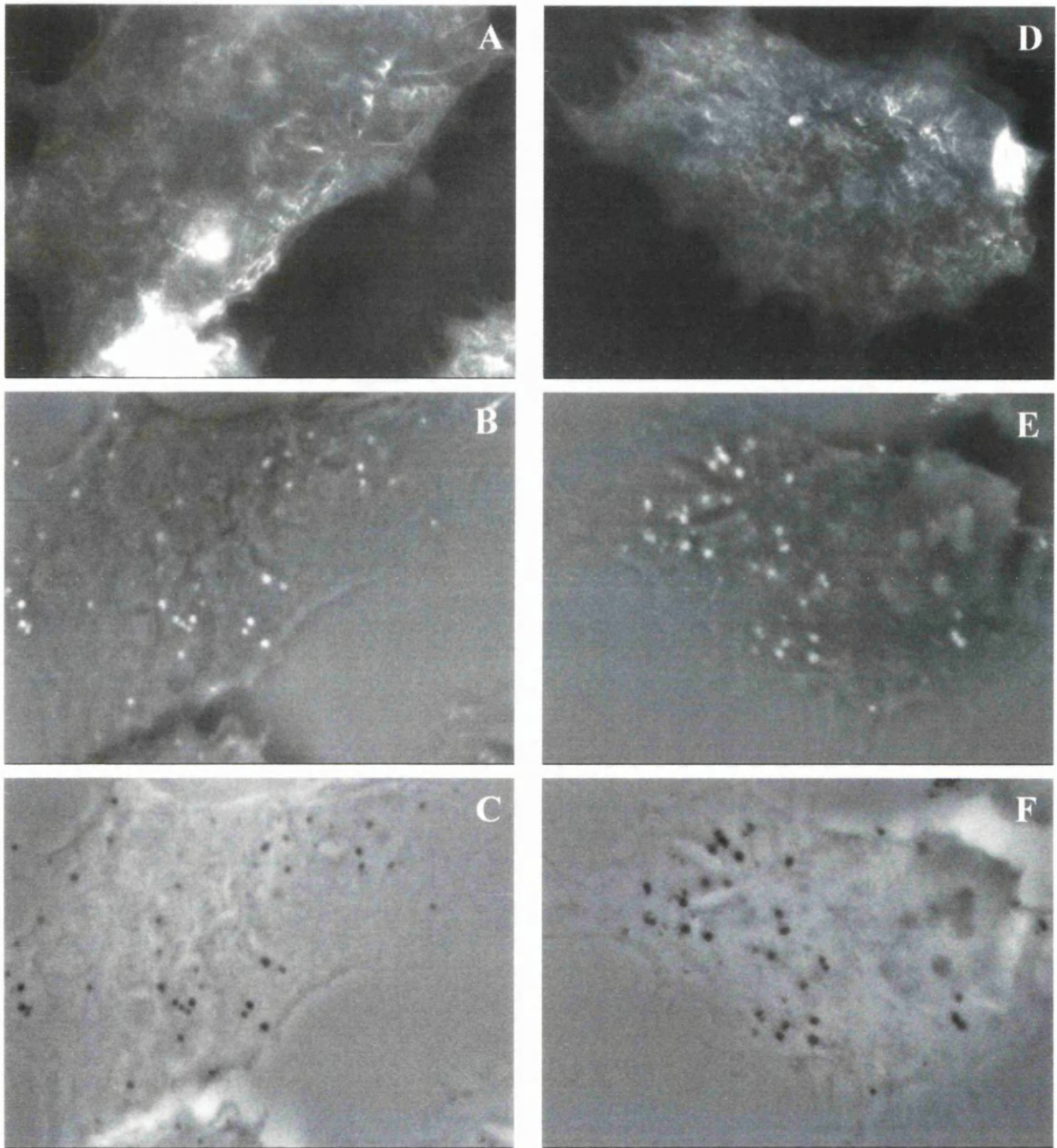


Figure 7.6B. Scanning Electron Microscopy-based assay to assess preS1 domain binding to plasma membranes of HepG2, cells.

HepG2 cells were grown in 24-well plates on glass coverslips for three days, then were incubated with preS1 domain, or mock antigen, in DMEM for one hour at 4°C. The unbound antigens were washed with DMEM and the cells were incubated with MAb RC28 for one hour. After washing, the cells were incubated with anti-mouse-IgG-30 nm. gold conjugate, washed and fixed in 2.5% glutaraldehyde. The cells were dehydrated in ethanol, dried by critical-point displacement with CO² and coated with carbon. The samples were analysed by secondary electron detection (panels **A** and **D**), by back-scatter analysis (panels **B** and **E**) and by reverse back-scatter (panels **C** and **F**).

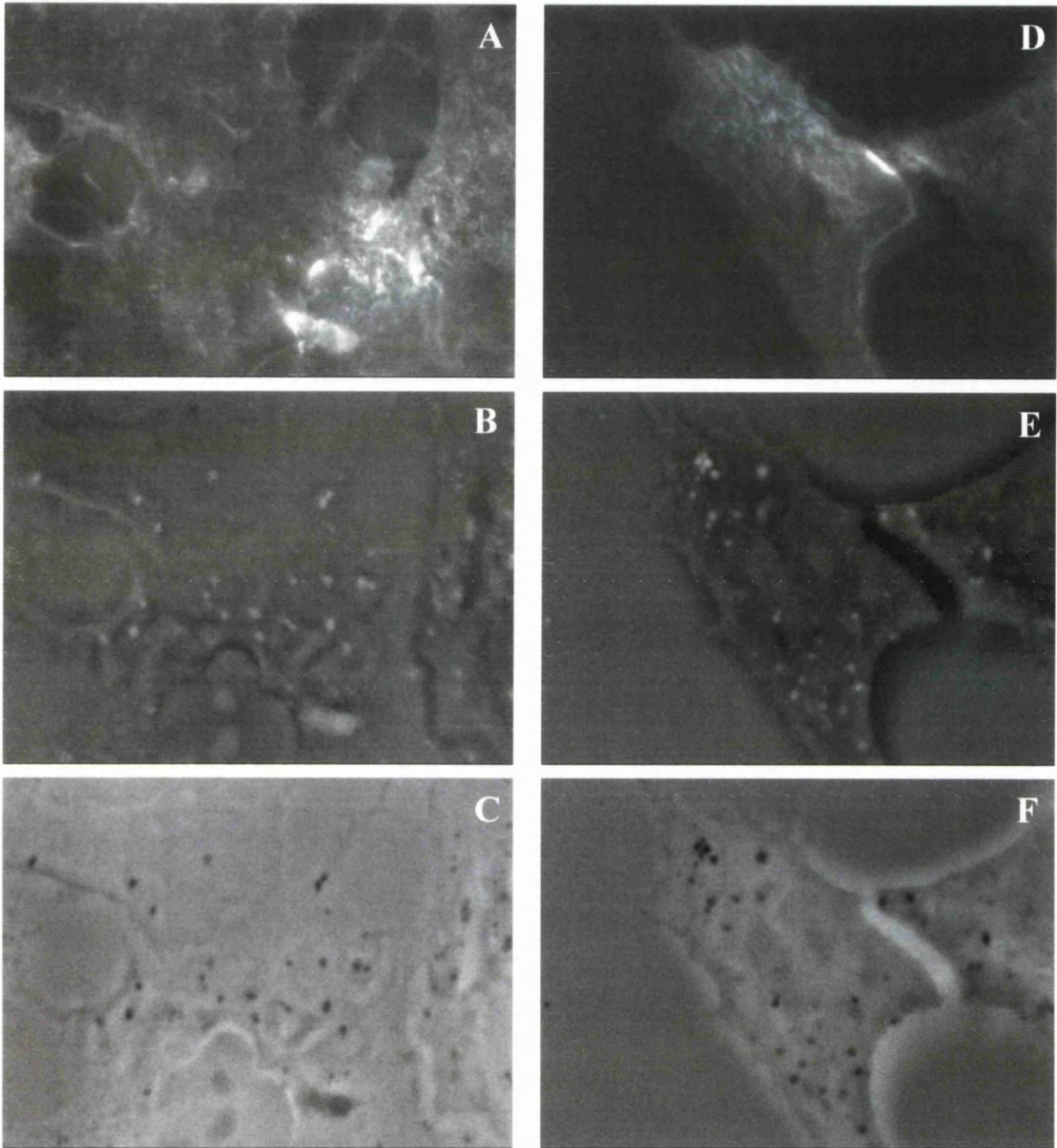


Figure 7.6C. Scanning Electron Microscopy-based assay to assess preS1 domain binding to plasma membranes of H5 cells.

H5 cells were grown in 24-well plates on glass coverslips for three days, then were incubated with preS1 domain, or mock antigen, in DMEM for one hour at 4°C. The unbound antigens were washed with DMEM and the cells were incubated with MAb RC28 for one hour. After washing, the cells were incubated with anti-mouse-IgG-30 nm. gold conjugate, washed and fixed in 2.5% glutaraldehyde. The cells were dehydrated in ethanol, dried by critical-point displacement with CO² and coated with carbon. The samples were analysed by secondary electron detection (panels **A** and **D**), by back-scatter analysis (panels **B** and **E**) and by reverse back-scatter (panels **C** and **F**).

Lx preparation. Due to the small amount of Lx protein recovered from the infected vLx cells, it was possible only to evaluate binding, but not specificity by inhibition in these experiments.

An attempt was also made to investigate the binding of the Lx protein preparation to the plasma membrane of HepG2, H5 and COS-7 cells by confocal microscopy. In this experiment, the cultured cells were incubated with the Lx protein preparation, a mock antigen, or a preparation obtained from the medium of WR-infected cells and then probed with the MAAb RC28 and anti-mouse IgG-FITC, then fixed and analysed for fluorescence. In Fig. 7.5, panels A-I, the images of the plasma membrane fluorescence from HepG2, H5 and COS-7 cells are shown. There was fluorescence discernible from all of the plasma membranes of the cells in each panel. The fluorescent images showed no localisation on the plasma membranes that are found only in the cells incubated with the Lx preparation. Furthermore, there was no discernible difference in the intensity of the fluorescence of the plasma membranes between the cell lines, or within the same cells incubated in the presence or absence of a ligand. It should be noted that during the course of this experimentation, the parameters used in the controlling software for the Laser Scanning Confocal Microscope remained constant throughout. The use of constant amplification and laser excitation parameters was intended to allow any discernible difference in the intensities of the plasma membrane fluorescence to become visible from examination of the image. However, it was the case here that there was no discernible difference between any of the images obtained.

It was apparent from the results obtained by flow cytometry, that the preS1 domain and Lx bound specifically to the plasma membrane of the HepG2 and H5 cell lines. The confocal assay used here (Fig. 7.4) to examine the plasma membrane binding of the Lx protein yielded no useful results, so the author utilised Scanning Electron Microscopy in order to attempt the visualisation of the preS1 domain to the plasma membrane of the HepG2 and H5 cell lines. Due to the larger increase in the fluorescent intensity of the HepG2 and H5 cells when incubated with the preS1 domain, in comparison with those incubated with the Lx preparation, it was prudent to examine the preS1 domain binding to the plasma membrane of cells in these experiments. The incubation of the cells with the preS1 domain was performed on

glass coverslips in 24-well plates and probed with MAb RC28, followed by anti-mouse IgG-gold conjugate (30nm). The samples were analysed for secondary electron detection, backscatter and reverse backscatter in a JEOL SEM T100. The results shown in Figs. 7.6 A to C show secondary electron detection (panel A), backscatter (panel B) and reverse backscatter (panel C). The negative control samples were incubated with mock antigen (PBSA) and then probed with the same primary and secondary antisera and analysed for secondary electron detection (panel D) backscatter (panel E) and reverse backscatter (panel F). The morphology of the COS-7 cell chosen for Fig. 7.6 is clearly apparent from the image in panel A and was typical of the COS-7 cells grown in this laboratory. Visualisation of the gold conjugate is readily apparent in panel B (white spots) and also in panel C (dark spots). The presence of the gold conjugates on the plasma membranes of COS-7, H5 and HepG2 cells is clearly visible in these figures. However, the negative controls for these experiments showed similar amounts of gold conjugate labelling on the plasma membranes of all the cells analysed in these experiments (panels D, E and F). The absence of any indication of binding of the preS1 domain to the plasma membrane may be due to one or more factors; it is possible that there is poor recognition of the MAb RC28 by the anti-mouse –gold conjugate: it may also be possible that the expression of MHC proteins on the plasma membrane of the cells binds the anti-mouse-gold conjugate, leading to a ubiquitous signal on all cells. This data contrasts with the data obtained from the cytometry experiments described earlier in this chapter.

7.3 Discussion.

The binding of the preS1 domain to hepatocytes and non-hepatocyte-derived cell lines has been investigated by flow cytometry. It has been shown that the preS1 domain binds to established and novel human hepatocyte cell lines, and binds specifically to HepG2 cells, and H5 cells. There was little or no binding of the preS1 domain to COS-7 cells, CEM-4 or CCRF-CEM4 cells in these assays. The demonstration of specific and inhibitable binding of the preS1 domain to established cell lines and to one of our novel cell lines, and the absence of binding to non-human and non-hepatic cell lines implies that the use of the preS1 domain for studying the interaction of the L protein with the plasma membrane proteins of the cell is appropriate for these types of investigation. The results are in agreement with previously published data that

implicates preS1 regions in binding to cell surface receptor. From the results described in this chapter it would appear that the preS1 domain recognises a human hepatocyte specific receptor(s). It is intriguing to note that the preS1 domain bound much more efficiently to H5 cells compared to HepG2, and moreover this binding was subject to dose-dependent inhibition by peptide 21-47 implicating this region in receptor recognition. Thus, the FACS-based assay developed in this study, together with the availability of a novel human hepatocyte cell line H5 would provide a basis to identify and clone the receptor(s) for preS1.

The absence of any meaningful results from the confocal microscopy-based and scanning electron microscopy-based assays for the binding of the preS1 domain to the plasma membranes demonstrates the difficulties associated with these assays. Clearly more work is required to eliminate the occurrence of high background presumably due to non-specific binding of primary and/or secondary antibodies or appropriate detection reagents to cells in these assays.

The demonstration of specific binding of HBV ligands to plasma membrane proteins has been notoriously difficult and has severely hampered progress in this field. It remains possible that the use of recombinant proteins such as the preS1 domain used here represents a sub-optimal assay system for investigation of the early events involved in receptor binding. The current regulations restricting workers to category three containment for use of viable HBV prevented the author investigating the early stages of infection of hepatocytes by HBV. Thus, the only avenue of investigation is to examine the early stages of the infection process is to use recombinant proteins instead of the infectious agent. A useful avenue of investigation would be to examine the binding of purified HBV in the presence and absence of inhibitory agents such as the preS1 domain and purified S from the serum of infected patients. However, in experimental investigation to identify the receptor for the L protein, it would be useful to use the preS1 domain to study the interaction of the protein of the L protein purported to be involved in the initial steps of binding to the plasma membrane proteins. It is likely that the S protein is involved in binding to annexin V on the plasma membrane, and the presence of the S domain in the L protein could lead to confusion in interpretation of results. Thus, the use of the preS1 domain in order to identify the cellular receptor for the L protein is a sound strategy, and has been used

to good effect in the search for the DHBV receptor (Breiner *et al.*, 1998) and subsequent characterisation of the ligand-receptor complex (Urban *et al.*, 1999).

Chapter 8

Conclusion.

In this study, the various roles played by the HBV surface antigens (S, M and L) in virus infection, assembly and morphogenesis has been investigated. To carry out this work, it was essential to generate a wide range of reagents. The surface antigens were expressed using a recombinant vaccinia virus and bacterial system. The bacterially expressed preS1 domain of the L antigen was used to generate a panel of MAbs and PABs. The antibodies generated in house and those obtained from elsewhere were used to confirm the expression of viral proteins by recombinant vaccinia virus system. A detailed analysis of the antigenicity of the HBV surface antigens and core was undertaken to confirm that the intracellular behaviour of the expressed proteins was in keeping with the previously published data. The reactivities of the MAbs and PABs were characterised in detail in ELISA, Western Blot, immunofluorescence and immunoprecipitation assays. Comprehensive analysis of the reactivities of the antibodies directed against the L protein has shown that all of the anti-preS1 MAbs generated here are reactive to amino acids 15-35 of the preS1 domain. Furthermore, a previously uncharacterised anti-S MAb, 6B1, was shown to recognise a discontinuous epitope in S and this MAb was used to generate new data concerning the antigenicity and conformation of the surface antigens. These antisera have been instrumental in the work described in Chapters 5, 6 and 7.

Given the hepatotropic nature of HBV and its inability to replicate efficiently in existing hepatocyte cell lines, the potential value of stable hepatocyte cell lines as a HBV research tool cannot be underestimated. The inability of HBV to replicate efficiently in culture is likely due to the lack of certain liver-specific functions in cells cultured *in vitro*. There is a considerable interest in generating novel hepatocyte cell lines as their relevance to hepatotropic virus research is obvious. Furthermore, the applicability of these lines on a wider scale to the biotechnology industry, e.g. for

examination of the metabolism and toxicity of compounds (which has so far seen HepG2 used as a preferred cell line) is immense. In this study, the novel hepatocytes (H5 and H16) generated in-house from a healthy human liver were characterised partially for expression of certain cellular markers. The analysis of intracellular markers such as cytokeratins 8 and 18, alpha-1-anti-trypsin and alpha-fetoprotein has lead the author to suggest that these novel cell lines (H5 and H16) are likely to have retained salient phenotypic markers of hepatocyte differentiation. The retention of these markers shows there is some likelihood that these cell lines are representative of the phenotype found in hepatocytes in the healthy liver. However, further evaluation of the appropriate proteins and mRNAs in the H5 and H16 cell lines is required to confirm the hepatocyte phenotype. This work was not done here as it was considered to be outside the scope of this project. The novel cell lines H5 and H16, as well as the well-characterised HepG2 and Huh7 cells were used in the work described in Chapters 5, 6 and 7. Overall, the results obtained are promising and suggest that these cell lines should be assessed for the ability to support infection and replication by HBV (and HCV) as soon as is practicable.

The structure of the surface antigens was evaluated immunologically to shed light on the conformation and transmembrane topology of these proteins. The anti-S MAb 6B1 that reacts with a conformational epitope present on S interestingly fails to recognise L. Thus, recognition of S, but not the S domain of L, in both immunofluorescence and immunoprecipitation by this MAb is evidence to suggest that there are significant differences present in structure of the S domains of the S and L proteins. Furthermore, the recognition of M by the MAb 6B1 is demonstrated, suggesting that the L protein has differently structured S domains than the M and S proteins. Current computer generated models of HBV surface antigen topology depict no overall differences in the structure of the S domain of L and M to HBsAg (see Introduction, Fig. 1.3). However, biochemical evidence to support this hypothesis has been lacking. In this study, using a novel MAb it has been shown experimentally for the first time the existence of structural differences between the S domain of L and the S protein. It would seem plausible that the MAb 6B1 epitope on S is masked by the preS domains of L, accounting for non-recognition of L, but given the dual topology of the L protein it is likely that at least 50% of S epitopes would be exposed for recognition by MAb 6B1. However, 6B1 does not recognise L at all,

clearly pointing to recognition of a structurally different S domain in L. Clearly, further experiments are required to ascertain where the differences may lie.

The MAb 6B1 has also been valuable in studying the intracellular distribution and behaviour of the L and S (and Lx and S, and M and S). It was shown that the intracellular retention of the L protein in the ER/ERGIC is abrogated by the expression of S, resulting in a membrane-associated complex of proteins distributed throughout the cell. The expression of Lx and S results in a wide distribution of tightly co-localised proteins throughout the cytoplasm, with S no longer associating with the intracellular membranes. Furthermore, to confirm both of these observations, anti-L antisera have been used to demonstrate the co-immunoprecipitation of L with S, and Lx with S. Taken together, these results clearly indicate that L and S specifically interact with each other. Wunderlich and Bruss (1996) demonstrated multimerisation between S and L, indicating that this event may potentially mediate budding of HBV particles. Thus, the author demonstrates in Chapter 5 the existence of a novel reagent capable of distinguishing between surface antigens, and analyses the intracellular behaviour of the proteins when expressed singularly or co-expressed.

The intracellular interactions of the surface antigens with core have been investigated using the reagents generated and described in Chapter 3. The expression and distribution of the core protein in hepatocytes and other cell lines when co-expressed with surface antigens has generated new data concerning the morphogenesis of HBV. The results presented here show that expression of core results in a nuclear and cytoplasmic distribution, but upon co-expression with L, the core protein is tightly retained in the ER/ERGIC, the same compartment known to retain the L protein (as demonstrated in Chapter 6). Redistribution of core is not observed when co-expressed with either M or S. This information adds useful data to the existing literature base. Recent reports have shown *in vitro* interactions between the S domain and core, and the preS1 domain and core. However, data presented here show that the presence of M or S alone is insufficient to redistribute the core indicating a lack of, or a weak intracellular interaction between the proteins. The lack of recognition by MAb RC28 of L bound to core points to involvement of the epitope on the preS1 in the interaction of the core. Taken together, these results lead the author to reason that the

predominant influence in the association of the envelope with the core is due to the presence of the preS1 domain of L. However, it is possible that the structure of the S domain in L is disposed to interaction with the core protein, since this domain in L has been shown in this study to be conformationally different from HBsAg. The association of core with Lx is also demonstrated throughout the cytoplasm of co-expressing cells, suggesting that although the Lx protein is not retained intracellularly in the same manner as L, the Lx retains the ability to colocalise and interact with core within the cytoplasm.

The investigations of the binding of the HBV-derived ligands to the cell lines described in Chapter 7 have shown several new findings. The binding of the preS1 domain to the plasma membrane of human hepatocytes (HepG2 and H5) has been shown to be specific and inhibitable. There was an absence of binding to cells of lymphoblastic origin (CEM 4) and non-human cell lines (COS-7). Inhibition of the preS1 domain by the 21-47 peptide is in keeping with the inhibition of binding of the virus to immobilised plasma membrane proteins described in the literature. That the preS1 domain binds in a similar manner to HBV to the plasma membrane of HepG2 and H5 cells, suggests that this ligand is a suitable substitute for L and could be utilised in the search for the cellular receptor for HBV. The differences between the H5 and H16 cell lines are of considerable interest. Both cell lines were derived from a healthy liver donor and have been immortalised and partially characterised indicating a high likelihood of retention of a hepatocyte phenotype. The inability of the H16 cell line to bind the preS1 domain in the same manner as the H5 and HepG2 cell lines may indicate that there is a difference in expression of an as yet unidentified receptor or co-receptor in these cell lines. Alternatively, the difference in binding of the preS1 domain to H16 may indicate that this cell line has differentiated over time to a non-hepatocytic phenotype. Thus, the importance of a detailed analysis of the H5 and H16 cell lines should offer considerable insight into the hepatocyte-specific binding of the HBV surface antigens. It is conceivable that expression of a co-receptor for the preS1 domain is occurring in only one of these novel cell lines and that the true retention of an hepatocyte phenotype may be responsible for expression of this co-receptor.

This research presented here has generated novel information concerning HBV surface antigen structure, virion morphogenesis and receptor binding. Additionally, a comprehensive array of novel reagents has been generated and characterised, many of which hold a great deal of promise for future HBV research in this laboratory.

Appendix 1

The hybridoma supernatants from MAbs RC9, RC28, RC109, RC152 were used at a dilution of 1:1000 for indirect immunofluorescence.

PABs 142 and 143 were used at a dilution of 1:4000 for indirect immunofluorescence.

MAB 6B1/1 (obtained from Dr. Connal McCaughey, Queen's university of Belfast) was used at a dilution of 1:100 for indirect immunofluorescence.

Anti-p53 MAB 91/93 was used at 1:100.

Anti-human serum albumin (Sigma) was used at 1:50.

Anti-human alpha-1-antitrypsin (Sigma) was used at 1:100.

Anti-apolipoprotein (Calbiochem) was used at 1:200.

Anti-human plasminogen (Sigma) was used at 1:100.

Concanavalin-A-FITC (Sigma) was used at 1:200.

MAbs H166, H35, RF7 and H53 used at 1:100 for immunofluorescence. These antibodies were obtained from the laboratory of Dr. W. F. Carman. Relevant literature concerning the reactivities of these antisera can be found in Chen *et. al.* (1996). Anti-Annexin V MAB was also obtained from Dr. Carman's laboratory and was used at 1:50.

MAB 18/7 was kindly donated by Prof. W. H. Gerlich (Geissen, Germany) and was used at a dilution of 1:1000.

MAB 2-12F2 was kindly donated by Prof. W. H. Gerlich (Geissen, Germany) and was used neat.

MAB 2A23 was obtained from the Institute of Immunology, Osaka, Japan, and was used at 1:100.

Anti-mouse-IgG-FITC (Sigma) was used at a concentration of 1:100, anti-rabbit IgG-FITC (Sigma) was used at 1:100, anti-rabbit-IgG-cy5 (Amersham) was used at 1:200, and anti-mouse-IgG-cy5 (Amersham) was used at 1:100.

Appendix 2

	M K Q Y I V L A C M C L A A	
AAGCTT	ATG AAA CAA TAT ATC GTC CTG GCA TGC ATG TGC CTG GCG GCA	48
<i>HindIII</i>		
	└─▶ L	
	R A M P A S L K	8
CGT GCT ATG CCT GCC AGT	<u>CTT AAG</u> ATG GGG CAG AAT CTT TCC ACC AGC	96
	<i>AflII</i>	
N	P L G F L P D H Q L D P A F R	24
AAT CCT CTA GGA TTC CTT CCC GAT CAC CAG TTG GAC CCA GCA TTC AGA		144
	A N T N N P D W D F N P K K D P	40
GCA AAT ACC AAC AAT CCA GAT TGG GAC TTC AAT CCC AAA AAG GAC CCT		192
	W P E A N K V G V G A Y G P G F	56
TGG CCA GAG GCC AAC AAG GTA GGA GTT GGA GCC TAT GGA CCC GGG TTC		240
	T P P H G G L L G W S P Q S Q G	72
ACC CCT CCA CAC GGA GGC CTT TTG GGG TGG AGC CCT CAG TCT CAG GGC		288
	T L T T L P A D P P P A S T N R	88
ACA CTA ACA ACT TTG CCA GCA GAT CCG CCT CCT GCC TCC ACC AAT CGT		336
	Q S G R Q P T P I S P P L R D S	104
CAG TCA GGG AGG CAG CCT ACT CCC ATC TCT CCA CCA CTA AGA GAC AGT		384
	└─▶ M	
	H P Q A M Q W N S T A F H Q A L	120
CAT <u>CCT CAG GCC</u> ATG CAG TGG AAC TCT ACA GCA TTC CAC CAA GCT CTA		432
	<i>Bsu36I</i>	
Q	N P K V R G L Y F P A G G S S	136
CAA AAT CCC AAA GTC AGG GGC CTG TAT TTT CCT GCT GGT GGC TCC AGT		480
	S G I V N L V P T I A S H I S S	152
TCA GGG ATA GTG AAC CTT GTT CCG ACT ATT GCC TCT CAC ATC TCG TCA		528
	└─▶ S	
	I F S R I G D P A P N M E N I T	168
ATC TTC TCC AGG ATT GGG GAC CCT GCA CCG AAC ATG GAG AAC ATC ACA		576
	S G F L G P L L V L Q A G F F L	184
TCA GGA TTC CTA GGA CCC CTG CTC GTG TTA CAG GCG GGG TTT TTC TTG		624
	L T R I L T I P Q S L D S W W T	200
TTG ACA AGA ATC CTC ACA ATA CCG CAG AGT CTA GAC TCG TGG TGG ACT		672
	S L N F L G G V P V C P G L N S	216
TCT CTC AAT TTT CTA GGG GGA GTG CCC GTG TGT CCT GGC CTA AAT TCG		720
	Q S P T S N H S P I S C P P T C	232
CAG TCC CCA ACC TCC AAT CAC TCA CCA ATC TCC TGT CCT CCA ACT TGT		768
	P G Y R W M C L R R F I I F L F	248
CCT GGC TAT CGC TGG ATG TGT CTG CGG CGT TTT ATC ATA TTC CTC TTC		816

I	L	L	L	C	L	I	F	L	L	V	L	L	D	Y	Q	264
ATC	CTG	CTG	CTA	TGC	CTC	ATC	TTC	TTG	TTG	GTT	CTT	CTG	GAC	TAT	CAA	864
G	M	L	P	V	C	P	L	I	P	G	S	S	T	T	S	280
GGT	ATG	TTG	CCC	GTT	TGT	CCT	CTG	ATT	CCA	GGA	TCC	TCG	ACC	ACC	AGT	912
T	G	P	C	K	T	C	T	T	P	A	Q	G	N	S	M	296
ACG	GGA	CCC	TGC	AAA	ACC	TGC	ACG	ACT	CCT	GCT	CAA	GGC	AAC	TCT	ATG	960
Y	P	S	C	C	C	T	K	P	S	D	G	N	C	T	C	312
TAT	CCC	TCA	TGT	TGC	TGT	ACA	AAA	CCT	TCG	GAC	GGA	AAT	TGC	ACC	TGT	1008
I	P	I	P	S	S	W	A	F	A	K	Y	L	W	E	W	328
ATT	CCC	ATC	CCA	TCA	TCT	TGG	GCT	TTC	GCA	AAA	TAC	CTA	TGG	GAG	TGG	1056
A	S	V	R	F	S	W	L	S	L	L	V	P	F	V	Q	344
GCC	TCA	GTC	CGT	TTC	TCT	TGG	CTC	AGT	TTA	CTA	GTG	CCA	TTT	GTT	CAG	1104
W	F	V	G	L	S	P	T	V	W	L	S	A	I	W	M	360
TGG	TTC	GTA	GGG	CTT	TCC	CCC	ACT	GTC	TGG	CTT	TCA	GCT	ATA	TGG	ATG	1152
M	W	Y	W	G	P	N	L	Y	N	I	L	S	P	F	I	376
ATG	TGG	TAT	TGG	GGG	CCA	AAT	CTG	TAC	AAC	ATC	TTG	AGT	CCC	TTT	ATA	1200
P	L	L	P	I	F	F	C	L	W	V	Y	I	-			389
CCG	CTG	TTA	CCA	ATT	TTC	TTT	TGT	CTT	TGG	GTA	TAC	ATT	TAA	ACCCTAACC		1251
<u>AAGCTT</u>																1257
<u>HindIII</u>																

The nucleotide sequence of the ORF encoding the secretory form of HBV (subtype *adw*) L (Lx). The amino acid sequence in blue box represents the secretory signal sequence of the vaccinia virus 35 kDa polypeptide. The translational start sites of HBV L, M and S are show by an arrow. The amino acid sequence is numbered from the initiating methionine of the L protein. The nucleotide sequences encoding HBV preS1 domain, L and M were derived by subcloning or PCR from that of Lx (see Methods and Materials, section.....). The relevant restriction enzyme sites used in cloning are shown. The amino acid sequence highlighted in burgandy represent the 21 to 47 region of the preS1 domain involved interaction with a putative receptor. Comparison of the amino acid sequence of our L with those in the SwissProt database identified several unique residues at variant and invariant positions. These are highlighted in red or green, respectively.

Bibliography.

- Aiba, N., McGarvey, M. J., Waters, J., Hadziyannis, S. J., Thomas, H. C., and Karayiannis, P. (1997). The precore sequence of hepatitis B virus is required for nuclear localization of the core protein. *Hepatology* **26**(5), 1311-7.
- Alberti, A., Pontisso, P., Fraiese, A., Caredda, F., Fattovich, G., Tagariello, G., and Realdi, G. (1987). Virus-associated receptor for polymerized human serum albumin and antibody to the receptor in HBV and in HDV infection. *Prog Clin Biol Res* **234**, 61-70.
- Atkins, G. J., Qiao, M., Coombe, D. R., Gowans, E. J., and Ashman, L. K. (1997). Hepatitis B virus binding to leucocyte plasma membranes utilizes a different region of the preS1 domain to the hepatocyte receptor binding site and does not require receptors for opsonins. *Immunol Cell Biol* **75**(3), 259-66.
- Bartenschlager, R., and Schaller, H. (1993). Mechanisms Governing Hepadnaviral Nucleocapsid Assembly. *Journal of Hepatology* **17**(S3), S15-S19.
- Barwise, J. L., and Walker, J. H. (1996). Subcellular localization of annexin V in human foreskin fibroblasts: Nuclear localization depends on growth state. *Febs Letters* **394**(2), 213-216.
- Bchini, R., Capel, F., Dauguet, C., Dubanchet, S., and Petit, M. A. (1990). In vitro infection of human hepatoma (HepG2) cells with hepatitis B virus. *Journal of Virology* **64**(6), 3025-32.
- Blaheta, R. A., Kronenberger, B., Woitaschek, D., Auth, M. K. H., Scholz, M., Weber, S., Schuldes, H., Encke, A., and Markus, B. H. (1998). Dedifferentiation of human hepatocytes by extracellular matrix proteins in vitro: quantitative and qualitative investigation of cytokeratin 7, 8, 18, 19 and vimentin filaments. *Journal of Hepatology* **28**(4), 677-690.
- Blum, H. E., Zhang, Z. S., Galun, E., von Weizsacker, F., Garner, B., Liang, T. J., and Wands, J. R. (1992). Hepatitis B virus X protein is not central to the viral life cycle in vitro. *Journal of Virology* **66**(2), 1223-7.
- Bottcher, B., Tsuji, N., Takahashi, H., Dyson, M. R., Zhao, S., Crowther, R. A., and Murray, K. (1998). Peptides that block hepatitis B virus assembly: analysis by cryomicroscopy, mutagenesis and transfection. *EMBO J* **17**(23), 6839-45.

- Breiner, K. M., Urban, S., and Schaller, H. (1998). Carboxypeptidase D (gp180), a Golgi-resident protein, functions in the attachment and entry of avian hepatitis B viruses. *Journal of Virology* **72**(10), 8098-8104.
- Bruss, V., and Ganem, D. (1991a). The role of envelope proteins in hepatitis B virus assembly. *Proceedings of the National Academy of Science* **88**(3), 1059-63.
- Bruss, V., and Ganem, D. (1991b). The Role of Envelope Proteins in Hepatitis-B Virus Assembly. *Proceedings of the National Academy of Sciences of the United States of America* **88**(3), 1059-1063.
- Bruss, V., Gerhardt, E., Vieluf, K., and Wunderlich, G. (1996a). Functions of the large hepatitis B virus surface protein in viral particle morphogenesis. *Intervirology* **39**(1-2), 23-31.
- Bruss, V., Hagelstein, J., Gerhardt, E., and Galle, P. R. (1996b). Myristylation of the large surface protein is required for hepatitis B virus in vitro infectivity. *Virology* **218**(2), 396-9.
- Bruss, V., and Thomssen, R. (1994a). Mapping a region of the large envelope protein required for hepatitis B virion maturation. *Journal of Virology* **68**(3), 1643-50.
- Bruss, V., and Thomssen, R. (1994b). Mapping a Region of the Large Envelope Protein Required For Hepatitis-B Virion Maturation. *Journal of Virology* **68**(3), 1643-1650.
- Bruss, V., and Vieluf, K. (1995a). Functions of the internal pre-S domain of the large surface protein in hepatitis B virus particle morphogenesis. *Journal of Virology* **69**(11), 6652-7.
- Bruss, V., and Vieluf, K. (1995b). Functions of the Internal Pre-S Domain of the Large Surface Protein in Hepatitis-B Virus Particle Morphogenesis. *Journal of Virology* **69**(11), 6652-6657.
- Budkowska, A., Quan, C., Groh, F., Bedossa, P., Dubreuil, P., Bouvet, J. P., and Pillot, J. (1993). Hepatitis B virus (HBV) binding factor in human serum: candidate for a soluble form of hepatocyte HBV receptor. *Journal of Virology* **67**(7), 4316-22.
- Busachi, C. A., Ferrari, S., Ballardini, P. L., Landi, P., Bazzocchi, F., Santini, D., Martinelli, G., Piccaluga, A., and Pisi, E. (1986). Tissue antigen distribution in hepatocellular carcinoma. *Tumori* **72**(1), 1-5.
- Chambers, M. A., Dougan, G., Newman, J., Brown, F., Crowther, J., Mould, A. P., Humphries, M. J., Francis, M. J., Clarke, B., Brown, A. L., and Rowlands, D.

- (1996). Chimeric hepatitis B virus core particles as probes for studying peptide-integrin interactions [published erratum appears in *J Virol* 1996 Aug;70(8):5740]. *Journal of Virology* **70**(6), 4045-52.
- Chen, J. Y., Harrison, T. J., Lee, C. S., Chen, D. S., and Zuckerman, A. J. (1986). Detection of hepatitis B virus DNA in hepatocellular carcinoma. *Br J Exp Pathol* **67**(2), 279-88.
- Chen, M., Hieng, S., Qian, X. B., Costa, R., and Ou, J. H. (1994). Regulation of Hepatitis-B Virus Enhancer Activity By Hepatocyte- Enriched Transcription Factor Hnf3. *Virology* **205**(1), 127-132.
- Chen, Y. C., Delbrook, K., Dealwis, C., Mimms, L., Mushahwar, I. K., and Mandeck, W. (1996). Discontinuous epitopes of hepatitis B surface antigen derived from a filamentous phage peptide library. *Proceedings of the National Academy of Science* **93**(5), 1997-2001.
- Cheng, K. C., Smith, G. L., and Moss, B. (1986). Hepatitis B virus large surface protein is not secreted but is immunogenic when selectively expressed by recombinant vaccinia virus. *Journal of Virology* **60**(2), 337-44.
- Chisari, F. V., Filippi, P., Buras, J., McLachlan, A., Popper, H., Pinkert, C. A., Palmiter, R. D., and Brinster, R. L. (1987). Structural and pathological effects of synthesis of hepatitis B virus large envelope polypeptide in transgenic mice. *Proceedings of the National Academy of Science* **84**(19), 6909-13.
- Chu, C. M., and Liaw, Y. F. (1992). Intrahepatic expression of pre-S1 and pre-S2 antigens in chronic hepatitis B virus infection in relation to hepatitis B virus replication and hepatitis delta virus superinfection. *Gut* **33**(11), 1544-8.
- Cianflone, K., Vu, H., Zhang, Z. J., and Sniderman, A. D. (1994). Effects of Albumin On Lipid-Synthesis, Apo-B-100 Secretion, and Ldl Catabolism in Hepg2 Cells. *Atherosclerosis* **107**(2), 125-135.
- Conway, J. F., Cheng, N., Zlotnick, A., Stahl, S. J., Wingfield, P. T., and Steven, A. C. (1998). Localization of the N terminus of hepatitis B virus capsid protein by peptide-based difference mapping from cryoelectron microscopy. *Proceedings of the National Academy of Science* **95**(25), 14622-7.
- Crowther, R. A., Kiselev, N. A., Bottcher, B., Berriman, J. A., Borisova, G. P., Ose, V., and Pumpens, P. (1994). Three-dimensional structure of hepatitis B virus core particles determined by electron cryomicroscopy. *Cell* **77**(6), 943-50.

- Dash, S., Panda, S. K., and Nayak, N. C. (1990). Polymerized albumin binding to serum in various liver diseases: its significance and relation to hepatitis B virus infection. *J Gastroenterol Hepatol* **5**(1), 16-24.
- Dash, S., Rao, K. V., and Panda, S. K. (1992). Receptor for pre-S1(21-47) component of hepatitis B virus on the liver cell: role in virus cell interaction. *J Med Virol* **37**(2), 116-21.
- Davison, A. J., and Moss, B. (1990). New Vaccinia Virus Recombination Plasmids Incorporating a Synthetic Late Promoter For High-Level Expression of Foreign Proteins. *Nucleic Acids Research* **18**(14), 4285-4286.
- de Bruin, W. C., Hertogs, K., Leenders, W. P., Depla, E., and Yap, S. H. (1995). Hepatitis B virus: specific binding and internalization of small HBsAg by human hepatocytes. *J Gen Virol* **76**(Pt 4), 1047-50.
- de Bruin, W. C., Leenders, W. P., Moshage, H., and van Haelst, U. J. (1996). Species specificity for HBsAg binding protein endonexin II. *J Hepatol* **24**(3), 265-70.
- Dejean, A., and de The, H. (1990). Hepatitis B virus as an insertional mutagen in a human hepatocellular carcinoma. *Mol Biol Med* **7**(3), 213-22.
- de-Medina, T., Haviv, I., Noiman, S., and Shaul, Y. (1994). The X protein of hepatitis B virus has a ribo/deoxy ATPase activity. *Virology* **202**(1), 401-7.
- De-Medina, T., and Shaul, Y. (1994). Functional and structural similarity between the X protein of hepatitis B virus and nucleoside diphosphate kinases. *FEBS Lett* **351**(3), 423-6.
- Dyson, M. R., and Murray, K. (1995). Selection of peptide inhibitors of interactions involved in complex protein assemblies: association of the core and surface antigens of hepatitis B virus. *Proceedings of the National Academy of Science* **92**(6), 2194-8.
- Eble, B. E., Lingappa, V. R., and Ganem, D. (1986). Hepatitis B surface antigen: an unusual secreted protein initially synthesized as a transmembrane polypeptide. *Mol Cell Biol* **6**(5), 1454-63.
- Eble, B. E., Lingappa, V. R., and Ganem, D. (1990). The N-terminal (pre-S2) domain of a hepatitis B virus surface glycoprotein is translocated across membranes by downstream signal sequences. *Journal of Virology* **64**(3), 1414-9.
- Eble, B. E., Macrae, D. R., Lingappa, V. R., and Ganem, D. (1987). Multiple Topogenic Sequences Determine the Transmembrane Orientation of Hepatitis-B Surface-Antigen. *Molecular and Cellular Biology* **7**(10), 3591-3601.

- Ehrlich, P. H., and Moyle, W. R. (1986). Ultrasensitive Cooperative Immunoassays With Mixed Monoclonal- Antibodies. *Methods in Enzymology* **121**, 695-702.
- Eng, F. J., Novikova, E. G., Kuroki, K., Ganem, D., and Fricker, L. D. (1998). gp180, a protein that binds duck hepatitis B virus particles, has metalloproteinase D-like enzymatic activity. *Journal of Biological Chemistry* **273**(14), 8382-8388.
- Fei, G. Z., Sylvan, S. P., Hellstrom, U. B., and Yao, G. B. (1995). Quantitative assessment of IgM antibodies towards an immunodominant B- cell epitope within the preS2 domain of HBV in the natural course and during combined prednisone/interferon alpha 2b treatment of chronic hepatitis B virus infection. *J Med Virol* **46**(2), 138-43.
- Flint, M., Maidens, C., LoomisPrice, L. D., Shotton, C., Dubuisson, J., Monk, P., Higginbottom, A., Levy, S., and McKeating, J. A. (1999). Characterization of hepatitis C virus E2 glycoprotein interaction with a putative cellular receptor, CD81. *Journal of Virology* **73**(8), 6235-6244.
- Franco, A., Paroli, M., Testa, U., Benvenuto, R., Peschle, C., Balsano, F., and Barnaba, V. (1992). Transferrin receptor mediates uptake and presentation of hepatitis B envelope antigen by T lymphocytes. *J Exp Med* **175**(5), 1195-205.
- Galle, P. R., Hagelstein, J., Kommerell, B., Volkmann, M., Schranz, P., and Zentgraf, H. (1994). In vitro experimental infection of primary human hepatocytes with hepatitis B virus. *Gastroenterology* **106**(3), 664-73.
- Gallina, A., Gazina, E., and Milanesi, G. (1995). A C-terminal PreS1 sequence is sufficient to retain hepatitis B virus L protein in 293 cells. *Virology* **213**(1), 57-69.
- Galun, E., Offensperger, W. B., von Weizsacker, F., Offensperger, S., Wands, J. R., and Blum, H. E. (1992). Human non-hepatocytes support hepadnaviral replication and virion production. *J Gen Virol* **73**(Pt 1), 173-8.
- Ganem, D. (1991). Assembly of Hepadnaviral Virions and Subviral Particles. *Current Topics in Microbiology and Immunology* **168**, 61-83.
- Garcia, A. D., Ostapchuk, P., and Hearing, P. (1993). Functional interaction of nuclear factors EF-C, HNF-4, and RXR alpha with hepatitis B virus enhancer I. *Journal of Virology* **67**(7), 3940-50.
- Gerlich, W. H., Lu, X., and Heermann, K. H. (1993a). Studies on the attachment and penetration of hepatitis B virus. *J Hepatol* **17**(Suppl 3), S10-4.

- Gerlich, W. H., Lu, X., and Heermann, K. H. (1993b). Studies On the Attachment and Penetration of Hepatitis-B Virus. *Journal of Hepatology* **17**(S3), S10-S14.
- Germaschewski, V., and Murray, K. (1995). Screening a monoclonal antibody with a fusion-phage display library shows a discontinuity in a linear epitope within PreS1 of hepatitis B virus. *J Med Virol* **45**(3), 300-5.
- Gillececastro, B. L., Fisher, S. J., Tarentino, A. L., Peterson, D. L., and Burlingame, A. L. (1987). Structure of the Oligosaccharide Portion of Human Hepatitis-B Surface-Antigen. *Archives of Biochemistry and Biophysics* **256**(1), 194-201.
- Gong, Z. J., De Meyer, S., van Pelt, J., Hertogs, K., Depla, E., Soumillion, A., Fevery, J., and Yap, S. H. (1999). Transfection of a rat hepatoma cell line with a construct expressing human liver annexin V confers susceptibility to hepatitis B virus infection. *Hepatology* **29**(2), 576-84.
- Gong, Z. J., DeMeyer, S., vanPelt, J. F., Hertogs, K., Soumillion, A., Fevery, J., and Yap, S. H. (1996). Human annexin V is the determining factor for cell infectability by hepatitis B virus. *Hepatology* **24**(4 Pt2 SS), 488.
- Gripon, P., Diot, C., and Guguenguillouzo, C. (1993). Reproducible High-Level Infection of Cultured Adult Human Hepatocytes By Hepatitis-B Virus - Effect of Polyethylene-Glycol On Adsorption and Penetration. *Virology* **192**(2), 534-540.
- Gripon, P., Diot, C., Theze, N., Fourel, I., Loreal, O., Brechot, C., and Guguenguillouzo, C. (1988). Hepatitis B virus infection of adult human hepatocytes cultured in the presence of dimethyl sulfoxide. *Journal of Virology* **62**(11), 4136-43.
- Hafeez, W., Ciliberto, G., and Perlmutter, D. H. (1992). Constitutive and Modulated Expression of the Human Alpha-1- Antitrypsin Gene - Different Transcriptional Initiation Sites Used in 3 Different Cell-Types. *Journal of Clinical Investigation* **89**(4), 1214-1222.
- Halpern, M. S., England, J. M., Deery, D. T., Petcu, D. J., Mason, W. S., and Molnar-Kimber, K. L. (1983). Viral nucleic acid synthesis and antigen accumulation in pancreas and kidney of Pekin ducks infected with duck hepatitis B virus. *Proceedings of the National Academy of Science* **80**(15), 4865-9.
- Harvey, T. J., Macnaughton, T. B., Park, D. S., and Gowans, E. J. (1999). A cellular protein which binds hepatitis B virus but not hepatitis B surface antigen. *J Gen Virol* **80**(Pt 3), 607-15.

- He, L., Isselbacher, K. J., Wands, J. R., Goodman, H. M., Shih, C., and Quaroni, A. (1984). Establishment and characterization of a new human hepatocellular carcinoma cell line. *In Vitro* **20**(6), 493-504.
- Heermann, K. H., Goldmann, U., Schwartz, W., Seyffarth, T., Baumgarten, H., and Gerlich, W. H. (1984). Large surface proteins of hepatitis B virus containing the pre-s sequence. *Journal of Virology* **52**(2), 396-402.
- Heermann, K. H., Kruse, F., Seifer, M., and Gerlich, W. H. (1987). Immunogenicity of the gene S and Pre-S domains in hepatitis B virions and HBsAg filaments. *Intervirology* **28**(1), 14-25.
- Hertogs, K., Depla, E., Crabbe, T., De Bruin, W., Leenders, W., Moshage, H., and Yap, S. H. (1994). Spontaneous development of anti-hepatitis B virus envelope (anti- idiotypic) antibodies in animals immunized with human liver endonexin II or with the F(ab')₂ fragment of anti-human liver endonexin II immunoglobulin G: evidence for a receptor-ligand-like relationship between small hepatitis B surface antigen and endonexin II. *Journal of Virology* **68**(3), 1516-21.
- Hertogs, K., Leenders, W. P., Depla, E., De Bruin, W. C., Meheus, L., Raymackers, J., Moshage, H., and Yap, S. H. (1993). Endonexin II, present on human liver plasma membranes, is a specific binding protein of small hepatitis B virus (HBV) envelope protein. *Virology* **197**(2), 549-57.
- Higginbottom, A., Quinn, E. R., Kuo, C. C., Flint, M., Wilson, L. H., Bianchi, E., Nicosia, A., Monk, P. N., McKeating, J. A., and Levy, S. (2000). Identification of amino acid residues in CD81 critical for interaction with hepatitis C virus envelope glycoprotein E2. *Journal of Virology* **74**(8), 3642-3649.
- Hildt, E., and Hofschneider, P. H. (1998). The PreS2 activators of the hepatitis B virus: activators of tumour promoter pathways. *Recent Results Cancer Res* **154**, 315-29.
- Hildt, E., Hofschneider, P. H., and Urban, S. (1996). The role of hepatitis B virus (HBV) in the development of hepatocellular carcinoma. *Seminars in Virology* **7**(5), 333-347.
- Hildt, E., Saher, G., Bruss, V., and Hofschneider, P. H. (1996). The hepatitis B virus large surface protein (LHBs) is a transcriptional activator. *Virology* **225**(1), 235-9.

- Hildt, E., Urban, S., Lauer, U., Hofschneider, P. H., and Kekule, A. S. (1993). Er-
 Localization and Functional Expression of the HBV Transactivator Mhbs(T).
Oncogene **8**(12), 3359-3367.
- Hu, J., and Seeger, C. (1996). Hsp90 is required for the activity of a hepatitis B virus
 reverse transcriptase. *Proceedings of the National Academy of Science* **93**(3),
 1060-4.
- Hu, Z., Zhang, Z., Doo, E., Coux, O., Goldberg, A. L., and Liang, T. J. (1999).
 Hepatitis B virus X protein is both a substrate and a potential inhibitor of the
 proteasome complex. *Journal of Virology* **73**(9), 7231-40.
- Huang, C. J., Chen, Y. H., and Ting, L. P. (2000). Hepatitis B virus core protein
 interacts with the C-terminal region of actin-binding protein. *Journal of*
Biomedical Science **7**(2), 160-168.
- Hui, J., Li, G., Kong, Y., and Wang, Y. (1999). Expression and characterization of
 chimeric hepatitis B surface antigen particles carrying preS epitopes. *J*
Biotechnol **72**(1-2), 49-59.
- Ishida, H., Ueda, K., Ohkawa, K., Kanazawa, Y., Hosui, A., Nakanishi, F., Mita, E.,
 Kasahara, A., Sasaki, Y., Hori, M., and Hayashi, N. (2000). Identification of
 multiple transcription factors, HLF, FTF, and E4BP4, controlling hepatitis B
 virus enhancer II. *Journal of Virology* **74**(3), 1241-1251.
- Itoh, Y., Kuroda, S., Miyazaki, T., Otaka, S., and Fujisawa, Y. (1992). Identification
 of polymerized-albumin receptor domain in the pre-S2 region of hepatitis B
 virus surface antigen M protein. *J Biotechnol* **23**(1), 71-82.
- Jeong, J. H., Kwak, D. S., Rho, H. M., and Jung, G. (1996). The catalytic properties
 of human hepatitis B virus polymerase. *Biochem Biophys Res Commun*
223(2), 264-71.
- Johnson, P. J. (1999). Role of alpha-fetoprotein in the diagnosis and management of
 hepatocellular carcinoma. *Journal of Gastroenterology and Hepatology*
14(SS), S32-S36.
- Johnson, P. J., Poon, T. C. W., Hjelm, N. M., Ho, C. S., Ho, S. K. W., Welby, C.,
 Stevenson, D., Patel, T., Parekh, R., and Townsend, R. R. (1999). Glycan
 composition of serum alpha-fetoprotein in patients with hepatocellular
 carcinoma and non-seminomatous germ cell tumour. *British Journal of*
Cancer **81**(7), 1188-1195.

- Klingmuller, U., and Schaller, H. (1993). Hepadnavirus Infection Requires Interaction Between the Viral Pre-S Domain and a Specific Hepatocellular Receptor. *Journal of Virology* **67**(12), 7414-7422.
- Kock, J., Theilmann, L., Galle, P., and Schlicht, H. J. (1996). Hepatitis B virus nucleic acids associated with human peripheral blood mononuclear cells do not originate from replicating virus. *Hepatology* **23**(3), 405-13.
- Laccotripe, M., Makrides, S. C., Jonas, A., and Zannis, V. I. (1997). The carboxyl-terminal hydrophobic residues of apolipoprotein A-I affect its rate of phospholipid binding and its association with high density lipoprotein. *Journal of Biological Chemistry* **272**(28), 17511-17522.
- Lanford, R. E., Chavez, D., Brasky, K. M., Burns, R. B., 3rd, and Rico-Hesse, R. (1998). Isolation of a hepadnavirus from the woolly monkey, a New World primate. *Proceedings of the National Academy of Science* **95**(10), 5757-61.
- Le Seyec, J., Chouteau, P., Cannie, I., Guguen-Guillouzo, C., and Gripon, P. (1998). Role of the pre-S2 domain of the large envelope protein in hepatitis B virus assembly and infectivity. *Journal of Virology* **72**(7), 5573-8.
- Lee, Y. I., Hong, Y. B., Kim, Y., Rho, H. M., and Jung, G. (1997). RNase H activity of human hepatitis B virus polymerase expressed in Escherichia coli. *Biochem Biophys Res Commun* **233**(2), 401-7.
- Leenders, W. P., Glansbeek, H. L., de Bruin, W. C., and Yap, S. H. (1990). Binding of the major and large HBsAg to human hepatocytes and liver plasma membranes: putative external and internal receptors for infection and secretion of hepatitis B virus [see comments]. *Hepatology* **12**(1), 141-7.
- Li, J. S., Tong, S. P., and Wands, J. R. (1996). Characterization of a 120-kilodalton pre-S-binding protein as a candidate duck hepatitis B virus receptor. *Journal of Virology* **70**(9), 6029-6035.
- Li, J. S., Tong, S. P., and Wands, J. R. (1999). Identification and expression of glycine decarboxylase (p120) as a duck hepatitis B virus pre-S envelope-binding protein. *Journal of Biological Chemistry* **274**(39), 27658-27665.
- Li, M., Xie, Y., Wu, X., Kong, Y., and Wang, Y. (1995). HNF3 binds and activates the second enhancer, ENII, of hepatitis B virus. *Virology* **214**(2), 371-8.
- Loffler-Mary, H., Werr, M., and Prange, R. (1997). Sequence-specific repression of cotranslational translocation of the hepatitis B virus envelope proteins coincides with binding of heat shock protein Hsc70. *Virology* **235**(1), 144-52.

- Lu, X. Y., Block, T. M., and Gerlich, W. H. (1996). Protease-induced infectivity of hepatitis B virus for a human hepatoblastoma cell line. *Journal of Virology* **70**(4), 2277-2285.
- Luckcuck, T., Trotter, P. J., and Walker, J. H. (1997). Localization of annexin V in the adult and neonatal heart Download Full Text of Article. *Biochemical and Biophysical Research Communications* **238**(2), 622-628.
- Mabit, H., Dubanchet, S., Capel, F., Dauguet, C., and Petit, M. A. (1994). In vitro infection of human hepatoma cells (HepG2) with hepatitis B virus (HBV): spontaneous selection of a stable HBV surface antigen- producing HepG2 cell line containing integrated HBV DNA sequences. *J Gen Virol* **75**(Pt 10), 2681-9.
- Mabit, H., Vons, C., Dubanchet, S., Capel, F., Franco, D., and Petit, M. A. (1996). Primary cultured normal human hepatocytes for hepatitis B virus receptor studies. *J Hepatol* **24**(4), 403-12.
- Massamiri, T., Tobias, P. S., and Curtiss, L. K. (1997). Structural determinants for the interaction of lipopolysaccharide binding protein with purified high density lipoproteins: Role of apolipoprotein A-I. *Journal of Lipid Research* **38**(3), 516-525.
- McGwire, G. B., Tan, F., Michel, B., Rehli, M., and Skidgel, R. A. (1997). Identification of a membrane-bound carboxypeptidase as the mammalian homolog of duck gp180, a hepatitis B virus-binding protein. *Life Sci* **60**(10), 715-24.
- Mehdi, H., Kaplan, M. J., Anlar, F. Y., Yang, X., Bayer, R., Sutherland, K., and Peeples, M. E. (1994). Hepatitis B virus surface antigen binds to apolipoprotein H. *Journal of Virology* **68**(4), 2415-24.
- Mehdi, H., Yang, X., and Peeples, M. E. (1996). An altered form of apolipoprotein H binds hepatitis B virus surface antigen most efficiently Download Full Text of Article. *Virology* **217**(1), 58-66.
- Michel, M. L., Pontisso, P., Sobczak, E., Malpiece, Y., Streeck, R. E., and Tiollais, P. (1984). Synthesis in animal cells of hepatitis B surface antigen particles carrying a receptor for polymerized human serum albumin. *Proceedings of the National Academy of Science* **81**(24), 7708-12.

- Milich, D. R., Jones, J., Hughes, J., and Maruyama, T. (1994). Hepatitis-B Virus-Infection, the Immune-Response and Hepatocellular- Carcinoma. *Ciba Foundation Symposia* **187**, 113-131.
- Molina, A., Oka, T., Munoz, S. M., ChikamoriAoyama, M., Kuwahata, M., and Natori, Y. (1997). Vitamin B-6 suppresses growth and expression of albumin gene in a human hepatoma cell line HepG2. *Nutrition and Cancer-an International Journal* **28**(2), 206-211.
- Molmenti, E. P., Perlmutter, D. H., and Rubin, D. C. (1993). Cell-Specific Expression of Alpha(1)-Antitrypsin in Human Intestinal Epithelium. *Journal of Clinical Investigation* **92**(4), 2022-2034.
- Molnar-Kimber, K. L., Jarocki-Witek, V., Dheer, S. K., Vernon, S. K., Conley, A. J., Davis, A. R., and Hung, P. P. (1988). Distinctive properties of the hepatitis B virus envelope proteins. *Journal of Virology* **62**(2), 407-16.
- Mondelli, M., Tedder, R. S., Ferns, B., Pontisso, P., Realdi, G., and Alberti, A. (1986). Differential distribution of hepatitis B core and E antigens in hepatocytes: analysis by monoclonal antibodies. *Hepatology* **6**(2), 199-204.
- Nassal, M. (1992a). The arginine-rich domain of the hepatitis B virus core protein is required for pregenome encapsidation and productive viral positive- strand DNA synthesis but not for virus assembly. *Journal of Virology* **66**(7), 4107-16.
- Nassal, M. (1992b). Conserved cysteines of the hepatitis B virus core protein are not required for assembly of replication-competent core particles nor for their envelopment. *Virology* **190**(1), 499-505.
- Nassal, M., and Rieger, A. (1993). An intramolecular disulfide bridge between Cys-7 and Cys61 determines the structure of the secretory core gene product (e antigen) of hepatitis B virus. *Journal of Virology* **67**(7), 4307-15.
- Neurath, A. R., Kent, S. B., Strick, N., and Parker, K. (1986). Identification and chemical synthesis of a host cell receptor binding site on hepatitis B virus. *Cell* **46**(3), 429-36.
- Neurath, A. R., Kent, S. B., Strick, N., and Parker, K. (1988). Delineation of contiguous determinants essential for biological functions of the pre-S sequence of the hepatitis B virus envelope protein: its antigenicity, immunogenicity and cell-receptor recognition. *Ann Inst Pasteur Virol* **139**(1), 13-38.

- Ohmachi, Y., Murata, A., Yasuda, T., Kitagawa, K., Yamamoto, S., Monden, M., Mori, T., Matsuura, N., and Matsubara, K. (1994). Expression of the pancreatic secretory trypsin inhibitor gene in the liver infected with hepatitis B virus. *J Hepatol* **21**(6), 1012-6.
- Ostapchuk, P., Hearing, P., and Ganem, D. (1994). A dramatic shift in the transmembrane topology of a viral envelope glycoprotein accompanies hepatitis B viral morphogenesis. *EMBO J* **13**(5), 1048-57.
- Ou, J. H., and Rutter, W. J. (1987). Regulation of Secretion of the Hepatitis-B Virus Major Surface- Antigen By the Pres-1 Protein. *Journal of Virology* **61**(3), 782-786.
- Panin, L. E., Polyakov, L. M., Kolosova, N. G., Russkikh, G. S., and Poteryaeva, O. N. (1997). Distribution of the tocopherol and apolipoprotein A-I-immunoreactivity in the rat liver chromatin. *Biologicheskie Membrany* **14**(5), 512-519.
- Patel, A. H., Gaffney, D. F., Subaksharpe, J. H., and Stow, N. D. (1990). Dna-Sequence of the Gene Encoding a Major Secreted Protein of Vaccinia Virus, Strain Lister. *Journal of General Virology* **71**(Pt9), 2013-2021.
- Patel, A. H., Subaksharpe, J. H., and Stow, N. D. (1992). The N-Terminal 22 Amino-Acids Encoded By the Gene Specifying the Major Secreted Protein of Vaccinia Virus, Strain Lister, Can Function As a Signal Sequence to Direct the Export of a Foreign Protein. *Virus Research* **26**(3), 197-212.
- Persing, D. H., Varmus, H. E., and Ganem, D. (1986). Inhibition of Secretion of Hepatitis-B Surface-Antigen By a Related Presurface Polypeptide. *Science* **234**(4782), 1388-1391.
- Persing, D. H., Varmus, H. E., and Ganem, D. (1987). The Pres1 Protein of Hepatitis-B Virus Is Acylated At Its Amino Terminus With Myristic Acid. *Journal of Virology* **61**(5), 1672-1677.
- Peterson, D. L. (1987). The structure of hepatitis B surface antigen and its antigenic sites. *Bioessays* **6**(6), 258-62.
- Petit, M. A., Capel, F., Dubanchet, S., and Mabit, H. (1992). PreS1-specific binding proteins as potential receptors for hepatitis B virus in human hepatocytes. *Virology* **187**(1), 211-22.

- Phillips, J. C., Wriggers, W., Li, Z. G., Jonas, A., and Schulten, K. (1997). Predicting the structure of apolipoprotein A-1 in reconstituted high-density lipoprotein disks. *Biophysical Journal* **73**(5), 2337-2346.
- Poisson, F., Severac, A., Hourieux, C., Goudeau, A., and Roingard, P. (1997). Both pre-S1 and S domains of hepatitis B virus envelope proteins interact with the core particle. *Virology* **228**(1), 115-20.
- Prange, R., Clemen, A., and Streeck, R. E. (1991). Myristylation is involved in intracellular retention of hepatitis B virus envelope proteins. *Journal of Virology* **65**(7), 3919-23.
- Prange, R., and Streeck, R. E. (1995). Novel Transmembrane Topology of the Hepatitis-B Virus Envelope Proteins. *EMBO Journal* **14**(2), 247-256.
- Qiao, M., Macnaughton, T. B., and Gowans, E. J. (1994). Adsorption and Penetration of Hepatitis-B Virus in a Nonpermissive Cell-Line. *Virology* **201**(2), 356-363.
- Rodriguez-Crespo, I., Nunez, E., Yelamos, B., Gomez-Gutierrez, J., Albar, J. P., Peterson, D. L., and Gavilanes, F. (1999). Fusogenic activity of hepadnavirus peptides corresponding to sequences downstream of the putative cleavage site. *Virology* **261**(1), 133-42.
- Runge, D., Runge, D. M., Jager, D., Lubecki, K. A., Stolz, D. B., Karathanasis, S., Kietzmann, T., Strom, S. C., Jungermann, K., Fleig, W. E., and Michalopoulos, G. K. (2000). Serum-free, long-term cultures of human hepatocytes: Maintenance of cell morphology, transcription factors, and liver-specific functions Download Full Text of Article. *Biochemical and Biophysical Research Communications* **269**(1), 46-53.
- Runge, D. M., Runge, D., Dorko, K., Pizarov, L. A., Leckel, K., Kostrubsky, V. E., Thomas, D., Strom, S. C., and Michalopoulos, G. K. (1999). Epidermal growth factor- and hepatocyte growth factor-receptor activity in serum-free cultures of human hepatocytes. *Journal of Hepatology* **30**(2), 265-274.
- Ryu, C. J., Cho, D. Y., Gripon, P., Kim, H. S., GuguenGuillouzo, C., and Hong, H. J. (2000). An 80-kilodalton protein that binds to the pre-S1 domain of hepatitis B virus. *Journal of Virology* **74**(1), 110-116.
- Sanger, F., Coulson, A.R., Barrell, B.J., Smith, J.H. and Roe, B. A. (1997). Cloning in single-stranded bacteriophage as an aid to rapid DNA sequencing. *Journal of Molecular Biology*. **143**, 161-178.

- Sansonno, D. E., Fiore, G., Bufano, G., and Manghisi, O. G. (1988). Cytoplasmic localization of hepatitis B core antigen in hepatitis B virus infected livers. *J Immunol Methods* **109**(2), 245-52.
- Sato, K., Tanaka, M., Kusaba, T., Fukuda, H., and Tanikawa, K. (1998). Immunohistochemical demonstration of alpha-fetoprotein in small hepatocellular carcinoma. *Oncology Reports* **5**(2), 355-358.
- Saul, F. A., Vulliez-le Normand, B., Lema, F., and Bentley, G. A. (1997). Crystal structure of a recombinant form of the maltodextrin-binding protein carrying an inserted sequence of a B-cell epitope from the preS2 region of hepatitis B virus. *Proteins* **27**(1), 1-8.
- Seifer, M., and Standing, D. N. (1995). Ribonucleoprotein complex formation by the human hepatitis B virus polymerase. *Intervirology* **38**(5), 295-303.
- Sells, M. A., Chen, M. L., and Acs, G. (1987). Production of hepatitis B virus particles in Hep G2 cells transfected with cloned hepatitis B virus DNA. *Proceedings of the National Academy of Science* **84**(4), 1005-9.
- Semenkova, L. N., Dudich, E. I., and Dudich, I. V. (1997). Induction of apoptosis in human hepatoma cells by alpha-fetoprotein. *Tumor Biology* **18**(5), 261-273.
- Semenkova, L. N., Dudich, E. I., Dudich, I. V., Shingarova, L. N., and Korobko, V. G. (1997). Alpha-fetoprotein as a TNF resistance factor for the human hepatocarcinoma cell line HepG2. *Tumor Biology* **18**(1), 30-40.
- Sheu, S. Y., and Lo, S. J. (1994). Biogenesis of the hepatitis B viral middle (M) surface protein in a human hepatoma cell line: demonstration of an alternative secretion pathway. *J Gen Virol* **75**(Pt 11), 3031-9.
- Sirma, H., Giannini, C., Poussin, K., Paterlini, P., Kremsdorf, D., and Brechot, C. (1999). Hepatitis B virus X mutants, present in hepatocellular carcinoma tissue abrogate both the antiproliferative and transactivation effects of HBx. *Oncogene* **18**(34), 4848-59.
- Sonveaux, N., Thines, D., and Ruyschaert, J. M. (1995). Characterization of the HBsAg particle lipid membrane. *Res Virol* **146**(1), 43-51.
- Stirk, H. J., Thornton, J. M., and Howard, C. R. (1992). A Topological Model For Hepatitis-B Surface-Antigen. *Intervirology* **33**(3), 148-158.
- Su, H., and Yee, J. K. (1992). Regulation of hepatitis B virus gene expression by its two enhancers. *Proceedings of the National Academy of Science* **89**(7), 2708-12.

- Sun, J., Salem, H. H., and Bird, P. (1992). Nucleolar and Cytoplasmic Localization of Annexin-V. *Febs Letters* **314**(3), 425-429.
- Tan, W. S., Dyson, M. R., and Murray, K. (1999). Two distinct segments of the hepatitis B virus surface antigen contribute synergistically to its association with the viral core particles. *J Mol Biol* **286**(3), 797-808.
- Tong, S. P., Li, J. S., and Wands, J. R. (1995). Interaction Between Duck Hepatitis-B Virus and a 170-Kilodalton Cellular Protein Is Mediated Through a Neutralizing Epitope of the Pre-S Region and Occurs During Viral-Infection. *Journal of Virology* **69**(11), 7106-7112.
- Treichel, U., Meyer zum Buschenfelde, K. H., Stockert, R. J., Poralla, T., and Gerken, G. (1994). The asialoglycoprotein receptor mediates hepatic binding and uptake of natural hepatitis B virus particles derived from viraemic carriers. *J Gen Virol* **75**(Pt 11), 3021-9.
- Tsuji, M., Kashihara, T., Terada, N., and Mori, H. (1999). An immunohistochemical study of hepatic atypical adenomatous hyperplasia, hepatocellular carcinoma, and cholangiocarcinoma with alpha-fetoprotein, carcinoembryonic antigen, CA19-9, epithelial membrane antigen, and cytokeratins 18 and 19 Download Full Text of Article. *Pathology International* **49**(4), 310-317.
- Urban, S., Breiner, K. M., Fehler, F., Klingmuller, U., and Schaller, H. (1998). Avian hepatitis B virus infection is initiated by the interaction of a distinct pre-S subdomain with the cellular receptor gp180. *Journal of Virology* **72**(10), 8089-8097.
- Urban, S., Kruse, C., and Multhaup, G. (1999). A soluble form of the avian hepatitis B virus receptor - Biochemical characterization and functional analysis of the receptor ligand complex. *Journal of Biological Chemistry* **274**(9), 5707-5715.
- vonderMark, K., and Mollenhauer, J. (1997). Annexin V interactions with collagen. *Cellular and Molecular Life Sciences* **53**(6), 539-545.
- Wang, X. W., and Xie, H. (1998). Alpha-fetoprotein enhances the proliferation of human hepatoma cells in vitro. *Life Sciences* **64**(1), 17-23.
- White, A. L., Guerra, B., and Lanford, R. E. (1997). Influence of allelic variation on apolipoprotein(a) folding in the endoplasmic reticulum. *Journal of Biological Chemistry* **272**(8), 5048-5055.
- Wu, J. Y., Zhou, Z. Y., Judd, A., Cartwright, C. A., and Robinson, W. S. (1990). The hepatitis B virus-encoded transcriptional trans-activator hbx appears to be a

- novel protein serine/threonine kinase [published erratum appears in *Cell* 1993 Nov 19;75(4):826]. *Cell* **63**(4), 687-95.
- Wunderlich, G., and Bruss, V. (1996). Characterization of early hepatitis B virus surface protein oligomers. *Archives of Virology* **141**(7), 1191-1205.
- Wynne, S. A., Crowther, R. A., and Leslie, A. G. (1999). The crystal structure of the human hepatitis B virus capsid. *Mol Cell* **3**(6), 771-80.
- Xu, Z. C., Bruss, V., and Yen, T. S. B. (1997). Formation of intracellular particles by hepatitis B virus large surface protein. *Journal of Virology* **71**(7), 5487-5494.
- Yen, T. S. B. (1993). Regulation of Hepatitis-B Virus Gene-Expression. *Seminars in Virology* **4**(1), 33-42.
- Zlotnick, A., Cheng, N., Stahl, S. J., Conway, J. F., Steven, A. C., and Wingfield, P. T. (1997). Localization of the C terminus of the assembly domain of hepatitis B virus capsid protein: implications for morphogenesis and organization of encapsidated RNA. *Proceedings of the National Academy of Science* **94**(18), 9556-61.

